UNIVERSITAT POLITÈCNICA DE CATALUNYA

CONTRIBUTION TO THE IMPROVEMENT OF INTEGRAL EQUATION METHODS FOR PENETRABLE SCATTERERS

Tesi Doctoral

presentada al Departament de Teoria del Senyal i Comunicacions

per a l'obtenció del títol de Doctor Enginyer de Telecomunicació

a càrrec de
Eduard Úbeda Farré

Director de tesi: dr. Juan Manuel Rius i Casals
Barcelona, TSC-UPC, novembre 2000

ACKNOWLEDGEMENTS

Vull agrair al meu Director, en Juan Manuel Rius, el seu docte i constant guiatge. Vull agrair a en Joaquim Fortuny el seu desinteressat suport al llarg de la meva estada al Joint Research Center (JRC). Agraeixo a en Josep Parron i l'Alex Heldring, companys del grup de Mètodes Numèrics, el contrast de llurs parers científics. A en Josep Maria Haro agraeixo el seu puntual suport informàtic.

És de justícia testimoniar la calidesa dels meus dos companys de despatx, en Marc Bara i en Lluís Sagués. És igualment obligat un esment per tots aquells amb qui regularment he intercanviat mots, gestos i atencions: els avisats osonencs David, Albert i Isma, els reposats Jaumes, tarragonins, el laboriós Gonzalo, de terra endins, o l'impetuós baixllobregatí Carlos. Adreço també una salutació als rodamons de la ciència amb qui he compartit camí sia aquí -Alex, Andreas, Laura, Elaine, Tim- sia a Itàlia - Gloria, Giovanni, Margherita -.

Però per damunt de tot, vull dedicar aquest treball a aquells que -des del principi fins a la fi- han romàs indefectiblement a prop: la meva família. És a ells a qui dedico de tot cor aquest treball. Només ells donen sentit a la presentació d'aquesta Tesi doctoral.

TABLE OF CONTENTS

Chapter 1 Introduction ---------- 10

Chapter 2 Integral Method of Moments ---------- 14
2.1 Maxwell equations ---------- 14
2.2 Linear, homogeneous and isotropic media ---------- 16
2.2.1 Lossless dielectric ---------- 17
2.2.2 Magnetised lossless medium ---------- 18
2.2.3 Dielectric lossy medium with conductivity ---------- 18
2.3 Boundary conditions ---------- 19
2.4 Differential operators. Wave equations ---------- 20
2.5 Integral operators. Green's function ---------- 20
2.6 Equivalence theorem ---------- 23
2.6.1 Volume equivalence ---------- 24
2.6.2 Surface equivalence ---------- 24
2.6.2.1 *Single PeC body* ---------- 25
2.6.2.2 *Single penetrable body* ---------- 30
2.6.2.3 *Structure composed of PeC and penetrable regions* -- 34
2.7 Reciprocity theorem ---------- 36
2.8 Numerical methods ---------- 36
2.8.1 Analytical formulation of the electromagnetic problem ---------- 37
2.8.2 Discretization of the problem ---------- 37
2.8.2.1 *Discretization of the unknown* ---------- 37
2.8.2.2 *Discretization of the boundary conditions* ---------- 40
2.8.3 The solution of the problem. Matrix inversion ---------- 41
2.8.3.1 *Iterative methods* ---------- 42
2.8.3.2 *Preconditioning* ---------- 42
2.9 Method of moments ---------- 43
2.9.1 Requirements for the expanding and weighting functions ---------- 44

Chapter 3 Method of Moments on PeC bodies of revolution ---- 46
3.1 Introduction ---- 46
3.1.1 Expanding functions ---- 47
3.1.2 Weighting functions ---- 48
3.1.3 Matrix elements ---- 48
3.1.3.1 *Impedance elements corresponding to vector potential* ---- 48
3.1.3.2 *Impedance elements corresponding to scalar potential* ---- 49
3.1.3.3 *Modal matrices. Othogonality* ---- 51
3.2 Quick review of the existing BoR-MoM techniques ---- 52
3.2.1 PeC-EFIE by J. R. Mautz and R. F. Harrington ---- 52
3.2.2 PMCHW for honogeneous dielectrics or E-PMCHW for completely coated PeC bodies ---- 52
3.2.3 Use of the FFT for the efficient solution of the PeC-EFIE by S. D. Gedney and R. Mittra ---- 54
3.3 MoM-BoR PeC-EFIE according to S. D. Gedney and R. Mittra ---- 55
3.3.1 Extraction of the ξ-singularity ---- 56
3.3.2 Limitations of the ξ-singularity extraction ---- 58
3.3.3 Extraction of the t-singularity ---- 59
3.3.4 Impedance matrix ---- 61
3.3.5 Incident field expansion ---- 63
3.3.5.1 *Tangential weighting* ---- 65
3.3.5.2 *Azimuthal weighting* ---- 66
3.4 MoM-BoR PeC-MFIE ---- 67
3.4.1 Discussion about the proper choice of basis functions ---- 68
3.4.2 PeC-MFIE singularity extraction ---- 68
3.4.3 PeC-MFIE Cauchy principal value raw development ---- 70
3.4.3.1 *Fundamental integrals* ---- 70
3.4.3.2 *t-weighted submatrices* ---- 71
3.4.3.3 *ϕ-weighted submatrices* ---- 76
3.4.3.4 *Extraction of the ξ-singularity* ---- 81
3.4.3.5 *Extraction of the t-singularity* ---- 85
3.4.4 Improvement of the PeC-MFIE accuracy ---- 86
3.4.4.1 *The $\partial(\ )/\partial\phi$ dependence* ---- 87
3.4.4.2 *The terms $\sin\xi\,\partial(\ )/\partial n$ in the odd submatrices* ---- 88
3.4.4.3 *The terms $\sin\xi\,\partial(\ )/\partial R$ in the even submatrices* ---- 89
3.4.4.4 *Symmetry derived from the reciprocity theorem* ---- 92
3.4.5 Incident field expansion ---- 93

Chapter 4 Results for PeC bodies of revolution ---- 96
4.1 PeC-EFIE results ---- 96
4.2 Nature of the PeC-MFIE misbehaviour ---- 98
4.3 Description of the dissimilarity between PeC-MFIE and PeC-EFIE ---- 100
4.4 PeC-MFIE results ---- 102
4.4.1 Substitution of the R^{-3}-terms by R^{-1}-terms ---- 102
4.4.2 Improvement due to the property of symmetry ---- 107
4.4.3 Behaviour for a cylinder ---- 108
4.5 Explanation of the PeC-MFIE misbehaviour ---- 113

Chapter 5 Method of Moments on penetrable bodies of revolution ---- 116
5.1 Suitable operators for an *unbalanced* set ---- 116
5.1.1 PeC operators ---- 117
5.1.2 Dielectric operators ---- 118
5.2 Numerical limitations on the development of the dielectric operators ---- 121
5.3 Homogeneous dielectric bodies ---- 121
5.4 PeC- bodies with full dielectric coating ---- 123

Chapter 6 *RWG* based method of moments for PeC 3D bodies ---- 124
6.1 Definition of the basis functions ---- 124
6.1.1 RWG basis functions ---- 125
6.1.2 unxRWG basis functions ---- 128
6.2 Valid PeC-operators ---- 129
6.2.1 PeC-EFIE(*RWG,RWG*) ---- 130
6.2.1.1 *Mathematical development* ---- 130
6.2.1.2 *Theoretical considerations* ---- 132
6.2.2 PeC-MFIE(*unxRWG,RWG*) ---- 132
6.2.2.1 *Mathematical development* ---- 132
6.2.2.2 *Theoretical considerations* ---- 133
6.2.3 PeC-MFIE(*RWG,unxRWG*) ---- 134
6.2.3.1 *Mathematical development* ---- 134
6.2.3.2 *Theoretical considerations* ---- 135
6.3 Dismissed PeC-operators ---- 136
6.3.1 Operators with an inappropriate expansion of the domain space ---- 137
6.3.1.1 *Computation of the accumulated charge* ---- 137
6.3.1.2 *Charge definition on the neighbouring triangles* ---- 137
6.3.2 Operators with an inappropriate expansion of the rank space ---- 139
6.3.2.1 PeC-EFIE(*unxRWG,RWG*) ---- 140
6.3.2.2 PeC-MFIE(*unxRWG,unxRWG*), PeC-MFIE(*RWG,RWG*) 141
6.4 Numerical development of the PeC-operators ---- 141
6.4.1 Analytical integration ---- 142
6.4.2 Integration according to a Gaussian quadrature rule ---- 144
6.4.3 PeC-EFIE(*RWG,RWG*) ---- 145
6.4.4 PeC-MFIE(*unxRWG,RWG*) ---- 145
6.4.5 PeC-MFIE(*RWG,unxRWG*) ---- 146
6.5 Physical properties on an arbitrary polyhedron ---- 147
6.5.1 Charge boundary conditions ---- 147
6.5.2 Field boundary conditions ---- 148
6.5.2.1 *Magnetic field conditions: MFIE* ---- 149
6.5.2.2 *Electric field conditions: EFIE* ---- 152
6.5.3 Conclusions ---- 156

Chapter 7 Results for 3D PeC bodies ---- 158
7.1 Verification of the theoretical conclusions in accordance with the planar approach ---- 158
7.2 Numerical computation of the operators ---- 159
7.3 Conditioning of the matrices ---- 159
7.4 Physical polyhedrons ---- 161
7.5 Curved objects ---- 168
7.4.1 Higher-order expansion in PeC-EFIE(*RWG*,*RWG*) than in PeC-MFIE(*RWG*,*unxRWG*) ---- 174
7.6 Improvement of the behaviour of the operators ---- 176
7.6.1 Solid angle correction for PeC-MFIE(*unxRWG*,*RWG*) ---- 176
7.6.2 PeC-EFIE(*RWG*,*RWG*) post-correction for coarsely meshed spheres ---- 178

Chapter 8 *RWG* based method of moments for dielectric 3D bodies ---- 182
8.1 Dielectric polyhedron ---- 182
8.1.1 Charge condition ---- 183
8.1.2 Electric and magnetic boundary conditions:EFIE-MFIE ---- 183
8.1.3 Linear combination of the electric and magnetic boundary conditions: CFIE, PMCHW ---- 187
8.1.3.1 *Field conditions on the edges to yield a compatible problem in PMCHW* ---- 188
8.1.3.2 *Discussion about the resemblance of the PMCHW-solution with the Maxwell-consistent solution of the polyhedron* ---- 191
8.1.4 Influence of the low-order expansion of the current on the performance of EFIE-MFIE ---- 193
8.1.5 Conclusions ---- 195
8.2 Results for bodies with two regions shaping the interface surface ---- 196
8.2.1 Conditioning of the matrices ---- 197
8.2.2 Electrically small bodies with only penetrable regions ---- 198
8.2.2.1 *Relevance of the EFIE-MFIE low-order error* ---- 198
8.2.2.2 *Physical polyhedrons* ---- 203
8.2.2.3 *Curved objects* ---- 207
8.2.3 Electrically bigger bodies with only penetrable regions ---- 208
8.2.4 Bodies with PeC and dielectric regions ---- 213
8.2.4.1 *Relevance of the PMCHW error due to the less stringent field requirements* ---- 213
8.2.4.2 *Reference results* ---- 215
8.3 Generalisation to bodies with more than two regions shaping the interface surface ---- 217
8.4 Conclusions ---- 220

Chapter 9 Efficient methods----------222
9.1 Introduction----------222
9.2 IE-MEI----------223
9.2.1 Quasi-continuous metrons----------224
9.3 Fast Multipole Method----------226
9.3.1 MLFMM----------229
9.3.2 MLFMM for penetrable bodies----------230

Chapter 10 Conclusions----------234

Chapter 11 Appendices----------240
Appendix A----------240
Appendix B----------243

Bibliography----------246

Chapter 1 INTRODUCTION

The study of the electromagnetic phenomena along the last two centuries has brought about outstanding contributions for the human progress. The electromagnetism represents still now, at the beginning of the third millenium, a very important research area. The radiation pattern of particular types of antennas -for example, fractal or microstrip-, the analysis of the effect of the cellular communications on human beings or the detection of buried mines represent specific examples of the wide variety of problems of great interest nowadays.

The study of such a variety of problems relies on the application of the Maxwell equations, which rule all the electromagnetic behaviour. Since the analytical solution can only be obtained for very particular cases of canonical forms -such as spheres, spheroids or infinite cylinders-, in general, to tackle the analysis of an arbitrary problem, one makes use of the numerical methods. The discretization of electromagnetic integral equations by the Method of Moments -MoM- [3][36], henceforth integral MoM, excels as a powerful and reliable tool for analysing bodies composed of locally homogeneous regions -penetrable or conducting- immerse in a wide and nearly uniform medium -typically the ground or the free-space-. These integral methods result from the surface equivalence theorem, which allows in general two different formulations, the *Electric Field Integral Equation* (EFIE) and the *Magnetic Field Integral Equation* (MFIE). For the case of penetrable bodies, the Poggio, Miller, Chang, Harrington and Wu (PMCHW) [7][8][31] formulation can also be employed -it results from the subtraction of the EFIE and MFIE at both sides of the surfaces-.

The Method of Moments is based on the full expansion of the physical magnitudes, field and current, over the interface surfaces between the regions. In consequence, the solution of the problem is obtained through the inversion of a full-matrix, which, for electrically large problems, requires excessive memory resources and computation time. That is why the MoM is widely considered a brute-force method. The expansion of the magnitudes is carried out through the *discretization* of the surface; that is, *patches* spreading over the interface. The set of patches expanding the -electric or magnetic- fields and currents are respectively called *Weighting* and *Expanding* functions.

The most outstanding contribution of this dissertation Thesis -Chapters 6, 7 and 8- is the study of the appropriate conditions to develop correctly the 3D operators EFIE, MFIE -PeC and dielectric- and PMCHW so as to yield accurate results for any structure. Since the discretization implies a break on the continuity properties of the physical magnitudes, the valid 3D-operators must ensure the physical electromagnetic requirements in the discretized surface. In mathematical terms, these requirements set the rank -field- and domain -current- spaces, which essentially require the enforcement of the continuity across the edges of either the tangential or the normal component of the expanded magnitudes.

The first half of this dissertation Thesis -Chapters 3, 4 and 5- tackles the development of the MoM applied to problems with bodies with symmetry of revolution -BoR-. Since in this case the physical magnitudes present an azimuthal periodicity, they can be expressed as a Fourier series. The orthogonality between the different modes enables to obtain separately each azimuthal mode of the solution. It is thus only required to spread the *patches* along the generating arc of the bodies for each mode, which is very advantageous because the electromagnetic analysis can be carried out indeed for dimensionally large problems. In Chapter 3, a well-known PeC-EFIE BoR [12] formulation is developed. Accordingly, PeC-MFIE and PMCHW formulations are developed from scratch, which represent an original contribution of this dissertation Thesis. Furthermore, it is commented in detail and corrected to some extent the numerical error associated to the fastest-varying part of the PeC-MFIE BoR operator. The BoR-codes are particularly useful in modelling the electromagnetic behaviour of buried mines, which very often show revolution symmetry.

In Chapter 6, the valid integral MoM approaches for the case of an arbitrary perfectly conducting -PeC- body are justified, which becomes a singular contribution of this work. It is thus recommended the use of the divergence-conforming and of the curl-conforming functions respectively in the development of the PeC-EFIE and the PeC-MFIE operators. Low-order sets over triangular facets, *RWG* [28] and *unxRWG* [35], -belonging respectively to these two fundamental groups- are chosen to develop the PeC-operators: PeC-EFIE(*RWG*) and PeC-MFIE(*unxRWG*). Furthermore, it is reasoned theoretically the inherent misbehaviour in the PeC-MFIE in case the current expansion relies on a divergence-conforming set. The accurate computation of the impedance terms for each operator is also presented in detail. It is particularly interesting the precise computation of the operator PeC-MFIE(*unxRWG*), which is an original contribution of this work.

In Chapter 7, a heuristic correction for the misbehaviour of PeC-MFIE(*RWG*) is provided, which stands for an original contribution of this dissertation Thesis. The better behaviour of PeC-EFIE(*RWG*) and PeC-MFIE(*unxRWG*) is confirmed with examples. In view of the results, it is reasoned the suitability of PeC-EFIE(*RWG*) for the analysis of physical polyhedrons, which makes PeC-MFIE(*unxRWG*) excel as a more appropriate operator for curved bodies. A procedure for improving the performance of PeC-EFIE(*RWG*) for coarsely meshed spheres is given, which represents another original contribution of this Thesis.

In Chapter 8, the operators that agree with the electromagnetic requirements for an arbitrary penetrable body are presented: EFIE [15], PMCHW [25] and MFIE - dual operator to EFIE and new contribution of this work-. Since the same low-order sets are used to expand the currents, it is shown their compatibility with the combination of the right PeC-operators. In the dielectric case, in addition to the required continuity of the magnitudes across the edges at each region, the fields at both sides of the surface must satisfy the interface continuity, which is ignored in the conducting case -the fields are null inside the conductor-. The impossibility of meeting both continuity requirements at the same time justifies the apparition of inherent and different errors in the dual EFIE-MFIE and in PMCHW. The dual EFIE-MFIE focus on ensuring the continuity of the electric-magnetic field across the edges separately on each medium meanwhile the PMCHW operator ensures the interface continuity of the fields. It is thoroughly reasoned and confirmed with examples the suitability of PMCHW for problems with only penetrable regions. It is also shown and discussed in detail the robustness of EFIE-MFIE since its behaviour is appropriate for electrically not too small structures with perfectly conducting

or penetrable regions. All this theoretical analysis constitutes an original contribution of this dissertation Thesis.

At the end of Chapter 8 the analysis of composite structures is presented, which is very useful for the case of microstrip antennas. These cases are considered as a group of disjoint bodies with null distances of separation. It is recommended the use of EFIE-MFIE since, unlike PMCHW, they can ensure the continuous transition to zero of a distance of separation increasingly small.

In Chapter 9, efficient methods -IE-MEI [53] and MLFMM [45]- relying on the 3D-operators of Chapters 6 and 8 are presented. The development of the PeC 3D IE-MEI cannot maintain the advantages present in the 2D case since the harmonic *metrons* are not valid in the 3D general case. A new and original contribution of this work is a set of *metrons* that ensures little discontinuity of the current across the edges. It is confirmed with examples how these *metrons,* so-called *quasi-continuous*, reduce the number of required coefficients per row for a certain current error. However, these *metrons* must be dismissed in practice since they must be pre-computed for each body and involve an extra multiplying matrix in the process of search of the coefficients.

With regard to the dielectric MLFMM implementation, it is reasoned the suitability of the dual EFIE and MFIE operators since they provide a lower condition number than PMCHW and because their low-order misbehaviour disappears for electrically large dielectric bodies. The dielectric MLFMM EFIE-MFIE operators are thus developed from an existing PeC-MLFMM package. Some examples of penetrable spheres with moderate electrical dimensions are shown and commented.

Chapter 2 INTEGRAL METHOD OF MOMENTS

2.1 MAXWELL EQUATIONS

The electromagnetic differential equations that rule all the electromagnetic phenomena stand for

$$\nabla \times \vec{h} = \vec{j} + \frac{\partial \vec{d}}{\partial t} \tag{2.1}$$

$$\nabla \times \vec{e} = -\frac{\partial \vec{b}}{\partial t} \tag{2.2}$$

$$\nabla \cdot \vec{d} = \alpha \tag{2.3}$$

$$\nabla \cdot \vec{b} = 0 \tag{2.4}$$

$$\nabla \cdot \vec{j} + \frac{\partial \alpha}{\partial t} = 0 \tag{2.5}$$

where $\vec{e}(\vec{r},t)$, $\vec{h}(\vec{r},t)$ are the electric and magnetic fields, $\vec{b}(\vec{r},t)$, $\vec{d}(\vec{r},t)$, the electric and magnetic flux densities and $\vec{j}(\vec{r},t)$, $\alpha(\vec{r},t)$, the electric current and charge densities.

The field expressions (2.1), (2.2), (2.3) and (2.4) form the widely-known Maxwell equations. The application of the Stokes theorem on (2.1) and (2.2) results in the Ampère and Faraday's expressions; similarly, the divergence theorems in (2.3) and (2.4) yield the Gauss law. The expression in (2.5) is the continuity equation, which allows for the charge conservation principle.

Whenever the sources are harmonic time-varying, the original magnitudes become

$$\begin{aligned} \vec{j}(\vec{r},t) &= \mathrm{Re}\left[\vec{J}(\vec{r})e^{j\omega t}\right] \;,\; \alpha(\vec{r},t) = \mathrm{Re}\left[\sigma(\vec{r})e^{j\omega t}\right] \\ \vec{e}(\vec{r},t) &= \mathrm{Re}\left[\vec{E}(\vec{r})e^{j\omega t}\right] \;,\; \vec{h}(\vec{r},t) = \mathrm{Re}\left[\vec{H}(\vec{r})e^{j\omega t}\right] \\ \vec{b}(\vec{r},t) &= \mathrm{Re}\left[\vec{B}(\vec{r})e^{j\omega t}\right] \;,\; \vec{d}(\vec{r},t) = \mathrm{Re}\left[\vec{D}(\vec{r})e^{j\omega t}\right] \end{aligned} \tag{2.6}$$

where $\sigma(\vec{r})$, $\vec{J}(\vec{r})$, $\vec{H}(\vec{r})$, $\vec{E}(\vec{r})$, $\vec{B}(\vec{r})$, $\vec{D}(\vec{r})$ are complex quantities under which the Maxwell equations become

$$\nabla \times \vec{H} = \vec{J} + j\omega\vec{D} \tag{2.7}$$

$$\nabla \times \vec{E} = -j\omega\vec{B} \tag{2.8}$$

$$\nabla \cdot \vec{D} = \sigma \tag{2.9}$$

$$\nabla \cdot \vec{B} = 0 \tag{2.10}$$

$$\nabla \cdot \vec{J} + j\omega\sigma = 0 \tag{2.11}$$

where ω corresponds to the angular frequency. This system must not be considered a particular case since any temporal dependence can be expanded in terms of its spectral coefficients. In general, the solution can be obtained for each spectral frequency component according to the Fourier Transform

$$\vec{J}(\vec{r}) = \int_{-\infty}^{+\infty} \vec{j}(\vec{r},t)e^{-j\omega t}dt \qquad \sigma(\vec{r}) = \int_{-\infty}^{+\infty} \alpha(\vec{r},t)e^{-j\omega t}dt \tag{2.12}$$

and one can recompose the time domain solution through the inverse Fourier transform. All the formulation presented along this dissertation Thesis has been developed in the frequency domain but one can readily pass to the time domain by means of the correspondences $j\omega \leftrightarrow \partial(\ )/\partial t$ and $-\omega^2 \leftrightarrow \partial^2(\ )/\partial t^2$.

Some of the equations above can be derived from others. This is the case of the continuity equation, that results from the application of the divergence operator $\nabla\cdot$ in (2.7) and from the further substitution in (2.9). One can similarly obtain (2.10) from (2.8). So, as a matter of fact, with three independent expressions one can unambiguously determine any electromagnetic problem: (2.7), (2.8) -curl dependent- and (2.11) -the continuity equation-.

The above-presented expression for the Maxwell equations allows only for electric sources, ρ and $\vec{J}$, because these are the only sources that have physical sense. Nonetheless, one can also theoretically define magnetic sources, $v(\vec{r})$ and $\vec{M}(\vec{r})$. These fictitious sources are used for simplifying the computation of the electromagnetic fields due to more complicated electric distributions. Therefore, the expressions in (2.8), (2.10) and (2.11) now become

$$\nabla \times \vec{E} = -\vec{M} - j\omega\vec{B} \tag{2.13}$$

$$\nabla \cdot \vec{B} = v \tag{2.14}$$

$$\nabla \cdot \vec{M} + j\omega v = 0 \tag{2.15}$$

2.2 LINEAR, HOMOGENEOUS AND ISOTROPIC MEDIA

In case the medium being the vacuum, the flux densities and the fields are related through the constants ε_0 and μ_0, the so-called electric permittivity and the magnetic permeability constants

$$\vec{D} = \varepsilon_0 \vec{E} \qquad \vec{B} = \mu_0 \vec{H} \tag{2.16}$$

where $\varepsilon_0 = (1/(36\pi)) \cdot 10^{-9}$ F/m and $\mu_0 = 4\pi \cdot 10^{-7}$ H/m.

One can thus equivalently express the Maxwell equations as

$$\nabla \times \vec{H} = \vec{J} + j\omega\varepsilon_0 \vec{E} \tag{2.17}$$

$$\nabla \times \vec{E} = -\vec{M} - j\omega\mu_0 \vec{H} \tag{2.18}$$

$$\nabla \cdot \vec{E} = \frac{\sigma}{\varepsilon_0} \tag{2.19}$$

$$\nabla \cdot \vec{H} = \frac{\nu}{\mu_0} \tag{2.20}$$

which are the equations adopted to rule the electromagnetic behaviour in the free-space -as required in the scattering problems- since its electromagnetic characteristics are very close to those of the vacuum.

If we define two systems of equations with no electric or magnetic sources, the resulting fields are related -as one may have foreseen in advance by viewing the dual symmetry in the Maxwell equations-. Particularly, for the vacuum, the expression that transforms the field magnitudes of both dual problems, 1, electric - $\vec{M}$ =0-, and 2, magnetic - $\vec{J}$ =0-, is

$$\vec{E}_2 = -\eta_0 \vec{H}_1 \qquad \vec{H}_2 = \frac{1}{\eta_0} \vec{E}_1 \tag{2.21}$$

and the compatibility between the sources yields

$$\nu = \eta_0 \sigma \qquad \vec{M} = \eta_0 \vec{J} \tag{2.22}$$

where $\eta_0 = \sqrt{\mu_0 / \varepsilon_0}$ is the so-called impedance in the vacuum.

In general, a medium is linear whenever the flux densities and the fields can be related through a first order approximation. In homogeneous media, the approximating parameters are uniform throughout the space. An isotropic medium behaves equally for the three vector components, whereby the parameters are scalars. The vacuum stands for an outstanding example of isotropic, linear and homogeneous medium. Some other examples of linear, homogeneous and isotropic media are presented right away and result in ruling equations analogous to those above-shown for the vacuum.

2.2.1 Lossless dielectric

The internal structure of the dielectric media is in general modelled in terms of a distribution of electric dipoles that are induced by the external field. These induced dipoles in turn create an electric field that opposes the original electric field -see Fig. 2.1-.

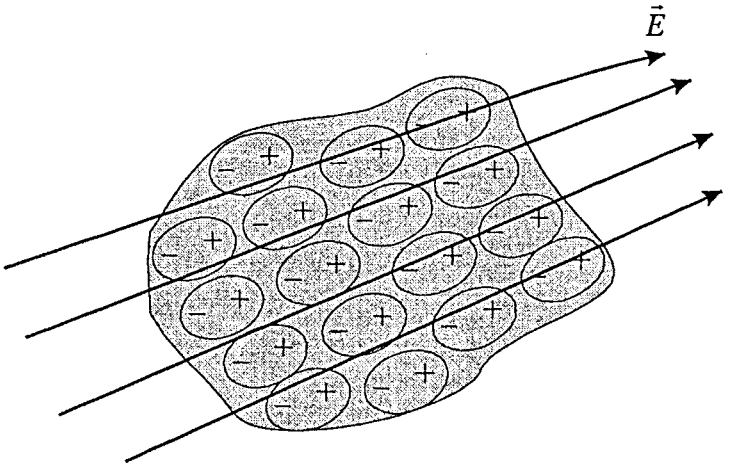

Fig. 2.1 Induced dipoles in a dielectric body

The electric induction, from the superposition of both influences, becomes now

$$\vec{D} = \varepsilon_0 \vec{E} + \vec{P} \tag{2.23}$$

where the first addend allows for the vacuum influence and $\vec{P}(\vec{r})$, the polarisation vector, is defined as $\vec{P} = d\vec{p}/dv$, where $\vec{p}(\vec{r})$ stands for the dielectric dipolar moment. The insertion of (2.23) in (2.17) and (2.19), yields

$$\nabla \times \vec{H} = \vec{J}_f + j\omega \vec{P} + j\omega \varepsilon_0 \vec{E} \tag{2.24}$$

$$\nabla \cdot \vec{E} = \frac{\sigma_f - \nabla \cdot \vec{P}}{\varepsilon_0} \tag{2.25}$$

where $-\nabla \cdot \vec{P}$ can be formally interpreted as the induced charge density. The free sources σ_f, $\vec{J}_f$ represent the real excitation of the problem, irrespective of the particular characteristics of the medium. They are called free to point out their independent origin from the charges throughout the dielectric, induced by the external field.

In general, one can empirically find a closed relation between the polarisation vector and the electric field. For the specific case of a linear, isotropic and homogeneous medium, it accomplishes

$$\vec{P} = \varepsilon_0 \chi_e \vec{E} \tag{2.26}$$

where χ_e, the electric susceptibility, is constant, scalar and non dependent on the field intensity. The introduction of (2.26) in (2.24) and (2.25) yields

$$\nabla\times\vec{H}=\vec{J}_f+j\omega\varepsilon_0(1+\chi_0)\vec{E} \tag{2.27}$$

$$\nabla\cdot\vec{E}=\frac{\sigma_f}{\varepsilon_0(1+\chi_0)} \tag{2.28}$$

By comparing (2.17) and (2.19) with (2.27) and (2.28), one remarks about the presence of an extra multiplying factor that is only due to the dielectric characteristics. Hence, through the definition $\varepsilon=\varepsilon_0\varepsilon_r$, with $\varepsilon_r=1+\chi_e$ being the so-called relative electric permittivity, one can accordingly apply the vacuum equations to the dielectric case as

$$\nabla\cdot\vec{E}=\frac{\sigma_f}{\varepsilon} \tag{2.29}$$

$$\nabla\times\vec{H}=\vec{J}_f+j\omega\varepsilon\vec{E} \tag{2.30}$$

The fact of χ_e being positive for all the cases confirms that the dipoles induce an electric field with opposite sense to $\vec{E}$, which unavoidably forces ε_r to be bigger than one.

2.2.2 Magnetised lossless medium

One can analogously analyse the magnetised bodies as a distribution of magnetic dipoles, which, for a linear, isotropic and homogeneous medium, lead to the permeability constants μ and μ_r. According to the internal physical origin of the magnetic behaviour, there can be different magnetised bodies, such as paramagnetic, diamagnetic or ferromagnetic. However, since the aim of the presented Thesis is to study the scattering due to penetrable -dielectric- bodies, it is always assumed $\mu_r=1$. In any case, any magnetised medium could be analysed as well through the same formulation by setting μ_r properly. The expressions in (2.18) and (2.20) in this case become

$$\nabla\times\vec{E}=-\vec{M}_f-j\omega\mu\vec{H} \tag{2.31}$$

$$\nabla\cdot\vec{H}=\frac{\nu}{\mu} \tag{2.32}$$

2.2.3 Dielectric lossy medium with conductivity σ_c

This section allows for those media with the presence of conduction current $\vec{J}_c$, which is related with $\vec{E}$ through the conductivity parameter σ_c, that is assumed constant,

$$\vec{J}_c=\sigma_c\vec{E} \tag{2.33}$$

The Ampere law, (2.30), now stands for

$$\nabla\times\vec{H}=\vec{J}_f+\vec{J}_c+j\omega\varepsilon\vec{E}=\vec{J}_f+(\sigma_c+j\omega\varepsilon)\vec{E} \tag{2.34}$$

from where one assesses the goodness in working in the frequency space since all the medium dependence can be confined in an equivalent or effective relative permittivity $\varepsilon_{r,ef}$ that is complex and frequency dependent

$$\varepsilon_{r,ef}=\varepsilon_r-j\frac{\sigma_c}{\omega\varepsilon_0} \tag{2.35}$$

which enables the expression in (2.34) to be rewritten as in (2.30)

$$\nabla\times\vec{H}=\vec{J}_f+j\omega\varepsilon_0\varepsilon_{r,ef}\vec{E} \tag{2.36}$$

The imaginary part from (2.35) accounts for the losses inherent to the conduction current because it results in an attenuating factor for the propagating waves.

A particular an extremely important case is that for which $\sigma_c=\infty$, widely known as perfectly conducting (PeC). In a PeC body, free current flows along the body surface, $\vec{E}$ is null inside the body and is normal to the outer side of the surface, which involves that no losses are assumed.

2.3 BOUNDARY CONDITIONS

As shown so far, the Maxwell equations are a set of differential equations that rule over determined portion of the space. So as to let the solution well-defined one has to provide also the conditions over the bordering surface around the volume where the differential equations rule. These are the so-called *boundary conditions.*

In case the problem rules the whole space, the boundary conditions are set in the infinite, S_∞, and compel the electromagnetic fields to be zero -as one can well intuitively foresee-. These are the so-called Sommerfeld radiation conditions.

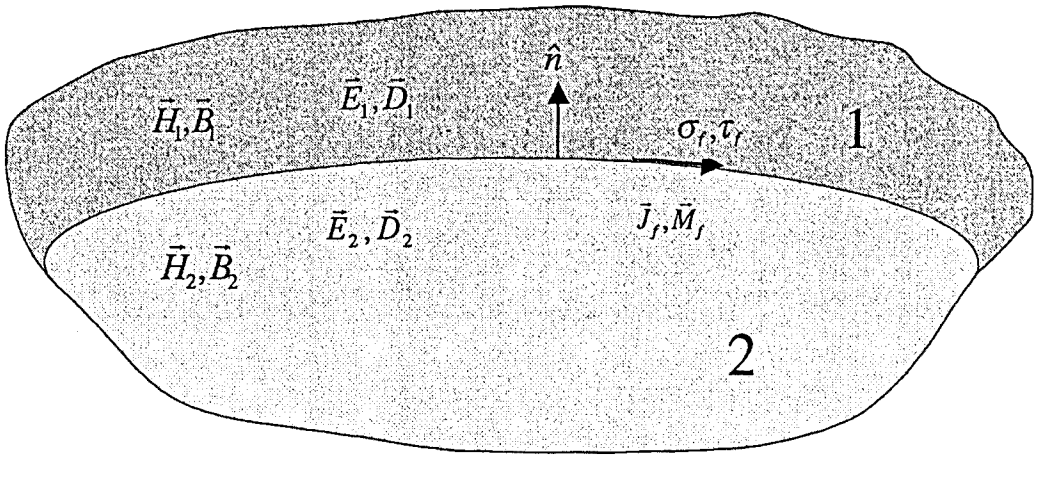

Fig. 2.2 Interface between two media

In general, the boundary conditions that rule the transition between two different media are -see Fig. 2.2-

$$\vec{n}\times\left(\vec{H}_1-\vec{H}_2\right)\Big|_{\vec{r}\in S_i}=\vec{J}_f \tag{2.37}$$

$$\vec{n}\times\left(\vec{E}_1-\vec{E}_2\right)\Big|_{\vec{r}\in S_i}=-\vec{M}_f \tag{2.38}$$

$$\vec{n}\cdot\left(\vec{D}_1-\vec{D}_2\right)\Big|_{\vec{r}\in S_i}=\sigma_f \tag{2.39}$$

$$\vec{n}\cdot\left(\vec{B}_1-\vec{B}_2\right)\Big|_{\vec{r}\in S_i}=\nu_f \tag{2.40}$$

where $\hat{n}$ stands for the unitary normal vector to the surface directed from the medium 2 to the medium 1 and $\vec{J}_f(\vec{r})$, $\sigma_f(\vec{r})$ and $\vec{M}_f(\vec{r})$, $\nu_f(\vec{r})$ are the surface electric and magnetic free sources [1] that lie throughout S_i, the interface surface.

2.4 DIFFERENTIAL OPERATORS. WAVE EQUATIONS

The application of $\nabla\times$ into the curl-dependent equations, (2.30) and (2.31), of an arbitrary linear, homogeneous and isotropic medium yields

$$\nabla\times\nabla\times\vec{H}=\nabla\times\vec{J}+j\omega\varepsilon\nabla\times\vec{E} \qquad \nabla\left(\nabla\cdot\vec{H}\right)-\nabla^2\vec{H}=\nabla\times\vec{J}+j\omega\varepsilon\nabla\times\vec{E} \tag{2.41}$$

$$\nabla\times\nabla\times\vec{E}=-\nabla\times\vec{M}-j\omega\mu\nabla\times\vec{H} \qquad \nabla\left(\nabla\cdot\vec{E}\right)-\nabla^2\vec{E}=-\nabla\times\vec{M}-j\omega\mu\nabla\times\vec{H} \tag{2.42}$$

which, in view of (2.29) and (2.32), become the $\vec{E}$ and $\vec{H}$ and wave equations

$$\nabla^2\vec{H}+k^2\vec{H}=-\nabla\times\vec{J}+j\omega\varepsilon\vec{M}+\frac{\nabla\nu}{\mu} \qquad \nabla^2\vec{E}+k^2\vec{E}=\nabla\times\vec{M}+j\omega\mu\vec{J}+\frac{\nabla\sigma}{\varepsilon} \tag{2.43}$$

They render solutions of wave nature with propagation velocity of $c=1/\sqrt{\mu\varepsilon}$. For harmonic time-varying sources one defines besides $k=\omega/c=\omega\sqrt{\mu\varepsilon}$, the wave number, which accomplishes $k=2\pi/\lambda$, where λ is the spatial wavelength. These differential equations are generally appropriate to obtain the solution without exciting sources; for instance, the wave-guide or cavity modes, or in the free-space, under a cartesian coordinate system, the plane waves.

2.5 INTEGRAL OPERATORS. GREEN'S FUNCTION

When dealing with an electromagnetic problem it is also possible to develop an integral formulation completely equivalent to the wave equations. It is firstly convenient to tackle

[1] In this dissertation Thesis, the currents $\vec{J}$, $\vec{M}$ and the charge densities σ, ν will be indistinctly named so, regardless their origin, volumetric or superficial. Here, unlike the precedent sections, the currents and the charge densities are superficial.

the study through the superposition of the formulation for each of the dual problems: 1 - $\vec{M}=0,\nu=0$- and 2 - $\vec{J}=0,\sigma=0$-.

$$\begin{aligned}\vec{E}(\vec{J},\vec{M})&=\vec{E}(\vec{J},\vec{M})\big|_{\vec{M}=0}+\vec{E}(\vec{J},\vec{M})\big|_{\vec{J}=0}=\vec{E}_1(\vec{J})+\vec{E}_2(\vec{M})\\ \vec{H}(\vec{J},\vec{M})&=\vec{H}(\vec{J},\vec{M})\big|_{\vec{M}=0}+\vec{H}(\vec{J},\vec{M})\big|_{\vec{J}=0}=\vec{H}_1(\vec{J})+\vec{H}_2(\vec{M})\end{aligned} \tag{2.44}$$

From the differential expression of the magnetic Gauss law (2.10), assuming $\nu=0$, for a linear, homogeneous and isotropic medium one can infer

$$\vec{H}_1=\frac{1}{\mu}\nabla\times\vec{A} \tag{2.45}$$

by resorting to $\nabla\cdot(\nabla\times(\ ))=0$, where $\vec{A}(\vec{r})$ stands for the electric vector potential. The insertion of (2.45) in the differential expression of the Faraday's law, (2.8), assuming $\vec{M}=0$, yields

$$\nabla\times(\vec{E}_1+j\omega\vec{A})=0 \tag{2.46}$$

from where, since $\nabla\times(\nabla\cdot(\ ))=0$, one can accordingly state

$$\vec{E}_1=-\nabla\Phi-j\omega\vec{A} \tag{2.47}$$

where $\Phi(\vec{r})$ is the electric scalar potential.

By introducing (2.45) and (2.47) in the other, electric source dependent, Maxwell equations, we get to the closed expressions in terms of the scalar and vector potentials;

$$\nabla^2\vec{A}+\omega^2\mu\varepsilon\vec{A}=-\mu\vec{J}+\nabla(\nabla\cdot\vec{A}+j\omega\mu\varepsilon\Phi) \tag{2.48}$$

$$\nabla^2\Phi=-\frac{\sigma}{\varepsilon}-j\omega(\nabla\cdot\vec{A}) \tag{2.49}$$

In addition, the Lorentz condition, compatible with the continuity equation, stands for

$$\nabla\vec{A}+j\omega\mu\varepsilon\Phi=0 \tag{2.50}$$

which, when applied in (2.48) and in (2.49), leads to the so-called Helmholtz equations

$$\nabla^2\vec{A}+k^2\vec{A}=-\mu\vec{J}\qquad\nabla^2\Phi+k^2\Phi=-\frac{\sigma}{\varepsilon} \tag{2.51}$$

which, as (2.43), are wave equations too. These equations are uncoupled, which means that the potential functions $\vec{A}(\vec{r})$, $\Phi(\vec{r})$ represent respectively the separate response for each of the source magnitudes $\vec{J}(\vec{r})$ and $\rho(\vec{r})$.

The Green's function $G(\vec{r},\vec{r}')$ is the solution of the differential equation in (2.51) under a point-source excitation; that is,

$$\nabla^2 G(\vec{r},\vec{r}') - k^2 G(\vec{r},\vec{r}') = -\delta(\vec{r}-\vec{r}') \tag{2.52}$$

where $\vec{r}'$ is the point where the point-source is placed.

According to the second scalar Green's theorem,

$$\iiint_V \left[\Phi\nabla^2 G - G\nabla^2\Phi\right] dv = \oiint_S \left[\Phi\frac{\partial G}{\partial n} - G\frac{\partial\Phi}{\partial n}\right] dS \tag{2.53}$$

which, in view of (2.51) and (2.52), can be expressed as

$$\Phi(\vec{r}) = \iiint_V G(\vec{r},\vec{r}')\frac{\sigma(\vec{r}')}{\varepsilon} dV' - \oiint_S \left[\Phi(\vec{r}')\frac{\partial G(\vec{r},\vec{r}')}{\partial n'} - G(\vec{r},\vec{r}')\frac{\partial\Phi(\vec{r}')}{\partial n'}\right] dS' \tag{2.54}$$

where V stands for the volume of the medium, S is the enclosing surface and $\vec{r}', \vec{r}$ denote respectively the source and field domains. $G(\vec{r},\vec{r}')$, which must be known beforehand, is key to obtain the solution for any arbitrary source excitation and enables the transformation of the original differential operators into an equivalent integral expression. In general, the surface integral in (2.54) is non-null and allows for the boundary conditions.

It is not easy to obtain $G(\vec{r},\vec{r}')$ for any medium and its corresponding boundary conditions. For the particular case of the medium being linear, homogeneous and isotropic over the whole space, one can obtain the analytical expression for $G(\vec{r},\vec{r}')$, the well-known free-space Green's function,

$$G(\vec{r},\vec{r}') = \frac{e^{-jkR}}{4\pi R} \tag{2.55}$$

being $R = |\vec{r}-\vec{r}'|$. Moreover, as in this case the enclosing surface is in the infinite, where according to the Sommerfeld radiation condition the fields must be null, the expression for $\Phi(\vec{r})$ becomes

$$\Phi(\vec{r}) = \iiint_V \frac{e^{-jk|\vec{r}-\vec{r}'|}}{4\pi|\vec{r}-\vec{r}'|}\frac{\sigma(\vec{r}')}{\varepsilon} dV' \tag{2.56}$$

and so does accordingly the vector potential function $\vec{A}$ since it is ruled by the same operator

$$\vec{A}(\vec{r}) = \iiint_V \mu\frac{e^{-jk|\vec{r}-\vec{r}'|}}{4\pi|\vec{r}-\vec{r}'|}\vec{J}(\vec{r}')dV' \tag{2.57}$$

The solutions for $\vec{E}_1(\vec{J})$ and $\vec{H}_1(\vec{J})$, (2.45) and (2.47), are straightforward from the two previous expressions, which represent a convolution integral of the Green's function with the sources.

One can equivalently reach the previous expressions for the electromagnetic fields $\vec{E}_2$, $\vec{H}_2$ of the dual problem - $\vec{J}=0$, $\sigma=0$ -. The potential functions in this case are defined as

$$\Psi(\vec{r})=\iiint_V \frac{e^{-jk|\vec{r}-\vec{r}'|}}{4\pi|\vec{r}-\vec{r}'|}\frac{\nu(\vec{r}')}{\mu}dV' \tag{2.58}$$

$$\vec{F}(\vec{r})=\iiint_V \varepsilon\frac{e^{-jk|\vec{r}-\vec{r}'|}}{4\pi|\vec{r}-\vec{r}'|}\vec{M}(\vec{r}')dV' \tag{2.59}$$

where $\Psi(\vec{r})$ and $\vec{F}(\vec{r})$ stand respectively for the magnetic scalar and vector potentials. The expressions for the fields accordingly yield

$$\vec{E}_2=-\frac{1}{\varepsilon}\nabla\times\vec{F} \tag{2.60}$$

$$\vec{H}_2=-\nabla\Psi-j\omega\vec{F} \tag{2.61}$$

which confirm the field and source transformations between both problems presented in (2.21) and (2.22) for the vacuum; indeed,

$$\begin{aligned}\vec{E}_2(\vec{M})&=-\eta\vec{H}_1\left(\frac{\vec{M}}{\eta}\right)=-\vec{H}_1(\vec{M})\\ \vec{E}_2(\vec{M})&=-\eta\vec{H}_1\left(\frac{\vec{M}}{\eta}\right)=-\vec{H}_1(\vec{M})\end{aligned} \tag{2.62}$$

where η stands for the medium impedance.

Therefore, the final expressions for $\vec{E}$ and $\vec{H}$ come from the addition of the solution for both the dual problems, as shown in (2.44),

$$\begin{aligned}\vec{E}(\vec{J},\vec{M})&=-\nabla\Phi-j\omega\vec{A}-\frac{1}{\varepsilon}\nabla\times\vec{F}\\ \vec{H}(\vec{J},\vec{M})&=\frac{1}{\mu}\nabla\times\vec{A}-\nabla\Psi-j\omega\vec{F}\end{aligned} \tag{2.63}$$

2.6 EQUIVALENCE THEOREM

The equivalence theorem allows to solve an electromagnetic problem by means of an equivalent problem where some new electric and magnetic currents - $\vec{J}_{eq}$, $\vec{M}_{eq}$ - are defined so as to enable the use of the free-space integral expressions of (2.63). The equivalent

problem renders the same field solution as the real problem because the boundary conditions are compelled to be the same.

In scattering problems, one defines the scattered fields, $\vec{E}^S$, $\vec{H}^S$, as the fields radiated by the equivalent currents, and the incident fields, $\vec{E}^i$ and $\vec{H}^i$, as the fields already existing before placing the scatterer. Nonetheless, one must never consider a body under the incidence of an external field a radiating structure. The equivalent currents are fictitious and the only real currents that appear in the body are induced by the external action. One must understand the scattered fields as the necessary field contribution to make suitable the original $\vec{E}^i$ and $\vec{H}^i$ to the change of boundary conditions imposed by the body.

$$\vec{E} = \vec{E}^S\left(\vec{J}_{eq}, \vec{M}_{eq}\right) + \vec{E}^i \qquad \vec{H} = \vec{H}^S\left(\vec{J}_{eq}, \vec{M}_{eq}\right) + \vec{H}^i \tag{2.64}$$

2.6.1 Volume equivalence

The group of equivalent sources $\vec{J}_{eq,V}(\vec{r})$, $\vec{M}_{eq,V}(\vec{r})$ are spread throughout the volume of the original problem. Assuming $\varepsilon = \varepsilon(\vec{r})$ and $\mu = \mu(\vec{r})$, the curl-dependent Maxwell equations become

$$\nabla \times \vec{H} = \vec{J}_s + j\omega\varepsilon(\vec{r})\vec{E} \tag{2.65}$$

$$\nabla \times \vec{E} = -\vec{M}_s - j\omega\mu(\vec{r})\vec{H} \tag{2.66}$$

Through the smart substitution,

$$\vec{J}_{eqV} = j\omega\left(\varepsilon(\vec{r}) - \varepsilon_0\right)\vec{E} \tag{2.67}$$

$$\vec{M}_{eq,V} = j\omega\left(\mu(\vec{r}) - \mu_0\right)\vec{H} \tag{2.68}$$

the expressions in (2.65) and (2.66) convert into the more manageable, free-space, equivalent equations

$$\nabla \times \vec{H} = \vec{J}_s + \vec{J}_{eq,V} + j\omega\varepsilon_0\vec{E} \tag{2.69}$$

$$\nabla \times \vec{E} = -\vec{M}_s - \vec{M}_{eq,V} - j\omega\mu_0\vec{H} \tag{2.70}$$

where one sees how the equivalent sources make up for the change of medium.

This procedure is actually only used for inhomogeneous bodies since it involves to spread the unknown inside the volume of the body. The following technique, on the other hand, allows for the definition of the unknowns over the interface surfaces.

2.6.2 Surface equivalence

A more advantageous expression of the equivalence theorem can be developed whenever the electromagnetic problem consists of a structure composed of locally linear, homogeneous and isotropic media. This approach is suitable for a very wide range of

scattering or antenna problems, which are normally modelled by the piecewise composition of penetrable and PeC patches.

The equivalent problem is defined through the superposition of simpler problems -corresponding to each region- that extend the validity of the electromagnetic constants to the whole space so as to allow the use of the expressions (2.56), (2.57) and (2.63). The definition of electric and magnetic equivalent sources along the interface surfaces is required.

2.6.2.1 Single PeC body

According to the particular characteristics of the conductors, the field inside the body is known beforehand to be null -see Fig. 2.3-. Only the field contribution outside the scattering structure has to be hence considered (the electric and magnetic constants, required to develop the operators, stand for ε_0, μ_0, η_0).

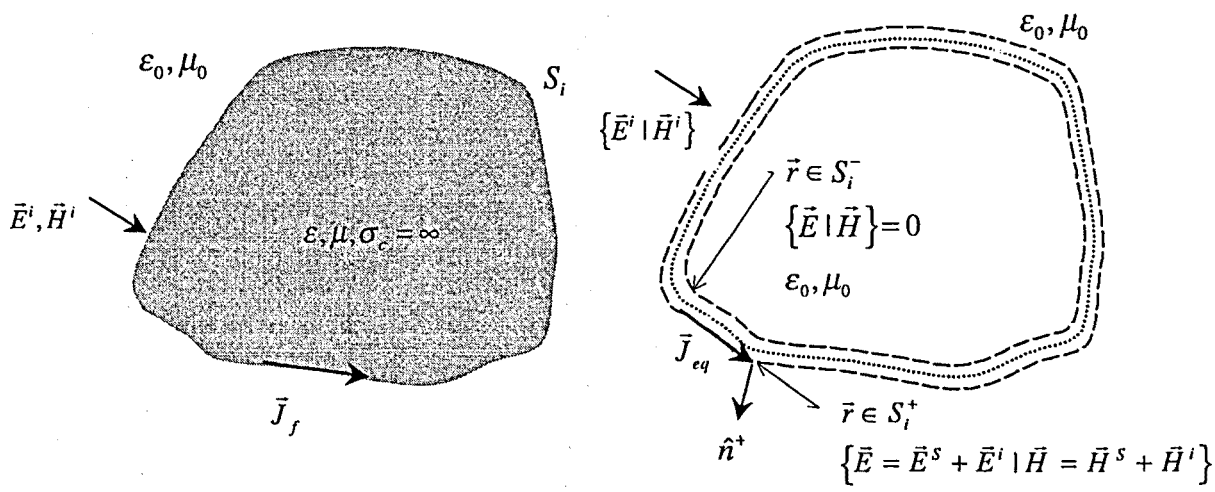

Fig. 2.3 Theorem of surface equivalence on a single PeC-body

- **Boundary conditions**

The electric equivalent current is defined along the outer face S_i^+ of the interface surface as

$$\vec{J}_{eq} = \hat{n}^+ \times \vec{H}\Big|_{\vec{r} \in S_i^+} \tag{2.71}$$

which coincides with the boundary condition since the fields of the equivalent problem are assumed null inside the body. The unitary vector normal to S_i $\hat{n}^+$ points at the volume where the problem is defined, as shown in Fig. 2.3.

The magnetic field boundary condition for the real problem is

$$\vec{J}_f = \hat{n}^+ \times \vec{H}\Big|_{\vec{r}\in S_i^+} \tag{2.72}$$

because the fields inside the PeC bodies are null.

The conditions (2.71) (2.72) are the same, which lets thus the problem correctly posed in the equivalent problem. One should not let be misunderstood by the fact of existing currents of the same value $\vec{J}_{eq}$ and $\vec{J}_f$ along S_i^+ in both problems. Although both are free currents $\vec{J}_{eq}$ is a radiating current inside an infinite medium of constants ε_0, μ_0, whereas $\vec{J}_f$ is a non-radiating current, that appears along the interface of a conducting body.

The electric boundary condition for PeC bodies is trivial

$$\hat{n}^+ \times \vec{E}\Big|_{\vec{r}\in S_i^+} = 0 \tag{2.73}$$

That is why no magnetic equivalent source is to be defined.

- **Definition of the equations**

By forcing the magnitudes, with the help of (2.64), to accomplish the magnetic field and the electric field boundary conditions, one renders two different equations to solve the problem

$$\hat{n}^+ \times \vec{H}^i\Big|_{\vec{r}\in S_i^+} = \vec{J}_{eq} - \hat{n}^+ \times \vec{H}^S\left(\vec{J}_{eq}\right)\Big|_{\vec{r}\in S_i^+} \tag{2.74}$$

$$-\hat{n}^+ \times \vec{E}^i\Big|_{\vec{r}\in S_i^+} = \hat{n}^+ \times \vec{E}^S\left(\vec{J}_{eq}\right)\Big|_{\vec{r}\in S_i^+} \tag{2.75}$$

which are respectively the *Magnetic Field Integral Equation* (MFIE) and the *Electric Field Integral Equation* (EFIE).

Some authors [15] have proposed to set the boundary conditions in the interior side of the surface S_i^-, where the fields are to be null. The ruling boundary equations in this case result in

$$\hat{n}^- \times \vec{H}\Big|_{\vec{r}\in S_i^-} = 0 \qquad \hat{n}^- \times \vec{E}\Big|_{\vec{r}\in S_i^-} = 0 \tag{2.76}$$

which lead the MFIE and the EFIE to

$$\hat{n}^- \times \vec{H}^i\Big|_{\vec{r}\in S_i^-} = -\hat{n}^- \times \vec{H}^S\left(\vec{J}_{eq}\right)\Big|_{\vec{r}\in S_i^-} \tag{2.77}$$

$$\hat{n}^- \times \vec{E}^i\Big|_{\vec{r}\in S_i^-} = -\hat{n}^- \times \vec{E}^S\left(\vec{J}_{eq}\right)\Big|_{\vec{r}\in S_i^-} \tag{2.78}$$

The EFIE and the MFIE are fully determined in any case since these PeC operators, $\vec{E}^S_{PeC} = \vec{E}^S\left(\vec{J}_{eq}\right)$, $\vec{H}^S_{PeC} = \vec{H}^S\left(\vec{J}_{eq}\right)$, whose integral expression lies in (2.45) and (2.47)[2], are univocally dependent on the Green's function in the free-space.

From (2.45) (2.47) (2.56) (2.57) (2.5), they can be developed in detail as

$$\vec{H}^S_{PeC} = \nabla\times\left[\iint_S G(\vec{r},\vec{r}')\vec{J}_{eq}(\vec{r}')dS'\right] = -\iint_S \vec{J}_{eq}(\vec{r}')\times\nabla G(\vec{r},\vec{r}')dS' \tag{2.79}$$

$$\begin{aligned}\vec{E}^S_{PeC} &= \nabla\left[\iint_S G(\vec{r},\vec{r}')\frac{\nabla'\cdot\vec{J}_{eq}}{j\omega\varepsilon_0}dS'\right] - j\omega\mu_0\iint_S G(\vec{r},\vec{r}')\vec{J}_{eq}(\vec{r}')dS' \\ &= -j\frac{\eta_0}{k_0}\iint_S \nabla'\cdot\vec{J}_{eq}\nabla G(\vec{r},\vec{r}')dS' - jk_0\eta_0\iint_S G(\vec{r},\vec{r}')\vec{J}_{eq}(\vec{r}')dS'\end{aligned} \tag{2.80}$$

The correct development of the operators $\vec{E}^S_{PeC}$, $\vec{H}^S_{PeC}$ is crucial since all the later operators -see (2.111)- derive from them. Particularly, avoiding any thorough insight into the integration method, which will be later provided, one must pay special attention on the singularity $-\vec{r}'\rightarrow\vec{r}$- of the integrands.

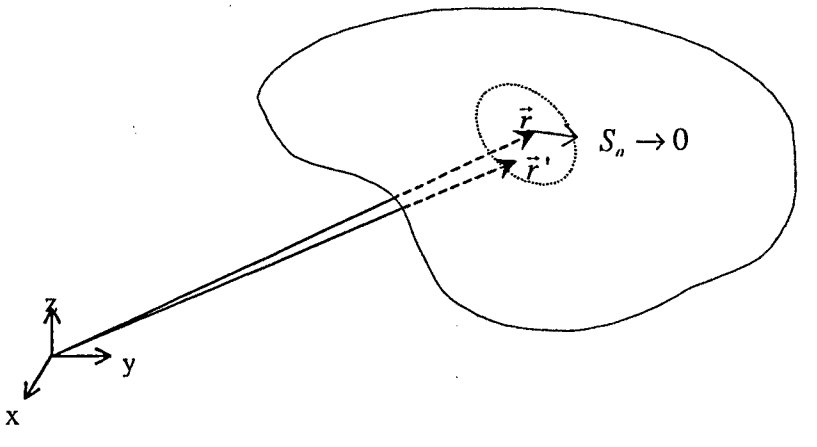

Fig. 2.4 Integration of the singularity over S_a

As shown in Fig. 2.4, the integration of the singularity necessarily involves the integration over an area tending to zero around the field point $\vec{r}$: $\vec{E}^S_{PeC}\big|_{S_a\rightarrow 0}$, $\vec{H}^S_{PeC}\big|_{S_a\rightarrow 0}$. The result of the integration due to the rest of the domain is called the Cauchy Principal Value and can be effectuated through the appropriate analytical or numerical techniques: $\vec{E}^S_{PeC}\big|_{PV}$, $\vec{H}^S_{PeC}\big|_{PV}$. The integral expressions of MFIE -(2.74) (2.77)- and EFIE -(2.75) (2.78)- can be separated in terms of these partial contributions as

[2] Although the integration is initially presented over a volume, in this case, due to the superficial nature of the sources, the integration must be done over a surface

$$\hat{n}^{\pm}\times\vec{H}^{S}_{PeC}\Big|_{\vec{r}\in S_i^{\pm}}=\hat{n}^{\pm}\times\vec{H}^{S}_{PeC}\Big|_{S_a^{\pm}\to 0}+\hat{n}^{\pm}\times\vec{H}^{S}_{PeC}\Big|_{PV^{\pm}} \tag{2.81}$$

$$\hat{n}^{\pm}\times\vec{E}^{S}_{PeC}\Big|_{\vec{r}\in S_i^{\pm}}=\hat{n}^{\pm}\times\vec{E}^{S}_{PeC}\Big|_{S_a^{\pm}\to 0}+\hat{n}^{\pm}\times\vec{E}^{S}_{PeC}\Big|_{PV^{\pm}} \tag{2.82}$$

Furthermore, as it is well-known [4][5], the integration of the singularity can be analytically solved for $G(\vec{r},\vec{r}\,')$ and $\nabla G(\vec{r},\vec{r}\,')$

$$\lim_{a\to 0}\int_{S_a} G(\vec{r},\vec{r}\,')dS'=0 \qquad \lim_{a\to 0}\int_{S_a^{\pm}} \nabla G(\vec{r},\vec{r}\,')dS'=-\frac{\Omega_0^{\pm}}{4\pi}\hat{n}^{\pm} \tag{2.83}$$

where $\Omega_0^{\pm}(\vec{r})$ is the portion of solid angle at both sides of S^i-see Fig. 2.5-. These values are related through the expression

$$\Omega_0^{+}=4\pi-\Omega_0^{-} \tag{2.84}$$

For smooth-varying surfaces, which is normally the case, $\Omega_0^{+}=\Omega_0^{-}=2\pi$.

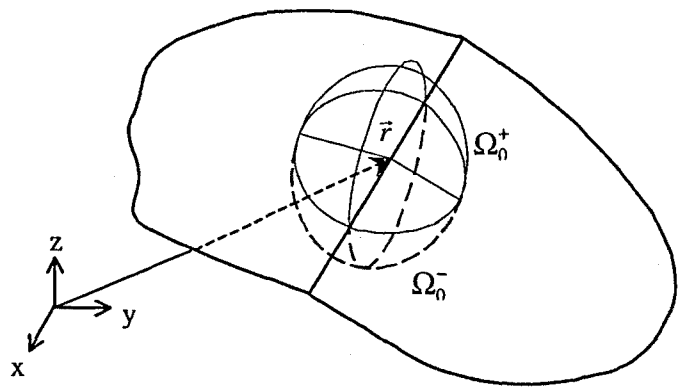

Fig. 2.5 Solid angle definition

The development of $\hat{n}^{\pm}\times\vec{H}^{S}_{PeC}\Big|_{S_a^{\pm}\to 0}$ and $\hat{n}^{\pm}\times\vec{E}^{S}_{PeC}\Big|_{S_a^{\pm}\to 0}$, according to (2.83), is easily obtained

$$\begin{aligned}\hat{n}^{\pm}\times\vec{E}^{S}_{PeC}\Big|_{S_a^{\pm}\to 0} &= -j\frac{\eta_0}{k_0}\nabla'\cdot\vec{J}_{eq}\left[\hat{n}^{\pm}\times\iint_{S_a^{\pm}}\nabla G(\vec{r},\vec{r}\,')dS'\right]-jk_0\eta_0\hat{n}^{\pm}\times\left[\vec{J}_{eq}(\vec{r}\,')\iint_{S_a^{\pm}}G(\vec{r},\vec{r}\,')dS'\right] \\ &= j\frac{\eta_0}{k_0}\nabla'\cdot\vec{J}_{eq}\left[\hat{n}^{\pm}\times\frac{\Omega_0^{\pm}}{4\pi}\hat{n}^{\pm}\right]=0\end{aligned} \tag{2.85}$$

$$\hat{n}^{\pm}\times\vec{H}^{S}_{PeC}\Big|_{S_a^{\pm}\to 0}=\hat{n}^{\pm}\times\left[-\vec{J}_{eq}(\vec{r})\times\iint_{S_a^{\pm}\to 0}\nabla G(\vec{r},\vec{r}\,')dS'\right]=\frac{\Omega_0^{\pm}}{4\pi}\hat{n}^{\pm}\times\left(\vec{J}_{eq}(\vec{r})\times\hat{n}^{\pm}\right)=\frac{\Omega_0^{\pm}}{4\pi}\vec{J}_{eq}(\vec{r}) \tag{2.86}$$

which, following (2.81) and (2.82), let the previous MFIE and EFIE expressions for $\vec{r} \in S_i^+$, (2.74) (2.75), as

$$\hat{n}^+ \times \vec{H}^i\Big|_{\vec{r}\in S_i^+} = \left[1 - \frac{\Omega_0^+}{4\pi}\right]\vec{J}_{eq} - n^+ \times \vec{H}^S_{PeC}\Big|_{PV^+} \tag{2.87}$$

$$\hat{n}^+ \times \vec{E}^i\Big|_{\vec{r}\in S_i^+} = -\hat{n}^+ \times \vec{E}^S_{PeC}\Big|_{PV^+} \tag{2.88}$$

The MFIE and EFIE expressions for $\vec{r} \in S_i^-$ (2.77) and (2.78), accordingly substituted, yield

$$\hat{n}^- \times \vec{H}^i\Big|_{\vec{r}\in S_i^-} = -\frac{\Omega_0^-}{4\pi}\vec{J}_{eq}(\vec{r}) - \hat{n}^- \times \vec{H}^S_{PeC}\Big|_{PV^-} \tag{2.89}$$

$$\hat{n}^- \times \vec{E}^i\Big|_{\vec{r}\in S_i^-} = -\hat{n}^- \times \vec{E}^S_{PeC}\Big|_{PV^-} \tag{2.90}$$

Allowing for the continuity of the incident fields and of the non-singular parts of the integrands across the surface, one should also note that

$$\vec{H}^S_{PeC}\Big|_{PV^+} = \vec{H}^S_{PeC}\Big|_{PV^-} \qquad \vec{E}^S_{PeC}\Big|_{PV^+} = \vec{E}^S_{PeC}\Big|_{PV^-}$$

$$\vec{H}^i\Big|_{\vec{r}\in S_i^-} = \vec{H}^i\Big|_{\vec{r}\in S_i^+} \qquad \vec{E}^i\Big|_{\vec{r}\in S_i^-} = \vec{E}^i\Big|_{\vec{r}\in S_i^+} \tag{2.91}$$

In addition, resorting to (2.84) and to the fact that $\hat{n}^+ = -\hat{n}^-$, one remarks that both expressions for the EFIE and the MFIE are equal. Indeed, it can only be so since the solution for $\vec{J}_{eq}$ is unique. This confirms again the right assumption for the fields being null at S_i^-. A formal advantageous aspect of the equations in (2.77) (2.78) is that one can express them by leaving out the $\hat{n}$ cross product since they respond to a field expression made equal to zero. Indeed, one can equivalently set the boundary conditions, (2.76), as

$$\left[\vec{H}\right]_{\tan,\vec{r}\in S_i^-} = 0 \qquad \left[\vec{E}\right]_{\tan,\vec{r}\in S_i^-} = 0 \tag{2.92}$$

and, accordingly, the MFIE and EFIE yield

$$\left[\vec{H}^i\right]_{\tan,\vec{r}\in S_i^-} = -\left[\vec{H}^S\left(\vec{J}_{eq}\right)\right]_{\tan,\vec{r}\in S_i^-} \tag{2.93}$$

$$\left[\vec{E}^i\right]_{\tan,\vec{r}\in S_i^-} = -\left[\vec{E}^S\left(\vec{J}_{eq}\right)\right]_{\tan,\vec{r}\in S_i^-} \tag{2.94}$$

which, though completely equal to the integral equations inferred from (2.71) and (2.73), are formally more interesting since the field operator embraces completely the unknown. The EFIE and MFIE formulations chosen to develop all the electromagnetic operators along this dissertation Thesis are based on the (2.93) and (2.94).

The EFIE and MFIE integral equations are theoretically valid for any kind of surface that encloses any arbitrary region. However, when the PeC-region has a shape in such

a way that one dimension is minuscule compared with the other dimensions, such as the strips, -see Fig. 2.6-, getting a precise value for the solution becomes difficult, since the opposite geometry values tend to merge.

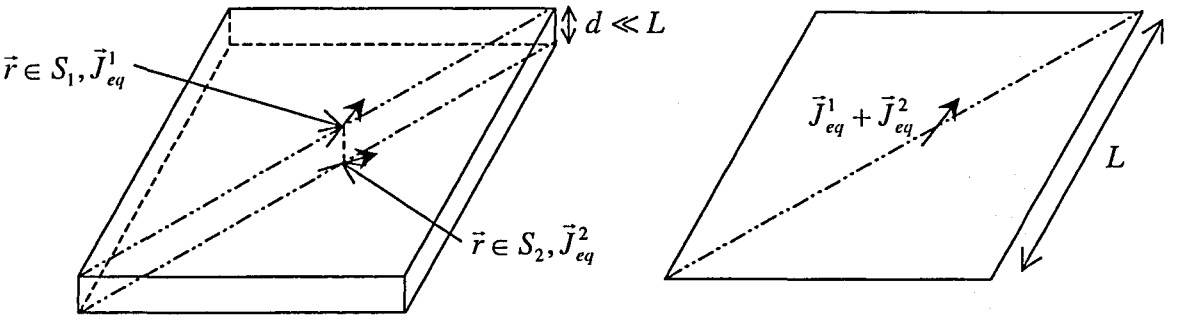

Fig. 2.6 Surface equivalence theorem simplification for strips

Due to the fact that $\left[\vec{E}^S_{PeC}\right]_{S_a^{\pm}\to 0} = 0$ -see (2.85)- under the assumption for the width to be null, $\vec{E}^S$ is equal at $\vec{r} \in \{S_1 \,|\, S_2\}$, being $\{S_1 \,|\, S_2\}$ each opposite portion of the enclosing surface -see Fig. 2.6-, and can be expressed as the addition of the contribution of the current from both sides: $\vec{J}^1_{eq}$, $\vec{J}^2_{eq}$

$$\vec{E}^S\left(\vec{J}_{eq}\right)\Big|_{\vec{r}\in S_1} = \vec{E}^S\left(\vec{J}_{eq}\right)\Big|_{\vec{r}\in S_2}$$
$$\vec{E}^S\left(\vec{J}_{eq}\right)\Big|_{\vec{r}\in\{S_1|S_2\}} = \vec{E}^S\left(\vec{J}^1_{eq}\right)\Big|_{\vec{r}\in\{S_1|S_2\}} + \vec{E}^S\left(\vec{J}^2_{eq}\right)\Big|_{\vec{r}\in\{S_1|S_2\}} = \vec{E}^S\left(\vec{J}^1_{eq} + \vec{J}^2_{eq}\right)\Big|_{\vec{r}\in\{S_1|S_2\}} \tag{2.95}$$

It can be thus set as new current unknown the addition of the current at both sides - $\vec{J}_n = \vec{J}^1_{eq} + \vec{J}^2_{eq}$ - because, in this case, the particular value for the current at each side is irrelevant with regard to the construction of the fields. One can theoretically assign this approach to the definition of an open surface with flowing current $\vec{J}_n$, which, though, has no physical significance.

On the other hand, one is unable to reproduce this simplification and improvement with the MFIE expression because, as shown in (2.86), the term $\left[\vec{H}^S_{PeC}\right]_{S_a^{\pm}\to 0,\vec{r}\in\{S_1|S_2\}} \propto \vec{J}^{\{1|2\}}_{eq} \neq 0$

2.6.2.2 Single penetrable body

The equivalence theorem proposes to divide the study into the superposition of two equivalent problems, defined all over the free-space, each of which allows for the solution inside their associated region, assuming the field zero in the rest of the space. Each equivalent problem spreads the electromagnetic constants corresponding to each region all over; in the original problem, in accordance with the sign convention adopted for PeC, ε_+, μ_+ are assigned to the outer medium and ε_-, μ_-, to the inner medium -see Fig. 2.7-.

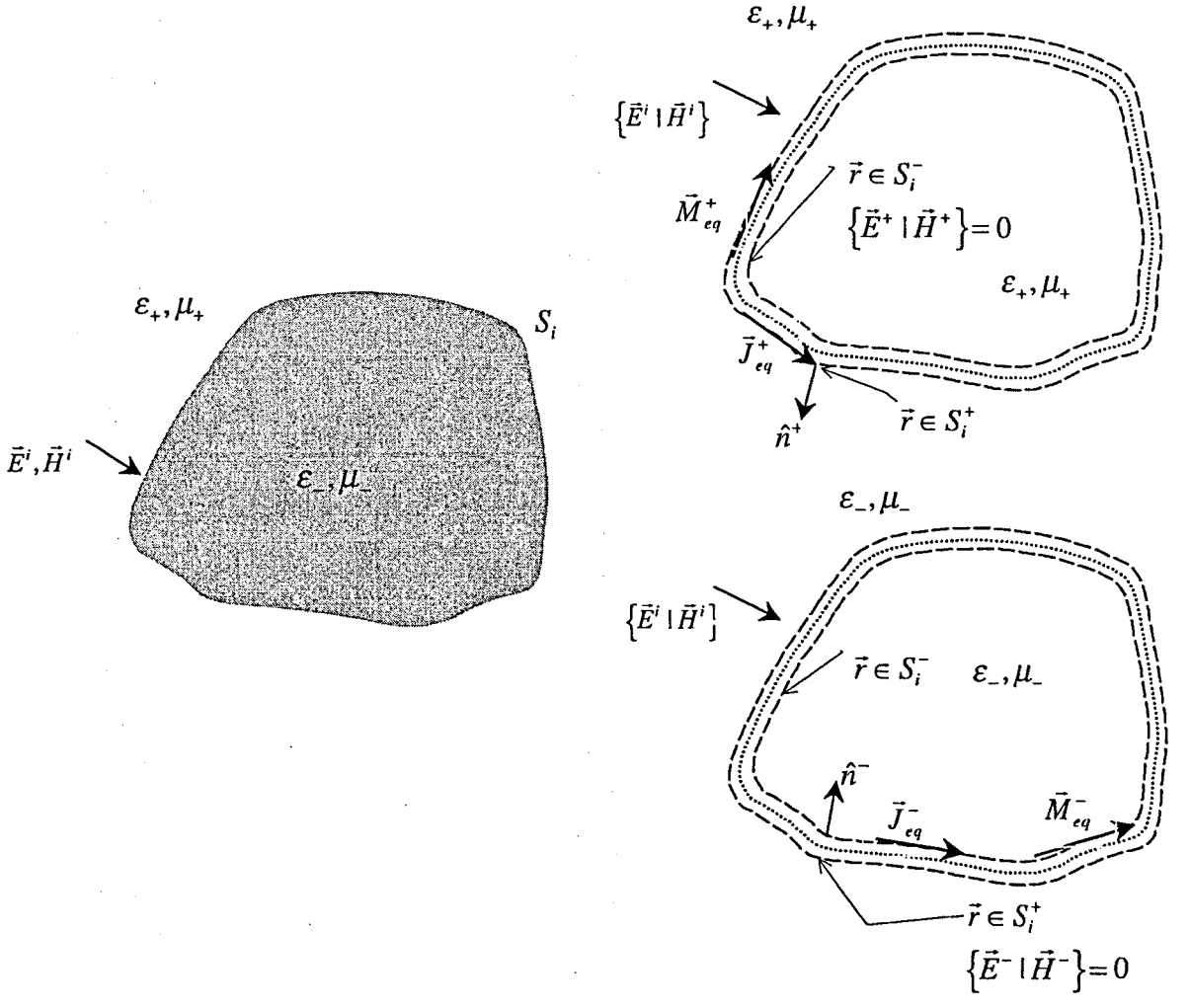

Fig. 2.7 Theorem of surface equivalence on a single penetrable body

- **Boundary conditions**

In accordance with (2.37) and (2.38), the boundary conditions along S_i for the original problem stand for

$$\vec{n}^+ \times \left(\vec{H}\big|_{\vec{r} \in S_i^+} - \vec{H}\big|_{\vec{r} \in S_i^-} \right) = 0 \qquad \vec{n}^+ \times \left(\vec{E}\big|_{\vec{r} \in S_i^+} - \vec{E}\big|_{\vec{r} \in S_i^-} \right) = 0 \tag{2.96}$$

because, with regard to the scattering problems with penetrable bodies, there must not be free sources either inside the body or along the bordering surface S_i.

The equivalent currents are defined at both sides of the interface surface S_i

$$\vec{J}_{eq}^{\pm} = \hat{n}^{\pm} \times \vec{H}^{\pm}\big|_{\vec{r} \in S_i^{\pm}} \qquad \vec{M}_{eq}^{\pm} = -\hat{n}^{\pm} \times \vec{E}^{\pm}\big|_{\vec{r} \in S_i^{\pm}} \tag{2.97}$$

where $\vec{H}^+, \vec{E}^+$ and $\vec{H}^-, \vec{E}^-$ stand for the resulting field in each equivalent problem, respectively corresponding to the medium constants ε_+, μ_+ and ε_-, μ_-.

The previous expressions coincide with the boundary conditions along $S_i^{\pm}$ in the equivalent problem. The fields outside the corresponding region, $\vec{H}^{\mp}\big|_{\vec{r}\in S_i^{\pm}}$ and $\vec{E}^{\mp}\big|_{\vec{r}\in S_i^{\pm}}$, are assumed null -see Fig. 2.7-, which involves

$$\hat{n}^{\pm}\times\vec{H}^{\mp}\big|_{\vec{r}\in S_i^{\pm}}=0 \qquad \hat{n}^{\pm}\times\vec{E}^{\mp}\big|_{\vec{r}\in S_i^{\pm}}=0 \tag{2.98}$$

The resulting field is then straightforwardly obtained through the superposition of the solution for both equivalent problems (2.97) (2.98);

$$\begin{aligned}\vec{H}\big|_{\vec{r}\in S_i^{\pm}}&=\vec{H}^{\pm}\big|_{\vec{r}\in S_i^{\pm}}+\vec{H}^{\mp}\big|_{\vec{r}\in S_i^{\pm}}=\vec{H}^{\pm}\big|_{\vec{r}\in S_i^{\pm}}\\ \vec{E}\big|_{\vec{r}\in S_i^{\pm}}&=\vec{E}^{\pm}\big|_{\vec{r}\in S_i^{\pm}}+\vec{E}^{\mp}\big|_{\vec{r}\in S_i^{\pm}}=\vec{E}^{\pm}\big|_{\vec{r}\in S_i^{\pm}}\end{aligned} \tag{2.99}$$

If the equivalent currents at both sides are related as

$$\vec{J}_{eq}^{+}=-\vec{J}_{eq}^{-} \qquad \vec{M}_{eq}^{+}=-\vec{M}_{eq}^{-} \tag{2.100}$$

the addition of the boundary conditions for each of the equivalent problems in (2.97), taking into consideration (2.99), becomes equal to the real conditions (2.96). This proves that the problem is equally defined in the equivalent and in the real problem and that, consequently, the assumption for the fields outside the corresponding region in the equivalent problem to be zero is correct.

- **Definition of the system equations**

$\vec{J}_{eq}^{+},\vec{M}_{eq}^{+}$ or $\vec{J}_{eq}^{-},\vec{M}_{eq}^{-}$ -related through (2.100)- form indistinctly the unknowns of the problem, which is solved by the introduction of (2.64) in the boundary conditions of the original problem (2.96)[3]

$$\vec{n}^{+}\times\vec{H}_i\big|_{\vec{r}\in S_i}=-\vec{n}^{+}\times\left(\vec{H}^{S^+}\left(\vec{J}_{eq}^{\pm},\vec{M}_{eq}^{\pm}\right)-\vec{H}^{S^-}\left(\vec{J}_{eq}^{\pm},\vec{M}_{eq}^{\pm}\right)\right)\Big|_{\vec{r}\in S_i} \tag{2.101}$$

$$\vec{n}^{+}\times\vec{E}_i\big|_{\vec{r}\in S_i}=-\vec{n}^{+}\times\left(\vec{E}^{S^+}\left(\vec{J}_{eq}^{\pm},\vec{M}_{eq}^{\pm}\right)-\vec{E}^{S^-}\left(\vec{J}_{eq}^{\pm},\vec{M}_{eq}^{\pm}\right)\right)\Big|_{\vec{r}\in S_i} \tag{2.102}$$

or in the boundary conditions corresponding to the equivalent problem (2.97)

$$\vec{n}^{+}\times\vec{H}^{i}\big|_{\vec{r}\in S_i^{+}}=\vec{J}_{eq}^{+}-\vec{n}^{+}\times\vec{H}^{S^+}\left(\vec{J}_{eq}^{\pm},\vec{M}_{eq}^{\pm}\right)\Big|_{\vec{r}\in S_i^{+}} \tag{2.103}$$

$$0=\vec{J}_{eq}^{-}-\vec{n}^{-}\times\vec{H}^{S^-}\left(\vec{J}_{eq}^{\pm},\vec{M}_{eq}^{\pm}\right)\Big|_{\vec{r}\in S_i^{-}} \tag{2.104}$$

$$\vec{n}^{+}\times\vec{E}^{i}\big|_{\vec{r}\in S_i^{+}}=-\vec{M}_{eq}^{+}-\vec{n}^{+}\times\vec{E}^{S^+}\left(\vec{J}_{eq}^{\pm},\vec{M}_{eq}^{\pm}\right)\Big|_{\vec{r}\in S_i^{+}} \tag{2.105}$$

---

[3] As shown in detail later on, this operator is independent of setting the field point either in S_i^{+} or in S_i^{-} since that influence is cancelled in $\vec{H}^{S^+}-\vec{H}^{S^-}$ and $\vec{E}^{S^+}-\vec{E}^{S^-}$. That is why it is adopted $\vec{r}\in S_i$.

$$0 = -\vec{M}_{eq}^{-} - \vec{n}^{-} \times \vec{E}^{S^-}\left(\vec{J}_{eq}^{\pm}, \vec{M}_{eq}^{\pm}\right)\Big|_{\vec{r}\in S_i^-} \tag{2.106}$$

In all these equations, in accordance with the characteristics of the scattering problems, the source of the incident field is assumed in the outer medium -see Fig. 2.7-. Through the choice of two of these equations, one can establish three formulations to determine the unknowns $\vec{J}_{eq}^{\pm}, \vec{M}_{eq}^{\pm}$.

(2.101) and (2.102) is the explicit formulation for the Boundary equations, which are better known all over the literature as PMCHW formulation since it was originally developed by Poggio, Miller, Chang, Harrington and Wu [7][8][31]. This formulation is consistent because the magnetic and the electric field boundary conditions are directly enforced. Strictly speaking this approach must not be understood as the decomposition into two equivalent problems, one for each region; indeed, this approach does not compel any field to be null in any part of the medium. That is why the equivalent currents do not appear explicitly in the field boundary conditions-(2.101) and (2.102)-. They are of course implicitly assumed in the integral expression of the fields.

(2.103) and (2.104) correspond to the EFIE and (2.105) and (2.106) represent the MFIE in the dielectric case. The definition of these systems is consistent because from the addition of each pair of equations, one accomplishes respectively the electric and the magnetic field boundary conditions. The other boundary condition, though explicitly not imposed, it is accomplished implicitly through the current definition.

The system of equations coming from the choice of (2.103) and (2.105) or (2.104) and (2.106) is erroneous since none of the boundary conditions is accomplished. This means that the electric and the magnetic fields are badly defined and hence the assumption for the field to be zero outside the corresponding region cannot be accomplished.

Some authors have suggested [15] to pose the integral equations by setting the boundary conditions outside the corresponding region, (2.98); that is

$$\vec{n}^{-} \times \vec{H}^{i}\Big|_{\vec{r}\in S_i^-} = -\vec{n}^{-} \times \vec{H}^{S^+}\left(\vec{J}_{eq}^{\pm}, \vec{M}_{eq}^{\pm}\right)\Big|_{\vec{r}\in S_i^-} \tag{2.107}$$

$$0 = \vec{n}^{+} \times \vec{H}^{S^-}\left(\vec{J}_{eq}^{\pm}, \vec{M}_{eq}^{\pm}\right)\Big|_{\vec{r}\in S_i^+} \tag{2.108}$$

$$\vec{n}^{-} \times \vec{E}^{i}\Big|_{\vec{r}\in S_i^-} = -\vec{n}^{+} \times \vec{E}^{S^+}\left(\vec{J}_{eq}^{\pm}, \vec{M}_{eq}^{\pm}\right)\Big|_{\vec{r}\in S_i^-} \tag{2.109}$$

$$0 = \vec{n}^{+} \times \vec{E}^{S^-}\left(\vec{J}_{eq}^{\pm}, \vec{M}_{eq}^{\pm}\right)\Big|_{\vec{r}\in S_i^+} \tag{2.110}$$

which, in analogous terms as expounded for the PeC case, correspond to the same expressions of (2.103) (2.104) (2.105) (2.106).

The duality properties of the Maxwell equations enable $\vec{E}^{S^\pm}\left(\vec{J}_{eq}^{\pm}, \vec{M}_{eq}^{\pm}\right)$ and $\vec{H}^{S^\pm}\left(\vec{J}_{eq}^{\pm}, \vec{M}_{eq}^{\pm}\right)$ to be derived from the PeC-operators. Indeed, (2.44) and (2.62) lead to

$$\vec{E}^{S^{\pm}}(\vec{J},\vec{M}) = \vec{E}^{S}_{PeC}{}^{\pm}(\vec{J}) - \vec{H}^{S}_{PeC}{}^{\pm}(\vec{M})$$
$$\vec{H}^{S^{\pm}}(\vec{J},\vec{M}) = \vec{H}^{S}_{PeC}{}^{\pm}(\vec{J}) + \frac{1}{\eta^2}\vec{E}^{S}_{PeC}{}^{\pm}(\vec{M}) \qquad (2.111)$$

2.6.2.3 Structure composed of PeC and Penetrable regions

This problem is solved through the application of the Equivalence theorem applied to each of the interface regions -see Fig. 2.8-, in agreement with the simpler cases presented in 2.6.2.1 and 2.6.2.2 -see Fig. 2.3 and Fig. 2.7-. There must be, though, compatibility between the Equivalence theorem approach chosen for each simple problem so as to let the field consistently defined. Therefore, by applying the EFIE or the MFIE on each simple problem one ensures respectively the electric or the magnetic field boundary condition over all the interface surfaces of the structure. Similarly, the use of the PMCHW formulation for each simpler problem ensures that both boundary conditions are accomplished in the original problem. In this case, for the interfaces bordering on PeC regions, the PMCHW derives indistinctly either in the EFIE or in the MFIE, which result in the so-called E-PMCHW or H-PMCHW formulations.

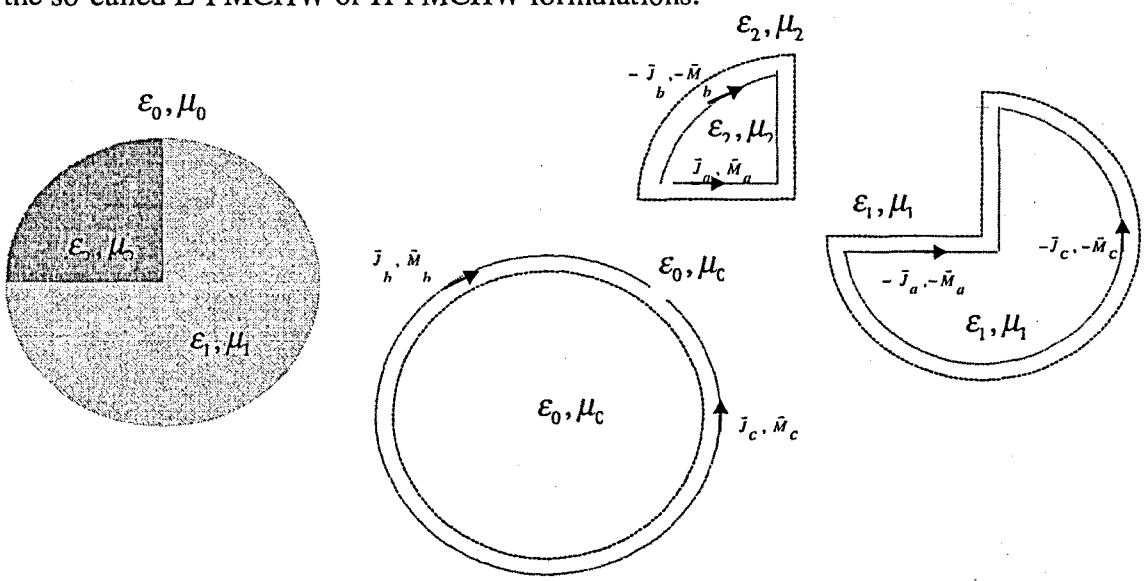

Fig. 2.8 Equivalent problem for a complex dielectric structure with three regions

Depending on the number of regions that shape the interface surfaces, one can sort out the diffraction problems as:

- **Two regions shaping the interface surfaces**

  A typical case is a group of disjoint objects -Fig. 2.9-. The equivalent problem assigned to the outer region can be treated in an analogous way as with a single body by placing some fictitious contours S_{ij} to join together the whole set of bodies.

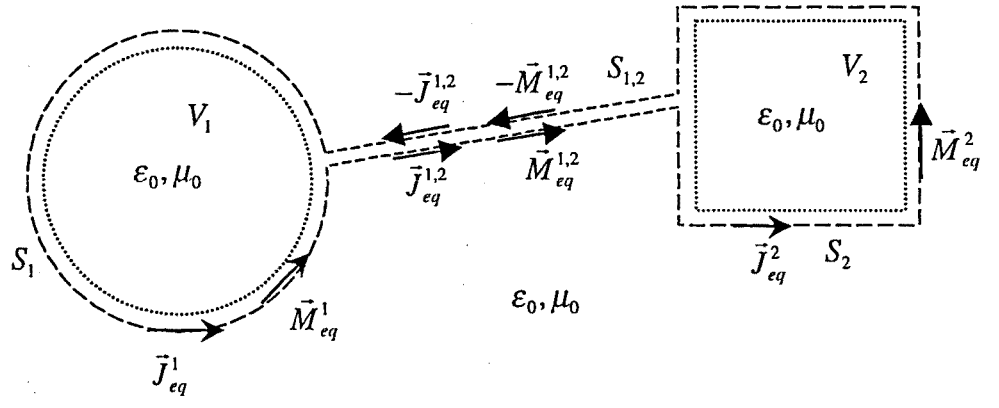

Fig. 2.9 Equivalent problem for the outer region for two single bodies

One can hence consider the new equivalent structure as a unique body, with an enclosing surface $S = \bigcup_{i=1..N} S_i \cup \bigcup_{i=1..N} S_{i,\mathrm{mod}(i,N)+1}$. These arbitrary fictitious contours $\bigcup_{i=1..N} S_{i,\mathrm{mod}(i,N)+1}$ do not contribute to the integral expressions since the currents placed at each side cancel each other because of the continuity of the fields -see Fig. 2.9-. Therefore, one can practically set $S = \bigcup_{i=1..N} S_i$ and apply the study described in the sections 2.6.2.1 and 2.6.2.2 as though the surface was really closed.

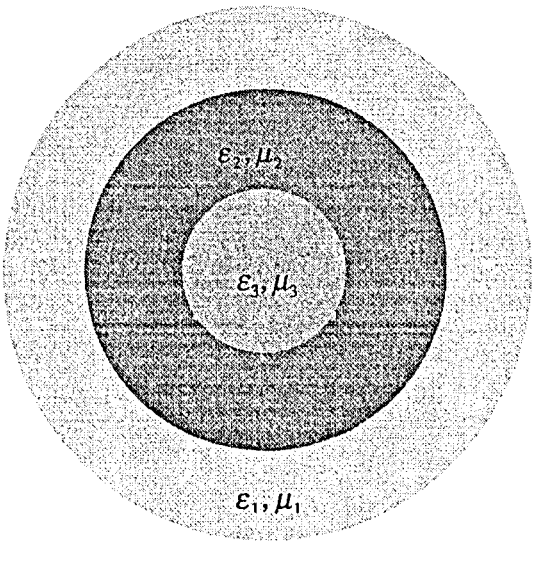

Fig. 2.10 Dielectric body with three dielectric layers

Another important case is that of layered bodies -see Fig. 2.10 -. They represent, as a matter of fact, the generalisation to several layers of the homogeneous case, which involves only one layer. A very typical case is that of a conducting core surrounded by a dielectric layer, so-called *coatedPeC.*

- **More than two regions shaping the interface surfaces**

  This is a very general case that includes most of structures. A very important one is that of patched or composite antennas, such as the microstrip antennas -see Fig. 2.11-, which are very widely used.

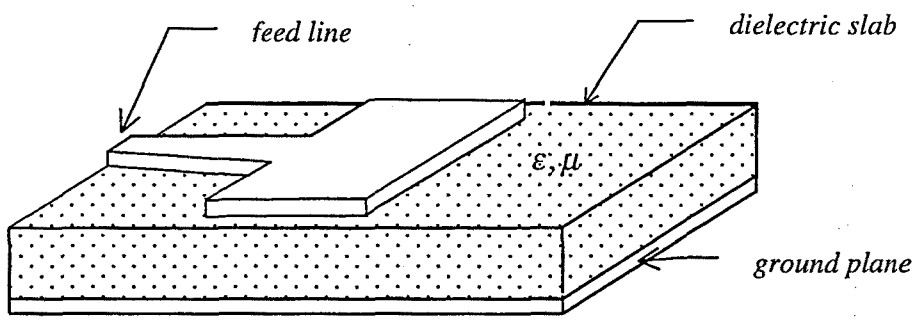

Fig. 2.11 Microstrip patch antenna over a finite ground plane

2.7 RECIPROCITY THEOREM

For a linear and isotropic medium with two groups of sources $\vec{J}^a$, $\vec{M}^a$ and $\vec{J}^b$, $\vec{M}^b$, the Reciprocity theorem relates the sources at one point with the fields produced by the other sources in that point,

$$\iiint_{V'}\left(\vec{E}\left(\vec{J}^a,\vec{M}^a\right)\cdot\vec{J}^b-\vec{H}\left(\vec{J}^a,\vec{M}^a\right)\cdot\vec{M}^b\right)dv'=\iiint_{V'}\left(\vec{E}\left(\vec{J}^b,\vec{M}^b\right)\cdot\vec{J}^a-\vec{H}\left(\vec{J}^b,\vec{M}^b\right)\cdot\vec{M}^a\right)dv' \qquad (2.112)$$

where V' is a volume including all the sources.

(2.112) is an expression with much physical sense, because it is only accomplished whenever the sources are physical and the fields are really electromagnetic. It will be mentioned along this dissertation Thesis to bring up the physical essence associated to some mathematical expressions.

2.8 NUMERICAL METHODS

One can exactly solve the Maxwell equations specifically for some canonical problems, such as the electromagnetic diffraction along spheres, ellipsoids or infinite cylinders, or the modal solutions for rectangular or cylindrical wave-guides. In these cases the application of the boundary conditions is effectuated over surfaces with some constant coordinate along which the wave equation is separable. For the large majority of problems, though, one cannot achieve an analytical expression for the solution. It is hence required to discretize the Maxwell equations -or other equations derived- so as to obtain a numerical solution. The ordinary steps in any numerical technique can be briefly highlighted below [5].

2.8.1 Analytical formulation of the Electromagnetic problem

Any of the ruling functional equations presented can be chosen to solve the electromagnetic problem. According to the domain, the formulation can be time-dependent or frequency-dependent. According to the nature of the operator, they can be differential, such as the wave equations (section 2.4) or integral, such as the theorem of equivalence (section 2.6). Particularly, this dissertation Thesis focuses on *frequency domain integral methods.*

One can also adapt the Maxwell equations to electrically large enough problems by modelling the electromagnetic behaviour through well-known high-frequency properties; for example, the optical physics theory, appropriate for large smooth-varying surfaces, or the use of predefined wires to model the radiation of zones bordering edges. These so-called high-frequency methods, that provide for the lack of computational resources of the ordinary lower-frequency techniques when increasing the electrical dimensions, are beyond the scope of this study. The size of the examples analysed along this dissertation Thesis, are on the order of the wavelength, inside the range commonly called the resonance region.

2.8.2 Discretization of the problem

The discretization of the functional equations is required to transform the functional domain into the numerical domain, which is manageable by computers. Therefore, one turns the functional equations into algebraic equations of finite dimension; that is, a matrix.

The general expression for a functional equation can be

$$Y = \Im(X) \tag{2.113}$$

where X stands for the unknown and Y, the independent term, relies on the excitation of the problem. According to the vector space theory, Y and X belong respectively to the rank and domain spaces of the operator $\Im$ and have to be discretized to build the new operator.

The domain magnitude for the differential operators, as shown in 2.4, is the field -$\vec{E}, \vec{H}$-. The integral operators, as shown in 2.5, make use of the equivalent currents, which are in any case univocally related with the currents and density charges be it in the surface formulation -$\hat{n}\times\vec{E}$, $\hat{n}\cdot\vec{E}$, $\hat{n}\times\vec{H}$, $\hat{n}\cdot\vec{H}$ - or in the volume formulation. Moreover, the functional equation in (2.113) is built in accordance with the boundary conditions.

2.8.2.1 Discretization of the unknown

According to the nature of the problem, the unknown is expanded accordingly in terms of a determined set of basis functions $\{x_n\}$, the so-called *Expanding Functions*

$$X \cong X_N = \sum_{n=1..N} a_n x_n \tag{2.114}$$

For particular cases of well-definite domains where the shape of the current is known in advance, one can define x_n over the whole domain of the operator; for example, the use of harmonic functions to expand the ϕ-variation on bodies with symmetry of revolution.

For an arbitrary domain, the expansion of x_n is carried out over elementary portions, so-called subdomains, which are interconnected to form the whole space. This work focuses on low-order expansions, whereby the electrical dimensions of the subdomains must be around $\lambda/10$ at the most. Three wide groups of functions can be presented depending on the part of the space where the unknown is expanded.

- ***Node-based finite elements***

  From the unknown placed at each node of the domain -previously meshed-, one interpolates the values, according to a predetermined rule (linear, parabolic), over the whole space. Hence, the characteristics of the current are not locally fixed in advance; on the contrary, the current and field properties rely merely on the use of an adequate electromagnetic operator, which must provide them implicitly. The interpolating subdomains, so-called *elements*, can be, depending on the shape of the domain, wire-shaped, triangular, rectangular. In Fig. 2.12, linear and parabolic triangular node-based finite elements are shown. In Chapter 6 it will be presented an improvement on the computation of the RCS resorting to the definition of nodal parabolic elements.

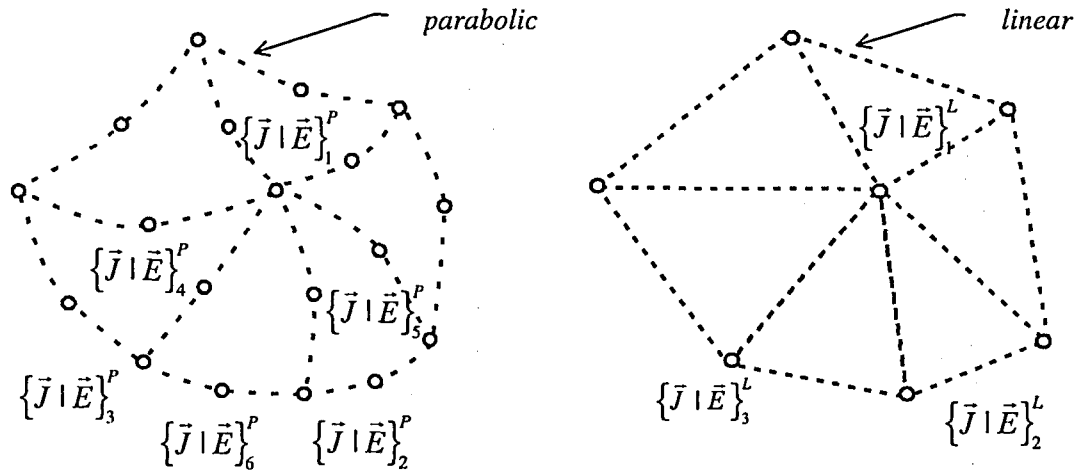

Fig. 2.12 Node-based finite elements on triangular facets

This approach embraces a very versatile group of functions; indeed, the characteristic of the operator can be differential or integral, the formulation can be superficial or volumetric and there are no constraints for the type of magnitude, field or current, to expand.

With regard to the scope of this dissertation Thesis, surface integral operators, the Finite elements version is the *Boundary Elements Method*; Marc S. Ingber and Randolph H. Ott [22] have developed a PeC-MFIE formulation with $\vec{J}$ as interpolated magnitude. Nuria Duffo [6] developed a formulation for dielectrics where the adopted interpolated magnitudes are the fields $\vec{E}$ and $\vec{H}$.

♦ *Patch-based* functions

The expansion of the current is carried out inside the subdomain; that is, the patch. The magnitudes over the junctions between patches, such as wire-currents or linear charges in a surface formulation[4], cannot be thus expanded. The patch-based functions are assumed zero over the junctions, which in any case is irrelevant with regard to the construction of the integral operators. Indeed, for surface integral operators, the excluded edges and vertices have null surface[5]. However, it is required through the good definition of the operator to ensure the differential characteristics across the junctions for the expanded physical magnitudes field and current. A thorough study will be provided in Chapter 6 for the 3D PeC-operators. The patch-based functions are chosen in this dissertation Thesis to develop the electromagnetic operators.

In 2D problems, or 3D problems with symmetry of revolution, the discretization is carried out along one dimension, which is the generating arc of the infinite cylinder or the body of revolution. The most used patches are pulses with rectangular or triangular shape -see Fig. 2.13-. For 3D problems with flat surfaces, such as strips, one can use 2D rectangular pulses or roof-top functions [13] -see Fig. 2.13 -.

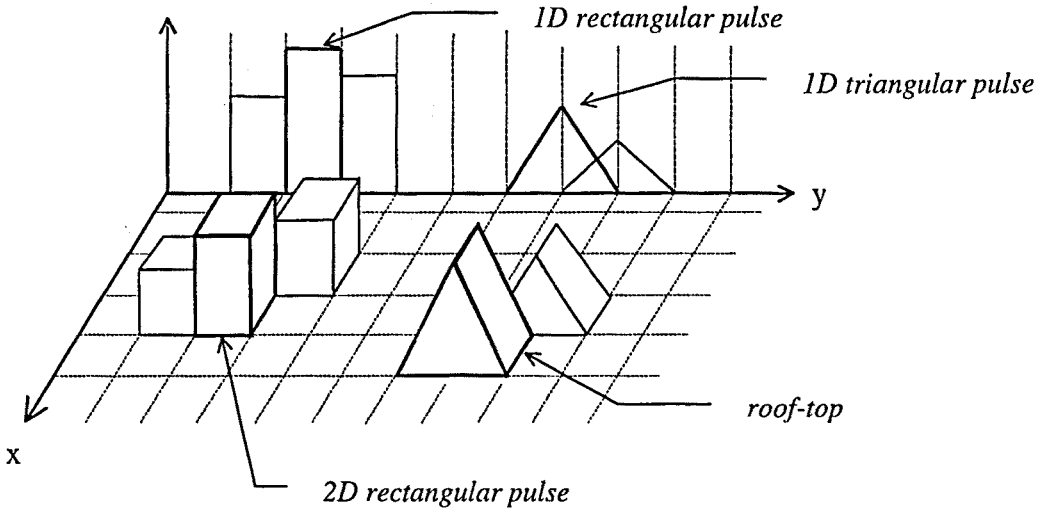

Fig. 2.13 Patch-based basis functions for problems of one or two dimensions

A very widespread set of functions is the *Rao, Glisson* and *Wilton* triangles [28], so-called *RWG* -see Fig. 2.14-, which ensure the normal component of the expanded magnitude to be continuous across the edges. The particular characteristics of *RWG* are shown in Chapter 6 because they are used to expand the surface current over 3D bodies. B. M. Kolundzija and B. D. Popovic have developed [14] expanding functions relying on rectangular patches enforcing as well the continuity of the normal component through the edges.

There are also patch-based functions that ensure the tangential component of the expanded magnitude to be continuous across the edges. An example is presented in Chapter 6, the *unxRWG* functions, called so in this work because they come from the cross product of the normal vector to the surface with *RWG*.

[4] planar currents or surface charge densities in volume formulations
[5] Analogously, for volume formulations the junctions are surfaces, which present null volume.

All these patch-based functions effectuate low-order expansions. For example, linear for *RWG*, *unxRWG* or roof-top and constant for the rectangular pulses.

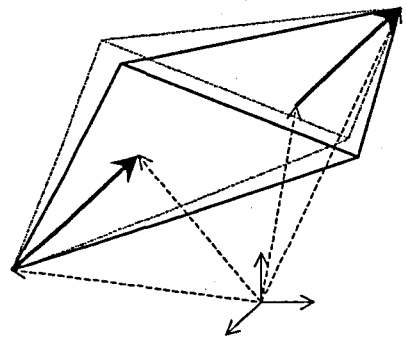

Fig. 2.14 RWG basis functions

In general, the patch-based functions ensure the charge throughout the surface to be null through the local enforcement over a reduced part of the domain, whose size depends on the simplicity of the chosen patch. That is, in 2D basis functions and in *unxRWG*, the charge condition is accomplished over each patch, in *RWG*, over each pair of triangles sharing an edge and for the Kolundzija's quadrangular functions, over even bigger structures of patches.

It is very important to note that this group of functions is often presented in the literature as *Vector Finite elements* [33][34][35]. They are named so because they turn out better to simulate vector electromagnetic fields than the *Node-based Finite elements*, which are suitable for modelling scalar quantities [34]. However, in this work it has been preferred the name *patch-based* because it alludes explicitly the fact that the magnitude can only be expanded over the patches but not over the junctions.

- ***Wire-based* functions**

In surface formulations, these functions undertake the expansion of the current only over the edges, which is a portion of the space that the patch-based functions ignore. This method has turned out appropriate to some extent for computing far-field parameters but, when compared with the other methods, it becomes less accurate for near-field magnitudes.

2.8.2.2 Discretization of the boundary conditions

In all problems regarding antenna radiation or scattering, one region must necessarily be the free space. This involves that the solution inside this region must accomplish the Sommerfeld radiation condition so that the fields propagating from the source to the infinite conserve the total power of the wave front. The integral methods allow implicitly for this fact since the Green's function accomplishes this condition. The differential methods, though, as it is unfeasible the meshing of the whole outer space, have to provide some special *radiation boundary conditions* throughout the end enclosing surface to make up for the required truncation of the space.

Furthermore, one has to apply the boundary conditions along the surface interfaces. Since the boundary conditions can only be imposed exactly over canonical shapes, one has to discretize the enclosing surfaces of the bodies. Being the modelling of solids a complex area, one usually associates, for the sake of convenience, the discretization of the geometry with the discretization of the unknown 2.8.2.1. However, in general terms it does not have to be necessarily so; indeed, the node-based finite elements tools can be used to model the enclosing surface and the unknown with a different order of interpolation, N_g and N_f

$$\vec{r} = \sum_{i=1}^{N_g} \phi_i \vec{r}_i \qquad \left\{\vec{J} \mid \vec{E}\right\} = \sum_{i=1}^{N_f} \phi_i \left\{\vec{J} \mid \vec{E}\right\}_i \tag{2.115}$$

where the three cases, $N_g = N_f$, $N_g > N_f$ and $N_g < N_f$, are possible and correspond respectively to the *isoparametric*, *superparametric* and *subparametric* node-based finite elements approaches.

One defines the residue, $R(\vec{r})$, as the difference between the theoretical -$Y(\vec{r})$, (2.113)- and the computed contribution $Y_N = \Im(X_N)$ to the boundary conditions; that is,

$$R(\vec{r}) = Y(\vec{r}) - Y_N(\vec{r}) \tag{2.116}$$

where $\vec{r} \in S$. In general, the imposition of the boundary conditions can be approximately undertaken over the model of the surface by forcing the residue to be null through the inner-product with a set of functions, so-called *Weighting functions*, $\vec{w}_m$.

$$\int_S R(\vec{r}) \cdot \vec{w}_m dS = 0 \qquad m = 1..M \tag{2.117}$$

This sets the definition of the *Weighted Residues Method*, which is widely better known as the *Method of Moments (MoM)* [3][36]. The proper behaviour of this method relies much on the right choice of $\vec{w}_m$. Since all the integral developments presented along this dissertation Thesis focus on the MoM, a thorough insight is given in 2.9.

A particular approach, derived from the MoM by setting $\vec{w}_m = \partial(\vec{r} - \vec{r}_m)$, is the *point-matching* method, which imposes the boundary conditions exactly over a finite set of points $\vec{r}_m$ from the surface model. One can also assume *point-matching* whenever the MoM field integration is numerically undertaken with one point.

2.8.3 The solution of the problem. Matrix inversion

Through the combination of the procedures presented in 2.8.2.1 and in 2.8.2.2, that eventually rule the discretization of the domain and rank spaces of the operator $\Im$, one turns the original functional equation in (2.113) into a matrix equation

$$[Y_m] = [Z_{mn}] \cdot [X_n] \qquad n = 1..N, m = 1..M \tag{2.118}$$

where the normal case in a well-determined linear system yields $N = M$ [6].

The problem must then be solved through the inversion of the matrix $[Z_{mn}]$, which can be in general routinely carried out through the well-known Gauss inverting techniques. Some complementary methods must be taken into account, though, for some specific cases.

2.8.3.1 Iterative methods

Unlike the differential methods, which result in sparse matrices, the integral methods always lead to full matrices. This represents a drawback since the inverting time is dependent on the number of non-null elements per row N as $t_{inv}=O(N^3)$. For big matrices, the Gauss procedure becomes too demanding with regard to the computational resources. In this case, one can alternatively reach $[Y_m]$ through iterative techniques, which lead to the solution more quickly for dimensionally big matrices. As it will be shown in Chapter 9, one develops along with the iterative techniques efficient computational methods for bodies with big enough electrical dimensions.

When $[Z_{mn}]$ is positive defined, one can apply the *conjugate gradient method*[7], which ensures the convergence. Another technique is the *biconjugate gradient method*, which, although it does not ensure the convergence, it reaches a reasonable value with less steps of iteration for any type of matrix.

2.8.3.2 Preconditioning

When ω is near a resonance frequency ω_r of the cavity inside the scattering body, the solution is not unique anymore since the solutions of the Maxwell equations without the excitation appear. These solutions are exclusively dependent on the characteristics of the geometry.

The consequent matricial system is ill-defined because $[Z_{mn}]$ is very close to be singular -it is actually singular when $\omega = \omega_r$-. Since $[Z_{mn}]$ is very difficult to invert precisely -the determinant of the matrix is very close to zero-, the computation of the matrix must be effectuated with a very high precision, which, in practice, relies much on the numerical precision of the computer for the real types. As the EFIE and the MFIE present different resonance frequencies, one can theoretically solve this problem for each integral operator by defining a new operator, so-called *Combined Field Integral Equation (CFIE)*, coming from the linear combination of the fundamental EFIE and MFIE.

The Bauer-Fike's theorem states that when solving $Aa = b$, the relative error at the input and at the output, that may allow for some lack of precision, is related by

---

[6] if $M > N$, the system is overdetermined and, in general, does not have an exact solution that makes the residue zero; the Least squares solution renders a minimum value for $\|R\|$.

[7] The conjugate gradient method can be applied by premultiplying the system by the transpose conjugate of the matrix, which lets the resulting matrix positive defined.

$$\frac{\|\Delta a\|}{\|a\|} \leq \kappa \frac{\|\Delta b\|}{\|b\|} \tag{2.119}$$

where κ stands for the condition number

$$\kappa = \|A\|\|A^{-1}\| \tag{2.120}$$

In (2.119), one sees that Δa is small as long as κ is small, from which it can be inferred that the fact of κ being small is a sufficient condition to let the system well-defined. If, on the contrary, κ is high, one can not tell much about the value of Δa since κ represents a high bound in (2.119). Hence, the condition number in any case can stand for a measure of the ambiguity of the solution. A well-known consequence of this is the increase in the number of steps for the inverting iterative algorithms to converge.

One can fasten the rate of convergence by improving the conditioning for a system $Aa = b$. This is very often effectuated by multiplying the system by an appropriate matrix, typically the inverse matrix of a matrix $\tilde{A}$ that resembles A but that is easy to invert because its condition number is lower

$$\left(\tilde{A}^{-1} \cdot A\right)a = \tilde{A}^{-1}b \tag{2.121}$$

if A is a positive defined matrix, one can use the eigenvalues matrix as $\tilde{A}$. In general, one obtains $\tilde{A}$ by inserting smartly zeros in A. This tool, so-called *preconditioning*, is very helpful to invert nearly singular systems or systems with a considerable value for the condition number. The iterative inverting methods are usually programmed together with this tool to improve the time of convergence.

2.9 METHOD OF MOMENTS

The MoM [3][36] is the ruling approach adopted along this dissertation Thesis to develop the integral operators. As mentioned in 2.8.2.2, the expression for the matrix yields

$$Z_{mn} = \int_S \vec{w}_m \cdot \Im(\vec{x}_n) dS \qquad n,m = 1..N \tag{2.122}$$

where $\vec{w}_m$, $\vec{x}_n$ stand for the Weighting and Expanding functions and $\Im$ is the integral operator, typically $\vec{H}^S_{PeC}$ or $\vec{E}^S_{PeC}$, from which the rest of the operators derive. One can equivalently express (2.122) as

$$Z_{mn} = \left\langle \vec{w}_m, \Im(\vec{x}_n) \right\rangle \qquad n,m = 1..N \tag{2.123}$$

where $\langle , \rangle = \int (\ )^* (\ ) dS$ stands for the well-known definition of the inner-product associated to the square-integrable space.

One can understand physically the matrix elements Z_{mn} as the mutual impedance between the elementary current distributions $\vec{w}_m$ and $\vec{x}_n$.

2.9.1 Requirements for the expanding and weighting functions

The right choice of $\vec{w}_m$ and $\vec{x}_n$ ensures the good behaviour of the system. The two fundamental ruling properties are listed below [5].

1. $\{\vec{x}_n\}$ must form a complete basis of the domain of the operator $\Im$. In this work, the equivalent currents -$\vec{J}$,$\vec{M}$ - are taken as domain magnitudes. Therefore, according to the charge conservation principle throughout the surface of the scatterer, the expanding functions must stand for

$$Q_T = \sum_{n=1..N} q_n = \sum_{n=1..N} c_n \int_{S_n} \nabla \cdot \vec{x}_n dS = 0 \tag{2.124}$$

which can only be accomplished, irrespective of the current coefficients c_n, by enforcing $\forall n$

$$\int_S \nabla \cdot \vec{x}_n dS = 0 \tag{2.125}$$

which is thus required for the correct definition of the patch-based expanding functions.

2. $\{\vec{w}_m\}$ must form a complete basis in the rank of the operator $\Im$ [37][38]. A sufficient condition for this is to form a complete basis along the domain of the adjoint operator $\Im^a$; that is,

$$\langle \vec{w}_m, \Im(\vec{x}_n) \rangle = \langle \Im^a(\vec{w}_m), \vec{x}_n \rangle = \langle \vec{x}_n, \Im^a(\vec{w}_m) \rangle^* \tag{2.126}$$

Of course, the worst choice for $\{\vec{w}_m\}$ is that of being orthogonal to $\Im(\vec{x}_n)$, which causes $Z_{mn} = 0$.

The rank space of the integral operators are the electromagnetic fields, which have to accomplish the boundary conditions. This will be used in Chapters 6 and 7 to confirm and to dismiss the use of some particular MoM-operators.

Keeping in mind the aforementioned requirements, one can determine the conditions for the good behaviour of the two widely spread MoM-formulations.

- **Galerkin**

It is characterised by the choice of the same set as Weighting and Expanding functions

$$\vec{w}_i = \vec{x}_i \qquad i = 1..N \tag{2.127}$$

If the operator is self-adjoint $-\Im^a = \Im$- the above-presented condition 2 is automatically accomplished as long as the expanding functions form a complete basis of the domain of $\Im$. The resulting matrix in this case is hermitian

$$Z_{mn} = \langle \vec{x}_m, \Im(\vec{x}_n) \rangle = \langle \Im^a(\vec{x}_m), \vec{x}_n \rangle = \langle \vec{x}_n, \Im^a(\vec{x}_m) \rangle^* = \langle \vec{x}_n, \Im(\vec{x}_m) \rangle^* = Z_{nm}^* \qquad (2.128)$$

♦ Least squares (LSQ)

The aim of the MoM is to make the residue zero

$$\langle \vec{w}_m, R \rangle = \langle \vec{w}_m, Y - Y_N \rangle = \left\langle \vec{w}_m, Y - \sum_{n=1..N} c_n \Im(\vec{x}_n) \right\rangle = 0 \qquad m = 1..N \qquad (2.129)$$

Moreover, as it is well-known from the vector theory, the error is minimum if $R \perp Y_N \Rightarrow R \perp \sum_{n=1..N} c_n \Im(\vec{x}_n) \Rightarrow R \perp \Im(\vec{x}_n)$. The LSQ approach defines the Weighting functions accordingly as

$$\vec{w}_i = \Im(\vec{x}_i) \qquad i = 1..N \qquad (2.130)$$

This approach is thus best because the previous condition 2 is accomplished by definition. However, this technique is seldom used since it is normally very difficult to obtain an analytical expression for the Weighting functions.

In view of (2.130), the LSQ weighting in (2.129) can be equivalently expressed as

$$\left\langle \vec{x}_m, \Im^a Y - \sum_{n=1..N} c_n \Im^a \Im(\vec{x}_n) \right\rangle = 0 \qquad m = 1..N \qquad (2.131)$$

which represents a Galerkin approach.

Chapter 3 METHOD OF MOMENTS ON PEC BODIES OF REVOLUTION

3.1 INTRODUCTION

The problem of electromagnetic radiation and scattering due to bodies with rotational symmetry was first treated by Mautz and Harrington [18]. They developed a MoM technique by expanding the current as a Fourier series. Because of the orthogonality between the modes, the matrix inversion could be effectuated independently for each mode. Furthermore, since only the contour was discretized, the number of unknowns decreased. As usual in MoM techniques, Mautz and Harrington used patch-based expanding functions periodically expanded along the azimuth direction; that is, annuli. They developed the EFIE operator for perfectly conducting -PeC- bodies.

Over the years, different authors have also worked in this subject in accordance with the original Mautz and Harrington's idea. Te-Kao Wu and Leonard L. Tsai [31] and L.N. Medgyesi-Mitschang and C. Eftimiu [19][20] developed other formulations, such as PMCHW (homogeneous dielectric bodies) and E-PMCHW (coated PeC bodies), according to the original triangular-shaped expanding functions. In 1980, Wilton and Glisson [13] obtained good results for PeC (EFIE) and Dielectric bodies (PMCHW) through the substitution of the Mautz and Harrington's triangular patches by rectangular pulses. In 1990, Stephen D. Gedney and Raj Mittra [12] improved the previous techniques for PeC bodies by using the rectangular pulse formulation from Wilton and Glisson and fast integrating along the ϕ direction by means of the Fast Fourier Transform (FFT).

The aim of this chapter has been firstly to implement the Gedney and Mittra's PeC-EFIE formulation for bodies of revolution (BoR). Secondly, the PeC-MFIE operator has been developed by assuming the general concepts presented over the years about the BoR PeC-EFIE operator. So as to allow for a later extension to dielectrics, the conception of Gedney and Mittra -FFT and recurrence formula- has been chosen to build the new PeC-MFIE operator. At last, all the possible Dielectric formulations have been considered and, after dismissing the EFIE and the MFIE, one has programmed the PMCHW operator -from the combination of PeC-EFIE and PeC-MFIE- for homogeneous dielectric and coated PeC bodies, consistent with the up-to-date literature. One has analysed in detail why the PeC-MFIE operator, even considering the same aspects as with the PeC-EFIE operator, has never worked with the MoM techniques -to my knowledge, nothing has ever been published-. In any case, some improvements are shown. The reach of validity of the PMCHW operator has also been considered.

3.1.1 Expanding functions

The key aspect in all the MoM-BoR formulation is the expansion of the current in terms of the Fourier series. This enables the electromagnetic operator to be solved independently for each mode. Thanks to the orthogonality of the expanding functions, the current coefficients must only be computed along the generating arc for each mode -see Fig. 3.1-.

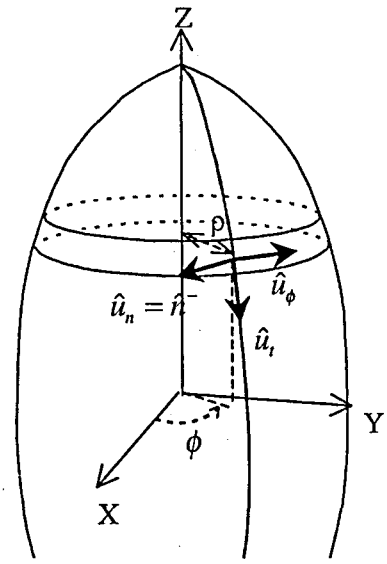

Fig. 3.1 Local coordinates over each segment along the generating arc

One can thus reach the solution for electrically bigger structures, which otherwise, through the ordinary MoM approach -with a general 3D oriented discretization- might be unfeasible with regard to the computation time and the memory resources. On the other hand, in the BoR-MoM more accuracy on the electromagnetic operators is required. Indeed, the source integration may be effectuated over annuli of considerable perimeter -with bigger size than the wavelength- and a different matrix to be inverted appears for each mode -the numeric conditions that rule their accuracy may not be the same-.

The current expansion in terms of the m modes yields:

$$\vec{J}(t,\phi) \cong \sum_{m=-M}^{m=+M} \vec{J}_m(t,\phi) \tag{3.1}$$

where $\vec{J}_m(t,\phi)$ is discretized along the generating arc and expanded in terms of two perpendicular components $\hat{u}_t$ and $\hat{u}_\phi$ at any point of the surface.

$$\vec{J}_m(t,\phi) \cong \left(\sum_{j=1}^{N_t} I^t_{mj} \hat{u}_t b^t_j(t) + \sum_{j=1}^{N_\phi} I^\phi_{mj} \hat{u}_\phi b^\phi_j(t) \right) e^{jm\phi} \tag{3.2}$$

where I^t_{mj} and I^ϕ_{mj} stand for the current coefficients in t and ϕ for each mode and N_t, N_ϕ, the number of segments over the contour for both directions; b^ϕ_j and b^t_j determine the shape of the expanding functions for both components on each segment along the generating arc.

3.1.2 Weighting functions

The weighting functions -inherent to the MoM- are analogously chosen because there is also periodicity over ϕ in the rank space. Therefore, through the discretization of the generating contour and by azimuthally expanding the functions, the weighting functions keep defined over each point of the geometry. Being p the mode number and q the arc segment or body annulus considered, we have

$$\begin{aligned}\left[\vec{W}^t(t,\phi)\right]^{pq} &= \hat{u}_t w^t_q(t) e^{-jp\phi} \quad q=1..N_t,\ p=-M..M \\ \left[\vec{W}^\phi(t,\phi)\right]^{pq} &= \hat{u}_\phi w^\phi_q(t) e^{-jp\phi} \quad q=1..N_\phi,\ p=-M..M\end{aligned} \tag{3.3}$$

where w^ϕ_j and w^t_j are the contour facets of the weighting functions. Since only first order interpolating methods are considered, which is the scope in this dissertation Thesis, they can be either rectangular, $\Pi(t,\Delta_1,\Delta_2)/\rho$, or triangular, $\Lambda(t,\Delta_1,\Delta_2)/\rho$, patches:

$$\Pi(t,\Delta_1,\Delta_2) = \begin{cases} 1 & -\Delta_1 \le t \le \Delta_2 \\ 0 & otherwise \end{cases}$$

$$\Lambda(t,\Delta_1,\Delta_2) = \begin{cases} 1-\dfrac{t}{\Delta_2} & 0 < t \le \Delta_2 \\ 1+\dfrac{t}{\Delta_1} & -\Delta_1 \le t < 0 \\ 0 & otherwise \end{cases} \tag{3.4}$$

and Δ_1, Δ_2 denote the left and right half-lengths of the pulse.

3.1.3 Matrix elements

3.1.3.1 Impedance elements corresponding to $\left(\vec{A}\,|\,\vec{F}\right), \nabla\times\left(\vec{A}\,|\,\vec{F}\right)$

The application of the set of expanding functions of (3.1) in the vector potential operators and the inner-product with the q annulus weighting function for any weighting-expanding functions components pair combination $\{\phi,t\}-\{\phi',t'\}$ can be ultimately expressed as

$$\left\langle \left[\vec{W}^{\{t,\phi\}}\right]^{pq}, \vec{S}^{\{t',\phi'\}} \right\rangle = \iint_{t\phi} \left[\vec{W}^{\{t,\phi\}}\right]^{pq}(t,\phi) \iint_{t',\phi'} K(t,t'/\phi,\phi')\vec{J}^{\{t',\phi'\}}(t',\phi')dS'$$

$$= \iint_{t,\phi} \hat{u}_{\{t,\phi\}} w_q^{\{t,\phi\}}(t) e^{-jp\phi} \iint_{t',\phi'} \left(K(t,t'/\phi,\phi') \sum_{m=-M}^{m=+M} \vec{J}_m^{\{t',\phi'\}}(t',\phi') e^{jm\phi'} \right) dS'dS \tag{3.5}$$

$$= \sum_{m=-M}^{m=+M} \sum_{j=1}^{N_{\{t',\phi'\}}} \left[I_{mj}^{\{t',\phi'\}} \iint_{t,\phi} \iint_{t',\phi'} \left\{ K\hat{u}_{\{t,\phi\}}\hat{u}_{\{t',\phi'\}} \right\}(t,t'/\phi,\phi') w_q^{\{t,\phi\}}(t) b_j^{\{t',\phi'\}}(t') e^{j(m\phi'-p\phi)} dS'dS \right]$$

for all the chosen modes $p \in \{-M..M\}$.

In $\left(\vec{A} \mid \vec{F}\right)$-PeC-EFIE-, the Kernel $K(t,t'/\phi,\phi')$ is the Green's function G. $\nabla\times\left(\vec{A} \mid \vec{F}\right)$-PeC-MFIE- follows this structure but the Kernel, also derived from the Green's function, is more elaborate. Because of $\nabla\times$, the normal field unit vector $\hat{u}_n$ takes also part in the field-source unit vector products; that is, $\hat{u}_{\{t,\phi,n\}}\hat{u}_{\{t',\phi'\}}$ must be considered in (3.5) for the sake of generality.

3.1.3.2 Impedance elements corresponding to $\nabla(\Phi \mid \Psi)$

For the scalar potential terms, which appear in the PeC-EFIE operator, since the domain magnitude is the surface charge density, the expression in (3.5) becomes

$$\left\langle \left[\vec{W}^{\{t,\phi\}}\right]^{pq}, \vec{S}^{\{t',\phi'\}} \right\rangle = \iint_{t\phi} \left[\vec{W}^{\{t,\phi\}}\right]^{pq}(t,\phi) \iint_{t',\phi'} \nabla G(t,t'/\phi,\phi')\nabla'\cdot\left(\vec{J}^{\{t',\phi'\}}(t',\phi')\right)dS'$$

$$= \iint_{t,\phi} \hat{u}_{\{t,\phi\}}(t,\phi) w_q^{\{t,\phi\}}(t) e^{-jp\phi} \iint_{t',\phi'} \left(\nabla G(t,t'/\phi,\phi')\nabla'\cdot\left(\sum_{m=-M}^{m=+M} \vec{J}_m^{\{t',\phi'\}}(t',\phi') e^{jm\phi'} \right) \right) dS'dS \tag{3.6}$$

which, by shifting properly field and source dependent magnitudes, yields

$$= \iint_{t',\phi'} \nabla'\cdot\left(\sum_{m=-M}^{m=+M} \vec{J}_m^{\{t',\phi'\}}(t',\phi') e^{jm\phi'} \right) \underbrace{\left(\iint_{t,\phi} \nabla G(t,t'/\phi,\phi')\hat{u}_{\{t,\phi\}} w_q^{\{t,\phi\}}(t) e^{-jp\phi} dS \right)}_{E^{\{t,\phi\}}} dS' \tag{3.7}$$

Through the indistinct equivalence $s = (t \mid \rho\phi)$, $\bar{s} = (\rho\phi \mid t)$, one can still arrange $E^{\{t,\phi\}}$ by remarking on $\nabla G(s,s'/\bar{s},\bar{s}')\cdot\hat{u}_s = \dfrac{\partial G(s,s'/\bar{s},\bar{s}')}{\partial s}$ and on the chain derivative rule: $(\partial G/\partial s)A = \partial(GA)/\partial s - G(\partial A/\partial s)$.

- **E^{ϕ} arrangement:**

$$E^{\phi}(t',\phi') = \iint_{t,\phi} \frac{1}{\rho} \frac{\partial(G(t,t'/\phi,\phi')w_q^{\phi}(t)e^{-jp\phi})}{\partial\phi} dS - \iint_{t,\phi} \frac{1}{\rho} G(t,t'/\phi,\phi') \frac{\partial(w_q^{\phi}(t)e^{-jp\phi})}{\partial\phi} dS$$

$$= \int_{t} \underbrace{\left[G(t,t'/\phi,\phi')w_q^{\phi}(t)e^{-jp\phi}\right]_0^{2\pi}}_{\| \\ 0} dt - (-jp) \iint_{t,\phi} \frac{1}{\rho} G(t,t'/\phi,\phi')w_q^{\phi}(t)e^{-jp\phi} dS \tag{3.8}$$

The first term is zero because the function is 2π-periodic along ϕ: $F(\phi+2\pi)-F(\phi)=0$. We then finally have,

$$E^{\phi}(t',\phi') = jp \iint_{t,\phi} G(t,t'/\phi,\phi')w_q^{\phi}(t)e^{-jp\phi} dS \tag{3.9}$$

- **E^{t} arrangement for** $w_q^{t}(t)=\Lambda(t-t_q,\Delta_q,\Delta_{q+1})$ $\left(\frac{d(w_q^{t}(t))}{dt}=\pm 1\right)$

$$E^{t}(t',\phi') = \iint_{t,\phi} \frac{\partial(G(t,t'/\phi,\phi')w_q^{t}(t)e^{-jp\phi})}{\partial t} dS - \iint_{t,\phi} G(t,t'/\phi,\phi') \frac{\partial(w_q^{t}(t)e^{-jp\phi})}{\partial t} dS \tag{3.10}$$

The first term is zero because the function becomes zero at the pulse ends; hence,

$$E^{t}(t',\phi') = -\iint_{t,\phi} G(t,t'/\phi,\phi') \frac{dw_q^{\phi}(t)}{dt} e^{-jp\phi} dS \tag{3.11}$$

- **E^{t} arrangement for** $w_q^{t}(t)=\Pi(t-t_{q-1/2},\Delta_q/2,\Delta_q/2)$ $\left(\frac{d(w_q^{t}(t))}{dt}=0\right)$

$$E^{t}(t',\phi') = \iint_{t,\phi} \frac{\partial(G(t,t'/\phi,\phi')w_q^{t}(t)e^{-jp\phi})}{\partial t} dS = \int_{\phi} \left[G(t,t'/\phi,\phi')\right]_{-\frac{\Delta q}{2}}^{+\frac{\Delta q}{2}} e^{-jp\phi} d\phi \tag{3.12}$$

One can equivalently reach this expression by bringing up the Dirac's delta function, that is physically more intuitive, and following (3.11) in an analogous way; in this case, $dw_q^{\{t\}}(t)/dt = \delta(t-\Delta_q/2)-\delta(t+\Delta_q/2)$, which accounts for the abrupt transition, and the pulse value at the ends must be taken zero.

The introduction of the simplified mathematics for $E^{\{t,\phi\}}$ in (3.7) and the source divergence computation yields, for the different field-source $\{t,\phi\}-\{t',\phi'\}$ pairs combinations,

$$\left\langle \left[\vec{W}^{t}\right]^{pq}, \vec{S}^{t'} \right\rangle = -\sum_{m=-M}^{+M} \sum_{j=1}^{N_{t'}} I_{mj}^{\{t',\phi'\}} \iint_{t,\phi} \iint_{t',\phi'} G(t,t'/\phi,\phi') \frac{dw_q^t(t)}{dt} \frac{db_j^{t'}(t')}{dt'} e^{j(m\phi'-p\phi)} dS' dS \tag{3.13}$$

$$\left\langle \left[\vec{W}^{t}\right]^{pq}, \vec{S}^{\phi'} \right\rangle = -\sum_{m=-M}^{+M} (jm) \sum_{j=1}^{N_{t'}} I_{mj}^{\{t',\phi'\}} \iint_{t,\phi} \iint_{t',\phi'} G(t,t'/\phi,\phi') \frac{dw_q^t(t)}{dt} b_j^{t'}(t') e^{j(m\phi'-p\phi)} dS' dS \tag{3.14}$$

$$\left\langle \left[\vec{W}^{\phi}\right]^{pq}, \vec{S}^{t'} \right\rangle = (jp) \sum_{m=-M}^{+M} \sum_{j=1}^{N_{t'}} I_{mj}^{\{t',\phi'\}} \iint_{t,\phi} \iint_{t',\phi'} G(t,t'/\phi,\phi') w_q^t(t) \frac{db_j^{t'}(t')}{dt'} e^{j(m\phi'-p\phi)} dS' dS \tag{3.15}$$

$$\left\langle \left[\vec{W}^{\phi}\right]^{pq}, \vec{S}^{\phi'} \right\rangle = -p \sum_{m=-M}^{+M} m \sum_{j=1}^{N_{t'}} I_{mj}^{\{t',\phi'\}} \iint_{t,\phi} \iint_{t',\phi'} G(t,t'/\phi,\phi') w_q^t(t) \frac{db_j^{t'}(t')}{dt'} e^{j(m\phi'-p\phi)} dS' dS \tag{3.16}$$

this modified formulation is more advantageous since the order of the Kernel diminishes; one can thus achieve a better precision through the ordinary quadrature rules.

3.1.3.3 Modal matrices. Orthogonality

Let $C(t,t'/\phi,\phi')$ be either $\left\{K\hat{u}_{\{t,\phi,n\}}\hat{u}_{\{t',\phi'\}}\right\}(t,t'/\phi,\phi')$ in 3.1.3.1 or $G(t,t'/\phi,\phi')$ in 3.1.3.2 then $C(t,t'/\phi,\phi')$ can be expanded, according to the azimuthal symmetry of the body, through a Fourier series; that is,

$$C(t,t'/\phi,\phi') = C(t,t'/\phi-\phi') = \frac{1}{2\pi} \sum_{s=-\infty}^{+\infty} C_s(t,t') e^{js(\phi-\phi')} \tag{3.17}$$

where

$$C_s(t,t') = \int_{-\pi}^{\pi} \left\{K\hat{u}_{\{t,\phi,n\}}\hat{u}_{\{t',\phi'\}}\right\}(t,t'/\xi) e^{-js\xi} d\xi \tag{3.18}$$

are the Fourier coefficients.

By introducing the expression (3.17) in (3.5) or in (3.13), (3.14), (3.15), (3.16), which show the same formal structure, $\left\langle \left[\vec{W}^{\{t,\phi\}}\right]^{pq}, \vec{S}^{\{t',\phi'\}} \right\rangle$ results in

$$\begin{aligned} &\sum_{m=-M}^{m=+M} \sum_{j=1}^{N_{\{t',\phi'\}}} \left[I_{mj}^{\{t',\phi'\}} \iint_{t,\phi} \iint_{t',\phi'} \left(\left(\frac{1}{2\pi} \sum_{s=-\infty}^{+\infty} C_s(t,t') e^{js(\phi-\phi')} \right) \alpha_q^{\{t,\phi\}}(t) \beta_j^{\{t',\phi'\}}(t') e^{j(m\phi'-p\phi)} dS' \right) dS \right] \\ &= \frac{1}{2\pi} \sum_{m=-M}^{m=+M} \sum_{j=1}^{N_{\{t',\phi'\}}} I_{mj}^{\{t',\phi'\}} \sum_{s=-\infty}^{+\infty} \left[\int_{-\pi}^{+\pi} e^{-j(p-s)\phi} d\phi \iint_{t,t'} C_s(t,t') \alpha_q^{\{t,\phi\}}(t) \beta_j^{\{t',\phi'\}}(t') \rho\rho' dt' dt \int_{-\pi}^{+\pi} e^{j(m-s)\phi'} d\phi' \right] \end{aligned} \tag{3.19}$$

where, in accordance with (3.5) and (3.13), (3.14), (3.15), (3.16), $\alpha_q^{\{t,\phi\}}(t)$ and $\beta_j^{\{t',\phi'\}}(t')$ stand respectively for $w_q^{\{t,\phi\}}(t), dw_q^{\{t,\phi\}}(t)/dt$ and $b_j^{\{t',\phi'\}}(t'), db_j^{\{t',\phi'\}}(t')/dt'$.

Because of the orthogonality of the harmonic-exponential functions in the $[-\pi,\pi]$ domain, we have

$$\int_{-\pi}^{+\pi} e^{\pm j(r-k)\phi'} d\phi' = 2\pi\delta(r-k) \tag{3.20}$$

which leads (3.19) to

$$\left\langle \left[\vec{W}^{\{t,\phi\}}\right]^{pq}, \vec{S}^{\{t',\phi'\}} \right\rangle = \sum_{j=1}^{N_{\{t',\phi'\}}} I_{pj}^{\{t',\phi'\}} \iint_{t,t'} C_p(t,t') \alpha_q^{\{t,\phi\}}(t) \beta_j^{\{t',\phi'\}}(t') \rho\rho' dt' dt \tag{3.21}$$

because only the addends corresponding to $p = m = s \in \{-M..M\}$ are non zero. Therefore, in view of (3.21), a unique linear system for each mode $p \in \{-M..M\}$ can be defined involving the t and ϕ current components along the discretized generating arc. That is why one has often considered the solution of the BoR problem for each mode as though it was 2D. Although roughly speaking one could consider it so somehow, BoR-MoM demands an extra integration in terms of the $\xi = (\phi - \phi')$ variable for computing the C_p Fourier coefficients, which must be precise enough. Indeed, the numerical evaluation of the impedance elements becomes quite difficult because of the complexity of the formulas and usually represents the bottleneck of these techniques.

3.2 QUICK REVIEW OF THE EXISTING BoR-MoM TECHNIQUES

3.2.1 PeC-EFIE by J. R. Mautz and R. F. Harrington [18]

In 1969, J. R. Mautz and R. F. Harrington developed the BoR-MoM PeC-EFIE operator by taking into consideration the following aspects:

- Triangular patches for both components of the weighting and expanding sets

$$b_n^{\{t,\phi\}}(t) = w_n^{\{t,\phi\}}(t) = \frac{1}{\rho_n} \Lambda(t - t_n, \Delta_n, \Delta_{n+1}) \tag{3.22}$$

- The computation of the Fourier coefficients is effectuated by a combination of analytical and numerical techniques. The continuous part -$m = 0$- of all the harmonics is analytically integrated meanwhile the rest of terms are numerically integrated. .

- The field integration is very efficiently accomplished by means of a Gaussian quadrature rule.

3.2.2 PMCHW for homogeneous dielectrics or E-PMCHW for completely coated PeC bodies.

From the original development of Mautz and Harrington for the PeC-EFIE case, several authors assessed its generalization for the dielectric scattering problems by programming the PMCHW operator.

In 1977, Te-Kao Wu and Leonard L.Tsai [31] attempted a PMCHW formulation by assuming all the principles presented in 3.2.1. Furthermore, the integration of the more

insidious term of the Cauchy principal value $-d()/dn-$, that comes from $\nabla\times(\vec{A}\,|\,\vec{F})$, is carried by finite-difference approximating the field-derivative of the scalar potential $(\Phi\,|\,\Psi)$, which can be source-integrated more easily. Results are presented for lossy dielectric structures.

In 1979, L.N. Medgyesi-Mitschang and C.Eftimiu [19][20] extended the reach of the PMCHW formulation to completely coated PeC Bodies by combining the PeC-EFIE formulation, as presented by Mautz and Harrington, and a PMCHW formulation where the $\nabla\times(\vec{A}\,|\,\vec{F})$ integrating term is solved by source-integrating the whole $d()/dn$ expression.

In 1989, Allen W. Glisson and Donald R. Wilton, though maintaining the criteria expounded in 3.1.3 for developing the operators, presented a breakthrough on the BoR-MoM methods. The weighting functions are imposed to be

$$\begin{aligned} w_n^{\phi}(t) &= \frac{1}{\rho}\Pi(t-t_{n-1/2},\frac{\Delta_n}{2},\frac{\Delta_n}{2}), && n=1..N+1 \\ w_n^{t}(t) &= \frac{1}{\rho}\Pi(t-t_{n},\frac{\Delta_n}{2},\frac{\Delta_{n+1}}{2}), && n=1..N \end{aligned} \tag{3.23}$$

which sets two collections of functions, along t and ϕ, regularly overlapped.

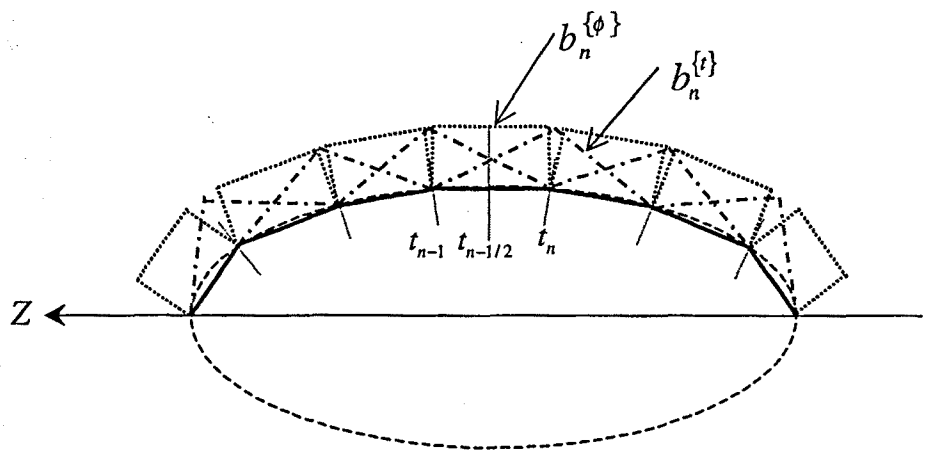

Fig. 3.2 Glisson and Wilton expanding functions choice

The expanding functions are accordingly set to -see Fig. 3.2-

$$\begin{aligned} b_n^{t}(t) &= \Lambda\left(t-t_n,\Delta_n,\Delta_{n+1}\right) \\ b_n^{\phi}(t) &= \Pi(t-t_{n-1/2},\frac{\Delta_n}{2},\frac{\Delta_n}{2}) \end{aligned} \tag{3.24}$$

which yields a different number of basis functions for each current component: $N_{\phi}=N_t+1$. In order to let the PeC-EFIE operator well-defined, the basis functions must expand properly not only the current but also the surface charge density. One must then check the good behaviour of the basis functions when applied into the surface divergence operator $-\nabla(\vec{v})=(1/\rho)\partial(v^{\phi})/\partial\phi+\partial(v^{t})/\partial t-$.

According to the MoM-BoR formulation, $(1/\rho)\partial(v^{\phi})/\partial\phi$ becomes perfectly defined since the ϕ-dependence does not affect the pulse $b^{\phi}(t)$ but $e^{jm\phi}$. Therefore, the divergence operator works perfectly no matter the kind of shape the pulses along the contour have. That is why A. W. Glisson and D. R. Wilton decided to use the less complicated, in computational terms, rectangular pulses.

However, one cannot force $b^{t}(t)$ to become rectangular pulses since $\partial(b^{t})/\partial t$ in this case would yield zero. As this is unacceptable for the proper expansion of the surface charge density, the t component current components must have a first derivative non null. This is fulfilled with the linear slope of the triangular patch, which renders a pulse-doublet charge representation.

According to the characteristics of the PeC-EFIE operator, A.W. Glisson and D. R. Wilton determined to turn the $b^{t}(t)$ triangles into half-length rectangles in the part of the PeC-EFIE operator dependent on the vector potential

$$b_n^t(t) = \Pi\left(t - t_n, \frac{\Delta_n}{2}, \frac{\Delta_{n+1}}{2}\right) \tag{3.25}$$

This change is perfectly consistent because of the much bigger importance of the scalar potential gradient at near distances of the radiating source distribution. Indeed, from the expression of the electric field radiated by any source surface distribution, we have

$$\vec{E}(\vec{J},\sigma) = \frac{1}{4\pi\varepsilon}\int_{S'}\left[\frac{e^{-jkR}}{R^2}\hat{R}\sigma(\vec{r}') + \left[jk\hat{R}\sigma(\vec{r}') - j\omega\mu\varepsilon\vec{J}(\vec{r}')\right]\frac{e^{-jkR}}{R}\right]dS' \tag{3.26}$$

In the matrix diagonal elements, the so-called *induced field* ($\propto 1/R^2$) dominates the *radiated field* ($\propto 1/R$). In the off-diagonal terms, the vector potential contribution must still have little effect and the result with triangular and rectangular pulses is to be alike since their current moments are the same. So, in practice, it barely makes any difference to replace the triangles by half-length rectangles inside the vector potential and it is even much more advantageous in terms of programming.

3.2.3 Use of the FFT for the efficient Solution of the PeC-EFIE by S. D. Gedney and R. Mittra.

In all the previous techniques, the inherent $1/R$ singularity in the Green's function is extracted as

$$\int_{-\pi}^{\pi}\left[\frac{e^{-jkR(\xi)}}{R(\xi)}\cos(m\xi) - \frac{1}{R(\xi)}\right]d\xi + \int_{-\pi}^{\pi}\frac{1}{R(\xi)}d\xi \tag{3.27}$$

which is easily effectuated since the second integral is the complete elliptic integral of the first kind.

Through the same weighting and expanding set choice of Glisson and Wilton -see section 3.2.2-, S. D. Gedney and R. M. Mittra proposed to improve the efficiency on the numerical computation of the first integral in (3.27) by extracting the singularity as

$$\int_{-\pi}^{\pi}\left[\frac{e^{-jkR(\xi)}}{R(\xi)}-\frac{1}{R(\xi)}\right]e^{-jm\xi}d\xi+\int_{-\pi}^{\pi}\frac{e^{-jm\xi}}{R(\xi)}d\xi \tag{3.28}$$

The first integral can be then evaluated via the FFT, more efficient than the previous ordinary numerical techniques. The analytical computation of the second integral can be carried out using a recursive relation from the analytical integrals for $m=0$, already needed for the previous approaches, and $m=1$.

This approach has been programmed in this dissertation Thesis for the PeC-EFIE case as described by Gedney and Mittra. Furthermore, the PeC-MFIE and the dielectric-PMCHW -with more elaborate Kernels- have also been programmed providing the same criteria with regard to the FFT faster computation and the recurrence relation for obtaining the higher modes integrals.

3.3 MoM-BoR PeC-EFIE ACCORDING TO S. D. GEDNEY AND R. MITTRA [12]

Let us consider a PeC-body of revolution placed in a homogeneous environment. The electric field $\vec{E}$ can be expressed, according to the Surface Equivalence Theorem, as the addition of the incident arbitrary electric field $\vec{E}^i$ and the scattered electric field $\vec{E}^s$. The boundary conditions on a PeC-scatterer require the tangential component of $\vec{E}$ to be zero on the surface; that is,

$$\left[\vec{E}^s\left(\vec{J}\right)\right]_{\tan,\vec{r}\in S^+}=-\left[\vec{E}^i\right]_{\tan,\vec{r}\in S^+} \tag{3.29}$$

The scattered field produced by the equivalent electric current source is

$$\vec{E}^s(\vec{r})=-j\omega\vec{A}(\vec{r})-\nabla\Phi(\vec{r}) \tag{3.30}$$

where the expressions of the vector and scalar potentials, $\vec{A}(\vec{r})$ and $\Phi(\vec{r})$, stand for -see section 2.5-

$$\begin{aligned}\vec{A}(\vec{r})&=\frac{\mu}{4\pi}\iint_{S'}G(\vec{r},\vec{r}')\vec{J}(\vec{r}')dS'\\ \Phi(\vec{r})&=\frac{1}{4\pi\varepsilon}\iint_{S'}G(\vec{r},\vec{r}')\sigma(\vec{r}')dS'\end{aligned} \tag{3.31}$$

where

$$G(\vec{r},\vec{r}')=\frac{e^{-jkR}}{R} \tag{3.32}$$

is the free-space Green's function, and

$$R = |\vec{r} - \vec{r}'| = \left[\rho^2 + \rho'^2 - 2\rho\rho'\cos(\phi - \phi') + (z - z')^2\right]^{1/2} \tag{3.33}$$

In view of the expressions (3.1), (3.2) and (3.24), the current expansion for this formulation entitles to

$$\vec{J}(t,\phi) = \sum_{m=-M}^{m=+M}\left(\sum_{j=1}^{N_t} I'_{mj}\hat{u}_t \frac{\Lambda(t_j,\Delta_j,\Delta_{j+1})}{2\pi\rho} + \sum_{j=1}^{N_t+1} I^{\phi}_{mj}\hat{u}_{\phi}\Pi(t_{j-1/2},\Delta_j/2,\Delta_j/2)\right)e^{jm\phi} \tag{3.34}$$

and I'_{mj} must be interpreted as the current intensity flowing in the tangential direction because $2\pi\rho$ is its section length. As shown in (3.25), the t current component in the vector potential term is set to $\Pi(t_j,\Delta_j/2,\Delta_{j+1}/2)$. In this work, the results obtained with this simplified choice have been compared with the original triangular pulse version for different objects. This is very important because the PeC-EFIE BoR-operator is taken as reference in Chapters 4 and 7 to test the behaviour respectively of the PeC-MFIE BoR-operator and the 3D PeC-operators. For spheres or cylinders, the simpler rectangular pulse version has been adopted -the performance of both approaches turns out to be almost identical-. Only for the cone of Chapter 7 the original version with triangular pulses has been preferred.

For building the operator one has to allow for the expressions in (3.5) and (3.13), (3.14), (3.15), (3.16), which rule the vector and the scalar potential terms. The Kernel is the Green's function in any case.

3.3.1 Extraction of the ξ-singularity

The goodness of the Gedney and Mittra's approach relies on the efficient computation of the Fourier coefficients, which, in view of (3.18), are

$$G_m(t,t') = \int_0^{2\pi} \frac{e^{-jkR(\xi)}}{R(\xi)} e^{-jm\xi} d\xi \tag{3.35}$$

S. D. Gedney and R. Mittra propose to extract the singularity as follows

$$\int_0^{2\pi}\left[\frac{e^{-jkR(\xi)}}{R(\xi)} - \frac{1}{R(\xi)}\right]e^{-jm\xi}d\xi + \underbrace{\int_0^{2\pi}\frac{e^{-jm\xi}}{R(\xi)}d\xi}_{\Phi_m} \tag{3.36}$$

The first term is computed numerically with the FFT. Φ_m is computed analytically. As $R(\xi) = R(-\xi)$ -for the Green's function is ξ-even symmetric- one can equivalently write

$$\Phi_m = \int_{-\pi}^{\pi} \frac{e^{-jm\xi}}{R(\xi)} d\xi = \int_{-\pi}^{\pi} \frac{\cos(m\xi)}{R(\xi)} d\xi \tag{3.37}$$

which can be simplified

$$\begin{aligned} \Phi_m &= 2\int_0^{\pi} \frac{\cos(m\xi)}{R(\xi)} d\xi = 2\int_0^{\pi} \frac{\cos(m\xi)}{\left[\rho^2 + \rho'^2 - 2\rho\rho'\cos(\xi) + (z-z')^2\right]^{1/2}} d\xi \\ &= 2\int_0^{\pi} \frac{\cos(m\xi)}{\left[(\rho-\rho')^2 + 2\rho\rho'(1-\cos(\xi)) + (z-z')^2\right]^{1/2}} d\xi \\ &= 2\int_0^{\pi} \frac{\cos(m\xi)}{\left[(\rho-\rho')^2 + 4\rho\rho'\sin^2(\xi/2) + (z-z')^2\right]^{1/2}} d\xi \end{aligned} \tag{3.38}$$

to which it follows that

$$\Phi_m = \frac{4}{R_1} \int_0^{\pi/2} \frac{\cos(2m\varphi)}{\left[1 + \beta_1^2 \sin^2\varphi\right]^{1/2}} d\varphi \tag{3.39}$$

where $R_1 = \left[(\rho-\rho'^2) + (z-z'^2)\right]^{1/2}$, $\beta_1^2 = \dfrac{4\rho\rho'}{R_1^2}$ are t and t' dependent parameters that do not interfere with the φ-angular integration.

It is advantageous an expansion of $\cos(2m\varphi)$ in terms of cosinus to even powers as

$$\cos(2m\varphi) = \sum_{k=1}^{m+1} \Psi_k^m \cos^{\alpha}\varphi \tag{3.40}$$

where $\alpha = 2m - 2(k-1)$, $\Psi_k^m = (-1)^{k-1} 2^{2m-(2k-1)} \gamma_k$ and $\gamma_k = \begin{cases} \dbinom{2m-k}{k-2} \dfrac{2m}{k-1} & k \neq 1 \\ 1 & k = 1 \end{cases}$

Thanks to the expansion in (3.40), the expression in (3.39) can be expressed in terms of elementary integrals I_{α} as

$$\Phi_m = \frac{4}{R_1} \sum_{k=1}^{m+1} \Psi_k^m I_{\alpha(k,m)} \tag{3.41}$$

where

$$I_{\alpha(k,m)} = \int_0^{\pi/2} \frac{\cos^{\alpha}\varphi}{\left[1+\beta_1^2\sin^2\varphi\right]^{1/2}} d\varphi \tag{3.42}$$

and the analytical expressions for I_0 nd I_2 are -see Appendix A-

$$I_0 = \frac{1}{\left[1+\beta_1^2\right]^{1/2}} K\left(\beta_1^2/\left(1+\beta_1^2\right)\right) \tag{3.43}$$

$$I_2 = \frac{\left[1+\beta_1^2\right]^{1/2}}{\beta_1^2}\left[K\left(\beta_1^2/\left(1+\beta_1^2\right)\right) - E\left(\beta^2{}_1/\left(1+\beta_1^2\right)\right)\right] \tag{3.44}$$

where $K(\ )$ and $E(\ )$ stand respectively for the complete elliptic integrals of first and second kind.

These elementary integrals are convenient since, as shown in the Appendix A, one can compute them fast through the recurrent relation $\forall \alpha \geq 4$, from the above-presented analytical expressions for I_0 and I_2,

$$I_\alpha = \left(\frac{\alpha-2}{\alpha-1}\right)\left(\beta_1^{-2}+2\right)I_{\alpha-2} - \left(\beta_1^{-2}+1\right)\left(\frac{\alpha-3}{\alpha-1}\right)I_{\alpha-4} \tag{3.45}$$

3.3.2 Limitations to the ξ-singularity extraction

There are no theoretical restrictions for the validity of the previous recurrent formula. However, when introduced into a computational code, some limitations, due to the finite accuracy of the machine, may appear.

These restrictions derive from the multiplicative effect of $\left(\beta_1^{-2}+2\right)$ and $\left(\beta_1^{-2}+1\right)$ that may overflow the capacity of the computer -the condition number increases much- and thus worsen the accuracy for big enough values of m. That is why it is recommended not to use large values for $\beta_1^{-2} = R_1^2/4\rho\rho'$. There must be an upper bound for R_1 and a lower bound for ρ and ρ'. In all the examples tested in this work, it has been adopted $\rho, \rho' > 0.1\lambda$ -as Gedney and Mittra recommend- and $R_1 < 0.2\lambda$.

On dimensionally large enough objects, whenever these limits are surpassed, not to use the recurrence formula is irrelevant. Indeed, since either the field or the source annuli are far enough or they present a rather small radius, they contribute poorly to the field radiation in comparison to the rest of influences. However, on rather small objects, a lack of accuracy may appear. In this case, the current error can be particularly evident on the points of the generating arc near the axis (where $\rho \to 0$).

3.3.3 Extraction of the t-singularity

The singularity extraction is completed with the precise integration along t. It is carried out a Gaussian quadrature rule for the contour source segments contributions different to the contour field segment.

When the field and source annuli coincide ($R_1 \to 0, \beta_1^2 \to \infty$), the integration of the singular terms of the integrand must be analytically undertaken since no numerical quadrature rule can undertake an integration of such a high order. The numerical integration for the lower order terms can be maintained.

With the goal of viewing the behaviour around the singularity for each mode, it is obligatory a first insight into the elementary integrals -embracing the whole t' dependence of the integrand- $(4/R_1)I_0$: and $(4/R_1)I_2$.

If we let $R_1 \to 0$; that is, $\beta_1^2 \to \infty$, $\beta_1/(1+\beta_1^2)^{1/2} \to 1$,

$$1/R_1 \to \infty,\ K\left(\beta_1/(1+\beta_1^2)^{1/2}\right) \to K(1) = \infty \tag{3.46}$$

$E(\ )$is always finite regardless the input value. Besides, the complete elliptic integral of the first kind $K(\ )$ can be well-approximated for input values close to one as $K(m) \cong -\frac{1}{2}\ln(1-m)$; that is,

$$K\left(\frac{\beta_1^2}{(1+\beta_1^2)}\right) \cong -\frac{1}{2}\ln\left(\frac{1}{(1+\beta_1^2)}\right) = \frac{1}{2}\ln\left(\frac{4\rho\rho'+R_1^2}{R_1^2}\right) = \frac{1}{2}\left[\ln\left(4\rho\rho'+R_1^2\right) - \ln\left(R_1^2\right)\right] \tag{3.47}$$

Hence, the highest order characteristic of both elementary integrals –outstanding when R_1 approaching zero- is, in view of the expressions (3.41), (3.43) and (3.44),

$$\chi_0 = \left\{\frac{4I_0}{R_1}\right\}(R_1 \to 0) = -\frac{4}{\left[4\rho\rho'+R_1^2\right]^{1/2}}\ln(R_1) \xrightarrow[R_1\to 0]{} -\frac{2}{[\rho\rho']^{1/2}}\ln(R_1) \tag{3.48}$$

$$\chi_2 = \left\{\frac{4I_2}{R_1}\right\}(R_1 \to 0) = -2\frac{\left[4\rho\rho'+R_1^2\right]^{1/2}}{\rho\rho'}\ln(R_1) \xrightarrow[R_1\to 0]{} -\frac{2}{[\rho\rho']^{1/2}}\ln(R_1) \tag{3.49}$$

In these two expressions one can assess that the singular behaviour of both integrals when tending approaching very closely the field point is nearly equal.

Similarly, for the integrals with $\alpha \geq 4$, as set in (3.45),

$$\chi_\alpha = \left\{\left(\frac{\alpha-2}{\alpha-1}\right)\left(\frac{1+2\beta_1^2}{\beta_1^2}\right)I_{\alpha-2} - \left(\frac{1+\beta_1^2}{\beta_1^2}\right)\left(\frac{\alpha-3}{\alpha-1}\right)I_{\alpha-4}\right\}\left(R_1 \to 0;\beta_1^2 \to \infty\right)$$
$$= 2\left(\frac{\alpha-2}{\alpha-1}\right)\chi_{\alpha-2} - \left(\frac{\alpha-3}{\alpha-1}\right)\chi_{\alpha-4} \tag{3.50}$$

For the particular case of $\alpha = 4$, -taking into consideration that $\chi_0 = \chi_2$-

$$\chi_4 = 2\left(\frac{\alpha-2}{\alpha-1}\right)\chi_2 - \left(\frac{\alpha-3}{\alpha-1}\right)\chi_0 = \frac{2\alpha-4-\alpha+3}{\alpha-1}\chi_0 = \chi_0 \tag{3.51}$$

and it can also be shown $\forall\alpha$

$$\chi_\alpha = \ldots = \chi_2 = \chi_0 \tag{3.52}$$

which is reasonable since the order of the singularity must not change when increasing the mode number. As a matter of fact, one could already realise about this on the singularity extractions undertaken in 3.2.1 and in 3.2.2. In this case the analytical integration of the singular term for all the modes does not depend on the mode number.

In Gedney and Mittra's technique, the singularity must be extracted for each mode but can be quickly computed thanks to the recurrence relation along ϕ and because the singular behaviour in t is eventually the same for each mode.

So as to fast integrate the singular dependence of the integrand in the self-annulus influence, Gedney and Mittra have analytically integrated the very fast t-varying part; that is,

$$\chi_\alpha = -\frac{2}{[\rho\rho']^{1/2}}\ln(R_1) \xrightarrow[\rho'\to\rho]{} -\frac{2}{\rho}\ln(R_1(t')) = \chi \tag{3.53}$$

which likewise eases the computation of (3.41) [8]

$$\Phi_m(R_1 \to 0) = \sum_{k=1}^{m+1}\Psi_k^m\chi_\alpha = \chi\sum_{k=1}^{m+1}\Psi_k^m = \chi \tag{3.54}$$

The integration of (3.53) along the generating arc, with 0 corresponding to the field point and t_-, t_+ being the distances from the segment ends to the field point -see Fig. 4.5-, leads to

$$-\frac{2}{\rho}\int_{-t_-}^{t_+}\ln(R_1(t'))dt' = \lim_{\varepsilon\to 0} -\frac{2}{\rho}\left[\int_{-t_-}^{-\varepsilon}\ln(-t')dt' + \int_{+\varepsilon}^{t_+}\ln(t')dt'\right]$$

[8] $[\cos(2m\varphi)](\varphi=0) = \left[\sum_{k=1}^{m+1}\Psi_k^m\cos^\alpha\varphi\right](\varphi=0) \Rightarrow \sum_{k=1}^{m+1}\Psi_k^m = 1$

$$= \lim_{\varepsilon \to 0} -\frac{2}{\rho}\left[\int_{\varepsilon}^{t_-} \ln(t')dt' + \int_{\varepsilon}^{t_+} \ln(t')dt'\right]$$

$$= \lim_{\varepsilon \to 0} -\frac{2}{\rho}\left[\left[t' \ln t' - t'\right]_{\varepsilon}^{t_-} + \left[t' \ln t' - t'\right]_{\varepsilon}^{t_+}\right]$$

$$= -\frac{2}{\rho}\left[t_- \ln t_- + t_+ \ln t_+ - (t_- + t_+)\right] \tag{3.55}$$

where Gedney and Mittra have assumed the slow-varying terms in the self-contribution constant in comparison to the singular part of the integrand.

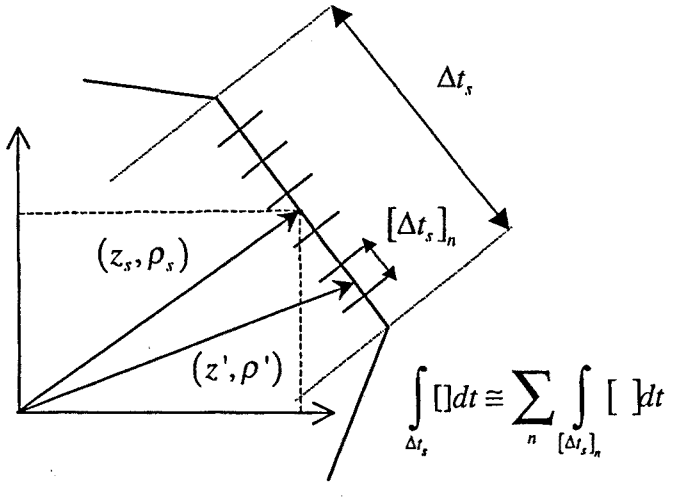

Fig. 3.3 Finer discretization over the segment for the computation of the self t-integral influence

When developing the PeC-EFIE code, the integration in (3.55) has been effectuated slightly differently so as to assess the influence of the multiplying terms that are assumed constant. As shown in Fig. 3.3, one has divided the contour segment into more little segments so that the integral has been computed as the sum of the contributions coming from each segment portion. The slow-varying multiplying terms are again assumed constant and (3.55) is locally redone. This change, though little, has added some complication to the code since the singular terms for each mode are not yet the same. In any case, the results are very similar to those presented by Gedney and Mittra, which shows that their assumption is precise enough.

This t singular integration is always needed no matter if the recurrent relation is applied or not according to the restrictions shown in 3.3.2.

3.3.4 Impedance matrix

As explained in 3.1.3.3, the $G_m(t,t')$ coefficients of (3.35), which derive from the Green's function, represent the Fourier coefficients for the scalar potential terms. The $C_m(t,t')$ definition for the vector potential terms shows that $G_m(t,t')$ needs to be modified with the product of the field-source unit vector $\{\hat{u}_{t,\phi}\hat{u}_{t',\phi'}\}(t,t'/\phi-\phi')$ combinations, which, by adopting the sign criterion and the angles shown in Fig. 3.1 and Fig. 3.4, become

$$\begin{aligned}\{\hat{u}_t\hat{u}_{t'}\} &= \begin{bmatrix}\sin\alpha\cos\phi\\ \sin\alpha\sin\phi\\ \cos\alpha\end{bmatrix}\cdot\begin{bmatrix}\sin\alpha'\cos\phi'\\ \sin\alpha'\sin\phi'\\ \cos\alpha'\end{bmatrix}\\ &= \sin\alpha\sin\alpha'(\cos\phi\cos\phi'+\sin\phi\sin\phi')+\cos\alpha\cos\alpha'\\ &= \sin\alpha\sin\alpha'\cos(\phi-\phi')+\cos\alpha\cos\alpha'\\ &= \sin\alpha\sin\alpha'\cos\xi+\cos\alpha\cos\alpha'\end{aligned} \tag{3.56}$$

$$\begin{aligned}\{\hat{u}_t\hat{u}_{\phi'}\} &= \begin{bmatrix}\sin\alpha\cos\phi\\ \sin\alpha\sin\phi\\ \cos\alpha\end{bmatrix}\cdot\begin{bmatrix}-\sin\phi\\ \cos\phi\\ 0\end{bmatrix}\\ &= -\sin\alpha(-\cos\phi\sin\phi'+\sin\phi\cos\phi')\\ &= -\sin\alpha\sin(\phi-\phi') = -\sin\alpha\sin\xi\end{aligned} \tag{3.57}$$

$$\begin{aligned}\{\hat{u}_\phi\hat{u}_{t'}\} &= \begin{bmatrix}-\sin\phi\\ \cos\phi\\ 0\end{bmatrix}\cdot\begin{bmatrix}\sin\alpha'\cos\phi'\\ \sin\alpha'\sin\phi'\\ \cos\alpha'\end{bmatrix}\\ &= \sin\alpha'(\cos\phi\sin\phi'-\sin\phi\cos\phi')\\ &= -\sin\alpha'\sin(\phi-\phi') = -\sin\alpha'\sin\xi\end{aligned} \tag{3.58}$$

$$\{\hat{u}_\phi\hat{u}_{\phi'}\} = \begin{bmatrix}-\sin\phi\\ \cos\phi\\ 0\end{bmatrix}\cdot\begin{bmatrix}-\sin\phi'\\ \cos\phi'\\ 0\end{bmatrix} = \cos(\phi-\phi') = \cos\xi \tag{3.59}$$

Obtaining the Fourier coefficients $C_m(t,t')$ from $G_m(t,t')$ and the previous expressions is straightforward thanks to the finite expansion of $\sin\xi$ and $\cos\xi$ in terms of the harmonic series:

$$\begin{aligned}\int_0^{2\pi}\left(\frac{e^{-jkR(\xi)}}{R(\xi)}\cos\xi\right)e^{-jm\xi}d\xi &= \int_0^{2\pi}\left(\frac{e^{-jkR(\xi)}}{R(\xi)}\frac{\left(e^{j\xi}+e^{-j\xi}\right)}{2}\right)e^{-jm\xi}d\xi\\ &= \frac{1}{2}\int_0^{2\pi}\frac{e^{-jkR(\xi)}}{R(\xi)}e^{-j(m-1)\xi}d\xi+\frac{1}{2}\int_0^{2\pi}\frac{e^{-jkR(\xi)}}{R(\xi)}e^{-j(m+1)\xi}d\xi\\ &= \frac{\left(G_{m-1}(t,t')+G_{m+1}(t,t')\right)}{2}\end{aligned} \tag{3.60}$$

and analogously

$$\int_0^{2\pi}\left(\frac{e^{-jkR(\xi)}}{R(\xi)}\sin\xi\right)e^{-jm\xi}d\xi = \frac{\left(G_{m+1}(t,t')-G_{m-1}(t,t')\right)}{2j} \tag{3.61}$$

The substitution of the terms $\cos\xi$ or $\sin\xi$ in (3.56), (3.57), (3.58), (3.59) by (3.60) or (3.61) leads to the complete vector potential development of (3.5). The matrix elements become thus a combination of G_{m+1}, G_{m-1} and G_m. They are thoroughly developed in [12].

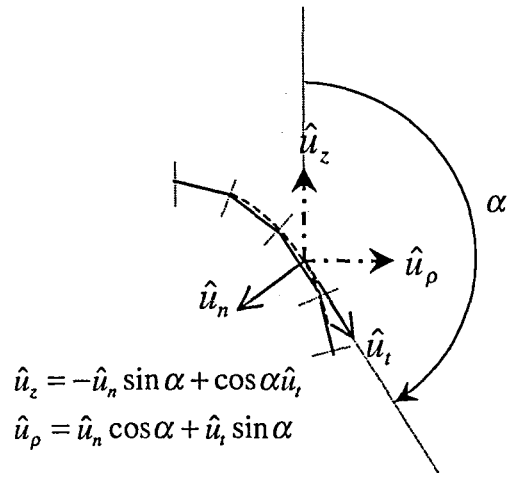

Fig. 3.4 Relation between the global cylindrical coordinates (ρ, z) and the local to the annulus (n, t)

The matrix form in (3.29) becomes

$$\begin{bmatrix} \underline{E}_t^{i\,m} \\ \underline{E}_\phi^{i\,m} \end{bmatrix} = \begin{bmatrix} \underline{\underline{Z}}_{t,t'}^{\;m} & \underline{\underline{Z}}_{t,\phi'}^{\;m} \\ \underline{\underline{Z}}_{\phi,t'}^{\;m} & \underline{\underline{Z}}_{\phi,\phi'}^{\;m} \end{bmatrix} \begin{bmatrix} \underline{I}_{t'}^{\;m} \\ \underline{I}_{\phi'}^{\;m} \end{bmatrix} \qquad m = -M..+M \tag{3.62}$$

and the submatrices are even if $\underline{\underline{Z}}_{s,s'}^{\;m}$ and odd if $\underline{\underline{Z}}_{\bar{s},s'}^{\;m}$; that is,

$$\begin{aligned} \underline{\underline{Z}}_{t,t'}^{\;m} &= \underline{\underline{Z}}_{t,t'}^{\;-m}, & \underline{\underline{Z}}_{\phi,\phi'}^{\;m} &= \underline{\underline{Z}}_{\phi,\phi'}^{\;-m} \\ \underline{\underline{Z}}_{t,\phi'}^{\;m} &= -\underline{\underline{Z}}_{t,\phi'}^{\;-m}, & \underline{\underline{Z}}_{\phi,t'}^{\;m} &= -\underline{\underline{Z}}_{\phi,t'}^{\;-m} \end{aligned} \tag{3.63}$$

which is intuitively reasonable since the electromagnetic coupling is best when the electric field and the electric current are parallel and null when they are perpendicular[9].

3.3.5 Incident electric field expansion

The electric incident field presents the general form

$$\vec{E}^i = \left(E_t^0 \hat{t}_{\phi_i} + E_\phi^0 \hat{\phi}_{\phi_i}\right) e^{-j\vec{k}_i \cdot \vec{r}} = \left(E_t^0 \hat{t}_{\phi_i} + E_\phi^0 \hat{\phi}_{\phi_i}\right) e^{jkz\cos\sigma_i} e^{jk\rho\sin\sigma_i\cos(\phi-\phi_i)} \tag{3.64}$$

[9] As mentioned in Chapter 2, the MoM matrix elements give a measure of the coupling between the weighting functions and the electromagnetic field radiated by the expanding functions. In Chapter 6, it will be provided a more elaborate description of this issue regarding the 3D integral operators.

If it is assumed $\phi_i = 0$, which is irrelevant in the bodies with symmetry of revolution -the current under a non null ϕ_i incidence is obtained through the ϕ_i shift of the resulting current for $\phi_i = 0-$, this expression, in accordance with the definition of the Bessel's function [10], becomes

$$\vec{E}^i = \left(E_t^0 \hat{t}_0 + E_\phi^0 \hat{\phi}_0\right) e^{jkz\cos\sigma_i} \sum_{n=-\infty}^{n=+\infty} j^{+n} J_n(k\rho \sin\sigma_i) e^{jn\phi} \tag{3.65}$$

The development of this expression is effectuated according to the definition of the weighting functions in (3.24) and allowing for the fact that any incident direction can be constructed from the two perpendicular directions $\hat{t}_0$, $\hat{\phi}_0$.

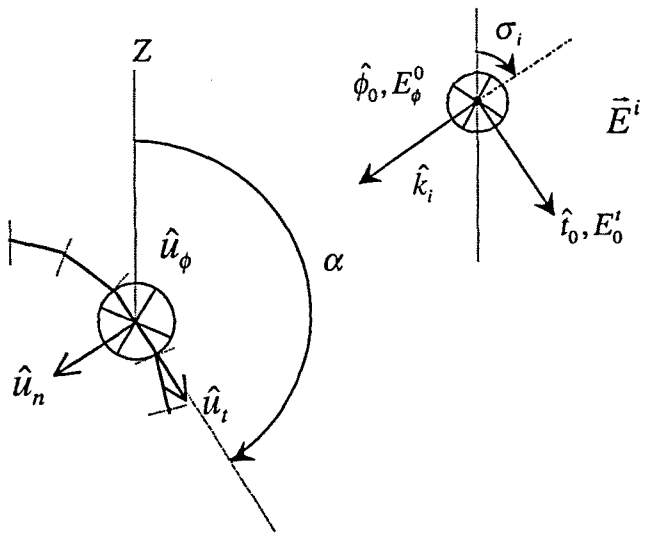

Fig. 3.5 Electric field incidence on the plane defined by the generating arc of the body

In view of (3.56), (3.57), (3.58) and (3.59) and of the angular disposition of Fig. 3.5, the expressions of the products of unit vector pairs stand for

$$\left\{\hat{u}_t \hat{t}_0\right\} = \sin\alpha\cos\sigma_i\cos\phi - \cos\alpha\sin\sigma_i \tag{3.66}$$

$$\left\{\hat{u}_t \hat{\phi}_0\right\} = -\sin\alpha\sin\phi \tag{3.67}$$

$$\left\{\hat{u}_\phi \hat{t}_0\right\} = -\cos\sigma_i\sin\phi \tag{3.68}$$

$$\left\{\hat{u}_\phi \hat{\phi}_0\right\} = \cos\phi \tag{3.69}$$

As usual in the BoR developments, the orthogonality between the azimuthal modes lets the weighting procedure independently defined for each mode $p \in \{-M..M\}$.

---

[10] $J_n(z) = \dfrac{(-j)^n}{2\pi} \int_0^{2\pi} e^{jz\cos\phi} e^{-jn\phi} d\phi$

3.3.5.1 Tangential weighting:

$$\left[\begin{matrix}E_\phi^i\\E_t^i\end{matrix}\right]_t^{pq}=\left\langle\left[\begin{matrix}\vec{E}_\phi^i\\\vec{E}_t^i\end{matrix}\right],w_q^t(t)\hat{t}e^{-jp\phi}\right\rangle=\left[\begin{matrix}E_\phi^0\\E_t^0\end{matrix}\right]\int_{t_q-\Delta_q/2}^{t_q+\Delta_{q+1}/2}\frac{e^{jkz\cos\sigma_i}}{\rho}\sum_{n=-\infty}^{n=+\infty}j^{+n}J_n(k\rho\sin\sigma_i)\rho\left(\int_{-\pi}^{\pi}\hat{u}_{t_r}\cdot\left[\begin{matrix}\hat{\phi}_0\\\hat{t}_0\end{matrix}\right]e^{j(n-p)\phi}d\phi\right)dt \quad (3.7$$

$$p=-M..M,\ q=1..N$$

which, in view of (3.66) and (3.67), leads to

$$\left[E_\phi^i\right]_t^{pq}=\left\langle\vec{E}_\phi^i,w_q^t(t)\hat{t}e^{-jp\phi}\right\rangle$$

$$=E_\phi^0\int_{t_q-\Delta_q/2}^{t_q+\Delta_{q+1}/2}e^{jkz\cos\sigma_i}\sum_{n=-\infty}^{n=+\infty}j^{+n}J_n(k\rho\sin\sigma_i)\left(\int_{-\pi}^{\pi}\hat{u}_{t_r}\cdot\hat{\phi}_0e^{j(n-p)\phi}d\phi\right)dt$$

$$=E_\phi^0\int_{t_q-\Delta_q/2}^{t_q+\Delta_{q+1}/2}e^{jkz\cos\sigma_i}\sum_{n=-\infty}^{n=+\infty}j^{+n}J_n(k\rho\sin\sigma_i)\left(\int_{-\pi}^{\pi}(-\sin\alpha\sin\phi)e^{j(n-p)\phi}d\phi\right)dt$$

$$=-2\pi E_\phi^0\int_{t_q-\Delta_q/2}^{t_q+\Delta_{q+1}/2}\frac{e^{jkz\cos\sigma_i}}{2j}\sin\alpha(j^{p+1}J_{p+1}(k\rho\sin\sigma_i)-j^{p-1}J_{p-1}(k\rho\sin\sigma_i))dt \quad (3.$$

$$p=-M..M,\ q=1..N$$

$$\left[E_\phi^i\right]_t^{pq}\cong-\pi E_\phi^0e^{jkz_q\cos\sigma_i}j^p(J_{p+1}(k\rho_q\sin\sigma_i)+J_{p-1}(k\rho_q\sin\sigma_i))\left(\frac{\sin\alpha_q\Delta_q+\sin\alpha_{q+1}\Delta_{q+1}}{2}\right) \quad (3.$$

$$p=-M..M,\ q=1..N$$

$$\left[E_t^i\right]_t^{pq}=\left\langle\vec{E}_t^i,w_q^t(t)\hat{t}e^{-jp\phi}\right\rangle$$

$$=E_t^0\int_{t_q-\Delta_q/2}^{t_q+\Delta_{q+1}/2}\frac{e^{jkz\cos\sigma_i}}{\rho}\sum_{n=-\infty}^{n=+\infty}j^{+n}J_n(k\rho\sin\sigma_i)\rho\left(\int_{-\pi}^{\pi}\hat{u}_{t_r}\cdot\hat{t}_0e^{j(n-p)\phi}d\phi\right)dt$$

$$=E_t^0\int_{t_q-\Delta_q/2}^{t_q+\Delta_{q+1}/2}e^{jkz\cos\sigma_i}\sum_{n=-\infty}^{n=+\infty}j^{+n}J_n(k\rho\sin\sigma_i)\left(\int_{-\pi}^{\pi}(\sin\alpha\cos\sigma_i\cos\phi-\cos\alpha\sin\sigma_i)e^{j(n-p)\phi}d\phi\right)dt$$

$$= 2\pi E_t^0 \int_{t_q-\Delta_q/2}^{t_q+\Delta_{q+1}/2} \frac{e^{jkz\cos\sigma_i}}{2} \sin\alpha\cos\sigma_i (j^{p+1}J_{p+1}(k\rho\sin\sigma_i) + j^{p-1}J_{p-1}(k\rho\sin\sigma_i))dt$$
$$-2\pi E_t^0 \int_{t_q-\Delta_q/2}^{t_q+\Delta_{q+1/2}} e^{jkz\cos\sigma_i} \cos\alpha\sin\sigma_i j^p J_p(k\rho\sin\sigma_i)dt \qquad (3.73)$$
$$p=-M..M,\ q=1..N$$

$$\left[E_t^i\right]_t^{pq} \cong \pi E_t^0 e^{jkz_q\cos\sigma_i} \left(\frac{\sin\alpha_q\Delta_q + \sin\alpha_{q+1}\Delta_{q+1}}{2}\right)\cos\sigma_i (j^{p+1}J_{p+1}(k\rho_q\sin\sigma_i) + j^{p-1}J_{p-1}(k\rho_q\sin\sigma_i))$$
$$-2\pi E_t^0 e^{jkz_q\cos\sigma_i} \sin\sigma_i \left(\frac{\cos\alpha_q\Delta_q + \cos\alpha_{q+1}\Delta_{q+1}}{2}\right) j^p J_p(k\rho_q\sin\sigma_i) \qquad (3.74)$$
$$p=-M..M,\ q=1..N$$

3.3.5.2 Azimuthal weighting:

Similarly, when weighting along the azimuthal direction according to the regular overlapping between the t and ϕ functions commented in (3.23), the expression yields

$$\begin{bmatrix} E_\phi^i \\ E_t^i \end{bmatrix}_\phi^{pq} = \left\langle \begin{bmatrix} \vec{E}_\phi^i \\ \vec{E}_t^i \end{bmatrix}, w_q^\phi(t)\hat{\phi}e^{-jp\phi} \right\rangle = \begin{bmatrix} E_\phi^0 \\ E_t^0 \end{bmatrix} \int_{t_{q-1/2}-\Delta_q/2}^{t_{q-1/2}+\Delta_q/2} e^{jkz\cos\sigma_i} \sum_{n=-\infty}^{n=+\infty} j^{+n}J_n(k\rho\sin\sigma_i)dt \int_{-\pi}^{\pi} \hat{u}_\phi \cdot \begin{bmatrix} \hat{\phi}_0 \\ \hat{t}_0 \end{bmatrix} e^{j(n-p)\phi}d\phi \qquad (3.75)$$
$$p=-M..M,\quad q=1..N+1$$

and, thanks to (3.68) and (3.69), we have

$$\left[E_\phi^i\right]_\phi^{pq} = \left\langle \vec{E}_\phi^i, w_q^\phi(t)\hat{\phi}e^{-jp\phi} \right\rangle = E_\phi^0 \int_{t_{q-1/2}-\Delta_q/2}^{t_{q-1/2}+\Delta_q/2} e^{jkz\cos\sigma_i} \sum_{n=-\infty}^{n=+\infty} j^{+n}J_n(k\rho\sin\sigma_i) \left(\int_{-\pi}^{\pi} \hat{u}_\phi \cdot \hat{\phi}_0 e^{j(n-p)\phi}d\phi \right) dt$$
$$= E_\phi^0 \int_{t_{q-1/2}-\Delta_q/2}^{t_{q-1/2}+\Delta_q/2} e^{jkz\cos\sigma_i} \sum_{n=-\infty}^{n=+\infty} j^{+n}J_n(k\rho\sin\sigma_i) \left(\int_{-\pi}^{\pi} \cos\phi e^{j(n-p)\phi}d\phi \right) dt$$
$$= \pi E_\phi^0 \int_{t_{q-1/2}-\Delta_q/2}^{t_{q-1/2}+\Delta_q/2} e^{jkz\cos\sigma_i} \left(j^{p+1}J_{p+1}(k\rho\sin\sigma_i) + j^{p-1}J_{p-1}(k\rho\sin\sigma_i)\right)dt \qquad (3.76)$$

$$\left[E_\phi^i\right]_\phi^{pq} \cong \pi E_\phi^0 e^{jkz_{q-1/2}\cos\sigma_i} \left(j^{p+1}J_{p+1}(k\rho_{q-1/2}\sin\sigma_i) + j^{p-1}J_{p-1}(k\rho_{q-1/2}\sin\sigma_i)\right)\Delta_q \qquad (3.77)$$
$$p=-M..M,\quad q=1..N+1$$

$$\left[E_t^i\right]_\phi^{pq} = \left\langle \vec{E}_t^i, w_q^\phi(t)\hat{\phi}e^{-jp\phi}\right\rangle = E_t^0 \int_{t_{q-1/2}-\Delta_q/2}^{t_{q-1/2}+\Delta_q/2} e^{jkz\cos\sigma_i} \sum_{n=-\infty}^{n=+\infty} j^{+n} J_n(k\rho\sin\sigma_i)\left(\int_{-\pi}^{\pi} \hat{u}_\phi \cdot \hat{t}_0 e^{j(n-p)\phi} d\phi\right) dt$$

$$= E_t^0 \int_{t_{q-1/2}-\Delta_q/2}^{t_{q-1/2}+\Delta_q/2} e^{jkz\cos\sigma_i} \sum_{n=-\infty}^{n=+\infty} j^{+n} J_n(k\rho\sin\sigma_i)\left(-\int_{-\pi}^{\pi} \sin\phi\cos\sigma_i e^{j(n-p)\phi} d\phi\right) dt$$

$$= -\pi E_t^0 \int_{t_{q-1/2}-\Delta_q/2}^{t_{q-1/2}+\Delta_q/2} e^{jkz\cos\sigma_i} j^p \left(J_{p+1}(k\rho\sin\sigma_i) + J_{p-1}(k\rho\sin\sigma_i)\right)\cos\sigma_i dt \tag{3.78}$$

$$\left[E_t^i\right]_\phi^{p,q} \cong -\pi E_t^0 e^{jkz_{q-1/2}\cos\sigma_i} j^p \left(J_{p+1}(k\rho_{q-1/2}\sin\sigma_i) + J_{p-1}(k\rho_{q-1/2}\sin\sigma_i)\right)\cos\sigma_i\Delta_q \tag{3.79}$$

$$p = -M..M, \quad q = 1..N+1$$

3.4 MoM-BoR PeC-MFIE

Let us consider a PeC body of revolution placed in a homogeneous environment. The magnetic field $\vec{H}$ can be expressed -see Chapter 2- according to the Surface Equivalence Theorem, as

$$\left[\vec{H}\left(\vec{J}\right)\right]_{\tan,\vec{r}\in S^-} = 0 \qquad \left[\vec{H}^s\left(\vec{J}\right)\right]_{\tan,\vec{r}\in S^-} = -\left[\vec{H}^i\left(\vec{J}\right)\right]_{\tan,\vec{r}\in S^-} \tag{3.80}$$

where S^- represents the side of the surface where the electromagnetic fields are null.

The scattered field, radiated by the equivalent electric sources, accomplishes

$$\vec{H}^s(\vec{r}) = \frac{1}{\mu}\nabla\times\vec{A}(\vec{r}) \tag{3.81}$$

As in (3.62) with PeC-EFIE, the form of the matrix becomes

$$\begin{bmatrix} \underline{H_t^i}^m \\ \underline{H_\phi^i}^m \end{bmatrix} = \begin{bmatrix} \underline{\underline{Z}}_{t,t'}^{\ m} & \underline{\underline{Z}}_{t,\phi'}^{\ m} \\ \underline{\underline{Z}}_{\phi,t'}^{\ m} & \underline{\underline{Z}}_{\phi,\phi'}^{\ m} \end{bmatrix} \begin{bmatrix} \underline{I_{t'}}^m \\ \underline{I_{\phi'}}^m \end{bmatrix} \qquad m = -M..+M \tag{3.82}$$

where $\underline{\underline{Z}}_{\{t,\phi\},\{t',\phi'\}}^{m}$ follows the general form in (3.21), with a more insidious Kernel dependent on the curl of the integrand.

The expression of the Kernel for the local field coordinates $\{n,\phi,t\}$ stands for

$$\nabla\times\vec{A} = \frac{1}{\rho}\left[\frac{\partial A_t}{\partial\phi} - \frac{\partial(\rho A_\phi)}{\partial t}\right]\hat{u}_n + \left[\frac{\partial A_n}{\partial t} - \frac{\partial A_t}{\partial n}\right]\hat{u}_\phi + \frac{1}{\rho}\left[\frac{\partial(\rho A_\phi)}{\partial n} - \frac{\partial A_n}{\partial\phi}\right]\hat{u}_t \tag{3.83}$$

where, according to the sign assumption for the curl operator with regard to the unit vectors, $\{n,\phi,t\}$ must accomplish, as shown in Fig. 3.1, $\hat{u}_t = \hat{u}_n \times \hat{u}_\phi$. Furthermore, since the weighting is carried out over the surface tangential directions, only the ϕ and t components of $\nabla \times \vec{A}$ need to be computed. Each of the matrices in (3.82) is developed in detail in the following sections with the expanding and weighting functions presented in 3.4.1.

As mentioned in Chapter 2, the PeC-MFIE integral operator has to be tackled by the right development of two parts, which are the singularity integration [4][5] and the Cauchy principal value integration (*PV*). Both developments are carried out respectively in the sections 3.4.2 and 3.4.3.

3.4.1 Discussion about the proper choice of the set of basis functions

Unlike the PeC-EFIE operator, there is no need for the PeC-MFIE operator to let the expanding functions apt for the divergence operator by means of a triangular shape. Therefore, the choice of rectangular pulses for the expanding functions, simpler with regard to programming, should be appropriate:

$$b_n^t(t) = b_n^\phi(t) = \frac{\Pi\left(t - t_{n-1/2}, \Delta_n/2, \Delta_n/2\right)}{\rho} \tag{3.84}$$

This has been very important to ease the entire development of the PeC-MFIE operator, which has been encoded from scratch following the original Gedney and Mittra's ideas for the PeC-EFIE. With the aim of a later generalisation to Dielectrics compatible with the Gedney and Mittra's PeC-EFIE, the most accurate PeC-MFIE version with the rectangular pulses has also been adapted to a triangular shape.

For the sake of simplicity, the weighting functions have been chosen to be the same as the expanding functions.

$$w_n^t(t) = w_n^\phi(t) = \frac{\Pi\left(t - t_{n-1/2}, \Delta_n/2, \Delta_n/2\right)}{\rho} \tag{3.85}$$

3.4.2 PeC-MFIE singularity integration

Being $\left[\vec{B}^{\{t',\phi'\}}(t',\phi')\right]^{mq} = \hat{u}_{\{t',\phi'\}} b_q^{\{t',\phi'\}}(t') e^{jm\phi'}$ any of the expanding functions, when $(\rho',\phi',t') \rightarrow (\rho,\phi,t)$, one can state

$$-\vec{H}^s\left(\left[\vec{B}^{\{t',\phi'\}}(t',\phi')\right]^{mq}\right)\Big|_{\text{sing},\vec{r}\in S^-} = \frac{\Omega_0^-}{4\pi}\hat{n}^- \times \left[\vec{B}^{\{t,\phi\}}(t,\phi)\right]^{mq} = \frac{\Omega_0^-}{4\pi}\left(\hat{n}^- \times \hat{u}_{\{t,\phi\}}\right) b_q^{\{t,\phi\}}(t) e^{jm\phi} \tag{3.86}$$

where $\Omega_0^-, \hat{n}^-$ stand for the solid angle value and the unitary vector normal, in S^-, where the total electromagnetic fields are null.

The impedance elements result from the inner product between (3.86) and the weighting functions $\vec{W}^{\{t,\phi\}}(t,\phi)^{pq} = \vec{W}^{\{t,\phi\}}(t,\phi) = \hat{u}_{\{t,\phi\}} w_q^{\{t,\phi\}}(t) e^{-jp\phi}$. The integration of the singularity must be only considered if the field and the source annuli coincide - $s = q$ -, whereby this contribution becomes

$$\left\langle \left[\vec{W}^r(t,\phi)\right]^{pq}, \frac{\Omega_0^-}{4\pi}\hat{n}^- \times \left[\vec{B}^v(t,\phi)\right]^{mq} \right\rangle = \frac{\Omega_0^-}{4\pi} \int_{t_{q-1/2}}^{t_{q+1/2}} \frac{1}{\rho} \int_0^{2\pi} \left(\hat{u}_r \cdot \left(\hat{n}^- \times \hat{u}_v\right)\right) e^{j(m-p)\phi} d\phi dt \qquad (3.87)$$
$$p = -M..+M \ , \ m = -M..+M \ , \ q = 1..N$$

where r and v stand for the components of the weighting and the expanding functions.

The product $\left(\hat{u}_r \cdot \left(\hat{n}^- \times \hat{u}_v\right)\right)$ is constant along the ϕ direction. Thanks to the orthogonality between harmonic functions, (3.87) becomes expressible as

$$\begin{aligned} \left\langle \vec{W}^r(t,\phi)^{pq}, \frac{\Omega_0^-}{4\pi}\hat{n}^- \times \left[\vec{B}^v(t,\phi)\right]^{mq} \right\rangle &= \frac{\Omega_0^-}{4\pi} \int_{t_{q-1/2}}^{t_{q+1/2}} \frac{\left(\hat{u}_r \cdot \left(\hat{n}^- \times \hat{u}_v\right)\right)}{\rho} \int_0^{2\pi} e^{j(m-p)\phi} d\phi dt \\ &= \frac{\Omega_0^-}{2} \int_{t_{q-1/2}}^{t_{q+1/2}} \frac{\left(\hat{u}_r \cdot \left(\hat{n}^- \times \hat{u}_v\right)\right)}{\rho} dt \delta_{p,m} \end{aligned} \qquad (3.88)$$
$$p = -M..+M \ \ m = -M..+M \ , \ q = 1..N$$

which takes part in the self-impedance terms

$$\left[Z_{r,s'}^m\right]_{\text{sing}}^{q,q} = \frac{\Omega_0^-}{2} \int_{t_{q-1/2}}^{t_{q+1/2}} \frac{\left(\hat{u}_r \cdot \left(\hat{n}^- \times \hat{u}_v\right)\right)}{\rho} dt \qquad (3.89)$$
$$m = -M..+M \ , \ q = 1..N$$

One should remark now on the fact that since $\hat{n}^-$ is perpendicular to either $\hat{u}_t$ or $\hat{u}_\phi$ -see Fig. 3.1- $\hat{u}_t \cdot \left(\hat{n}^- \times \hat{u}_t\right) = \hat{u}_\phi \cdot \left(\hat{n}^- \times \hat{u}_\phi\right) = 0$; therefore,

$$\left[Z_{t,t'}^m\right]_{\text{sing}}^{q,q} = \left[Z_{\phi,\phi'}^m\right]_{\text{sing}}^{q,q} = 0 \qquad (3.90)$$
$$m = -M..+M \ , \ q = 1..N$$

Moreover, for $\left[Z_{t,\phi'}^m\right]_{\text{sing}}^{q,q}$, $\left[Z_{\phi,t'}^m\right]_{\text{sing}}^{q,q}$, the aforementioned cross product is maximum in absolute value. Particularly, in view again of Fig. 3.1 and Fig. 3.4, we note that $\hat{u}_n = \hat{n}^-$ is chosen as general criterion when developing the operators. In accordance with $\hat{u}_t = \hat{u}_n \times \hat{u}_\phi$, assumed in (3.83) , we have $\hat{u}_t \cdot \left(\hat{n}^- \times \hat{u}_\phi\right) = 1$ and $\hat{u}_\phi \cdot \left(\hat{n}^- \times \hat{u}_t\right) = -1$, which lets the contributions due to the integration of the singularity as

$$\left[Z^{m}_{t,\phi'}\right]^{q,q}_{\text{sing}} = \frac{\Omega_0^-}{2}\int_{t_{q-1/2}}^{t_{q+1/2}} \frac{1}{\rho}dt = \pi\int_{t_{q-1/2}}^{t_{q+1/2}} \frac{1}{\rho}dt$$
$$\left[Z^{m}_{\phi,t'}\right]^{q,q}_{\text{sing}} = -\frac{\Omega_0^-}{2}\int_{t_{q-1/2}}^{t_{q+1/2}} \frac{1}{\rho}dt = -\pi\int_{t_{q-1/2}}^{t_{q+1/2}} \frac{1}{\rho}dt \qquad (3.91)$$
$$m = -M..+M\ ,\ q = 1..N$$

where it is assumed $\Omega_0^- = 2\pi$.

Therefore, among the submatrices in (3.82), only $Z^{m}_{t,\phi'}$ and $Z^{m}_{\phi,t'}$ are affected by the integration of the singularity. This is reasonable since the PeC-MFIE operator manages the coupling between a magnetic and an electric source, which is maximum when they are orthogonal. One can likewise notice that these terms, unlike those from 3.4.3, are independent of the mode number.

3.4.3 PeC-MFIE Cauchy principal value raw development

3.4.3.1 Fundamental integrals

The application of the curl operator on the potential vector adds some complication in the computation of the Fourier coefficients. $C_m(t,t')$ -see (3.35)-, which represents the core of all the PeC-EFIE submatrices, becomes also a fundamental integral for the PeC-MFIE.

The application of the curl operator brings about some other basic integrals, which are

$$K_m(t,t') = \int_0^{2\pi} \frac{\partial}{\partial n}\left(\frac{e^{-jkR}}{R}\right)(\xi)e^{-jm\xi}d\xi \qquad (3.92)$$

and

$$R_m(t,t') = \int_0^{2\pi} \frac{\partial}{\partial \phi}\left(\frac{e^{-jkR}}{R}\right)(\xi)e^{-jm\xi}d\xi \qquad (3.93)$$

both of which can be developed in accordance with the chain rule

$$\frac{\partial}{\partial(n\,|\,\phi)}\left(\frac{e^{-jkR}}{R}\right) = \frac{\partial}{\partial R}\left(\frac{e^{-jkR}}{R}\right)\cdot\frac{\partial R}{\partial(n\,|\,\phi)} \qquad (3.94)$$

where

$$\frac{\partial}{\partial R}\left(\frac{e^{-jkR}}{R}\right) = -\frac{e^{-jkR}}{R^2}(jkR+1) \qquad (3.95)$$

♦ $K_m(t,t')$ **development**

$\partial R/\partial n$ can be rewritten at the same time, according to the dependence of the n local component with the co-planar global cylindrical components z and ρ, as

$$\frac{\partial R}{\partial n}=\left(\frac{\partial R}{\partial z}\frac{\partial z}{\partial n}+\frac{\partial R}{\partial \rho}\frac{\partial \rho}{\partial n}\right) \tag{3.96}$$

In view of Fig. 3.4,

$$\frac{\partial z}{\partial n}=-\sin\alpha,\ \frac{\partial \rho}{\partial n}=\cos\alpha \tag{3.97}$$

and each of the partial derivatives yield

$$\begin{aligned}\frac{\partial R}{\partial z}&=\frac{z-z'}{R}\\ \frac{\partial R}{\partial \rho}&=\frac{\rho-\rho'\cos\xi}{R}\end{aligned} \tag{3.98}$$

Hence, (3.94) is readily expressed as

$$\frac{\partial}{\partial n}\left(\frac{e^{-jkR}}{R}\right)=\frac{e^{-jkR(\xi)}}{R(\xi)^3}\left(jkR(\xi)+1\right)\left((\rho'\cos\xi-\rho)\cos\alpha+(z-z')\sin\alpha\right) \tag{3.99}$$

♦ $R_m(t,t')$ **development**

$$\frac{\partial R}{\partial \phi}=\frac{\rho\rho'\sin(\phi-\phi')}{R} \tag{3.100}$$

In this case (3.94) becomes

$$\frac{\partial}{\partial \phi}\left(\frac{e^{-jkR}}{R}\right)=-\frac{e^{-jkR(\xi)}}{R(\xi)^3}\left(jkR(\xi)+1\right)\rho\rho'\sin\xi \tag{3.101}$$

3.4.3.2 t-weighted submatrices: $Z^m_{t,t'}=<t,\mathrm{Hs}(t)>;\ Z^m_{t,\phi'}=<t,\mathrm{Hs}(\phi)>$

♦ **Analytical considerations**

From the t dependent part in (3.83), we have

$$\left[\nabla\times\vec{A}\right]_{\cdot}=\frac{1}{\rho}\left[\frac{\partial(\rho A_{\phi})}{\partial n}-\frac{\partial A_{n}}{\partial\phi}\right]=\frac{1}{\rho}\left[\frac{\partial\rho}{\partial n}A_{\phi}+\rho\frac{\partial A_{\phi}}{\partial n}-\frac{\partial A_{n}}{\partial\phi}\right] \tag{3.102}$$

which implicitly requires the expression of the unit vectors products pairs $\{\hat{u}_{\phi}\hat{u}_{t'}\}$, $\{\hat{u}_{\phi}\hat{u}_{\phi'}\}$, common to PeC-EFIE -see (3.58), (3.59)-, and those only related to PeC-MFIE; that is,

$$\begin{aligned}\{\hat{u}_{n}\hat{u}_{t'}\}&=\begin{bmatrix}\cos\alpha\cos\phi\\ \cos\alpha\sin\phi\\ -\sin\alpha\end{bmatrix}\cdot\begin{bmatrix}\sin\alpha'\cos\phi'\\ \sin\alpha'\sin\phi'\\ \cos\alpha'\end{bmatrix}\\ &=\cos\alpha\sin\alpha'(\cos\phi\cos\phi'+\sin\phi\sin\phi')-\sin\alpha\cos\alpha'\\ &=\cos\alpha\sin\alpha'\cos(\phi-\phi')-\sin\alpha\cos\alpha'\\ &=\cos\alpha\sin\alpha'\cos\xi-\sin\alpha\cos\alpha'\end{aligned} \tag{3.103}$$

$$\begin{aligned}\{\hat{u}_{n}\hat{u}_{\phi'}\}&=\begin{bmatrix}\cos\alpha\cos\phi\\ \cos\alpha\sin\phi\\ -\sin\alpha\end{bmatrix}\cdot\begin{bmatrix}-\sin\phi'\\ \cos\phi'\\ 0\end{bmatrix}=\cos\alpha(-\cos\phi\sin\phi'+\sin\phi\cos\phi')\\ &=\cos\alpha\sin(\phi-\phi')=\cos\alpha\sin\xi\end{aligned} \tag{3.104}$$

- ***t* current component term:** $Z^{m}_{t,t'}=\langle t,\mathrm{Hs}(t)\rangle$

The discretization of the operators yields

$$\left[Z^{m}_{t,t'}\right]^{s,q}_{PV}=-\left\langle\ \hat{u}_{t}\frac{w^{t}_{s}(t)}{\rho}\ ,\ \vec{H}^{s}\left(\frac{\hat{u}_{t}w^{t}_{q}(t')}{\rho'}\right)_{\vec{r}\in S^{-},PV}\right\rangle \tag{3.105}$$

which is partially undertaken for each of the addends in (3.102) in terms of the fundamental integrals (3.35) and (3.92) and according to the rectangular shape of the pulses so that

$$\begin{aligned}&-\left\langle\ \hat{u}_{\phi}\frac{w^{t}_{s}(t)}{\rho}\ ,\ \frac{1}{\mu\rho}\frac{\partial\rho}{\partial n}\vec{A}\left(\hat{u}_{t}\frac{w^{t}_{q}(t')}{\rho'}\right)_{\vec{r}\in S^{-},PV}\right\rangle\\ &\quad=-\frac{\cos\alpha}{4\pi}\int_{t_{s-1/2}}^{t_{s+1/2}}\frac{1}{\rho}\int_{t_{q-1/2}}^{t_{q+1/2}}\left[\int_{0}^{2\pi}G(t,t',\xi)\{\hat{u}_{\phi}\hat{u}_{t'}\}e^{-jm\xi}d\xi\right]dt'\,dt\end{aligned}$$

$$
\begin{aligned}
&= \frac{\cos\alpha}{4\pi} \int_{t_{s-1/2}}^{t_{s+1/2}} \frac{1}{\rho} \int_{t_{q-1/2}}^{t_{q+1/2}} \left[\int_0^{2\pi} G(t,t',\xi) \sin\alpha' \sin\xi e^{-jm\xi} d\xi \right] dt' dt \\
&= \frac{\sin\alpha' \cos\alpha}{4\pi} \int_{t_{s-1/2}}^{t_{s+1/2}} \frac{1}{\rho} \int_{t_{q-1/2}}^{t_{q+1/2}} \left[\frac{G_{m+1}(t,t') - G_{m-1}(t,t')}{2j} \right] dt' dt \\
&\qquad m = -M..+M \;, q = 1..N \;, \; s = 1..N
\end{aligned}
\tag{3.106}
$$

$$
\begin{aligned}
&- \left\langle \; \frac{w_s^t(t)}{\rho} \;,\; \frac{1}{\mu} \left(\frac{\partial \left(\hat{u}_\phi \cdot \vec{A}\left(\hat{u}_{t'} w_q^t(t') / \rho' \right) \right)}{\partial n} \right)_{\vec{r} \in S^-, PV} \; \right\rangle \\
&= -\frac{1}{4\pi} \int_{t_{s-1/2}}^{t_{s+1/2}} \int_{t_{q-1/2}}^{t_{q+1/2}} \left[\int_0^{2\pi} \frac{\partial \left(G\left\{ \hat{u}_\phi \hat{u}_{t'} \right\} \right)(t,t',\xi)}{\partial n} e^{-jm\xi} d\xi \right] dt' dt \\
&= -\frac{1}{4\pi} \int_{t_{s-1/2}}^{t_{s+1/2}} \int_{t_{q-1/2}}^{t_{q+1/2}} \left[\int_0^{2\pi} \frac{\partial G(t,t',\xi)}{\partial n} \left\{ \hat{u}_\phi \hat{u}_{t'} \right\} e^{-jm\xi} d\xi \right] dt' dt \\
&= \frac{1}{4\pi} \int_{t_{s-1/2}}^{t_{s+1/2}} \int_{t_{q-1/2}}^{t_{q+1/2}} \left[\int_0^{2\pi} \frac{\partial G(t,t',\xi)}{\partial n} \sin\alpha' \sin\xi e^{-jm\xi} d\xi \right] dt' dt \\
&= \frac{\sin\alpha'}{4\pi} \int_{t_{s-1/2}}^{t_{s+1/2}} \int_{t_{q-1/2}}^{t_{q+1/2}} \left[\frac{K_{m+1}(t,t') - K_{m-1}(t,t')}{2j} \right] dt' dt \\
&\qquad m = -M..+M \;, \; q = 1..N \;, \; s = 1..N
\end{aligned}
\tag{3.107}
$$

$$
\begin{aligned}
&\left\langle \; \hat{u}_n \frac{w_s^t(t)}{\rho} \;,\; \frac{1}{\mu\rho} \left(\frac{\partial \vec{A}\left(\hat{u}_{t'} w_q^t(t') / \rho' \right)}{\partial \phi} \right)_{\vec{r} \in S^-, PV} \; \right\rangle \\
&= \frac{1}{4\pi} \int_{t_{s-1/2}}^{t_{s+1/2}} \frac{1}{\rho} \int_{t_{q-1/2}}^{t_{q+1/2}} \left[\int_0^{2\pi} \frac{\partial \left(G\left\{ \hat{u}_n \hat{u}_{t'} \right\} \right)}{\partial \phi}(t,t',\xi) e^{-jm\xi} d\xi \right] dt' dt \\
&= \frac{1}{4\pi} \int_{t_{s-1/2}}^{t_{s+1/2}} \frac{1}{\rho} \int_{t_{q-1/2}}^{t_{q+1/2}} \left[\int_0^{2\pi} \frac{\partial G(t,t',\xi)}{\partial \phi} \left\{ \hat{u}_n \hat{u}_{t'} \right\} + G \frac{\partial \left\{ \hat{u}_n \hat{u}_{t'} \right\}(t,t',\xi)}{\partial \phi} e^{-jm\xi} d\xi \right] dt' dt \\
&= \frac{1}{4\pi} \int_{t_{s-1/2}}^{t_{s+1/2}} \frac{1}{\rho} \int_{t_{q-1/2}}^{t_{q+1/2}} \left[\int_0^{2\pi} \frac{\partial G(t,t',\xi)}{\partial \phi} \left(\cos\alpha \sin\alpha' \cos\xi - \sin\alpha \cos\alpha' \right) e^{-jm\xi} d\xi \right] dt' dt \\
&\quad - \frac{\cos\alpha \sin\alpha'}{4\pi} \int_{t_{s-1/2}}^{t_{s+1/2}} \frac{1}{\rho} \int_{t_{q-1/2}}^{t_{q+1/2}} \left[\int_0^{2\pi} G(t,t',\xi) \sin\xi e^{-jm\xi} d\xi \right] dt' dt
\end{aligned}
$$

$$= \frac{\cos\alpha \sin\alpha'}{4\pi} \int_{t_{s-1/2}}^{t_{s+1/2}} \frac{1}{\rho} \int_{t_{q-1/2}}^{t_{q+1/2}} \left[\frac{R_{m+1}(t,t') + R_{m-1}(t,t')}{2} \right] dt'\,dt - \frac{\sin\alpha \cos\alpha'}{4\pi} \int_{t_{s-1/2}}^{t_{s+1/2}} \frac{1}{\rho} \int_{t_{q-1/2}}^{t_{q+1/2}} R_m(t,t')\,dt'\,dt$$

$$- \frac{\cos\alpha \sin\alpha'}{4\pi} \int_{t_{q-1/2}}^{t_{q+1/2}} \frac{1}{\rho} \int_{t_{q-1/2}}^{t_{q+1/2}} \left[\frac{G_{m+1}(t,t') - G_{m-1}(t,t')}{2j} \right] dt'\,dt \qquad (3.10$$

$$m = -M..+M,\ q = 1..N,\ s = 1..N$$

By adding the three previous expressions, we remark that (3.106) is cancelled by the G_m depending part of (3.108), which leads to

$$\left[Z^m_{t,t'} \right]^{s,q}_{PV} = \frac{\sin\alpha'}{8\pi j} \int_{t_{s-1/2}}^{t_{s+1/2}} \int_{t_{q-1/2}}^{t_{q+1/2}} \left[K_{m+1}(t,t') - K_{m-1}(t,t') \right] dt'\,dt$$

$$+ \frac{\cos\alpha \sin\alpha'}{8\pi} \int_{t_{s-1/2}}^{t_{s+1/2}} \frac{1}{\rho} \int_{t_{q-1/2}}^{t_{q+1/2}} \left[R_{m+1}(t,t') + R_{m-1}(t,t') \right] dt'\,dt$$

$$- \frac{\sin\alpha \cos\alpha'}{4\pi} \int_{t_{s-1/2}}^{t_{s+1/2}} \frac{1}{\rho} \int_{t_{q-1/2}}^{t_{q+1/2}} R_m(t,t')\,dt'\,dt \qquad (3.109)$$

$$m = -M..+M,\ q = 1..N,\ s = 1..N$$

- **ϕ current component term: $Z^m_{t,\phi'} = \langle t, \mathrm{Hs}(\phi) \rangle$**

$$\left[Z^m_{t,\phi'} \right]^{s,q}_{PV} = -\left\langle \hat{u}_t \frac{w^t_s(t)}{\rho},\ \vec{H}s\left(\frac{\hat{u}_\phi w^\phi_q(t')}{\rho'} \right)_{\vec{r} \in S^-, PV} \right\rangle \qquad (3.110)$$

$$m = -M..+M,\ q = 1..N,\ s = 1..N$$

can be expressed analogously by means of the three addends:

$$-\left\langle \hat{u}_\phi \frac{w^t_s(t)}{\rho},\ \frac{1}{\mu\rho} \frac{\partial\rho}{\partial n} \vec{A}\left(\hat{u}_\phi \frac{w^\phi_q(t')}{\rho'} \right)_{\vec{r} \in S^-, PV} \right\rangle$$

$$= -\frac{\cos\alpha}{4\pi} \int_{t_{s-1/2}}^{t_{s+1/2}} \frac{1}{\rho} \int_{t_{q-1/2}}^{t_{q+1/2}} \left[\int_0^{2\pi} G(t,t',\xi) \left\{ \hat{u}_\phi \hat{u}_{\phi'} \right\} e^{-jm\xi} d\xi \right] dt'\,dt$$

$$
\begin{aligned}
&= -\frac{\cos\alpha}{4\pi}\int_{t_{s-1/2}}^{t_{s+1/2}}\frac{1}{\rho}\int_{t_{q-1/2}}^{t_{q+1/2}}\left[\int_0^{2\pi} G(t,t',\xi)\cos\xi e^{-jm\xi}d\xi\right]dt'dt \\
&= -\frac{\cos\alpha}{4\pi}\int_{t_{s-1/2}}^{t_{s+1/2}}\frac{1}{\rho}\int_{t_{q-1/2}}^{t_{q+1/2}}\left[\frac{G_{m+1}(t,t')+G_{m-1}(t,t')}{2}\right]dt'dt \qquad (3.111)
\end{aligned}
$$

$$m=-M..+M\ ,\ q=1..N\ ,\ s=1..N$$

$$
\begin{aligned}
&-\left\langle \frac{w_s^t(t)}{\rho}\ ,\ \frac{1}{\mu}\left(\frac{\partial\left(\hat{u}_\phi\cdot\vec{A}\left(\hat{u}_\phi w_q^\phi(t')/\rho'\right)\right)}{\partial n}\right)_{\vec{r}\in S^-,PV}\right\rangle \\
&= -\frac{1}{4\pi}\int_{t_{s-1/2}}^{t_{s+1/2}}\int_{t_{q-1/2}}^{t_{q+1/2}}\left[\int_0^{2\pi}\frac{\partial\left(G\left\{\hat{u}_\phi\hat{u}_{\phi'}\right\}\right)(t,t',\xi)}{\partial n}e^{-jm\xi}d\xi\right]dt'dt \\
&= -\frac{1}{4\pi}\int_{t_{s-1/2}}^{t_{s+1/2}}\int_{t_{q-1/2}}^{t_{q+1/2}}\left[\int_0^{2\pi}\frac{\partial G(t,t',\xi)}{\partial n}\left\{\hat{u}_\phi\hat{u}_{\phi'}\right\}e^{-jm\xi}d\xi\right]dt'dt \\
&= -\frac{1}{4\pi}\int_{t_{s-1/2}}^{t_{s+1/2}}\int_{t_{q-1/2}}^{t_{q+1/2}}\left[\int_0^{2\pi}\frac{\partial G(t,t',\xi)}{\partial n}\cos\xi e^{-jm\xi}d\xi\right]dt'dt \\
&= -\frac{1}{4\pi}\int_{t_{s-1/2}}^{t_{s+1/2}}\int_{t_{q-1/2}}^{t_{q+1/2}}\left[\frac{K_{m+1}(t,t')+K_{m-1}(t,t')}{2}\right]dt'dt \qquad (3.112)
\end{aligned}
$$

$$m=-M..+M\ ,\ q=1..N\ ,\ s=1..N$$

$$
\begin{aligned}
&\left\langle \frac{w_s^t(t)}{\rho}\ ,\ \frac{1}{\mu\rho}\left(\frac{\partial\left(\hat{u}_n\vec{A}\left(\hat{u}_\phi w_q^\phi(t')/\rho'\right)\right)}{\partial\phi}\right)_{\vec{r}\in S^-,PV}\right\rangle \\
&= \frac{1}{4\pi}\int_{t_{s-1/2}}^{t_{s+1/2}}\frac{1}{\rho}\int_{t_{q-1/2}}^{t_{q+1/2}}\left[\int_0^{2\pi}\frac{\partial\left(G\left\{\hat{u}_n\hat{u}_{\phi'}\right\}\right)}{\partial\phi}(t,t',\xi)e^{-jm\xi}d\xi\right]dt'dt \\
&= \frac{1}{4\pi}\int_{t_{s-1/2}}^{t_{s+1/2}}\frac{1}{\rho}\int_{t_{q-1/2}}^{t_{q+1/2}}\left[\int_0^{2\pi}\left[\frac{\partial G(t,t',\xi)}{\partial\phi}\cos\alpha\sin\xi+G\frac{\partial\left\{\hat{u}_{\{n\}}\hat{u}_{\{\phi'\}}\right\}(t,t',\xi)}{\partial\phi}\right]e^{-jm\xi}d\xi\right]dt'dt \\
&= \frac{1}{4\pi}\int_{t_{s-1/2}}^{t_{s+1/2}}\frac{1}{\rho}\int_{t_{q-1/2}}^{t_{q+1/2}}\left[\int_0^{2\pi}\frac{\partial G(t,t',\xi)}{\partial\phi}\cos\alpha\sin\xi e^{-jm\xi}\right]dt'dt \\
&\qquad +\frac{\cos\alpha}{4\pi}\int_{t_{q-1/2}}^{t_{q+1/2}}\frac{1}{\rho}\int_{t_{q-1/2}}^{t_{q+1/2}}\int_0^{2\pi}G(t,t',\xi)\cos\xi e^{-jm\xi}d\xi
\end{aligned}
$$

$$= \frac{\cos\alpha}{4\pi} \int_{t_{s-1/2}}^{t_{s+1/2}} \frac{1}{\rho} \int_{t_{q-1/2}}^{t_{q+1/2}} \left[\frac{R_{m+1}(t,t') - R_{m-1}(t,t')}{2j} \right] dt'\,dt$$

$$+ \frac{\cos\alpha}{4\pi} \int_{t_{q-1/2}}^{t_{q+1/2}} \frac{1}{\rho} \int_{t_{q-1/2}}^{t_{q+1/2}} \left[\frac{G_{m+1}(t,t') + G_{m-1}(t,t')}{2} \right] dt'\,dt \qquad (3.113)$$

$$m = -M..+M,\ q = 1..N,\ s = 1..N$$

and the result of the addition yields

$$\left[Z^{m}_{t,\phi'} \right]^{s,q}_{PV} = -\frac{1}{8\pi} \int_{t_{s-1/2}}^{t_{s+1/2}} \int_{t_{q-1/2}}^{t_{q+1/2}} \left[K_{m+1}(t,t') + K_{m-1}(t,t') \right] dt'\,dt + \frac{\cos\alpha}{8\pi j} \int_{t_{s-1/2}}^{t_{s+1/2}} \frac{1}{\rho} \int_{t_{q-1/2}}^{t_{q+1/2}} \left[R_{m+1}(t,t') - R_{m-1}(t,t') \right] dt'\,dt \qquad (3.114)$$

$$m = -M..+M,\ q = 1..N,\ s = 1..N$$

- **Field integration:**

Both submatrices (3.109) and (3.114) are field integrated with one point at the middle of the field segment s; that is,

$$\left[Z^{m}_{t,t'} \right]^{s,q}_{PV} \cong \frac{\sin\alpha'_q\,\Delta t_s}{8\pi j} \int_{t_{q-1/2}}^{t_{q+1/2}} \left[K_{m+1}(t_s,t') - K_{m-1}(t_s,t') \right] dt' - \frac{\sin\alpha_s \Delta t_s \cos\alpha'_q}{4\pi\rho_s} \int_{t_{q-1/2}}^{t_{q+1/2}} R_m(t_s,t')\,dt'$$

$$+ \frac{\cos\alpha_s \Delta t_s \sin\alpha'_q}{8\pi\rho_s} \int_{t_{q-1/2}}^{t_{q+1/2}} \left[R_{m+1}(t_s,t') + R_{m-1}(t_s,t') \right] dt \qquad (3.115)$$

$$m = -M..+M,\ q = 1..N,\ s = 1..N$$

$$\left[Z^{m}_{t,\phi'} \right]^{s,q}_{PV} \cong -\frac{\Delta t_s}{8\pi} \int_{t_{q-1/2}}^{t_{q+1/2}} \left[K_{m+1}(t_s,t') + K_{m-1}(t_s,t') \right] dt' + \frac{\Delta t_s \cos\alpha_s}{8\pi j \rho_s} \int_{t_{q-1/2}}^{t_{q+1/2}} \left[R_{m+1}(t_s,t') - R_{m-1}(t_s,t') \right] dt' \qquad (3.116)$$

$$m = -M..+M,\ q = 1..N,\ s = 1..N$$

3.4.3.3 ϕ-weighted submatrices: $Z^{m}_{\phi,t'}$= <ϕ,Hs(t)>; $Z^{m}_{\phi,\phi'}$=<ϕ,Hs(ϕ)>

- **Analytical considerations**

The ϕ dependent part in (3.83) is:

$$\left[\nabla \times \vec{A} \right]_{\phi} = \left[\frac{\partial A_n}{\partial t} - \frac{\partial A_t}{\partial n} \right] \qquad (3.117)$$

The unit vectors pairs required are $\{\hat{u}_n\hat{u}_{t'}\}$, $\{\hat{u}_n\hat{u}_{\phi'}\}$, $\{\hat{u}_t\hat{u}_{t'}\}$, $\{\hat{u}_t\hat{u}_{\phi'}\}$ -see (3.103), (3.104), (3.56), (3.57)-.

- ***t* current component term: $Z^m_{\phi,t'}$ =<ϕ,Hs(*t*)>**

The discretization of the operator stands for

$$\left[Z^m_{\phi,t'}\right]^{s,q}_{PV} = -\left\langle \hat{u}_\phi \frac{w^\phi_s(t)}{\rho} \;,\; \vec{H}^s\left(\frac{\hat{u}_t w^{t'}_q(t')}{\rho'}\right)_{\vec{r}\in S^-,PV} \right\rangle \qquad (3.118)$$

$$m=-M..+M,\ q=1..N,\ s=1..N$$

which, in accordance with (3.117), can be computed step by step by means of the addends

$$\begin{aligned}
&-\left\langle \frac{w^\phi_s(t)}{\rho} \;,\; \frac{1}{\mu}\left(\frac{\partial\left(\hat{u}_n\cdot\vec{A}\left(\hat{u}_t w^{t'}_q(t')/\rho'\right)\right)}{\partial t}\right)_{\vec{r}\in S^-,PV} \right\rangle \\
&\quad=\frac{-1}{4\pi}\int_{t_{s-1/2}}^{t_{s+1/2}}\int_{t_{q-1/2}}^{t_{q+1/2}}\left[\int_0^{2\pi}\frac{\partial\left(G\{\hat{u}_n\hat{u}_{t'}\}\right)}{\partial t}(t,t',\xi)e^{-jm\xi}d\xi\right]dt'dt \\
&=\frac{-\cos\alpha\sin\alpha'}{4\pi}\int_{t_{s-1/2}}^{t_{s+1/2}}\int_{t_{q-1/2}}^{t_{q+1/2}}\frac{\partial}{\partial t}\left(\int_0^{2\pi}G(t,t',\xi)\cos\xi e^{-jm\xi}d\xi\right)dt'dt \\
&\quad+\frac{\sin\alpha\cos\alpha'}{4\pi}\int_{t_{s-1/2}}^{t_{s+1/2}}\int_{t_{q-1/2}}^{t_{q+1/2}}\frac{\partial}{\partial t}\left(\int_0^{2\pi}G(t,t',\xi)e^{-jm\xi}d\xi\right)dt'dt \\
&=\frac{-\cos\alpha\sin\alpha'}{4\pi}\int_{t_{s-1/2}}^{t_{s+1/2}}\int_{t_{q-1/2}}^{t_{q+1/2}}\frac{\partial}{\partial t}\left(\frac{G_{m+1}(t,t')+G_{m-1}(t,t')}{2}\right)dt'dt \\
&\quad+\frac{\sin\alpha\cos\alpha'}{4\pi}\int_{t_{s-1/2}}^{t_{s+1/2}}\int_{t_{q-1/2}}^{t_{q+1/2}}\frac{\partial G_m(t,t')}{\partial t}dt'dt
\end{aligned} \qquad (3.119)$$

$$m=-M..+M,\ q=1..N,\ s=1..N$$

and

$$\begin{aligned}
&\left\langle \frac{w^\phi_s(t)}{\rho} \;,\; \frac{1}{\mu}\left(\frac{\partial\left(\hat{u}_{t'}\cdot\vec{A}\left(\hat{u}_{t'} w^{t'}_q(t')/\rho'\right)\right)}{\partial n}\right)_{\vec{r}\in S^-,PV} \right\rangle \\
&\quad=\frac{1}{4\pi}\int_{t_{s-1/2}}^{t_{s+1/2}}\int_{t_{q-1/2}}^{t_{q+1/2}}\left[\int_0^{2\pi}\frac{\partial\left(G\{\hat{u}_{\{t\}}\hat{u}_{\{t'\}}\}\right)}{\partial n}(t,t',\xi)e^{-jm\xi}d\xi\right]dt'dt
\end{aligned}$$

$$= \frac{1}{4\pi} \int_{t_{s-1/2}}^{t_{s+1/2}} \int_{t_{q-1/2}}^{t_{q+1/2}} \left[\int_0^{2\pi} \frac{\partial \left(G(t,t',\xi)(\sin\alpha \sin\alpha' \cos\xi + \cos\alpha \cos\alpha') \right)}{\partial n} e^{-jm\xi} d\xi \right] dt' dt$$

$$= \frac{\sin\alpha \sin\alpha'}{4\pi} \int_{t_{s-1/2}}^{t_{s+1/2}} \int_{t_{q-1/2}}^{t_{q+1/2}} \left(\frac{K_{m+1}(t,t') + K_{m-1}(t,t')}{2} \right) dt' dt \qquad (3.120)$$

$$+ \frac{\cos\alpha \cos\alpha'}{4\pi} \int_{t_{s-1/2}}^{t_{s+1/2}} \int_{t_{q-1/2}}^{t_{q+1/2}} K_m(t,t') dt' dt$$

$$m = -M..+M,\ q = 1..N,\ s = 1..N$$

and the total addition results in

$$\left[Z_{\phi,t'}^{m} \right]_{PV}^{s,q} = \frac{-\cos\alpha \sin\alpha'}{8\pi} \int_{t_{s-1/2}}^{t_{s+1/2}} \frac{\partial}{\partial t} \left(\int_{t_{q-1/2}}^{t_{q+1/2}} \left(G_{m+1}(t,t') + G_{m-1}(t,t') \right) \right) dt' dt$$

$$+ \frac{\sin\alpha \cos\alpha'}{4\pi} \int_{t_{s-1/2}}^{t_{s+1/2}} \frac{\partial}{\partial t} \left(\int_{t_{q-1/2}}^{t_{q+1/2}} G_m(t,t') \right) dt' dt$$

$$+ \frac{\sin\alpha \sin\alpha'}{8\pi} \int_{t_{s-1/2}}^{t_{s+1/2}} \int_{t_{q-1/2}}^{t_{q+1/2}} \left(K_{m+1}(t,t') + K_{m-1}(t,t') \right) dt' dt$$

$$+ \frac{\cos\alpha \cos\alpha'}{4\pi} \int_{t_{s-1/2}}^{t_{s+1/2}} \int_{t_{q-1/2}}^{t_{q+1/2}} K_m(t,t') dt' dt \qquad (3.121)$$

$$m = -M..+M,\ q = 1..N,\ s = 1..N$$

- **ϕ current component term: $Z_{\phi,\phi'}^{m}$=<ϕ,Hs(ϕ)>**

$$\left[Z_{\phi,\phi'}^{m} \right]_{PV}^{s,q} = -\left\langle \hat{u}_\phi \frac{w_s^\phi(t)}{\rho},\ \vec{H}^s \left(\frac{\hat{u}_\phi w_q^\phi(t')}{\rho'} \right)_{\vec{r} \in S^-, PV} \right\rangle \qquad (3.122)$$

$$m = -M..+M,\ q = 1..N,\ s = 1..N$$

and again by dividing the development into two steps according to (3.117), we have

$$-\left\langle \frac{w_s^\phi(t)}{\rho},\ \frac{1}{\mu} \left(\frac{\partial \left(\hat{u}_n \cdot \vec{A}\left(\hat{u}_\phi w_q^\phi(t') / \rho' \right) \right)}{\partial t} \right)_{\vec{r} \in S^-, PV} \right\rangle$$

$$= \frac{-1}{4\pi} \int_{t_{s-1/2}}^{t_{s+1/2}} \int_{t_{q-1/2}}^{t_{q+1/2}} \left[\int_0^{2\pi} \frac{\partial \left(G\left\{ \hat{u}_{\{n\}} \hat{u}_{\{\phi'\}} \right\} \right)}{\partial t}(t,t',\xi) e^{-jm\xi} d\xi \right] dt' dt$$

$$
\begin{aligned}
&= \frac{-\cos\alpha}{4\pi} \int_{t_{s-1/2}}^{t_{s+1/2}} \int_{t_{q-1/2}}^{t_{q+1/2}} \frac{\partial}{\partial t} \left(\int_0^{2\pi} G(t,t',\xi) \sin\xi e^{-jm\xi} d\xi \right) dt' dt \\
&= \frac{-\cos\alpha}{4\pi} \int_{t_{s-1/2}}^{t_{s+1/2}} \int_{t_{q-1/2}}^{t_{q+1/2}} \frac{\partial}{\partial t} \left(\frac{G_{m+1}(t,t') - G_{m-1}(t,t')}{2j} \right) dt' dt \\
&\qquad\qquad m = -M..+M,\ q = 1..N,\ s = 1..N
\end{aligned}
\tag{3.123}
$$

and

$$
\begin{aligned}
&\left\langle \frac{w_s^{\phi}(t)}{\rho},\ \frac{1}{\mu} \left(\frac{\partial \left(\hat{u}_t \cdot \vec{A}\left(\hat{u}_{\phi'} w_q^{\phi}(t') / \rho' \right) \right)}{\partial n} \right)_{\vec{r} \in S^-, PV} \right\rangle \\
&= \frac{1}{4\pi} \int_{t_{s-1/2}}^{t_{s+1/2}} \int_{t_{q-1/2}}^{t_{q+1/2}} \left[\int_0^{2\pi} \frac{\partial \left(G\{\hat{u}_{\{t\}} \hat{u}_{\{\phi'\}}\} \right)}{\partial n} (t,t',\xi) e^{-jm\xi} d\xi \right] dt' dt \\
&= \frac{-\sin\alpha}{4\pi} \int_{t_{s-1/2}}^{t_{s+1/2}} \int_{t_{q-1/2}}^{t_{q+1/2}} \left[\int_0^{2\pi} \frac{\partial G(t,t',\xi)}{\partial n} \sin\xi e^{-jm\xi} d\xi \right] dt' dt \\
&= \frac{-\sin\alpha}{4\pi} \int_{t_{s-1/2}}^{t_{s+1/2}} \int_{t_{q-1/2}}^{t_{q+1/2}} \left[\int_0^{2\pi} \frac{\partial \left(G(t,t',\xi) \sin\xi \right)}{\partial n} e^{-jm\xi} d\xi \right] dt' dt \\
&= \frac{-\sin\alpha}{4\pi} \int_{t_{s-1/2}}^{t_{s+1/2}} \int_{t_{q-1/2}}^{t_{q+1/2}} \left(\frac{K_{m+1}(t,t') - K_{m-1}(t,t')}{2j} \right) dt' dt \\
&\qquad\qquad m = -M..+M,\ q = 1..N,\ s = 1..N
\end{aligned}
\tag{3.124}
$$

and the total addition yields

$$
\begin{aligned}
\left[Z_{\phi,\phi'}^{m} \right]_{PV}^{s,q} &= \frac{-\cos\alpha}{8\pi j} \int_{t_{s-1/2}}^{t_{s+1/2}} \frac{\partial}{\partial t} \left(\int_{t_{q-1/2}}^{t_{q+1/2}} \left(G_{m+1}(t,t') - G_{m-1}(t,t') \right) dt' \right) dt \\
&\quad - \frac{\sin\alpha}{8\pi j} \int_{t_{s-1/2}}^{t_{s+1/2}} \int_{t_{q-1/2}}^{t_{q+1/2}} \left(K_{m+1}(t,t') - K_{m-1}(t,t') \right) dt' dt \\
&\qquad\qquad m = -M..+M,\ q = 1..N,\ s = 1..N
\end{aligned}
\tag{3.125}
$$

- **Field integration:**

The first $\partial / \partial t$ dependent term in the expressions (3.121) and (3.125) can be easily simplified by means of the field integration since, in general,

$$
\int_{t_0}^{t_1} \frac{\partial F}{\partial t} dt = F(t) \Big|_{t_0}^{t_1} = F(t_1) - F(t_0) \tag{3.126}
$$

The second term of (3.121) and (3.125) is field-integrated through a field point in the middle of the s field-segment, analogously to (3.115) and (3.116).

Therefore, the expression of both submatrices $Z^m_{\phi,t'}, Z^m_{\phi,\phi'}$ stands for

$$\begin{aligned}
\left[Z^m_{\phi,t'}\right]^{s,q}_{PV} = & \frac{-\cos\alpha_s \sin\alpha'_q}{8\pi}\left[\int_{t_{q-1/2}}^{t_{q+1/2}}\left(G_{m+1}(t_{s+1/2},t')+G_{m-1}(t_{s+1/2},t')\right)dt'\right. \\
& \left. -\int_{t_{q-1/2}}^{t_{q+1/2}}\left(G_{m+1}(t_{s-1/2},t')+G_{m-1}(t_{s-1/2},t')\right)dt'\right] \\
& +\frac{\sin\alpha_s \cos\alpha'_q}{4\pi}\left[\int_{t_{q-1/2}}^{t_{q+1/2}} G_m(t_{s+1/2},t')dt' - \int_{t_{q-1/2}}^{t_{q+1/2}} G_m(t_{s-1/2},t')dt'\right] \\
& +\frac{\sin\alpha_s \Delta t_s \sin\alpha'_q}{8\pi}\int_{t_{q-1/2}}^{t_{q+1/2}}\left(K_{m+1}(t_s,t')+K_{m-1}(t_s,t')\right)dt' \\
& +\frac{\cos\alpha_s \Delta t_s \cos\alpha'_q}{4\pi}\int_{t_{q-1/2}}^{t_{q+1/2}} K_m(t_s,t')dt' \qquad (3.127) \\
& \qquad m=-M..+M,\ q=1..N,\ s=1..N
\end{aligned}$$

$$\begin{aligned}
\left[Z^m_{\phi,\phi'}\right]^{s,q}_{PV} = & \frac{-\cos\alpha_s}{8\pi j}\left[\int_{t_{q-1/2}}^{t_{q+1/2}}\left(G_{m+1}(t_{s+1/2},t')-G_{m-1}(t_{s+1/2},t')\right)dt'\right. \\
& \left. -\int_{t_{q-1/2}}^{t_{q+1/2}}\left(G_{m+1}(t_{s-1/2},t')-G_{m-1}(t_{s-1/2},t')\right)dt'\right] \\
& -\frac{\Delta t_s \sin\alpha_s}{8\pi j}\int_{t_{q-1/2}}^{t_{q+1/2}}\left(K_{m+1}(t_s,t')-K_{m-1}(t_s,t')\right)dt' \qquad (3.128) \\
& \qquad m=-M..+M,\ q=1..N,\ s=1..N
\end{aligned}$$

The ξ-even or odd characteristic of the integrand prevails in m. Particularly, according to the ξ-even property of the integrands in $K_m(t,t')$ and in $G_m(t,t')$ and the ξ-odd behaviour of the integrand in $R_m(t,t')$, these fundamental integrals accomplish $K_m(t,t') = K_{-m}(t,t')$, $G_m(t,t') = G_{-m}(t,t')$ and $R_m(t,t') = -R_{-m}(t,t')$. If we inspect the expressions of (3.115), (3.116), (3.127), (3.128), one can easily infer

$$\begin{aligned}
\underline{\underline{Z}}_{t,t'}{}^{m} &= -\underline{\underline{Z}}_{t,t'}{}^{-m}, & \underline{\underline{Z}}_{\phi,\phi'}{}^{m} &= -\underline{\underline{Z}}_{\phi,\phi'}{}^{-m} \\
\underline{\underline{Z}}_{t,\phi'}{}^{m} &= \underline{\underline{Z}}_{t,\phi'}{}^{-m}, & \underline{\underline{Z}}_{\phi,t'}{}^{m} &= \underline{\underline{Z}}_{\phi,t'}{}^{-m}
\end{aligned} \qquad (3.129)$$

which are antagonistic with the properties of the PeC-EFIE -see (3.63)- and are reasonable because the electromagnetic coupling is best when the magnetic field and the electric current are perpendicular and null when they are parallel.

3.4.3.4 Extraction of the ξ-singularity

By watching the submatrices expressions from (3.115), (3.116), (3.127), (3.128), one realises that the fundamental terms from page 70 must be source-integrated along the t' direction. As in 3.3.1 for the PeC-EFIE, the terms of highest order from PeC-MFIE must be accurately integrated. It is thus required a precise analytic integration.

Meanwhile $G_m(t,t')$, present in (3.127) and (3.128), is managed as described 3.3.1 for the PeC-EFIE, the extraction of the highest order addends for the other fundamental terms $K_m(t,t')$ -(3.115), (3.116), (3.127), (3.128)- and $R_m(t,t')$ -(3.115), (3.116)- needs to be effectuated.

Starting from the expressions

$$\begin{aligned} K_m(t,t') &= \int_0^{2\pi} \frac{\partial}{\partial n}\left(\frac{e^{-jkR}}{R}\right)(\xi)e^{-jm\xi}d\xi \\ &= \int_0^{2\pi} \frac{e^{-jkR(\xi)}}{R(\xi)^3}\left(jkR(\xi)+1\right)\left((\rho'\cos\xi-\rho)\cos\alpha+(z-z')\sin\alpha\right)e^{-jm\xi}d\xi \end{aligned} \tag{3.130}$$

$$R_m(t,t') = \int_0^{2\pi} \frac{\partial}{\partial \phi}\left(\frac{e^{-jkR}}{R}\right)(\xi)e^{-jm\xi}d\xi = -\int_0^{2\pi} \frac{e^{-jkR(\xi)}}{R(\xi)^3}(jkR(\xi)+1)\rho\rho'\sin\xi e^{-jm\xi}d\xi \tag{3.131}$$

both of which contain in $(e^{-kR}/R^3)(jkR+1)$ the high order dependence. This expression allows the definition of a still more fundamental integration $T_m(t,t')$,

$$T_m(t,t') = -\int_0^{2\pi} \frac{1}{R}\frac{\partial}{\partial R}\left(\frac{e^{-jkR}}{R}\right)(\xi)e^{-jm\xi}d\xi = \int_0^{2\pi} \frac{e^{-jkR(\xi)}}{R(\xi)^3}\left(jkR(\xi)+1\right)e^{-jm\xi}d\xi \tag{3.132}$$

from which $K_m(t,t')$ and $R_m(t,t')$ can be derived in view of the properties from (3.60) and (3.61)

$$\begin{aligned} K_m(t,t') &= \cos\alpha\left[\rho'\left(\frac{T_{m+1}(t,t')+T_{m-1}(t,t')}{2}\right)-\rho T_m(t,t')\right]+\sin\alpha(z-z')T_m(t,t') \\ R_m(t,t') &= -\rho\rho'\left(\frac{T_{m+1}(t,t')-T_{m-1}(t,t')}{2j}\right) \end{aligned} \tag{3.133}$$

The $T_m(t,t')$ high-order terms when $R \to 0$ can be found thanks to the Taylor expansion,

$$\begin{aligned} \frac{e^{-jkR}}{R^3}(jkR+1) &= \frac{1-jkR-(k^2R^2/2)+j(k^3R^3/6)+\ldots}{R^3}(jkR+1) \\ &= \frac{1+k^2R^2-(k^2R^2/2)-jk^3R^3/2+jk^3R^3/6-k^4R^4/6+\ldots}{R^3} \end{aligned}$$

$$= \frac{1+(k^2R^2/2)-jk^3R^3/3-k^4R^4/6+\ldots}{R^3} = \frac{1}{R^3}+\frac{k^2}{2}\frac{1}{R}-j\frac{k^3}{3}+o(R) \qquad (3.134)$$

which sets perfectly the singularity extraction as

$$T_m(t,t') = \left[\int_0^{2\pi} \frac{e^{-jkR(\xi)}}{R(\xi)^3}\left(jkR(\xi)+1\right)-\frac{1}{R^3}-\frac{k^2}{2}\frac{1}{R}\right]e^{-jm\xi}d\xi + \underbrace{\int_0^{2\pi}\frac{e^{-jm\xi}}{R^3}d\xi}_{\Psi_m} + \frac{k^2}{2}\underbrace{\int_0^{2\pi}\frac{e^{-jm\xi}}{R}d\xi}_{\phi_m} \qquad (3.135)$$

As in the approach of Gedney and Mittra for PeC-EFIE -page 56-, the first integral, with a low order dependence on R, can be accomplished through the very efficient FFT, due to the circular symmetry of the integrand. Nonetheless, the two other steep-varying terms need to be analytically computed to make the singularity extraction feasible.

Meanwhile the recurrent computation on Φ_m is well-known since it is the same used in the PeC-EFIE, one should expect an analogous recurrent development for Ψ_m. Mr. Joaquim Fortuny, with whom the author of this dissertation Thesis worked during a stage of three months in the Joint Research Centre, has figured out a recurrent formulation analogous to the one developed by Gedney and Mittra.

Indeed, because of the even symmetry of $1/R^3$, Ψ_m is expressible as

$$\Psi_m(t,t') = \int_{-\pi}^{\pi}\frac{e^{-jm\xi}}{R^3(\xi)}d\xi = \int_{-\pi}^{\pi}\frac{\cos(m\xi)}{R^3(\xi)}d\xi = 2\int_0^{\pi}\frac{\cos(m\xi)}{R^3(\xi)}d\xi \qquad (3.136)$$

and in an analogous way to (3.39),

$$\Psi_m(t,t') = \frac{4}{R_1^3}\int_0^{\pi/2}\frac{\cos(2m\varphi)}{\left[1+\beta_1^2\sin^2\varphi\right]^{3/2}}d\varphi \qquad (3.137)$$

where $R_1 = \left[\left(\rho-\rho'^2\right)+\left(z-z'^2\right)\right]^{1/2}$, $\beta_1^2 = \frac{4\rho\rho'}{R_1^2}$ are t and t' dependent parameters that do not interfere with the φ-angular integration.

According to the same cosinus expansion from (3.40), one can readily express

$$\Psi_m = \frac{4}{R_1^3}\sum_{k=1}^{m+1}\Psi_k^m N_{\alpha(k,m)} \qquad (3.138)$$

where

$$N_{\alpha(k,m)} = \int_0^{\pi/2}\frac{\cos^{\alpha}\varphi}{\left[1+\beta_1^2\sin^2\varphi\right]^{3/2}}d\varphi \qquad (3.139)$$

and the analytical expressions for N_0 and N_2 stand for -see Appendix B-

$$N_0 = \frac{1}{\left(1+\beta_1^2\right)^{1/2}} E\left(\beta_1^2/(1+\beta_1^2)\right) \tag{3.140}$$

$$N_2 = -\frac{1}{\beta_1^2(1+\beta_1^2)^{1/2}} K\left(\beta_1^2/(1+\beta_1^2)\right) + \frac{(1+\beta_1^2)^{1/2}}{\beta_1^2} E\left(\beta_1^2/(1+\beta_1^2)\right) \tag{3.141}$$

$N_{\alpha(k,m)}$ are convenient since, as shown in the Appendix B, one can readily compute them through the recurrent relation $\forall \alpha \geq 4$, from the above-presented analytical expressions for N_0 and N_2

$$N_\alpha = \left(\frac{\alpha-2}{\alpha-3}\right)\left(\frac{\alpha-4}{\alpha-2} + \beta_1^{-2} + 1\right) N_{\alpha-2} - \left(\beta_1^{-2}+1\right) N_{\alpha-4} \tag{3.142}$$

The limitations about the validity of this recurrent formulation are the same as those expounded in 3.3.2 for the PeC-EFIE and I_α.

3.4.3.5 Extraction of the *t*-singularity

The singularity extraction is completed with the precise integration along *t*. It is carried out a Gaussian quadrature rule for the contributions of the contour source segments different to the field segment -non singular terms-. When the field and source annuli coincide ($R_1 \to 0, \beta_1^2 \to \infty, \beta_1/\left(1+\beta_1^2\right)^{1/2} \to 1$), an analytical integration of the singular terms of the integrand must be undertaken.

The behaviour around the singularity ($\rho \to \rho', z \to z'$) for each mode eventually depends, through the recurrent expression in (3.142), on the elementary integrals $(4/R_1^3)N_0$ and $(4/R_1^3)N_2$ when updated in the fundamental *t*-integrands present in (3.115), (3.116), (3.127), (3.128): $K_m(t,t')$, $R_m(t,t')$ and $G_m(t,t')$.

The highest-order characteristic of both elementary integrals -outstanding when R_1 approaching zero-, is -see (3.47)-

$$v_0 = \left\{\frac{4N_0}{R_1^3}\right\}(R_1 \to 0) = \frac{4R_1}{R_1^3\left(4\rho\rho'+R_1^2\right)^{1/2}} E(1) \xrightarrow[R_1 \to 0]{} \frac{2}{R_1^2[\rho\rho']^{1/2}} \tag{3.143}$$

$$v_2 = \left\{\frac{4N_2}{R_1^3}\right\}(R_1 \to 0) = \frac{1}{\rho\rho'(4\rho\rho'+R_1^2)^{1/2}} \ln(R_1) + \frac{(4\rho\rho'+R_1^2)^{1/2}}{\rho\rho' R_1^2} E(1)$$

$$\downarrow$$

$$\frac{1}{2(\rho\rho')^{3/2}} \ln(R_1) + \frac{2}{R_1^2(\rho\rho')^{1/2}} \tag{3.144}$$

In the following section, it is shown how the first term of (3.144) turns out to be not even singular since the contribution of the rest of the terms makes up for the singularity of $\ln(R_1)$. One can see hence that the singular behaviour of both expressions when tending closely to the field point is the same for the second term of v_2 -of considerable higher order than $\ln(R_1)$- and v_0. As $\rho'=\rho$ is completely assumable inside a segment portion very close to ρ, the highest order terms in $(4/R_1^3)N_0$ and in $(4/R_1^3)N_2$ accomplish

$$v_0 = v_2 = \frac{2}{\rho R_1^2} \tag{3.145}$$

which accordingly agrees with the singular terms in $(4/R_1)I_0$ and $(4/R_1)I_2$ becoming coincident when $R_1 \to 0$.

Likewise, for the integrals with $\alpha \geq 4$, in view of (3.142), we have

$$\begin{aligned} v_\alpha &= \left\{ \left(\frac{\alpha-2}{\alpha-3} \right) \left(\frac{\alpha-4}{\alpha-2} + \beta_1^{-2} + 1 \right) N_{\alpha-2} - \left(\frac{1+\beta_1^2}{\beta_1^2} \right) N_{\alpha-4} \right\} \left(R_1 \to 0; \beta_1^2 \to \infty \right) \\ &= 2 \left(\frac{\alpha-2}{\alpha-3} \right) \left(\frac{\alpha-3}{\alpha-2} \right) v_{\alpha-2} - v_{\alpha-4} = 2v_{\alpha-2} - v_{\alpha-4} \end{aligned} \tag{3.146}$$

and since $v_0 = v_2$, it can be shown $\forall \alpha$

$$v_\alpha = \ldots = v_2 = v_0 \tag{3.147}$$

which makes sense since the order of the singularity must not change when increasing the mode number.

The computation of $\Psi_m(R_1 \to 0)$ is then easily accomplished

$$\Psi_m(R_1 \to 0) = \sum_{k=1}^{m+1} \Psi_k^m v_\alpha = v_\alpha \sum_{k=1}^{m+1} \Psi_k^m = v_\alpha \qquad \forall m \tag{3.148}$$

which is analogous to (3.54).

The analysis of the behaviour of the t'-integrand in the proximity of the singularity for the general expressions of the submatrices in (3.115), (3.116), (3.127), (3.128) requires the thorough analysis of the expressions $G_m(t,t')$, $R_m(t,t')$ and $K_m(t,t')$ when $R_1 \to 0$.

- **$G_m(t,t')$ in the vicinity of the singularity**

  $G_m(t,t')$, $G_{m-1}(t,t')$ and $G_{m+1}(t,t')$ appear only in the expressions (3.127) and (3.128). The behaviour of all these expressions when $R_1 \to 0$ has already been analysed in detail for the PeC-EFIE operator, as shown in (3.53), which leads to

$$G_m(R_1 \to 0) = G_{m+1}(R_1 \to 0) = G_{m-1}(R_1 \to 0) = \chi_0 \tag{3.149}$$

When inserting this in the part of (3.127) depending on G_m, G_{m+1} and G_{m-1}, taking for granted the fact that for the self-annulus contribution $s = q$, we can infer

$$\frac{-\cos\alpha_s \sin\alpha'_q}{4\pi}\int_{t_{q-1/2}}^{t_{q+1/2}}(\chi_0(t'\to t_{s+1/2})-\chi_0(t'\to t_{s-1/2}))dt' + \frac{\sin\alpha_s \cos\alpha'_q}{4\pi}\int_{t_{q-1/2}}^{t_{q+1/2}}(\chi_0(t'\to t_{s+1/2})-\chi_0(t'\to t_{s-1/2}))dt' = 0 \qquad (3.150)$$

$$m = -M..+M,\ q = s = 1..N$$

Likewise, the introduction of (3.149) in the proper part of (3.128) yields

$$\frac{-\cos\alpha_s}{8\pi j}\left[\int_{t_{q-1/2}}^{t_{q+1/2}}(\chi_0(t'\to t_{s+1/2})-\chi_0(t'\to t_{s+1/2}))dt' - \int_{t_{q-1/2}}^{t_{q+1/2}}(\chi_0(t'\to t_{s-1/2})-\chi_0(t'\to t_{s-1/2}))dt'\right] = 0 \qquad (3.151)$$

$$m = -M..+M,\ q = s = 1..N$$

- **$R_m(t,t')$ in the vicinity of the singularity**

The insertion of $\Psi_m(R_1 \to 0)$ in $R_m(t,t')$ - (3.131) and (3.133) – also produces a zero

$$R[\Psi]_m(R_1 \to 0) = -\rho\rho'\left(\frac{\Psi_{m+1}(R_1 \to 0') - \Psi_{m-1}(R_1 \to 0)}{2j}\right) = 0 \qquad (3.152)$$

- **$K_m(t,t')$ in the vicinity of the singularity**

Of course the t'-integration must be completed by the terms expounded in (3.133), so that the total expression of the integrand depending on Ψ_m yields

$$K[\Psi]_m = \cos\alpha\left[\rho'\left(\frac{\Psi_{m+1}(t,t') + \Psi_{m-1}(t,t')}{2}\right) - \rho\Psi_m(t,t')\right] + \sin\alpha(z-z')\Psi_m(t,t') \qquad (3.153)$$

which, when $R_1 \to 0$ and considering (3.148), becomes

$$K[\Psi]_m(R_1 \to 0) = \cos\alpha\cdot\left[\rho'\left(\frac{\nu_\alpha + \nu_\alpha}{2}\right) - \rho\nu_0\right] + \sin\alpha\cdot(z-z')\nu_0 = \cos\alpha\cdot(\rho'-\rho)\nu_0 - \sin\alpha\cdot(z'-z)\nu_0 \qquad (3.154)$$

The key terms $(\rho-\rho')$ and $(z-z')$ enable v_α to be integrated along t' and account for the cancellation of the singularity coming from $\ln R_1$ in (3.144) when $R_1 \to 0$.

The analytic integration of the products $(\rho-\rho')v_0$ and $(z-z')v_0$ along the generating arc, with 0 corresponding to the field point and t_-, t_+ being the distances from the segment ends to the field point, can be carried out trough

$$\begin{aligned}\frac{2}{\rho}\int_{-t_-}^{t_+}\frac{t'}{t'^2}dt' &= \frac{2}{\rho}\int_{-t_-}^{t_+}\frac{dt'}{t'} = \lim_{\varepsilon\to 0}\frac{2}{\rho}\left[\int_{-t_-}^{-\varepsilon}\frac{dt'}{t'}+\int_{+\varepsilon}^{t_+}\frac{dt'}{t'}dt'\right]\\ &= \lim_{\varepsilon\to 0}\frac{2}{\rho}\left[-\int_{\varepsilon}^{t_-}\frac{dt'}{t'}+\int_{\varepsilon}^{t_+}\frac{dt'}{t'}\right] = \lim_{\varepsilon\to 0}\frac{2}{\rho}\left[-[\ln t']_{\varepsilon}^{t_-}+[\ln t']_{\varepsilon}^{t_+}\right]\\ &= \frac{2}{\rho}\ln\frac{t_+}{t_-}\end{aligned} \qquad (3.155)$$

since $(\rho-\rho')=-t\cdot\sin\alpha$, $(z-z')=t'\cdot\cos\alpha$ and $R_1=|t|$ -see Fig. 4.5-.

The t-integration of (3.155) derived from the weighting yields zero. Indeed, let us take a number of points symmetrically distributed along the t-segment, one compensates the contribution of its symmetric point; particularly, in the mid point of the segment (3.155) is zero.

Therefore, the highest order self-annulus contribution, which is to be the most relevant, is null for all the submatrices, since $K_m(R_1\to 0), R_m(R_1\to 0)$ and $G_m(R_1\to 0)$ yield zero. A Gaussian quadrature rule may thus be sufficient to tackle the t' integration.

In any case, the numerical integration of the rest of low order terms on the self-annulus contribution for each mode through the division of the t'-segment according to the procedure described in Fig. 3.3 brings about worse results for all the examples tested. As a matter of fact, the results turn out best whenever these low order contributions are set to zero.

3.4.4 Improvement of the PeC-MFIE accuracy

The PeC-MFIE operator was first programmed according to the expression of the submatrices in (3.115), (3.116), (3.127) and (3.128). This first raw version, though, when compared with the PeC-EFIE [12] results -spheres and cylinders- proved to be highly inaccurate -only some good accuracy was achieved for the very high ξ-frequency modes, which are actually those that present a negligible contribution for the current-. Therefore, with the further goal of developing a BoR-operator for dielectrics, it was first required to improve the accuracy of the PeC-MFIE operator by modifying this first raw PeC-MFIE formulation. In view of the good performance of the PeC-EFIE -it relies only on $R^{-1}(t,t',\xi)$ integrals-, some procedures have been implemented to compute alternatively the Fourier coefficients of the PeC-MFIE in order to lessen the order of the integration

3.4.4.1 The $\frac{\partial()}{\partial\phi}$ dependence in <t,Hs(t)>, <t,Hs(φ)>

The fundamental integration in (3.93), $R_m(t,t')$, can be fully simplified by integrating by parts; indeed,

$$\begin{aligned} R_m(t,t') &= \int_0^{2\pi} \frac{\partial}{\partial\phi}\left(\frac{e^{-jkR}}{R}\right)(\xi)e^{-jm\xi}d\xi = \int_0^{2\pi} \frac{\partial}{\partial(\phi-\phi')}\left(\frac{e^{-jkR}}{R}\right)(\xi)e^{-jm\xi}d\xi \\ &= \int_0^{2\pi} \frac{\partial}{\partial\xi}\left(\frac{e^{-jkR}}{R}\right)(\xi)e^{-jm\xi}d\xi = \frac{e^{-jkR(\xi)}}{R(\xi)}e^{-jm\xi}\Big|_0^{2\pi} - \int_0^{2\pi}(-jm)\frac{e^{-jkR(\xi)}}{R(\xi)}e^{-jm\xi}d\xi \end{aligned} \tag{3.156}$$

which yields

$$R_m(t,t') = \int_0^{2\pi} jm\frac{e^{-jkR(\xi)}}{R(\xi)}e^{-jm\xi} = jm\cdot G_m(t,t') \qquad m=-M..+M \tag{3.157}$$

Thanks to this change, the results improve considerably. From an integral, see (3.131), with dependence on $R^{-3}(t',t,\xi)$ we pass to an equivalent expression that relies on a smoother $R^{-1}(t',t,\xi)$. This modification affects only the submatrices $Z^m_{t,t'}, Z^m_{t,\phi'}$, whose expressions -see (3.115) and (3.116)- can now be rewritten as follows

$$\begin{aligned} \left[Z^m_{t,t'}\right]^{s,q}_{PV} \cong{}& \frac{\sin\alpha'_q\,\Delta t_s}{8\pi j}\int_{t_{q-1/2}}^{t_{q+1/2}}\left[K_{m+1}(t_s,t')-K_{m-1}(t_s,t')\right]dt' - jm\frac{\sin\alpha_s\Delta t_s\cos\alpha'_q}{4\pi\rho_s}\int_{t_{q-1/2}}^{t_{q+1/2}}G_m(t,t')dt' \\ &+\frac{j\cos\alpha_s\Delta t_s\sin\alpha'_q}{8\pi\rho_s}\int_{t_{q-1/2}}^{t_{q+1/2}}\left[(m+1)G_{m+1}(t_s,t')+(m-1)G_{m-1}(t_s,t')\right]dt \end{aligned} \tag{3.158}$$

$$m=-M..+M,\ q=1..N,\ s=1..N$$

$$\begin{aligned} \left[Z^m_{t,\phi'}\right]^{s,q}_{PV} \cong{}& -\frac{\Delta t_s}{8\pi}\int_{t_{q-1/2}}^{t_{q+1/2}}\left[K_{m+1}(t_s,t')+K_{m-1}(t_s,t')\right]dt' \\ &+\frac{\Delta t_s\cos\alpha_s}{8\pi\rho_s}\int_{t_{q-1/2}}^{t_{q+1/2}}\left[(m+1)G_{m+1}(t_s,t')-(m-1)G_{m-1}(t_s,t')\right]dt' \end{aligned} \tag{3.159}$$

$$m=-M..+M,\ q=1..N,\ s=1..N$$

3.4.4.2 The terms $\sin\xi \cdot \partial(\ )/\partial n$ in the odd submatrices <t,Hs(t)>, <ϕ,Hs(ϕ)>

The m-odd characteristic of the submatrices $Z^m_{t,t'}$ and $Z^m_{\phi,\phi'}$ derives from the product of a sinus by a term with ξ-even behaviour. The expressions (3.128) and (3.158) implicitly show the presence of such term through $[K_{m+1}(t,t')-K_{m-1}(t,t')]/(2j)$, which corresponds to -see (3.92)-

$$\frac{[K_{m+1}(t,t')-K_{m-1}(t,t')]}{2j}=\int_0^{2\pi}\sin\xi\,\frac{\partial}{\partial n}\left(\frac{e^{-jkR}}{R}\right)e^{-jm\xi}d\xi \qquad m=-M..+M \tag{3.160}$$

Resorting to (3.99) and (3.101), the integrand in (3.157) can be equivalently expressed as

$$\sin\xi\,\frac{\partial}{\partial n}\left(\frac{e^{-jkR}}{R}\right)=-\frac{\partial}{\partial\phi}\left(\frac{e^{-jkR}}{R}\right)\frac{((\rho'\cos\xi-\rho)\cos\alpha+(z-z')\sin\alpha)}{\rho\rho'} \tag{3.161}$$

which is readily integrated taking into account the previous section -see (3.156)-

$$\int_0^{2\pi}\sin\xi\,\frac{\partial}{\partial n}\left(\frac{e^{-jkR}}{R}\right)e^{-jm\xi}d\xi=-\cos\alpha\left(\frac{(j(m+1)G_{m+1}(t,t')+j(m-1)G_{m-1}(t,t'))}{2\rho}-\frac{jmG_m}{\rho'}\right)$$
$$-\frac{(z-z')\sin\alpha}{\rho\rho'}jmG_m(t,t') \qquad m=-M..+M \tag{3.162}$$

This is again a very advantageous expression since it is removed the dependence on $R^{-3}(t',t,\xi)$ inherent to $K_m(t,t')$. A lower order dependence - $R^{-1}(t',t,\xi)$ - appears instead in $G_m(t,t')$, $G_{m+1}(t,t')$ and $G_{m-1}(t,t')$. This second modification has lessened significantly the error, but still an error has remained for the low ξ-frequency current modes, which present the uppermost values.

The introduction of (3.162) in (3.158) and in (3.128) yield the new expressions for $Z^m_{t,t'}$ and $Z^m_{\phi,\phi'}$, that the author of this dissertation Thesis considers definitive because they only depend on G_{m-1}, G_m and G_{m+1}, as in the well behaving PeC-EFIE operator.

$$\left[Z^m_{t,t'}\right]^{s,q}_{PV}\cong -j\frac{\sin\alpha'_q\cos\alpha_s\Delta t_s}{8\pi\rho_s}\int_{t_{q-1/2}}^{t_{q+1/2}}((m+1)G_{m+1}(t_s,t')+(m-1)G_{m-1}(t_s,t'))dt'$$
$$+jm\frac{\sin\alpha'_q\cos\alpha_s\Delta t_s}{4\pi}\int_{t_{q-1/2}}^{t_{q+1/2}}\frac{G_m(t_s,t')}{\rho'}dt'$$
$$-jm\frac{\sin\alpha'_q\sin\alpha_s\Delta t_s}{4\pi\rho_s}\int_{t_{q-1/2}}^{t_{q+1/2}}\frac{(z_s-z')G_m(t_s,t')}{\rho'}dt'$$

$$-jm\frac{\sin\alpha_s\Delta t_s\cos\alpha'_q}{4\pi\rho_s}\int_{t_{q-1/2}}^{t_{q+1/2}}G_m(t_s,t')dt'$$
$$+j\frac{\cos\alpha_s\Delta t_s\sin\alpha'_q}{8\pi\rho_s}\int_{t_{q-1/2}}^{t_{q+1/2}}\left[(m+1)G_{m+1}(t_s,t')+(m-1)G_{m-1}(t_s,t')\right]dt \qquad (3.163)$$
$$m=-M..+M,\ q=1..N,\ s=1..N$$

$$\left[Z^m_{\phi,\phi'}\right]^{s,q}_{PV}=\frac{-\cos\alpha_s}{8\pi j}\left[\int_{t_{q-1/2}}^{t_{q+1/2}}\left(G_{m+1}(t_{s+1/2},t')-G_{m-1}(t_{s+1/2},t')\right)dt'\right.$$
$$\left.-\int_{t_{q-1/2}}^{t_{q+1/2}}\left(G_{m+1}(t_{s-1/2},t')-G_{m-1}(t_{s-1/2},t')\right)dt'\right]$$
$$+j\frac{\Delta t_s\cos\alpha_s\sin\alpha_s}{8\pi\rho_s}\int_{t_{q-1/2}}^{t_{q+1/2}}\left((m+1)G_{m+1}(t_s,t')+(m-1)G_{m-1}(t_s,t')\right)dt'$$
$$-jm\frac{\Delta t_s\cos\alpha_s\sin\alpha_s}{4\pi}\int_{t_{q-1/2}}^{t_{q+1/2}}\frac{G_m(t_s,t')}{\rho'}dt'$$
$$+jm\frac{\Delta t_s\sin^2\alpha_s}{4\pi\rho_s}\int_{t_{q-1/2}}^{t_{q+1/2}}\frac{(z_s-z')}{\rho'}G_m(t_s,t')dt' \qquad (3.164)$$
$$m=-M..+M,\ q=1..N,\ s=1..N$$

3.4.4.3 The terms $\sin\xi\cdot\partial()/\partial R$ in the even submatrices <*t*,Hs(*t*)>, <ϕ,Hs(ϕ)>

The submatrices $Z^m_{t,\phi'}$ and $Z^m_{\phi,t'}$, with m-even characteristic because their integrand is ξ-even, cannot in principle take advantage of the equality in (3.162). The corresponding expressions (3.159) and (3.127) still show dependence on $R^{-3}(t',t,\xi)$ due to the product $\cos\xi\cdot\partial()/\partial n$, which results in $[K_{m+1}(t,t')+K_{m-1}(t,t')]/2$. A detailed development of this expression -see (3.132)- leads to

$$\frac{[K_{m+1}(t,t')+K_{m-1}(t,t')]}{2}=\int_0^{2\pi}\cos\xi\frac{\partial}{\partial n}\left(\frac{e^{-jkR}}{R}\right)e^{-jm\xi}d\xi$$
$$=-\int_0^{2\pi}\cos\xi\frac{1}{R}\frac{\partial}{\partial R}\left(\frac{e^{-jkR}}{R}\right)(\xi)\left((\rho'\cos\xi-\rho)\cos\alpha+(z-z')\sin\alpha\right)e^{-jm\xi}d\xi$$
$$=-\int_0^{2\pi}\frac{1}{R}\frac{\partial}{\partial R}\left(\frac{e^{-jkR}}{R}\right)(\xi)\left((\rho'\cos^2\xi-\rho\cos\xi)\cos\alpha+(z-z')\sin\alpha\cos\xi\right)e^{-jm\xi}d\xi$$

$$
\begin{aligned}
&= -\rho'\cos\alpha \int_0^{2\pi} \frac{1}{R}\frac{\partial}{\partial R}\left(\frac{e^{-jkR}}{R}\right)(\xi)\cos^2\xi e^{-jm\xi}d\xi + \rho\cos\alpha \int_0^{2\pi} \frac{1}{R}\frac{\partial}{\partial R}\left(\frac{e^{-jkR}}{R}\right)(\xi)\cos\xi e^{-jm\xi}d\xi \\
&\qquad -(z-z')\sin\alpha \int_0^{2\pi} \frac{1}{R}\frac{\partial}{\partial R}\left(\frac{e^{-jkR}}{R}\right)(\xi)\cos\xi e^{-jm\xi}d\xi \\
&= -\rho'\cos\alpha \int_0^{2\pi} \frac{1}{R}\frac{\partial}{\partial R}\left(\frac{e^{-jkR}}{R}\right)(\xi)\cos^2\xi e^{-jm\xi}d\xi \\
&\qquad +\left((z-z')\sin\alpha - \rho\cos\alpha\right)\frac{\left[T_{m+1}(t,t')+T_{m-1}(t,t')\right]}{2}
\end{aligned}
\tag{3.165}
$$

The first addend can be straightforwardly computed, as a rule of thumb, as

$$
\begin{aligned}
-\int_0^{2\pi} \frac{1}{R}\frac{\partial}{\partial R}\left(\frac{e^{-jkR}}{R}\right)(\xi)\cos^2\xi e^{-jm\xi}d\xi &= -\int_0^{2\pi} \frac{1}{R}\frac{\partial}{\partial R}\left(\frac{e^{-jkR}}{R}\right)(\xi)\frac{(1+\cos 2\xi)}{2}e^{-jm\xi}d\xi \\
&= \frac{1}{2}\left[T_m(t,t') + \frac{T_{m+2}(t,t')+T_{m-2}(t,t')}{2}\right]
\end{aligned}
\tag{3.166}
$$

But this does not provide any improvement on the order of integration. Nonetheless, as in (3.161), through the comparison of (3.132) and (3.101) one can write

$$
\sin\xi \frac{1}{R}\frac{\partial}{\partial R}\left(\frac{e^{-jkR}}{R}\right) = \frac{\partial}{\partial\phi}\left(\frac{e^{-jkR}}{R}\right)\frac{1}{\rho\rho'}
\tag{3.167}
$$

which enables some modification on the first term of (3.165) by means of the well-known trigonometric fundamental identity

$$
\begin{aligned}
-\int_0^{2\pi} \frac{1}{R}\frac{\partial}{\partial R}\left(\frac{e^{-jkR}}{R}\right)(\xi)\cos^2\xi e^{-jm\xi}d\xi &= -\int_0^{2\pi} \frac{1}{R}\frac{\partial}{\partial R}\left(\frac{e^{-jkR}}{R}\right)(\xi)\left(1-\sin^2\xi\right)e^{-jm\xi}d\xi \\
&= T_m(t,t') + \frac{1}{\rho\rho'}\int_0^{2\pi} \frac{\partial}{\partial\phi}\left(\frac{e^{-jkR}}{R}\right)(\xi)\sin\xi e^{-jm\xi}d\xi
\end{aligned}
\tag{3.168}
$$

which, referring again

(3.157), becomes

$$
-\int_0^{2\pi} \frac{1}{R}\frac{\partial}{\partial R}\left(\frac{e^{-jkR}}{R}\right)(\xi)\cos^2\xi e^{-jm\xi}d\xi = T_m(t,t') + \frac{\left((m+1)G_{m+1}(t,t')-(m-1)G_{m-1}(t,t')\right)}{2\rho\rho'}
\tag{3.169}
$$

which lets the original $\cos\xi \cdot \partial()/\partial n$ product expressed in terms of $T_m(t,t')$, $T_{m+1}(t,t')$, $T_{m-1}(t,t')$ -with still a $R^{-3}(t,t',\xi)$ influence- and $G_{m+1}(t,t')$, $G_{m-1}(t,t')$, which compensate the contribution to the error due to $T_{m-2}(t,t')$ and $T_{m+2}(t,t')$.

The final expression for $Z^m_{t,\phi'}$ thus stands for

$$\begin{aligned}\left[Z^m_{t,\phi'}\right]^{s,q}_{PV} \cong & -\frac{\Delta t_s \cos\alpha_s}{4\pi}\int_{t_{q-1/2}}^{t_{q+1/2}} \rho' T_m(t_s,t')dt' \\ & -\frac{\Delta t_s \cos\alpha_s}{8\pi\rho_s}\int_{t_{q-1/2}}^{t_{q+1/2}} \left[(m+1)G_{m+1}(t_s,t')-(m-1)G_{m-1}(t_s,t')\right]dt' \\ & -\frac{\Delta t_s \cos\alpha_s\left(z_s\sin\alpha_s-\rho_s\cos\alpha_s\right)}{8\pi}\int_{t_{q-1/2}}^{t_{q+1/2}} \left(T_{m+1}(t_s,t')+T_{m-1}(t_s,t')\right)dt' \\ & +\frac{\Delta t_s \cos\alpha_s \sin\alpha_s}{8\pi}\int_{t_{q-1/2}}^{t_{q+1/2}} z'\left[T_{m+1}(t_s,t')+T_{m-1}(t_s,t')\right]dt' \\ & +\frac{\Delta t_s \cos\alpha_s}{8\pi\rho_s}\left[(m+1)\int_{t_{q-1/2}}^{t_{q+1/2}} G_{m+1}(t_s,t')dt' -(m-1)\int_{t_{q-1/2}}^{t_{q+1/2}} G_{m-1}(t_s,t')dt'\right] \\ & \qquad\qquad m=-M..+M,\ q=1..N,\ s=1..N\end{aligned} \tag{3.170}$$

where the dependence on G_{m+1} and G_{m-1} disappears, so that

$$\begin{aligned}\left[Z^m_{t,\phi'}\right]^{s,q}_{PV} \cong & -\frac{\Delta t_s \cos\alpha_s}{4\pi}\int_{t_{q-1/2}}^{t_{q+1/2}} \rho' T_m(t_s,t')dt' \\ & -\frac{\Delta t_s \cos\alpha_s\left(z_s\sin\alpha_s-\rho_s\cos\alpha_s\right)}{8\pi}\int_{t_{q-1/2}}^{t_{q+1/2}} \left(T_{m+1}(t_s,t')+T_{m-1}(t_s,t')\right)dt' \\ & +\frac{\Delta t_s \cos\alpha_s \sin\alpha_s}{8\pi}\int_{t_{q-1/2}}^{t_{q+1/2}} z'\left[T_{m+1}(t_s,t')+T_{m-1}(t_s,t')\right]dt' \\ & \qquad\qquad m=-M..+M,\ q=1..N,\ s=1..N\end{aligned} \tag{3.171}$$

Analogously, the final expression for $Z^m_{\phi,t'}$ yields

$$\begin{aligned}\left[Z^m_{\phi,t'}\right]^{s,q}_{PV} = & \frac{-\cos\alpha_s \sin\alpha'_q}{8\pi}\left[\int_{t_{q-1/2}}^{t_{q+1/2}} \left(G_{m+1}(t_{s+1/2},t')+G_{m-1}(t_{s+1/2},t')\right)dt'\right. \\ & \left. -\int_{t_{q-1/2}}^{t_{q+1/2}} \left(G_{m+1}(t_{s-1/2},t')+G_{m-1}(t_{s-1/2},t')\right)dt'\right]\end{aligned}$$

$$
\begin{aligned}
&+\frac{\sin\alpha_s\cos\alpha'_q}{4\pi}\left[\int_{t_{q-1/2}}^{t_{q+1/2}} G_m(t_{s+1/2},t')dt' - \int_{t_{q-1/2}}^{t_{q+1/2}} G_m(t_{s-1/2},t')dt'\right] \\
&+\frac{\sin^2\alpha_s\Delta t_s\sin\alpha'_q}{8\pi}\int_{t_{q-1/2}}^{t_{q+1/2}} (z-z')\left[T_{m+1}(t_s,t')+T_{m-1}(t_s,t')\right]dt' \\
&-\frac{\rho_s\sin\alpha_s\cos\alpha_s\Delta t_s\sin\alpha'_q}{8\pi}\int_{t_{q-1/2}}^{t_{q+1/2}} \left[T_{m+1}(t_s,t')+T_{m-1}(t_s,t')\right]dt' \\
&+\frac{\sin\alpha_s\cos\alpha_s\sin\alpha'_q\Delta t_s}{4\pi}\int_{t_{q-1/2}}^{t_{q+1/2}} \rho' T_m(t_s,t')dt' \\
&+\frac{\sin\alpha_s\cos\alpha_s\sin\alpha'_q\Delta t_s}{8\pi\rho_s}\left[(m+1)\int_{t_{q-1/2}}^{t_{q+1/2}} G_{m+1}(t_s,t')dt' - (m-1)\int_{t_{q-1/2}}^{t_{q+1/2}} G_{m-1}(t_s,t')dt'\right] \\
&+\frac{\cos^2\alpha_s\Delta t_s\cos\alpha'_q}{8\pi}\int_{t_{q-1/2}}^{t_{q+1/2}} \rho'\left(T_{m-1}(t_s,t')+T_{m+1}(t_s,t')\right)dt' \\
&-\frac{\rho_s\cos^2\alpha_s\Delta t_s\cos\alpha'_q}{4\pi}\int_{t_{q-1/2}}^{t_{q+1/2}} T_m(t_s,t')dt' \\
&+\frac{\sin\alpha_s\cos\alpha_s\Delta t_s\cos\alpha'_q}{4\pi}\int_{t_{q-1/2}}^{t_{q+1/2}} (z_s-z')T_m(t_s,t')dt'
\end{aligned}
\qquad (3.172)
$$

$$m=-M..+M,\ q=1..N,\ s=1..N$$

In accordance with the good behaviour of PeC-EFIE, it would have been better for all the PeC-MFIE submatrices to depend only on $G_m(t,t')$, $G_{m+1}(t,t')$ and $G_{m-1}(t,t')$. However, this has not been achieved for the m-even matrices $Z^m_{t,\phi'}$ and $Z^m_{\phi,t'}$. So, the author of this dissertation Thesis attributes the partial disagreement between PeC-MFIE and PeC-EFIE - more precise terms about this dissimilarity are expounded in Chapter 4- to the presence of $T_m(t,t')$, $T_{m+1}(t,t')$ and $T_{m-1}(t,t')$ in $Z^m_{t,\phi'}$ and $Z^m_{\phi,t'}$. Unfortunately, any attempt to compute differently these fundamental integrals so that the error declined has turned out fruitless.

3.4.4.4 Symmetry derived from the reciprocity theorem on <t,Hs(ϕ)>, <ϕ,Hs(t)>

As the m-even submatrices $Z^m_{t,\phi'}$ and $Z^m_{\phi,t'}$ cannot be fully corrected, the author of this dissertation Thesis has figured out a procedure, later to the computation of the matrices, to reduce the error. The reciprocity theorem between $\vec{J}^q$ and $\vec{M}^s$-arbitrary magnetic and electric source currents respectively over the surface elements S^q and S^s - yields [5]:

$$\int_{S^q}\vec{E}^s\cdot\vec{J}^q dS' = -\int_{S^s}\vec{H}^q\cdot\vec{M}^s dS' \qquad (3.173)$$

where $\vec{E}^s$ and $\vec{H}^q$ are the electric and magnetic fields due to $\vec{M}^s$ and $\vec{J}^q$.

According to the definition of the dielectric operators effectuated in Chapter 2, this expression can be rewritten in terms of the PeC-operators as

$$-\int_{S^q} \vec{H}^{PEC}(\vec{M}^s)\cdot\vec{J}^q dS' = -\int_{S^s} \vec{H}^{PEC}(\vec{J}^q)\cdot\vec{M}^s dS' \tag{3.174}$$

According to the definitions in (3.3), and deliberately choosing the same mode number m for both sets of functions so as to render a non-null weighting, we have

$$\int_{S^q} \vec{H}^{PEC}\left(\hat{u}_\phi w_s^\phi(t)e^{-jm\phi}\right)\cdot\hat{u}_{t'}w_q^{t'}(t)e^{-jm\phi'}dS' = \int_{S^s} \vec{H}^{PEC}(\hat{u}_{t'}w_q^{t'}(t)e^{-jm\phi'})\cdot\hat{u}_\phi w_s^\phi(t)e^{-jm\phi}dS \tag{3.175}$$
$$m=-M..+M,\ q=1..N,\ s=1..N$$

which consequently relates the impedance elements of $Z^m_{t,\phi'}$ and $Z^m_{\phi,t'}$ as

$$\left[Z^m_{\phi,t'}\right]^{s,q} = \left[Z^m_{\phi,t'}\right]^{q,s} \tag{3.176}$$
$$m=-M..+M,\ q=1..N,\ s=1..N, s\neq q$$

In view of this, the two insidious submatrices $Z^m_{t,\phi'}$ and $Z^m_{\phi,t'}$ are transposed when $s\neq q$ [11]. As both matrices are affected by the same error but with completely different formulations, one might think that it could be possible to lessen the error by either substituting one matrix by the other or by replacing both of them by a new equivalent matrix that was a weighted average of both.

This post-correction has turned out quite helpful for those cases where the error, though not negligible, was not very high; for instance, for the mode $m=0$. However, for those low ξ-frequency modes where the error is already too high, the post-correction becomes useless.

3.4.5 Incident field expansion

The incident magnetic field expansion can be easily deduced from the incident electric field expansion presented in 3.3.5. By means of the well-known property regarding plane waves $\hat{e}_i = \hat{h}_i \times \hat{k}_i$, one can determine straightforwardly the independent terms - $\underline{H}_t^{i^m}$, $\underline{H}_\phi^{i^m}$ - of the system in (3.82), for each of the two canonical perpendicular directions $\hat{t}_0$ and $\hat{\phi}_0$.

According to the unit vectors triad choice referred in Fig. 3.5, the correspondence of the H-components with each of the incident E-components yields

[11] As it will be shown in detail later in Chapter 6, although the expression in (3.175), derived from the Reciprocity Theorem, is true $\forall s,q$, the relation in (3.176) is only true when $s\neq q$, which affects the terms due to the Cauchy Principal Value.

$$\begin{aligned} &\text{if } \hat{h}_i = \hat{t}_0 \;\Rightarrow\; \hat{e}_i = \hat{t}_0 \times \hat{k}_i = -\hat{\phi}_0 \\ &\text{if } \hat{h}_i = \hat{\phi}_0 \;\Rightarrow\; \hat{e}_i = \hat{\phi}_0 \times \hat{k}_i = \hat{t}_0 \end{aligned} \tag{3.177}$$

which accordingly lets the final weighted incident H-components defined in terms of the weighted E-components -see 3.3.5- as

$$\left[H_t^i\right]_s^{p,q} = -\frac{\left[E_\phi^i\right]_s^{p,q}}{\eta_0}; \qquad \left[H_\phi^i\right]_s^{p,q} = \frac{\left[E_t^i\right]_s^{p,q}}{\eta_0} \tag{3.178}$$
$$p = -M..M,\ q = 1..N$$

where η_0 stands for the free-space impedance and s can be any of the weighting dimensions - t or ϕ-. Note that in the PeC-MFIE operator, as mentioned in 3.4.1, $q = 1..N$ for both components.

Chapter 4 RESULTS FOR PEC BODIES OF REVOLUTION

4.1 PEC-EFIE RESULTS

For a closed PeC-cylinder of radius 2λ and height 2λ, under an incident plane wave with $\sigma_i = 45°$ and $\phi_i = 90°$, it is presented the bistatic cross section in Fig. 4.1 and Fig. 4.2 -scanned along the observation plane placed at $\phi_{obs} = 60°$-, and the current components along the generating arc: $J_t(\phi = 0)$ -Fig. 4.3- and $J_\phi(\phi = \pi/2)$ -Fig. 4.4-. The discretization parameters are: $N_\phi = 60$, $N_{\text{modes}} = 2M + 1 = 31$ and $N_{FFT} = 128$. To confirm the good behaviour of the PeC-EFIE code, it is compared with some reference results in [12].

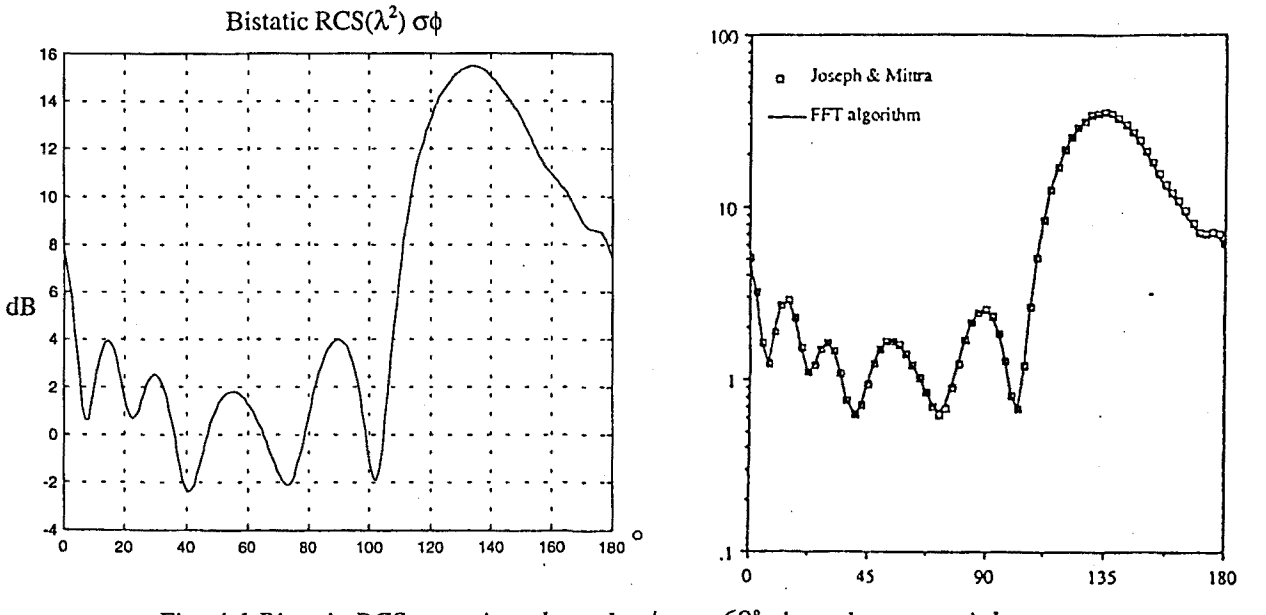

Fig. 4.1 Bistatic RCS scanning along the $\phi_{obs} = 60°$ plane the tangential component

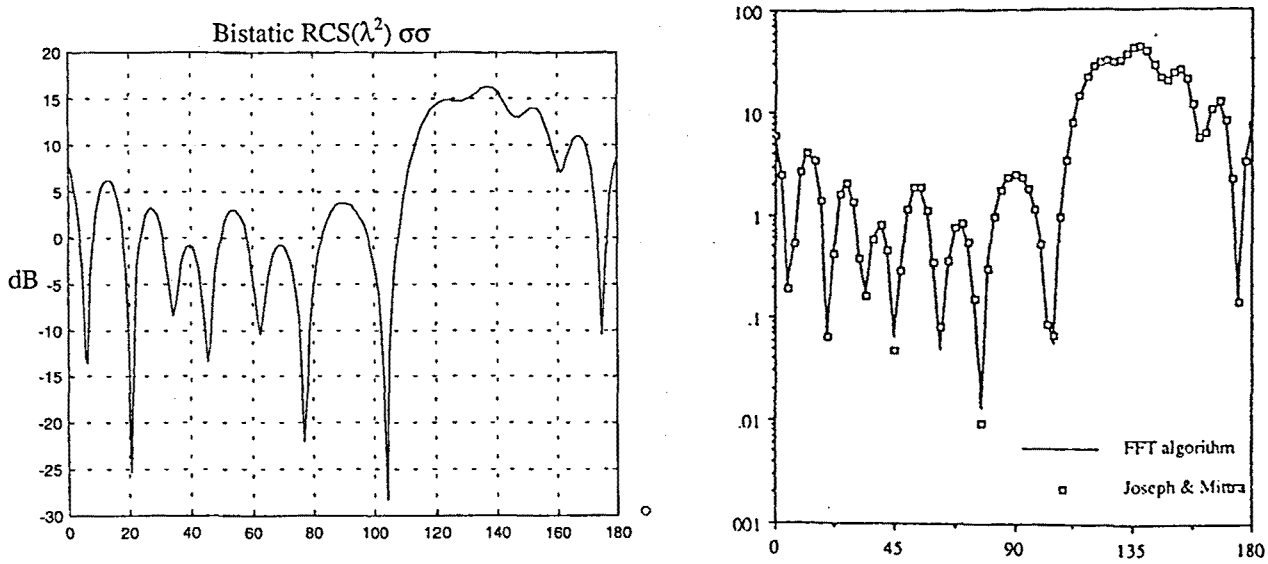

Fig. 4.2 Bistatic RCS scanning along the $\phi_{obs} = 60°$ plane the ϕ-component

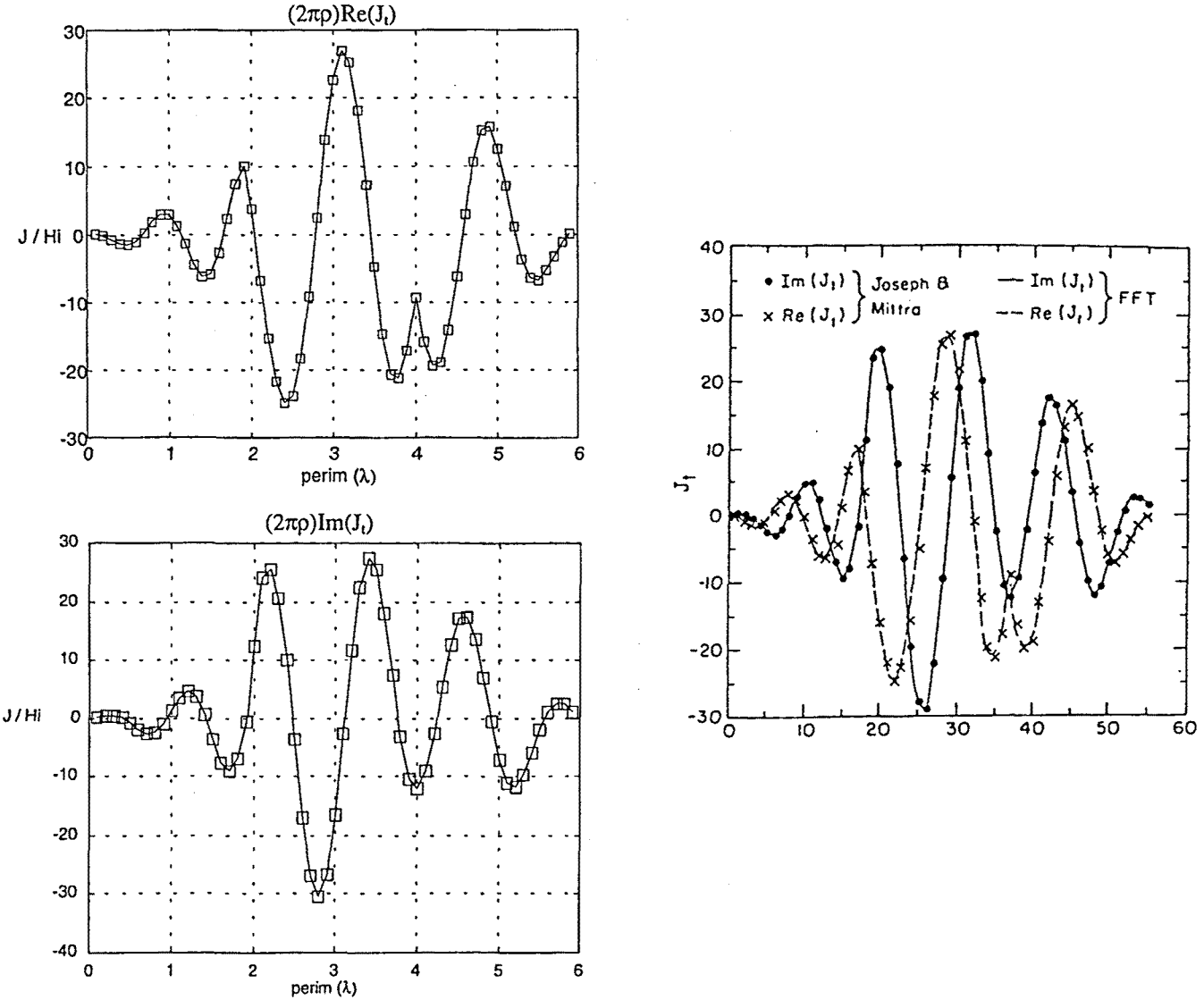

Fig. 4.3 J_t current component along the generating arc $(\phi = 0)$

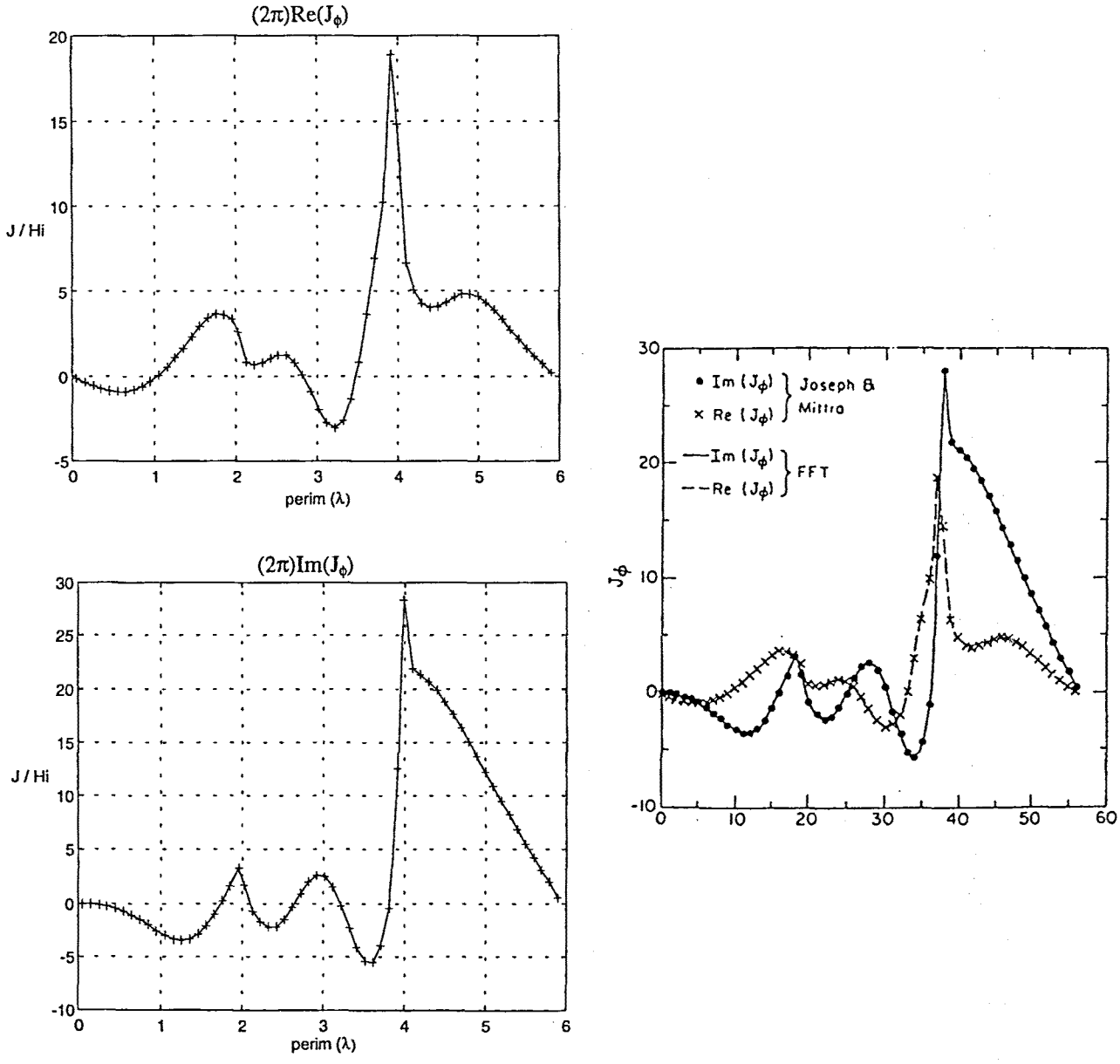

Fig. 4.4 J_ϕ current component along the generating arc $(\phi = \pi/2)$

4.2 NATURE OF THE PEC-MFIE MISBEHAVIOUR

Along the study of the PeC-MFIE in Chapter3, many clues have suggested that the computation of $T_m(t,t')$, $T_{m+1}(t,t')$ and $T_{m-1}(t,t')$ are the bottleneck in the development of this operator. According to the changes described so far, the fundamental integrals $R_m(t,t')$, $[K_{m+1}(t,t') - K_{m-1}(t,t')]$ and $[T_{m+1}(t,t') - T_{m-1}(t,t')]$, depending on $R^{-3}(t,t',\xi)$, are not precise enough because they cannot reproduce the better numerical results coming from the analytical equivalent expressions on $G_{m+1}(t,t')$ and $G_{m-1}(t,t')$ -see the sections 3.4.4.1, 3.4.4.2 and 3.4.4.3-. Hence, for the remaining $R^{-3}(t,t',\xi)$-terms in the definitive

version of the PeC-MFIE $T_m(t,t')$, $T_{m+1}(t,t')$ and $T_{m-1}(t,t')$, the numerical integration along t' and the analytical integration along ξ are to be likewise unsatisfactory.

The accurate computation of $K_m(t,t')$ has appeared to me as very complicated since the integrand at near distances becomes quickly very high and the integral must even yield a finite value. This tends to compensate the contribution of the symmetric source-annulus at the other side of the field point, according to the $(\rho'-\rho, z'-z)$-odd characteristic. Moreover, the computation of this integral for different modes aggravates the problem since a harmonic modulation must be allowed for along ξ.

Some changes have been carried out with the aim to improve the accuracy on the computation of K_m although in the end none of them improved the results for the formulation presented in (3.163), (3.164), (3.171) and (3.172).

1. It has been developed another recurrent formula for $K_m(t,t')$ -in an analogous way as in the appendices- using an equivalent mathematical expression for $\partial R/\partial n$;

$$\begin{aligned}\frac{\partial R}{\partial n} &= -(\rho'\cos\xi-\rho_s)\cos\alpha-(z_s-z')\sin\alpha \\ &= \left(-(\rho'-\rho_s)\cos^2(\xi/2)+(\rho'+\rho_s)\sin^2(\xi/2)\right)\cos\alpha+(z'-z_s)\sin\alpha\end{aligned} \tag{4.1}$$

The consequent integrals along t' are tackled numerically for the addend of $(\rho'+\rho_s)$, which shows a much comparatively lower order. The high-order integrals $(\rho-\rho')/R_1^2(t,t')$ and $(z-z')/R_1^2(t,t')$, present in the other two addends, can be carried out analytically; as a matter of fact, the analytical t-integration for the self-segment influence in (3.155) is a particular case. Indeed, by means of the expression of R_1, $(\rho'-\rho_s)$ and $(z'-z_s)$ in terms of the parameters presented in Fig. 4.5

$$\begin{aligned}&\rho'-\rho_s=\rho'-\rho_0+\rho_0-\rho_s=t'\sin\alpha+P_0\sin\beta=t'\sin\alpha-P_0\cos\alpha \\ &z'-z_s=z'-z_0+z_0-z_s=-t'\cos\alpha+P_0\cos\beta=-t'\cos\alpha+P_0\sin\alpha \\ &R_1=\left[(\rho_s-\rho')^2+(z_s-z')^2\right]^{1/2}=\left[t'^2+P_0^2\right]^{1/2}\end{aligned} \tag{4.2}$$

the elementary high-order integrals thus become

$$\int_{t^-}^{t^+}\frac{(\rho'-\rho_s)}{R_1^2}dt'=\sin\alpha\int_{t^-}^{t^+}\frac{t'dt'}{\left[t'^2+P_0^2\right]}-P_0\cos\alpha\int_{t^-}^{t^+}\frac{dt'}{\left[t'^2+P_0^2\right]} \tag{4.3}$$

$$\int_{t^-}^{t^+}\frac{(z'-z_s)}{R_1^2}dt'=-\cos\alpha\int_{t^-}^{t^+}\frac{t'dt'}{\left[t'^2+P_0^2\right]}+P_0\sin\alpha\int_{t^-}^{t^+}\frac{dt'}{\left[t'^2+P_0^2\right]} \tag{4.4}$$

where each of the basic integrals along t' can be developed easily.

Furthermore, the subdivision shown in Fig. 3.2 has been undertaken for the source-annuli in the proximity of the field-annulus so as to allow for the multiplying lower order terms associated to these addends, which have to be assumed constant while

integrating analytically the higher order terms. In any case, the results turn out alike or even worse, whereby this procedure has been dismissed.

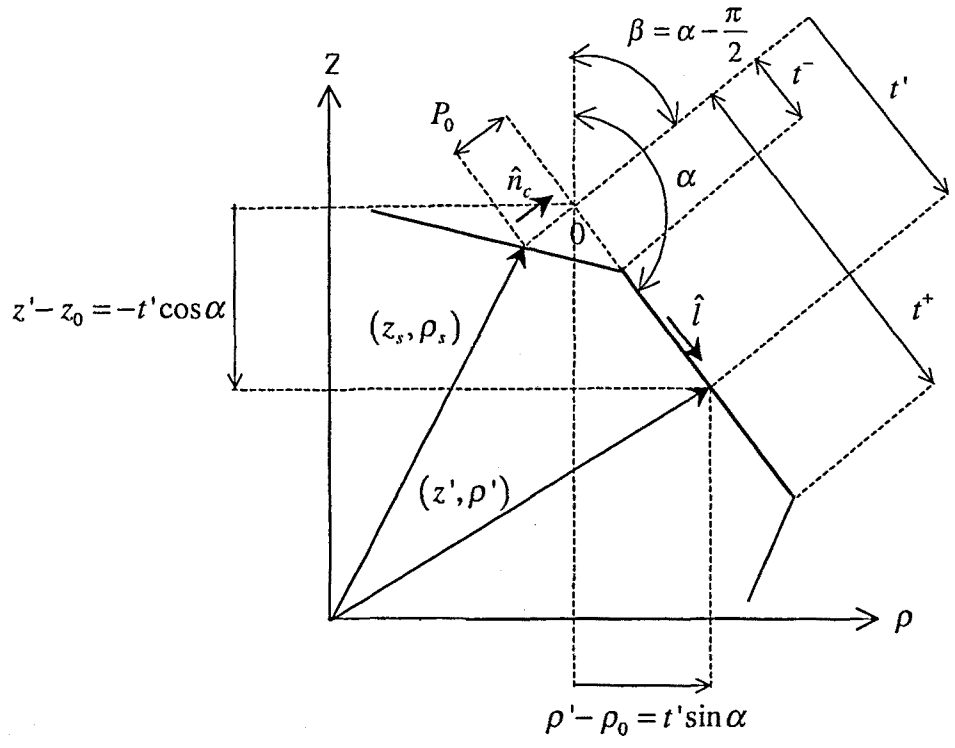

Fig. 4.5 Parameters of the analytical source-integration over a segment

2. The t-weighting has been effectuated with three field integrating points in the parts of (3.163), (3.164), (3.171) and (3.172) where only the mid point had been used. The results are very similar and no remarkable improvement is noticed.

4.3 DESCRIPTION OF THE DISSIMILARITY BETWEEN PEC-MFIE AND PEC-EFIE

The disagreement in all the tested bodies -spheres and cylinders- between the PeC-MFIE current coefficients and the PeC-EFIE ones, which are taken as reference, can be described through the aspects below.

1. The error is increasingly perceptible as long as one heads for the low ξ-frequency current coefficients. In all the bodies analysed, $m = \pm 1$ are the modes with the worst behaviour meanwhile $m = 0$ shows a much more acceptable similarity.

2. The range of low ξ-frequency modes of considerable error augments with the electrical dimensions of the object.

3. The shape of the generating arc of the body also influences the error. The results for a cylinder are slightly worse than for a sphere of similar electrical dimensions.

4. The number of low ξ-frequency modes that differ appreciably increases as the incident field reaches the transversal incidence ($\sigma_i = 90°$). Under the axial incidence ($\sigma_i = 0°$), with a series expansion with only two modes -$m = \pm 1$-[12], the current error is comparatively minor, though non-negligible.

The error due to the unsatisfactory computation of the fundamental integrals $T_m(t,t')$, $T_{m+1}(t,t')$ and $T_{m-1}(t,t')$, reasoned in section 4.2, can perfectly bring about each of the anomalies above.

Through the inspection of the final expressions for all the submatrices in (3.163), (3.164), (3.170) and (3.173), we remark on the more important presence of the $G_m(t,t')$, $G_{m+1}(t,t')$ and $G_{m-1}(t,t')$ terms as $|m|$ augments. Particularly, when m=0, the sumatrices $Z^m_{t,t'}$ and $Z^m_{\phi,\phi'}$, fully dependent on $G_m(t,t')$, $G_{m+1}(t,t')$ and $G_{m-1}(t,t')$, are null, according to its m-odd behaviour. In addition, for increasing values of $|m|$, the influence of $G_m(t,t')$, $G_{m+1}(t,t')$ and $G_{m-1}(t,t')$ becomes gradually enhanced -and so does accordingly the accuracy- in all the submatrices through the terms $mG_m(t,t')$, $(m+1)G_{m+1}(t,t')$ and $(m-1)G_{m-1}(t,t')$.

This fact, which can account for the first anomaly, can also be assessed intuitively. Indeed, for high ξ-frequency modes, the electromagnetic contribution of the ξ-lobes, due to the ξ harmonic expansion, may partially cancel each other, which eases the computation. On the other hand, as one heads for the lower ξ-frequencies, the contribution of each globe becomes itself increasingly important; that's why $|m| = 1$, 2, 3 can well be the worst cases. When $m = 0$, though, no globes need to be allowed for and so the accuracy, compared with the near low ξ-frequency modes, improves.

The second anomaly is reasonable. Meanwhile in the 3D approach one can successfully tackle the integration of such a high order integrand by diminishing the electrical dimensions of the patches and by increasing the order of the quadrature rule, in BoR problems the basic discretizing entity is an annulus with -in principle- any arbitrary radius. Of course, being the source integration not precise enough, the error must unavoidably increase when augmenting the value of the radius.

The third anomaly makes sense when analysing the order of the integrand near the singularity, which is shown in the expressions (4.3) and (4.4). When integrating along t', one sees how the order of the term tending to infinite, $\left[t'^2 + P_0^2\right]^{-1/2}$, evolves in a steeper way for cylinders - $P_0 = 0$ - than for spheres, which accomplish $P_0 \neq 0$ for any segment of the generating arc -see Fig. 4.5-.

---

[12] The mode p of the incident field is based on a linear combination of $J_{p+1}(k\rho \sin\sigma_i)$ and $J_{p-1}(k\rho \sin\sigma_i)$, which under an axial incidence -$\sigma_i = 0, \pi$ -, become $J_{p+1}(0)$ and $J_{p-1}(0)$. On the other hand, $J_k(0)$ is non-null only if $k = 0$, which allows non-null modes only for $p = \pm 1$ -see section 3.3.5-.

4.4 PeC-MFIE RESULTS

The fundamental integrals have been t'-integrated by means of a Gaussian quadrature rule of four points, which were sufficient for the PeC-EFIE. Whenever the number of points was augmented or the size of the segment was decreased, no real improvement was noticed. To assess the behaviour of the PeC-MFIE, the PeC-EFIE results are taken as reference.

4.4.1 Substitution of the $1/R^3$-terms by $1/R$

Results are presented according to the substitutions shown in the sections 3.4.4.1, 3.4.4.2 and 3.4.4.3 for a sphere of diameter 0.6λ under an impinging plane wave with $\sigma_i = 45°$ - $\phi_i = 0°$ - and $\hat{e}_i = \hat{t}_0$. The parameters of discretization are: $N_\phi = 25$, $N_{\text{modes}} = 2M + 1 = 15$ and $N_{FFT} = 64$.

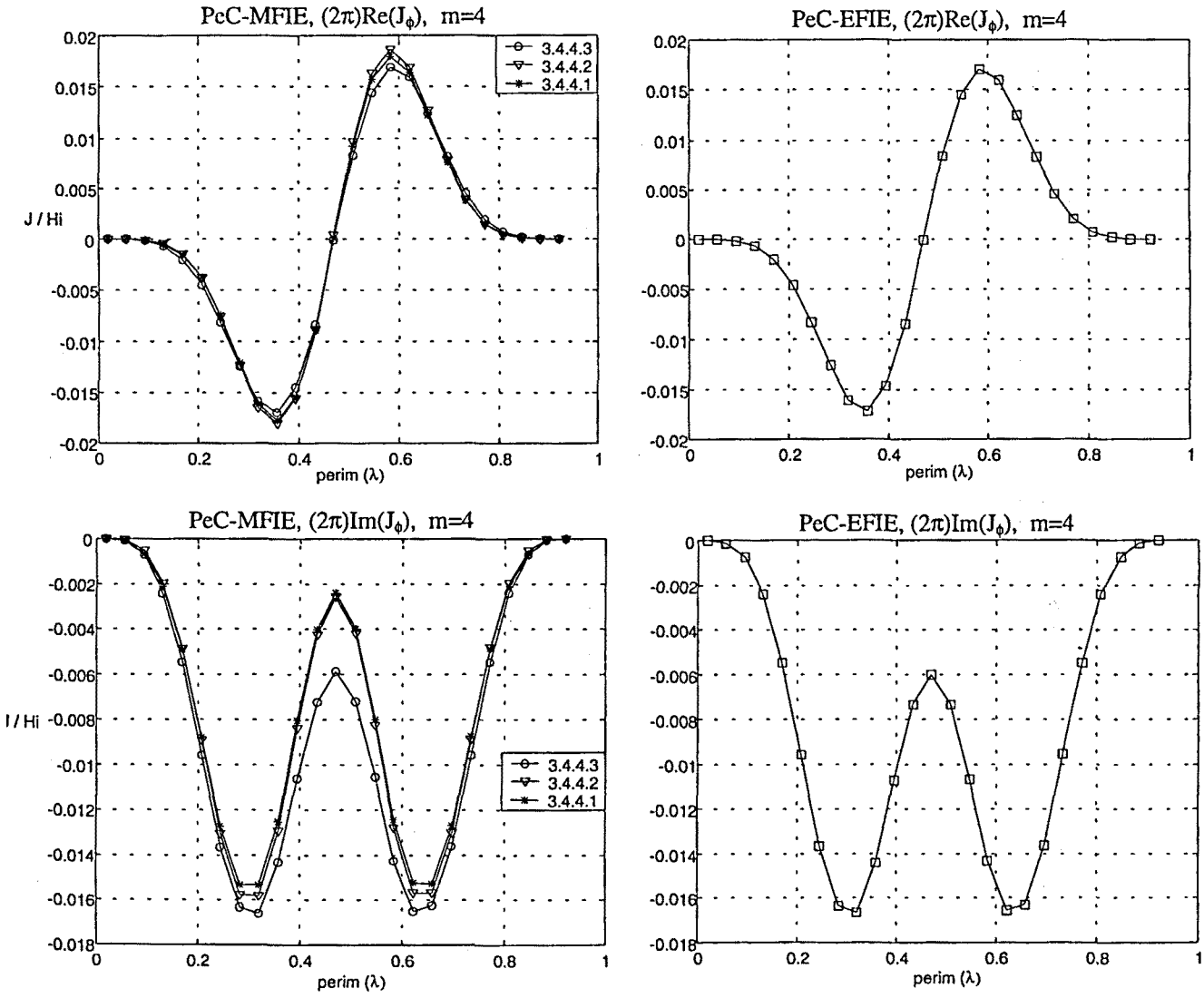

Fig. 4.6 J_ϕ component of the mode m=4 along the cut-plane $\phi = 0$

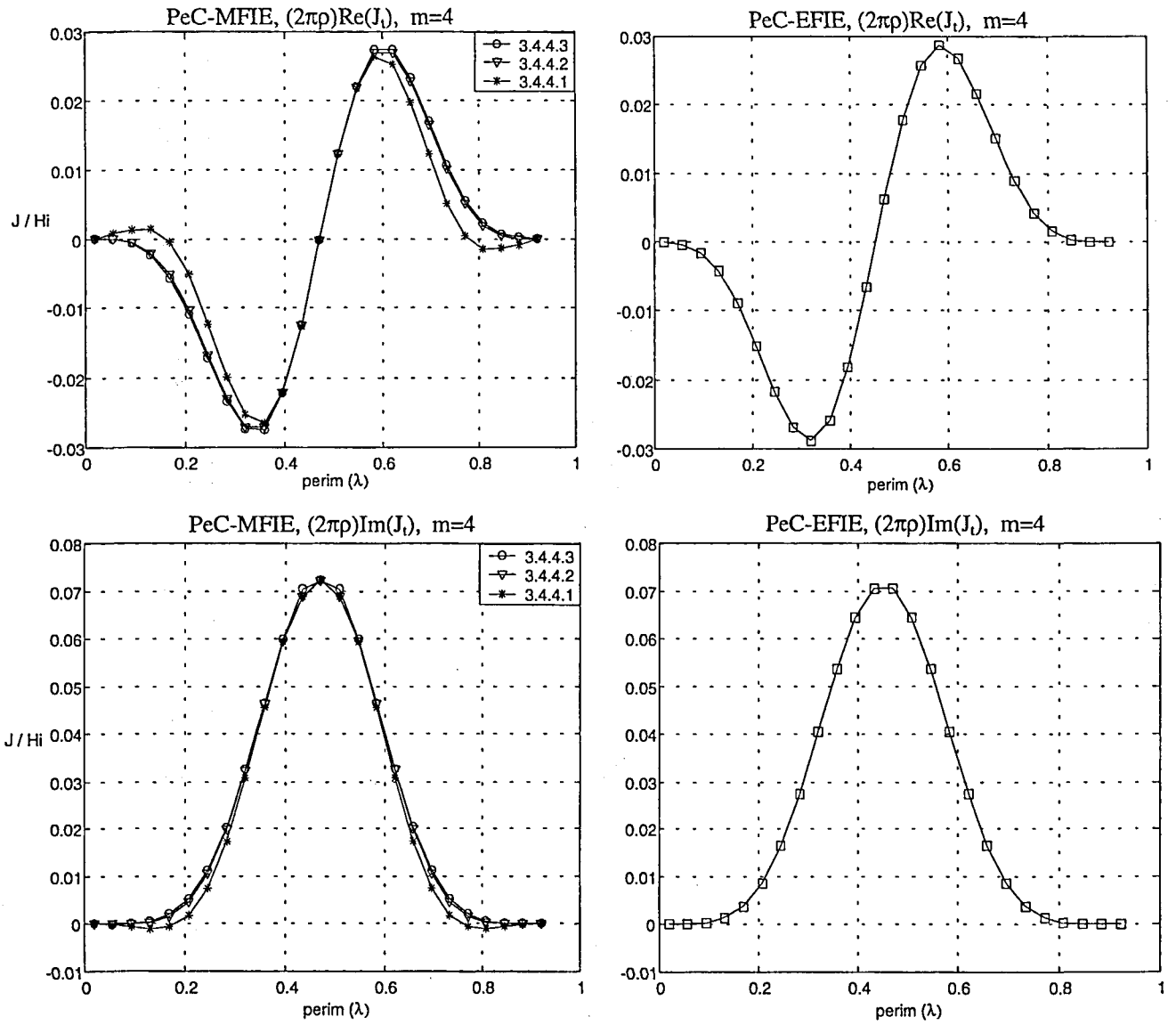

Fig. 4.7 J_t component of the mode m=4 along the cut-plane $\phi = 0$

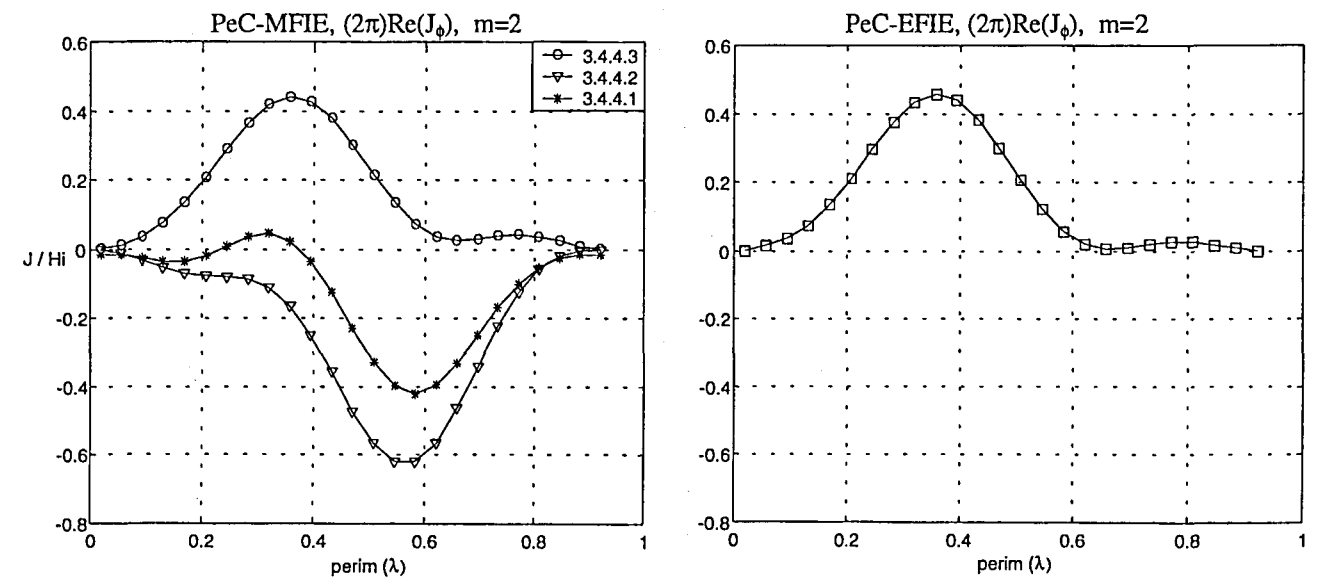

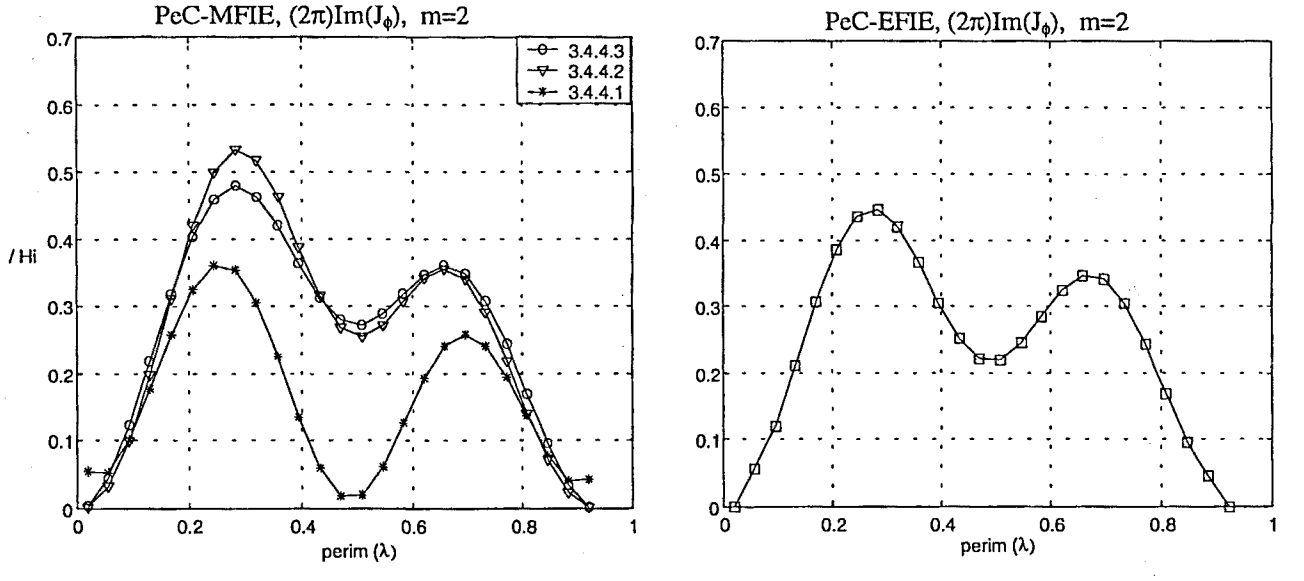

Fig. 4.8 J_ϕ component of the mode m=2 along the cut-plane $\phi = 0$

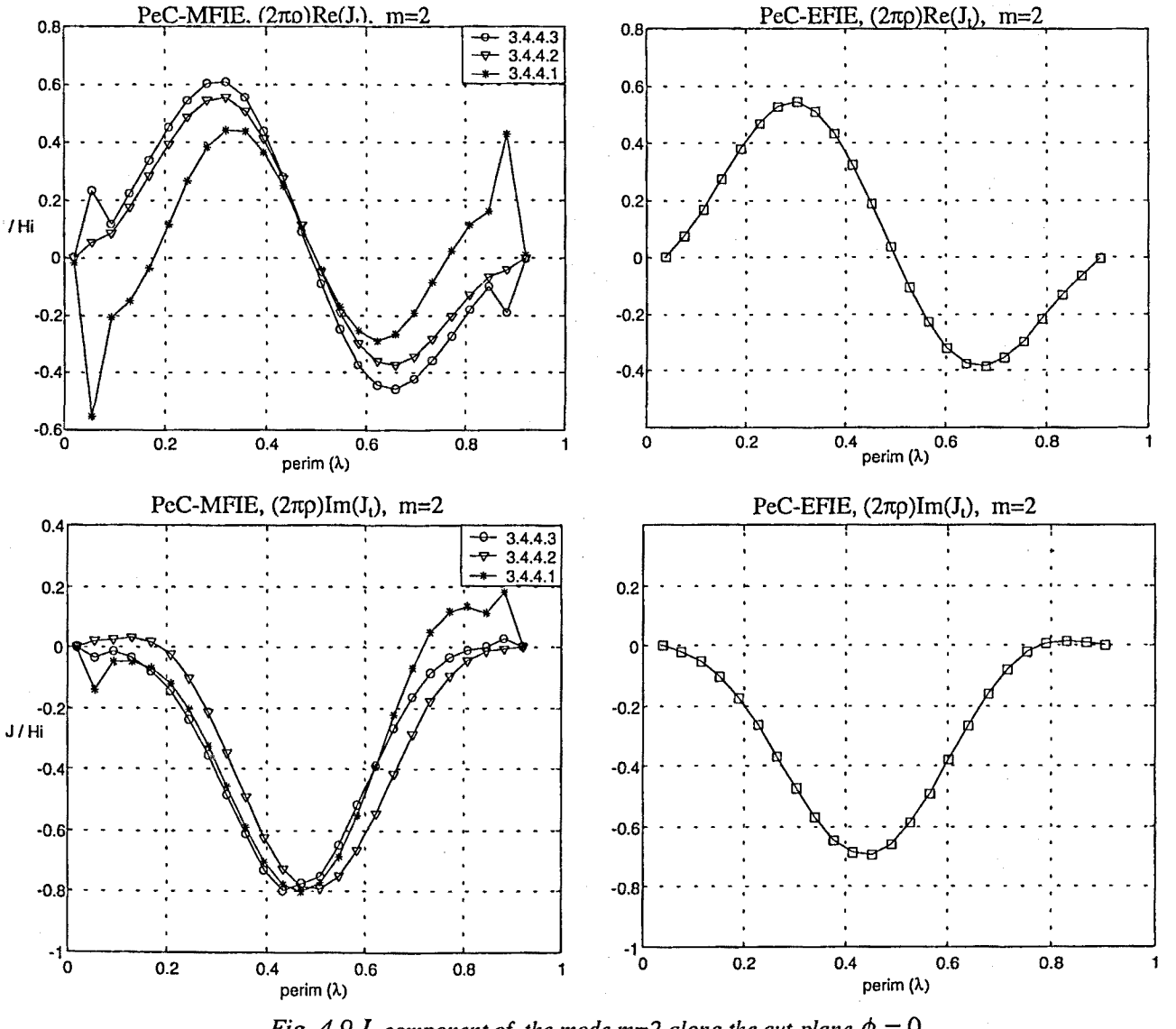

Fig. 4.9 J_t component of the mode m=2 along the cut-plane $\phi = 0$

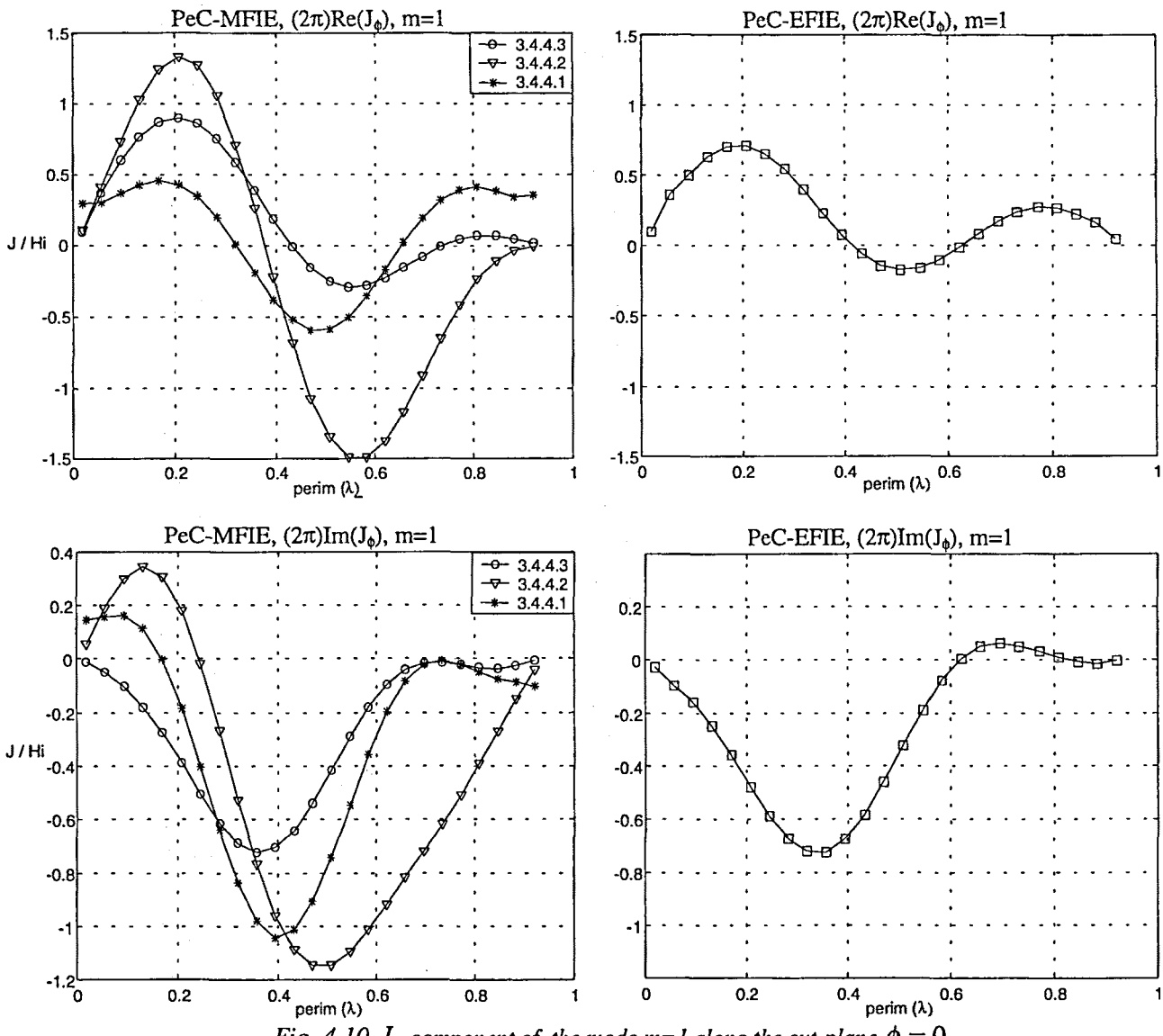

Fig. 4.10 J_ϕ component of the mode m=1 along the cut-plane $\phi = 0$

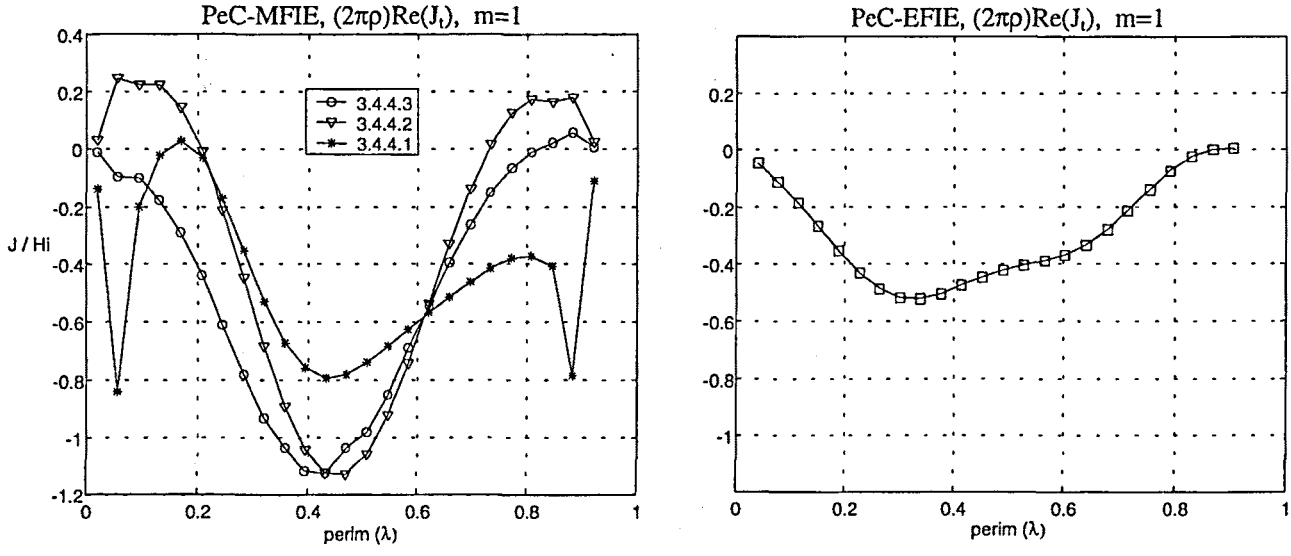

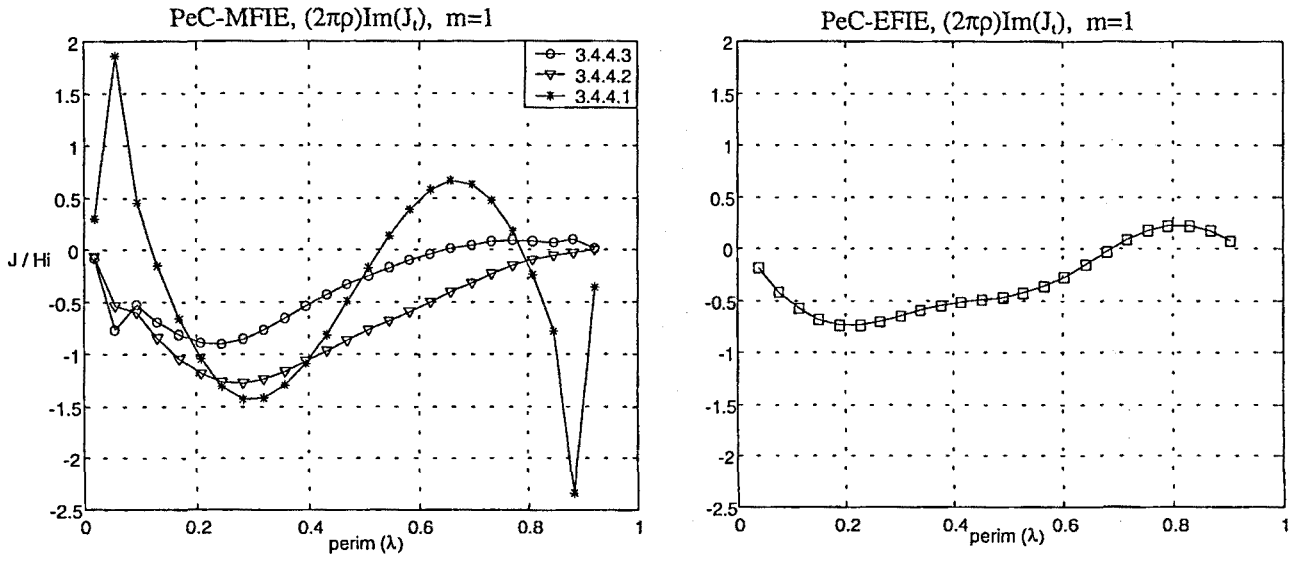

Fig. 4.11 J_t component of the mode m=1 along the cut-plane $\phi = 0$

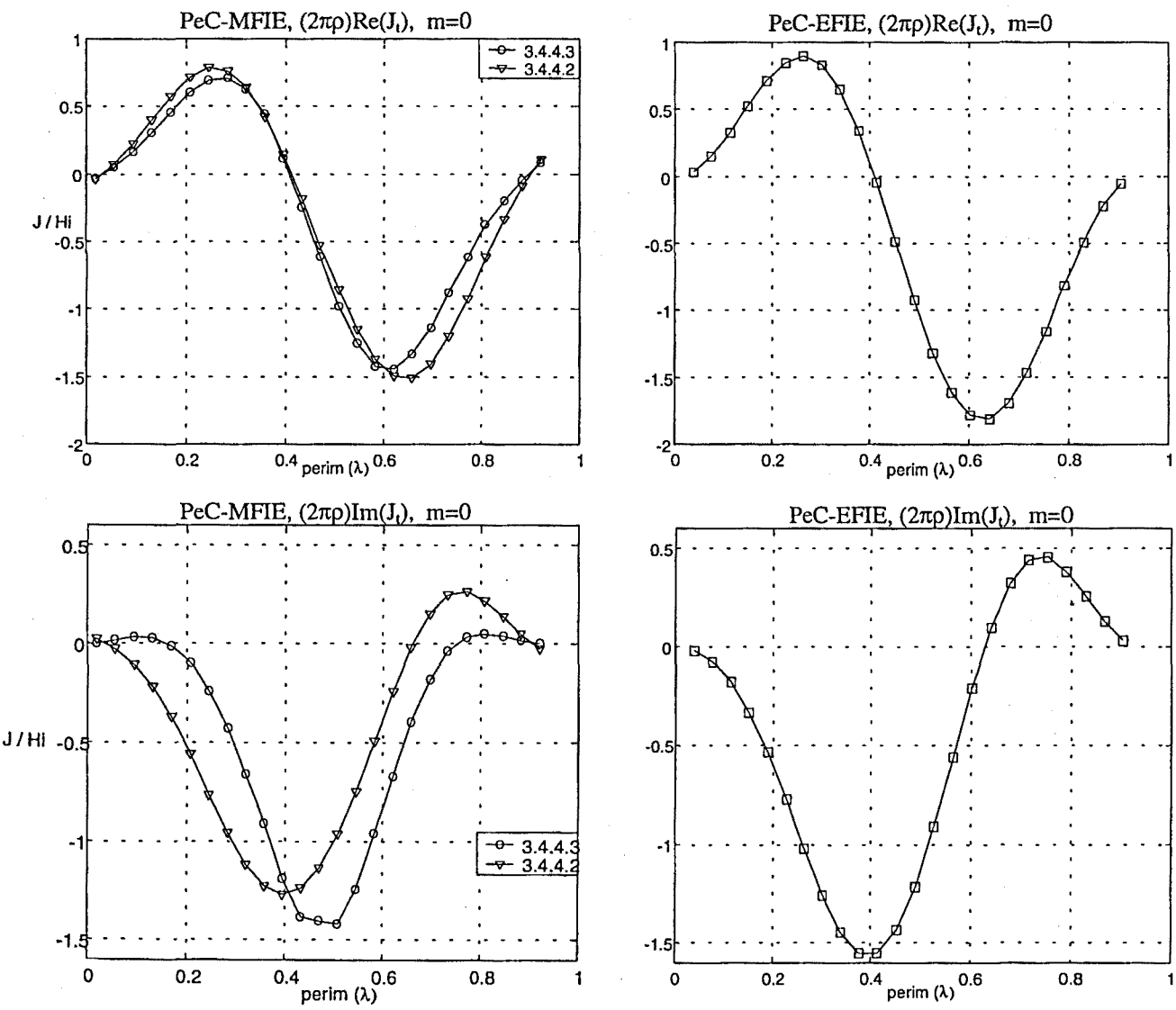

Fig. 4.12 J_t component of the mode m=0 along the cut-plane $\phi = 0$

The error due to $R^{-3}(t,t',\xi)$ diminishes in all the modes because of the substitution by the equivalent lower order integrals dependent on $R^{-1}(t,t',\xi)$. The correction due to 3.4.4.3 is best for all the modes, which makes sense because it allows for 3.4.4.2 and 3.4.4.1 as well. Note how for the high-frequency modes -Fig. 4.6, Fig. 4.7, Fig. 4.8 and Fig. 4.9-, the correction is satisfactory and less noticeable, which involves that the action of $R^{-3}(t,t',\xi)$ is comparatively less important. For $m=1$ -Fig. 4.10 and Fig. 4.11-, the correction is not good enough.

According to the results, it is clear that the computation of the current for $m=0$ -Fig. 4.12- is less sensitive to the error than $m=1$, which shows clearly the worst behaviour. Hence, this is the bottleneck of the BoR-PeC-MFIE implementation. For spheres of bigger electrical dimensions, the range of inaccurate low-frequency modes grows.

4.4.2 Improvement due to the property of symmetry

As explained in 3.4.4.4, one can achieve a further correction for the mode $m=0$, where the error is less evident, -see Fig. 4.12- by applying the symmetry property between $Z^0_{\phi,t'}$ and $Z^0_{t,\phi'}$ derived from the reciprocity theorem. Indeed, the 3.4.4.4 correction yields

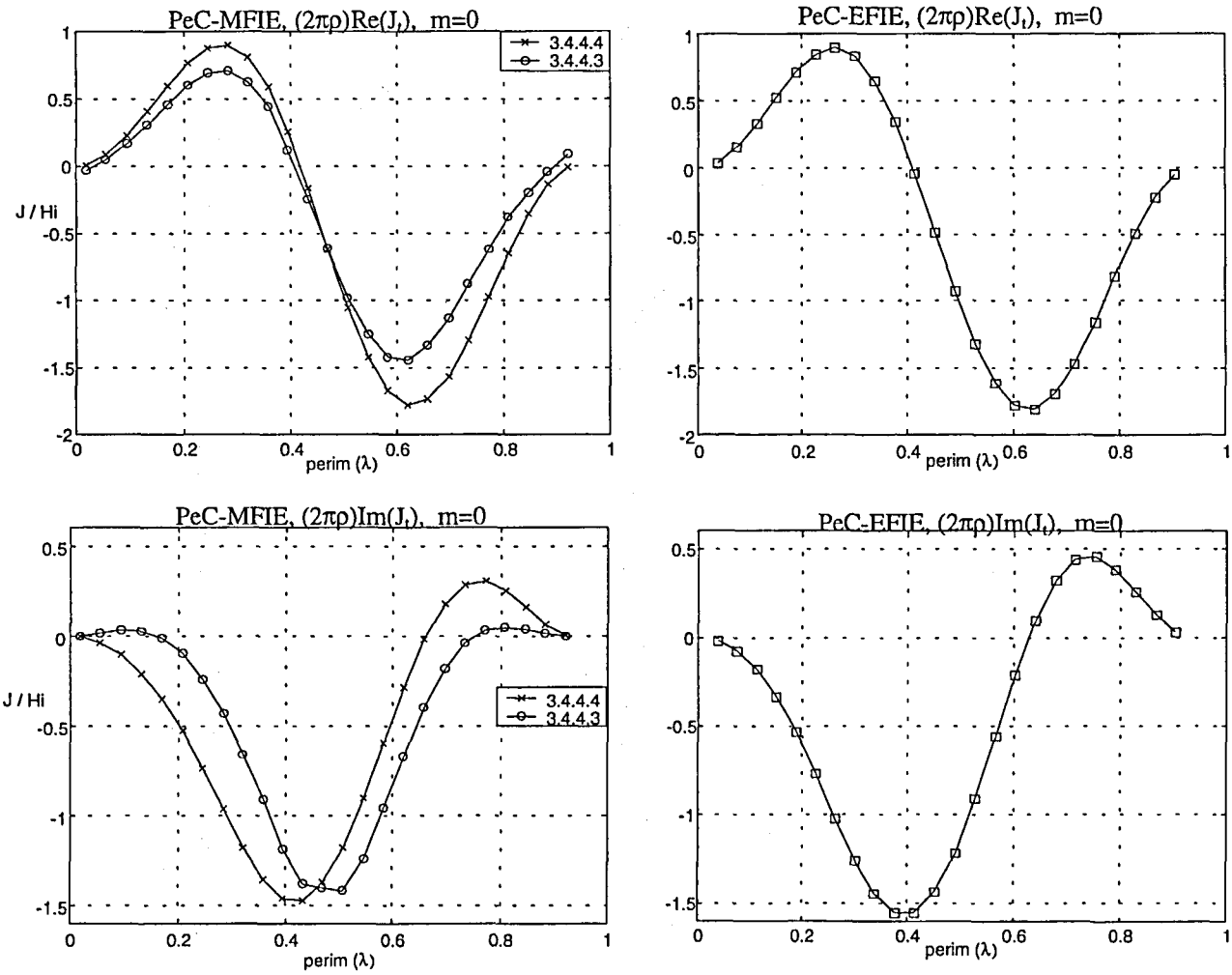

Fig. 4.13 J_t component of the mode m=0 along the cut-plane $\phi=0$

where the improvement comes from the substitution of $Z^0_{\phi,t'}$ by $Z^0_{t,\phi'}$ -see 3.4.4.4-.

4.4.3 Behaviour for a cylinder

Some results are presented for the case of a cylinder with diameter 0.5λ and height 0.5λ under an impinging plane wave with $\sigma_i = 45°$ -$\phi_i = 0°$- and $\hat{e}_i = \hat{t}_0$. Note that this case presents a radius and a length of the generating arc -1λ- close to the characteristics of the sphere commented in 4.4.1 and 4.4.2. The PeC-MFIE is encoded following 3.4.4.3 for the correction is best.

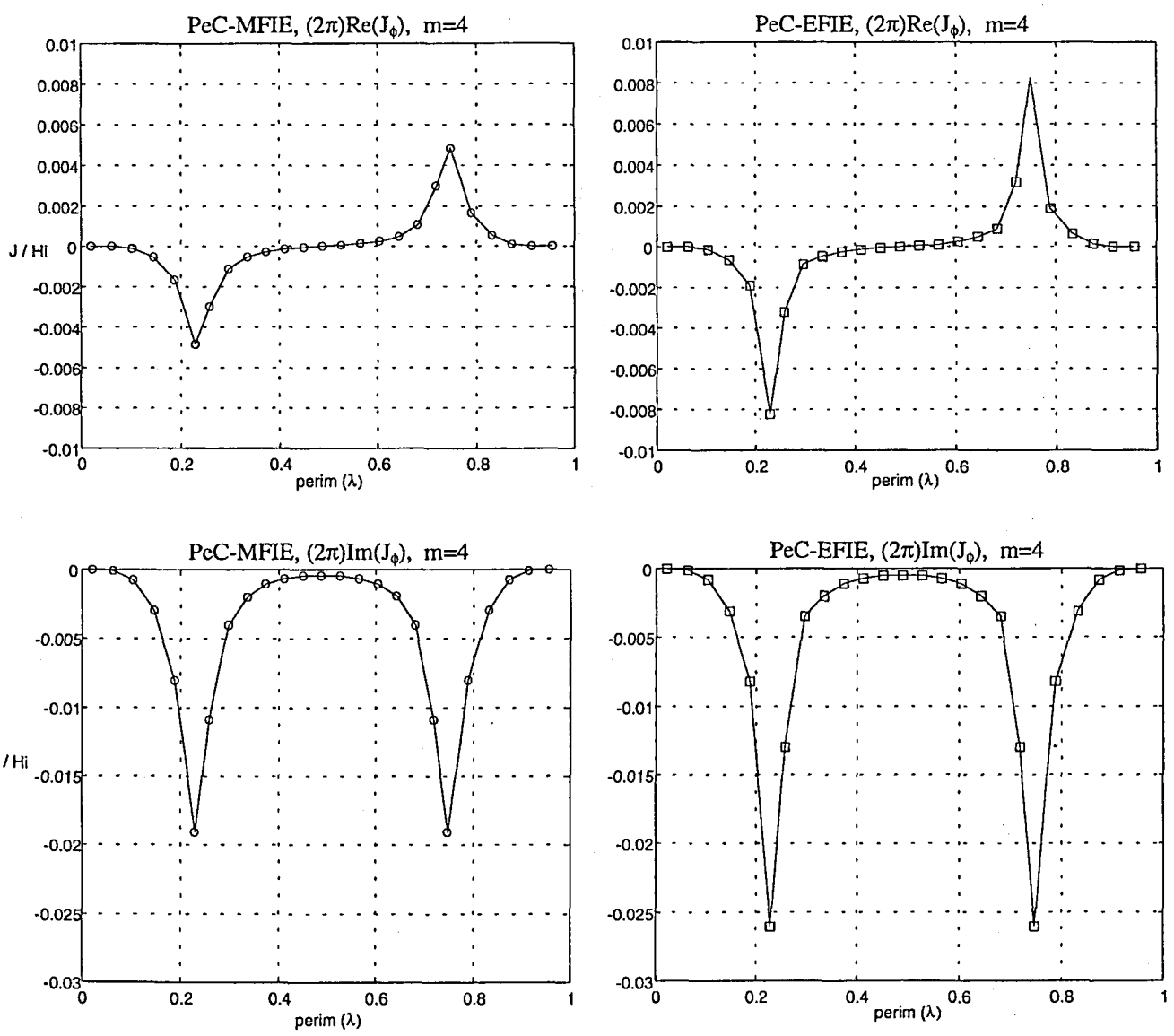

Fig. 4.14 J_ϕ component of the mode m=4 along the cut-plane $\phi = 0$

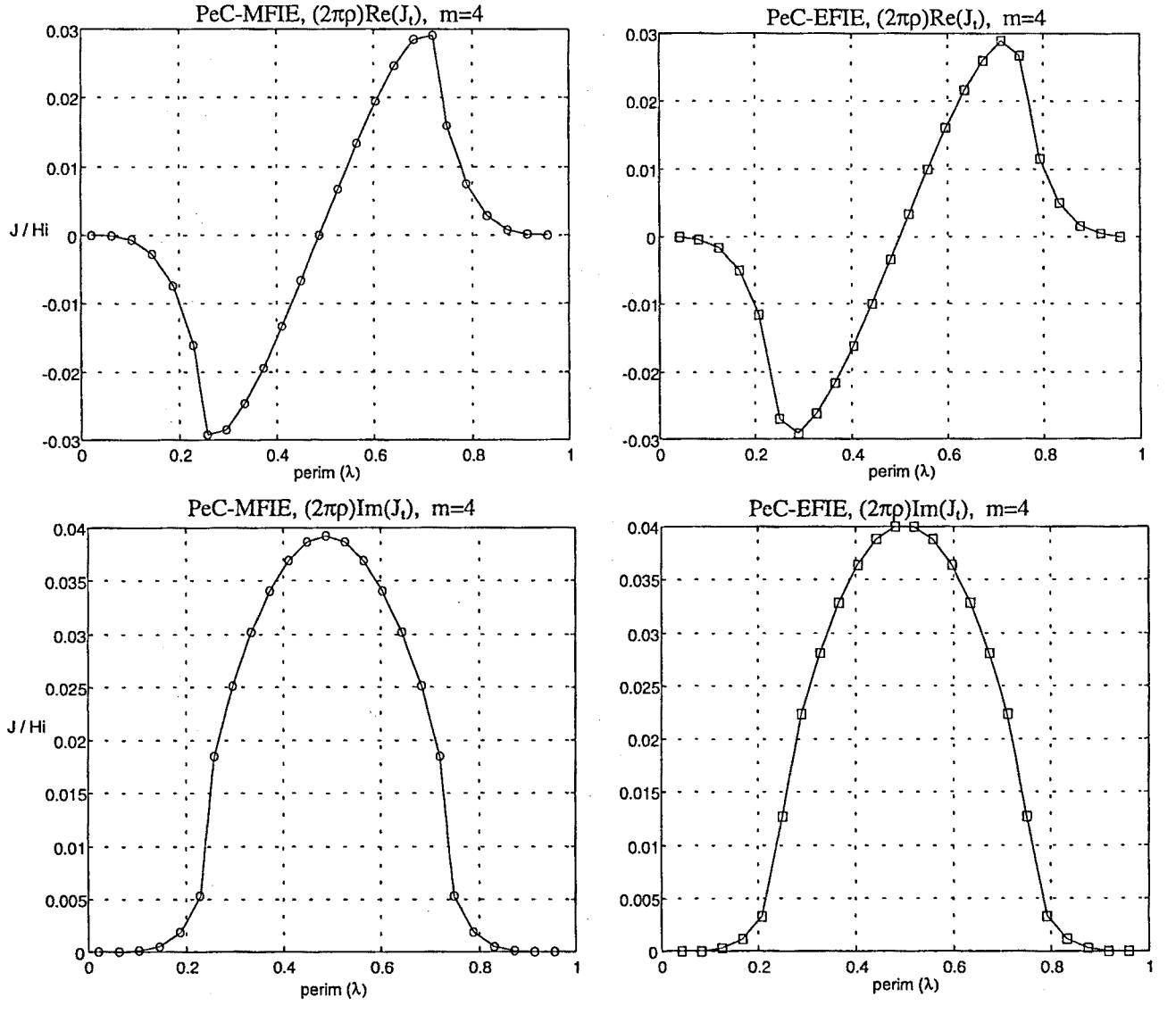

Fig. 4.15 J_t component of the mode m=4 along the cut-plane $\phi = 0$

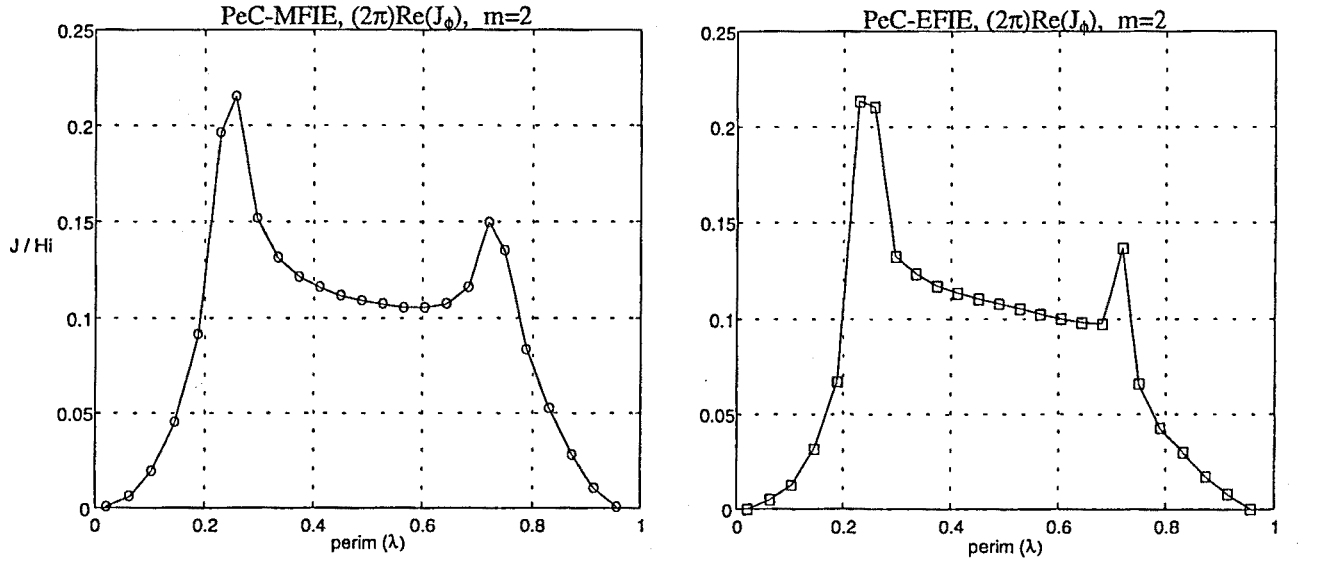

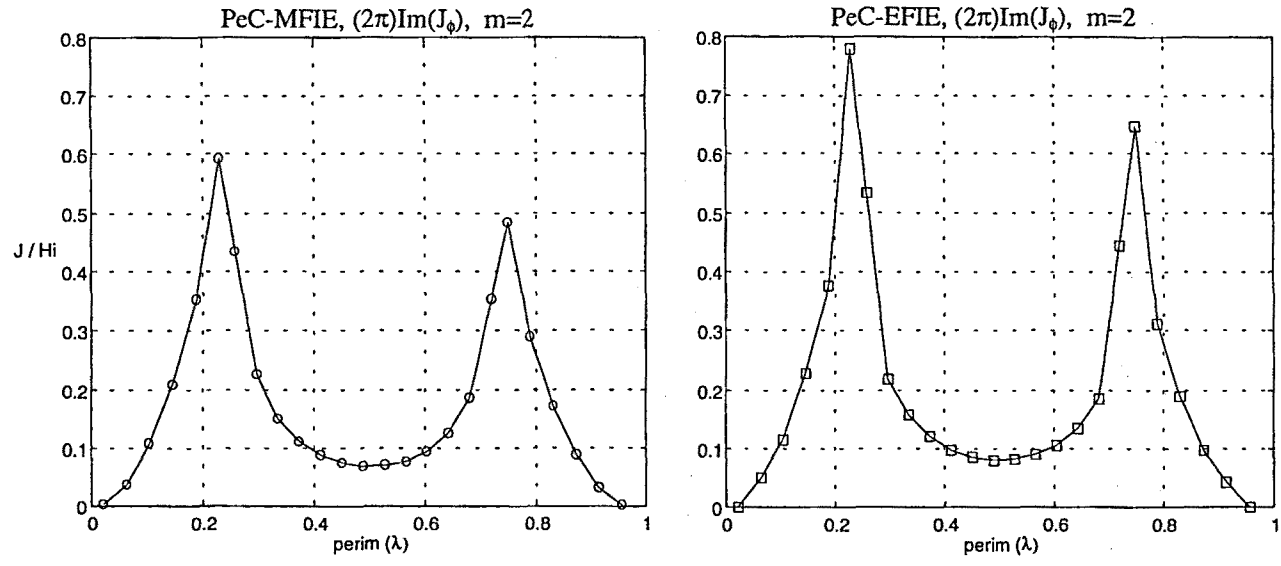

Fig. 4.16 J_ϕ component of the mode m=2 along the cut-plane $\phi = 0$

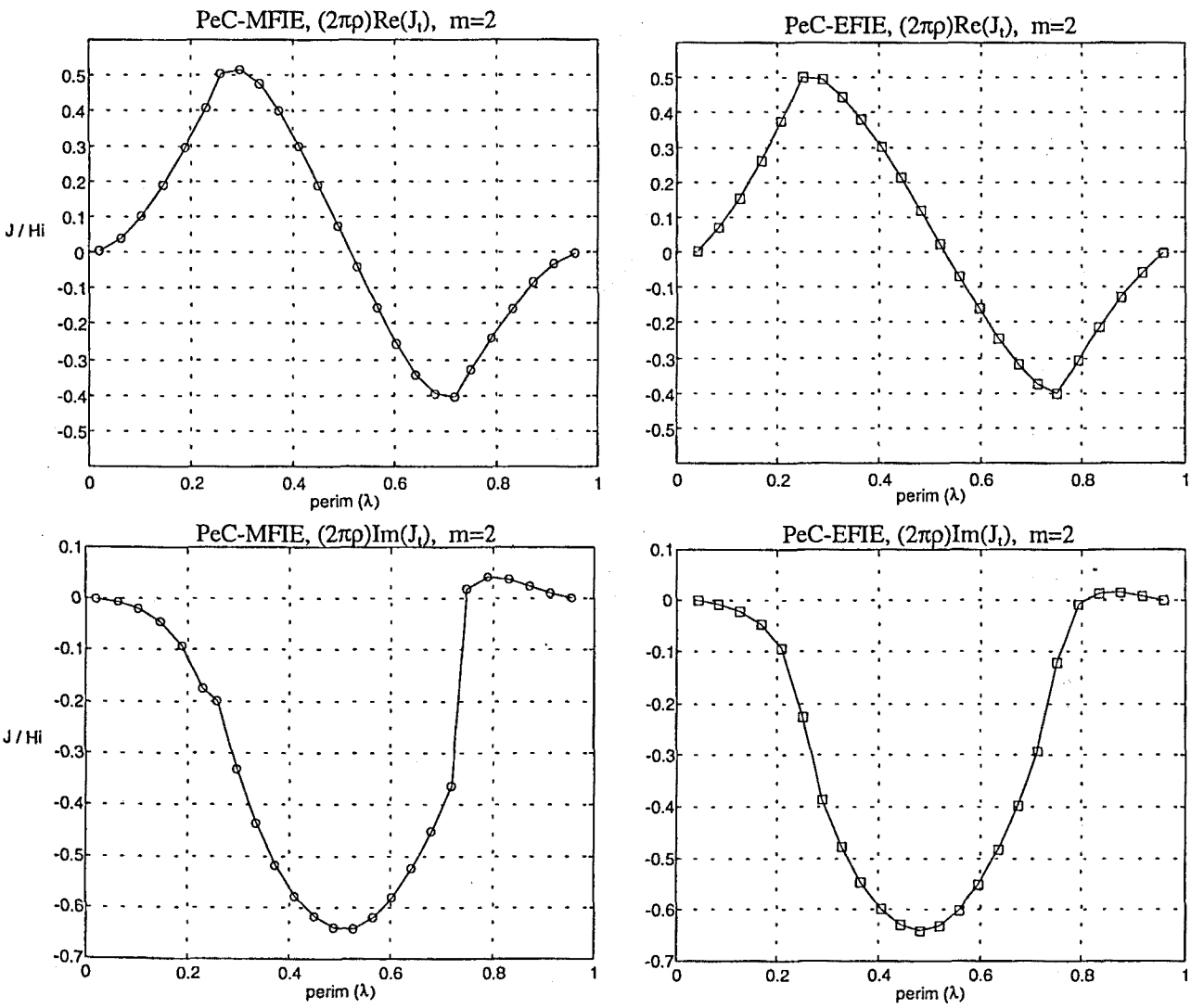

Fig. 4.17 J_t component of the mode m=2 along the cut-plane $\phi = 0$

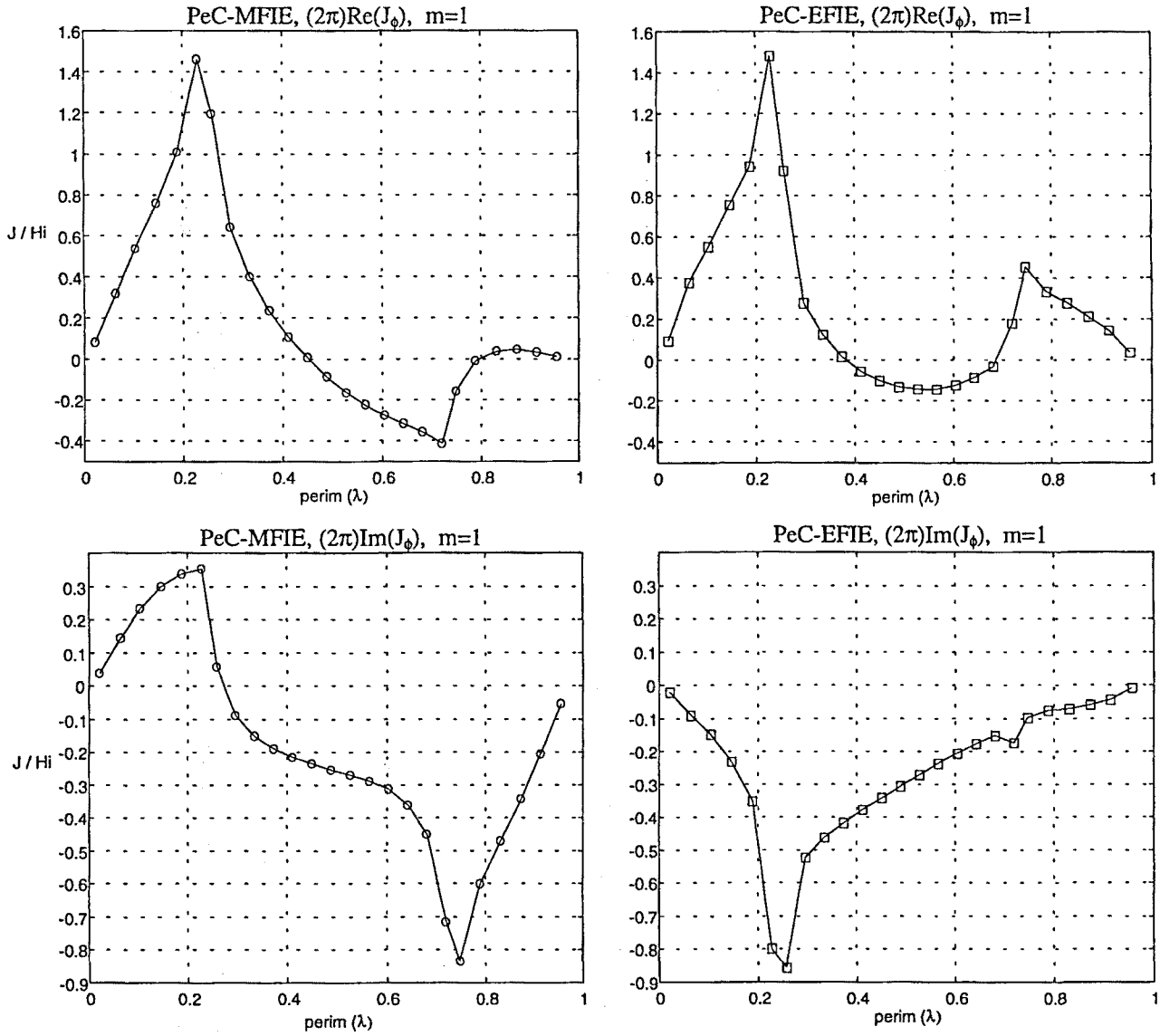

Fig. 4.18 J_ϕ component of the mode m=1 along the cut-plane $\phi = 0$

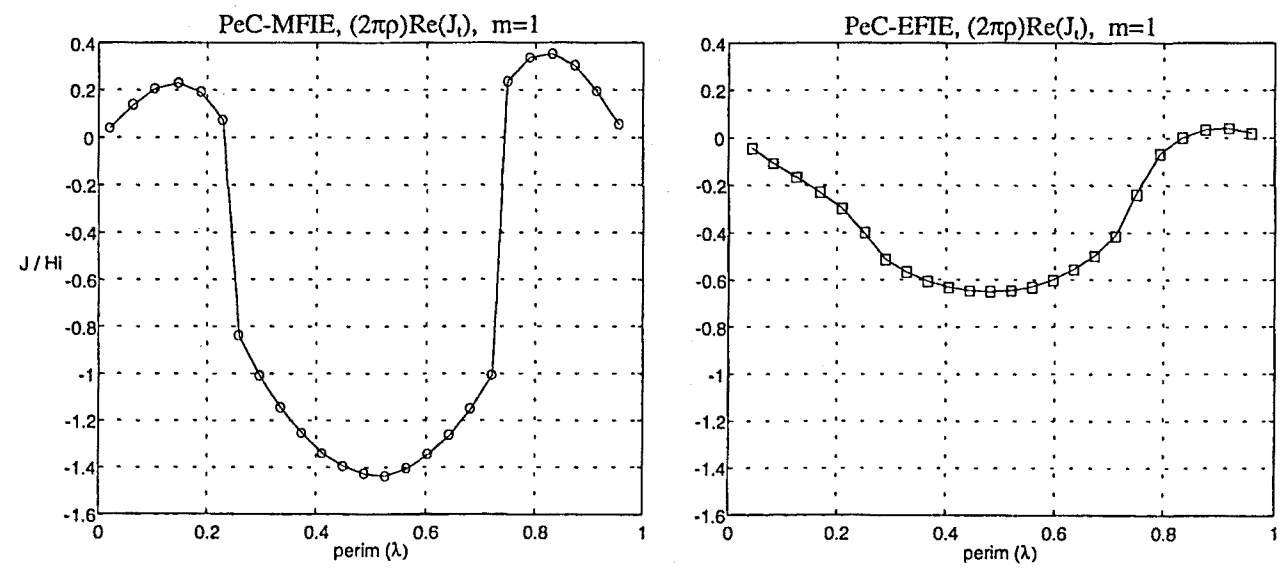

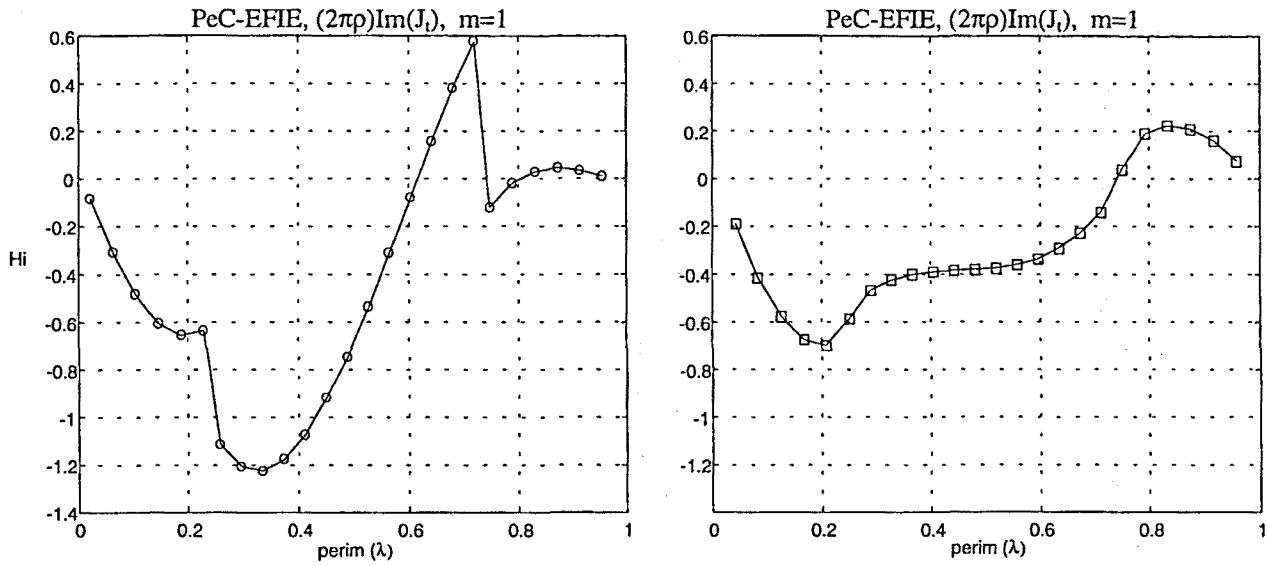

Fig. 4.19 J_t component of the mode m=1 along the cut-plane $\phi = 0$

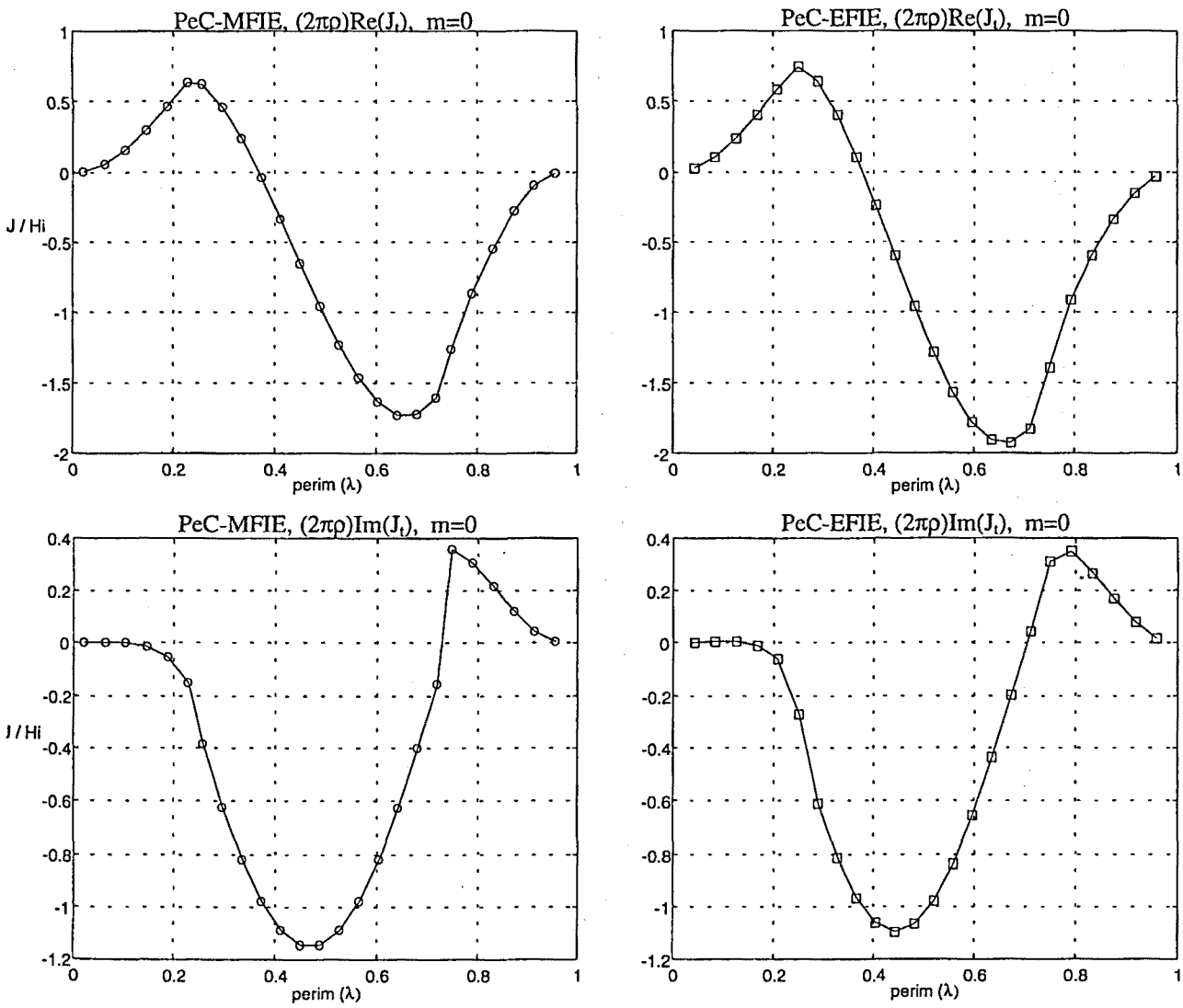

Fig. 4.20 J_t component of the mode m=0 along the cut-plane $\phi = 0$

The evolution of the results for the cylinder is analogous to the sphere. It must be noted, in addition, that for the higher frequency mode $m=4$, the J_ϕ results -Fig. 4.14- differ appreciably on the corners of the geometry; for $m=1$ the error is considerable and turns out again the worst. Finally, it is interesting to notice that the results for $m=0$ are very good.

Comparing the results for the sphere and the cylinder, both of similar electrical dimensions, it can be seen that the values are in general worse for the cylinder. This is especially evident for $m=1$, where the error is most remarkable. This behaviour can be attributed to the steeper slope of the high-order varying term in the case of the cylinder, as mentioned in 4.3.

4.5 EXPLANATION OF THE PEC-MFIE MISBEHAVIOUR

It has been proved with examples the misbehaviour of the PeC-MFIE in comparison with the PeC-EFIE. It has been reasoned in detail that this error comes from the inaccurate computation of the higher order integrals in the PeC-MFIE operator depending on $R^{-3}(t,t',\xi)$.

The source integrals involved in any BoR approach are two. One is the t'-integral, undertaken by means of a Gaussian numerical rule. The other one is the integral along ξ, which does not appear explicitly in the definitive BoR-formulation but it is implicitly incorporated since it rules the computation of the Fourier coefficients.

The author of this dissertation Thesis considers that the analytical integration of the ξ-dependent part can provide this error. In the Appendix B, it is theoretically proved the recurrence formula adopted, which relies on two basic integrals: N_0 and N_2. As one can well see either in the Appendix B or in (3.140) and (3.141), these integrals rely on the complete elliptic integral of the second kind: $E\left(\beta_1^2/(1+\beta_1^2)\right)$. Moreover, as discussed in 3.4.3.5, the contributions of highest order in N_0 and N_2 -those more relevant in the source-annuli near the field-annulus- depend on the addends with these integrals.

The complete elliptic integrals of the second kind are defined as [1]

$$E(m)=\int_0^{\pi/2}\left(1-m\sin^2\phi\right)^{1/2}d\phi \tag{4.5}$$

However, as shown in Appendix B, these elliptic integrals of second kind do not really come from a true second kind integral. Indeed, they come from the ϕ-integral

$$\Pi(m)=\int_0^{\pi/2}\left(1-m\sin^2\phi\right)^{-3/2}d\phi \tag{4.6}$$

which stands for a type of elliptic integral of third kind. These types of elliptic integrals, in general, are defined as [1]

$$\Pi(n;\varphi)=\int_0^{\pi/2}\left(1-n\sin^2\phi\right)^{-1}\left(1-\sin^2\varphi\sin^2\phi\right)^{-1/2}d\phi \tag{4.7}$$

Thanks to the properties of the elliptic integrals of the third kind [1], only for the case of $n=\sin^2\varphi$, which corresponds to the case of interest in (4.6), one can express (4.6) analytically as

$$\Pi(m)=\sec^2\left(\operatorname{asin}(m^{1/2})\right)E(m) \tag{4.8}$$

which is very advantageous because it transforms an integral with a term depending on $(\ )^{-3/2}$ in another integral relying on $(\ )^{1/2}$ and allows thus the apparition of the elliptic integrals of second kind in N_0 and N_2.

The author of this dissertation Thesis considers that this analytical transformation, although it is theoretically correct, can be the ultimate cause of the PeC-MFIE error. Indeed, note that a computer -with finite precision- cannot provide exactly $n=\sin^2\varphi$ as the transformation requires. Therefore, one has to assume in practice that $n\neq\sin^2\varphi$, which, as shown in the properties of the elliptic integrals in [1], leads to much more complicated equivalent expressions. One can well assess that as (4.8) cannot be assumed in practice, the high-order terms present in the *t'*-integral cannot be assumed either, because they come from (4.8).

In general, this explanation can also account for the historical failure of the BoR PeC-MFIE attempts because it points out the difficulty in computing with precision the terms of highest order. Note that terms with $E(\ )$ appear also in the recurrent analytical formulation of the PeC-EFIE -see Appendix A- but in this case they correspond truly to the type of integrals in (4.5), which is a proof again of its accuracy.

Chapter 5 METHOD OF MOMENTS ON PENETRABLE BODIES OF REVOLUTION

All the possible dielectric formulations derive from the combination of the PeC-EFIE and the PeC-MFIE operators. The BoR PeC-EFIE operator -see Chapter 3- assumes the basis functions to be different for each component. Indeed, rectangular and triangular pulses are used respectively for the expansion of the ϕ and t components of the current. The sets along both components become regularly overlapped along the generating arc -see Fig. 3.2-, which forces the number of unknowns for each component to be different - $N_\phi = N_t + 1$ -. This asymmetric arrangement of the expanding functions is alluded henceforth as *unbalanced.*

The development of the PeC-MFIE operator in Chapter 3 has been effectuated with rectangular pulses for both ϕ and t components. This symmetric disposition will be referred henceforth as *balanced.* The performance of the PeC-MFIE operator has to be really checked with the sets of expanding and weighting functions used by Gedney and Mittra for the PeC-EFIE [12] -chosen to develop the dielectric operators-. In any case, the lack of precision for the terms of highest-order of the PeC-MFIE operator must prevail because the origin of the inaccuracy is independent of the type of pulse shape chosen.

The objective in this chapter is to assess the possible implementations for the dielectric formulations in accordance with the limitations of the chosen *unbalanced* basis functions [13]. In 5.1, the operators -PeC and dielectric- that allow the use of an *unbalanced* set are presented. In 5.2, the influence of the numerical inaccuracy of PeC-MFIE in the dielectric operators -EFIE, MFIE and PMCHW- is assessed.

5.1 SUITABLE OPERATORS FOR AN *UNBALANCED* SET

One PeC-operator -PeC-EFIE-, see 5.1.1, and one dielectric operator -PMCHW-, see 5.1.2, allow the use of an *unbalanced* set as weighting and expanding functions. The other operators present in this case a singular matrix for the mode $m = 0$ because the number of expanding functions for both directions -t and ϕ - is not the same. The *balanced* sets are in principle accepted by all the operators.

5.1.1 PeC operators

The impedance matrix for the mode $m=0$ for PeC-EFIE operator - $Z_E{}^0$ - becomes

$$\underline{\underline{Z}}_E{}^0 = \begin{bmatrix} \underline{\underline{Z}}^0_{t,t'} & \underline{\underline{0}} \\ \underline{\underline{0}} & \underline{\underline{Z}}^0_{\phi,\phi'} \end{bmatrix} \tag{5.1}$$

The determinant of $Z_E{}^0$ is non null as long as the determinants of each of the submatrices are non null. Indeed, as $\underline{\underline{Z}}^m_{t,t'}$ and $\underline{\underline{Z}}^m_{\phi,\phi'}$ are square matrices, $\det\left(\underline{\underline{Z}}_E{}^0\right) = \det(\underline{\underline{Z}}^0_{t,t'}) \cdot \det(\underline{\underline{Z}}^0_{\phi,\phi'})$, irrespective of the set being either *unbalanced* [12] or *balanced* [18].

The impedance matrix for the mode $m=0$ for PeC-MFIE operator - $Z_H{}^0$ - becomes

$$\underline{\underline{Z}}_H{}^0 = \begin{bmatrix} \underline{\underline{0}} & \underline{\underline{Z}}^0_{t,\phi'} \\ \underline{\underline{Z}}^0_{\phi,t'} & \underline{\underline{0}} \end{bmatrix} \tag{5.2}$$

If the set is *balanced*, $\det\left(Z^0_H\right) = \det\left(\underline{\underline{Z}}^0_{\phi,t'}\right)\det\left(\underline{\underline{Z}}^0_{t,\phi'}\right)$, which lets the problem well posed provided that determinants of each of the submatrices are non null.

In case the set of expanding functions being *unbalanced*, $Z_H{}^0$ is singular no matter which the values of N_ϕ, N_t are. Indeed, the computation of $\det\left(Z_H{}^0\right)$ through the weighted addition of the minors associated to the elements along a row -or a column- leads in any case to the final dependence on the elementary matrices $\underline{\underline{A}}$, $\underline{\underline{B}}$, of size $(N_t+1)\times(N_t+1)$,

$$\underline{\underline{A}} = \begin{bmatrix} \neq 0 & \neq 0 & \cdots & \neq 0 & 0 \\ \neq 0 & \neq 0 & \cdots & \neq 0 & 0 \\ \vdots & \vdots & \vdots & \vdots & \vdots \\ \neq 0 & \neq 0 & \cdots & \neq 0 & 0 \end{bmatrix} \qquad \underline{\underline{B}} = \begin{bmatrix} \neq 0 & \neq 0 & \cdots & \neq 0 & \neq 0 \\ \neq 0 & \neq 0 & \cdots & \neq 0 & \neq 0 \\ \vdots & \vdots & \vdots & \vdots & \vdots \\ 0 & 0 & \cdots & 0 & 0 \end{bmatrix} \tag{5.3}$$

Both accomplish $\det(\underline{\underline{A}}) = 0$, $\det(\underline{\underline{B}}) = 0$ because they have either a null row or a null column.

Therefore, in PeC problems, the *unbalanced* set only allows the use of the PeC-EFIE operator. Indeed, it is present in the literature in [12][13].

5.1.2 Dielectric operators

The general expression for a problem with a homogeneous dielectric body must be

$$\begin{bmatrix} \langle \underline{EH}_t^{i\,m} \rangle_1 \\ \langle \underline{EH}_\phi^{i\,m} \rangle_1 \\ \langle \underline{EH}_t^{i\,m} \rangle_2 \\ \langle \underline{EH}_\phi^{i\,m} \rangle_2 \end{bmatrix} = \begin{bmatrix} \langle \underline{\underline{Z}}_{t,t'}^{\,m} \rangle_{J,1} & \langle \underline{\underline{Z}}_{t,\phi'}^{\,m} \rangle_{J,1} & \langle \underline{\underline{Z}}_{t,t'}^{\,m} \rangle_{M,1} & \langle \underline{\underline{Z}}_{t,\phi'}^{\,m} \rangle_{M,1} \\ \langle \underline{\underline{Z}}_{\phi,t'}^{\,m} \rangle_{J,1} & \langle \underline{\underline{Z}}_{\phi,\phi'}^{\,m} \rangle_{J,1} & \langle \underline{\underline{Z}}_{\phi,t'}^{\,m} \rangle_{M,1} & \langle \underline{\underline{Z}}_{\phi,\phi'}^{\,m} \rangle_{M,1} \\ \langle \underline{\underline{Z}}_{t,t'}^{\,m} \rangle_{J,2} & \langle \underline{\underline{Z}}_{t,\phi'}^{\,m} \rangle_{J,2} & \langle \underline{\underline{Z}}_{t,t'}^{\,m} \rangle_{M,2} & \langle \underline{\underline{Z}}_{t,\phi'}^{\,m} \rangle_{M,2} \\ \langle \underline{\underline{Z}}_{\phi,t'}^{\,m} \rangle_{J,2} & \langle \underline{\underline{Z}}_{\phi,\phi'}^{\,m} \rangle_{J,2} & \langle \underline{\underline{Z}}_{\phi,t'}^{\,m} \rangle_{M,2} & \langle \underline{\underline{Z}}_{\phi,\phi'}^{\,m} \rangle_{M,2} \end{bmatrix} \cdot \begin{bmatrix} \underline{I}_{t'}^{\,m} \\ \underline{I}_{\phi'}^{\,m} \\ \underline{M}_{t'}^{\,m} \\ \underline{M}_{\phi'}^{\,m} \end{bmatrix} \qquad (5.4)$$

$$m = -M..+M$$

where $\langle\ \rangle_{1,2}$ denote one of the two equations defined over the surface of the bodies and $\langle\ \rangle_{J,M}$ indicates if the field contribution comes from the electric or the magnetic current.

The correspondence of the submatrices in (5.4) with the PeC operators for the PMCHW dielectric operator stands for -see Chapter 2-

$$\begin{aligned} \langle Z^m \rangle_{J,1} &= [Z_E^m]^{\mathrm{O}} - [Z_E^m]^{\mathrm{I}} \quad ; \quad \langle Z^m \rangle_{M,1} = [Z_H^m]^{\mathrm{I}} - [Z_H^m]^{\mathrm{O}} \\ \langle Z^m \rangle_{J,2} &= [Z_H^m]^{\mathrm{O}} - [Z_H^m]^{\mathrm{I}} \quad ; \quad \langle Z^m \rangle_{M,2} = \frac{[Z_E^m]^{\mathrm{O}}}{\eta_{\mathrm{O}}^{\,2}} - \frac{[Z_E^m]^{\mathrm{I}}}{\eta_{\mathrm{I}}^{\,2}} \end{aligned} \qquad (5.5)$$

where the matrices with superindices I and O correspond to the operators respectively inside or outside the dielectric body.

Because of the m-odd property of the submatrices $\underline{\underline{Z}}_{H\phi,\phi'}^{\,m}$, $\underline{\underline{Z}}_{Ht,t'}^{\,m}$ -PeC MFIE- $\underline{\underline{Z}}_{E\phi,t'}^{\,m}$, $\underline{\underline{Z}}_{Et,\phi'}^{\,m}$ - PeC EFIE-, the matrix in (5.4) becomes

$$Z_{PCHMW}^{0} = \begin{bmatrix} \langle \underline{\underline{Z}}_{t,t'}^{\,m} \rangle_{J,1} & \underline{\underline{0}} & \underline{\underline{0}} & \langle \underline{\underline{Z}}_{t,\phi'}^{\,m} \rangle_{M,1} \\ \underline{\underline{0}} & \langle \underline{\underline{Z}}_{\phi,\phi'}^{\,m} \rangle_{J,1} & \langle \underline{\underline{Z}}_{\phi,t'}^{\,m} \rangle_{M,1} & \underline{\underline{0}} \\ \underline{\underline{0}} & \langle \underline{\underline{Z}}_{t,\phi'}^{\,m} \rangle_{J,2} & \langle \underline{\underline{Z}}_{t,t'}^{\,m} \rangle_{M,2} & \underline{\underline{0}} \\ \langle \underline{\underline{Z}}_{\phi,t'}^{\,m} \rangle_{J,2} & \underline{\underline{0}} & \underline{\underline{0}} & \langle \underline{\underline{Z}}_{\phi,\phi'}^{\,m} \rangle_{M,2} \end{bmatrix} \qquad m = -M..+M \qquad (5.6)$$

which, arranging properly the rows, yields

$$\begin{bmatrix} \left\langle \underline{\underline{Z}}_{t,t'}^{\,m} \right\rangle_{J,1} & \underline{\underline{0}} & \underline{\underline{0}} & \left\langle \underline{\underline{Z}}_{t,\phi'}^{\,m} \right\rangle_{M,1} \\ \left\langle \underline{\underline{Z}}_{\phi,t'}^{\,m} \right\rangle_{J,2} & \underline{\underline{0}} & \underline{\underline{0}} & \left\langle \underline{\underline{Z}}_{\phi,\phi'}^{\,m} \right\rangle_{M,2} \\ \underline{\underline{0}} & \left\langle \underline{\underline{Z}}_{t,\phi'}^{\,m} \right\rangle_{J,2} & \left\langle \underline{\underline{Z}}_{t,t'}^{\,m} \right\rangle_{M,2} & \underline{\underline{0}} \\ \underline{\underline{0}} & \left\langle \underline{\underline{Z}}_{\phi,\phi'}^{\,m} \right\rangle_{J,1} & \left\langle \underline{\underline{Z}}_{\phi,t'}^{\,m} \right\rangle_{M,1} & \underline{\underline{0}} \end{bmatrix} \qquad m = -M..+M \tag{5.7}$$

and the arrangement of the columns finally leads to

$$\begin{bmatrix} \left\langle \underline{\underline{Z}}_{t,t'}^{\,m} \right\rangle_{J,1} & \left\langle \underline{\underline{Z}}_{t,\phi'}^{\,m} \right\rangle_{M,1} & \underline{\underline{0}} & \underline{\underline{0}} \\ \left\langle \underline{\underline{Z}}_{\phi,t'}^{\,m} \right\rangle_{J,2} & \left\langle \underline{\underline{Z}}_{\phi,\phi'}^{\,m} \right\rangle_{M,2} & \underline{\underline{0}} & \underline{\underline{0}} \\ \underline{\underline{0}} & \underline{\underline{0}} & \left\langle \underline{\underline{Z}}_{t,t'}^{\,m} \right\rangle_{M,2} & \left\langle \underline{\underline{Z}}_{t,\phi'}^{\,m} \right\rangle_{J,2} \\ \underline{\underline{0}} & \underline{\underline{0}} & \left\langle \underline{\underline{Z}}_{\phi,t'}^{\,m} \right\rangle_{M,1} & \left\langle \underline{\underline{Z}}_{\phi,\phi'}^{\,m} \right\rangle_{J,1} \end{bmatrix} \qquad m = -M..+M \tag{5.8}$$

This matrix is conditioned as the original matrix in (5.6) since the determinant of both matrices coincide in absolute value -according to the properties of matrices and determinants, there might be only a sign change[13], which is irrelevant-. Since the two groups of submatrices in (5.8) form square matrices dimensionally equal - $(N_t + N_\phi)\times(N_t + N_\phi)$-, the PMCHW operator becomes well defined even for an *unbalanced* set. Indeed, it is present in the literature in [13].

It is widely known from the theorem of equivalence that two other dielectric operators can be implemented as well: EFIE and MFIE. The elements of the matrix in (5.4) for EFIE stand for

$$\begin{aligned} \left\langle Z^m \right\rangle_{J,1} &= \left[Z_E^m\right]^0 \quad ; \quad \left\langle Z^m \right\rangle_{J,2} = -\left[Z_H^m\right]^0 \\ \left\langle Z^m \right\rangle_{J,2} &= \left[Z_E^m\right]^1 \quad ; \quad \left\langle Z^m \right\rangle_{M,2} = -\left[Z_H^m\right]^1 \end{aligned} \tag{5.9}$$

which for the mode $m = 0$ set the matrix in (5.4) as

$$Z_{EFIE}^0 = \begin{bmatrix} \left\langle \underline{\underline{Z}}_{t,t'}^{\,m} \right\rangle_{J,1} & \underline{\underline{0}} & \underline{\underline{0}} & \left\langle \underline{\underline{Z}}_{t,\phi'}^{\,m} \right\rangle_{M,1} \\ \underline{\underline{0}} & \left\langle \underline{\underline{Z}}_{\phi,\phi'}^{\,m} \right\rangle_{J,1} & \left\langle \underline{\underline{Z}}_{\phi,t'}^{\,m} \right\rangle_{M,1} & \underline{\underline{0}} \\ \left\langle \underline{\underline{Z}}_{t,t'}^{\,m} \right\rangle_{J,2} & \underline{\underline{0}} & \underline{\underline{0}} & \left\langle \underline{\underline{Z}}_{t,\phi'}^{\,m} \right\rangle_{M,2} \\ \underline{\underline{0}} & \left\langle \underline{\underline{Z}}_{\phi,\phi'}^{\,m} \right\rangle_{J,2} & \left\langle \underline{\underline{Z}}_{\phi,t'}^{\,m} \right\rangle_{M,1} & \underline{\underline{0}} \end{bmatrix} \qquad m = -M..+M \tag{5.10}$$

If the columns and the rows are switched conveniently, the matrix becomes

[13] If two rows or columns are switched, the determinant of the resulting matrix is that of the original matrix multiplied by -1

$$Z^0_{EFIE}=\begin{bmatrix} \left\langle \underline{\underline{Z}}_{t,t'}^{\,m}\right\rangle_{J,1} & \left\langle \underline{\underline{Z}}_{t,\phi'}^{\,m}\right\rangle_{M,1} & \underline{\underline{0}} & \underline{\underline{0}} \\ \left\langle \underline{\underline{Z}}_{t,t'}^{\,m}\right\rangle_{J,2} & \left\langle \underline{\underline{Z}}_{t,\phi'}^{\,m}\right\rangle_{M,2} & \underline{\underline{0}} & \underline{\underline{0}} \\ \underline{\underline{0}} & \underline{\underline{0}} & \left\langle \underline{\underline{Z}}_{\phi,t'}^{\,m}\right\rangle_{M,1} & \left\langle \underline{\underline{Z}}_{\phi,\phi'}^{\,m}\right\rangle_{J,1} \\ \underline{\underline{0}} & \underline{\underline{0}} & \left\langle \underline{\underline{Z}}_{\phi,t'}^{\,m}\right\rangle_{M,1} & \left\langle \underline{\underline{Z}}_{\phi,\phi'}^{\,m}\right\rangle_{J,2} \end{bmatrix} \qquad m=-M..+M \tag{5.11}$$

The dimensions of the two groups of submatrices are $2N_t\times(N_t+N_\phi)$ and $2N_\phi\times(N_t+N_\phi)$. For an *unbalanced* set, both groups yield a non square matrix whereby, in view of the reasoning expounded for (5.3), one can infer that $\det(Z^0_{EFIE})=0$.

For the MFIE, the submatrices in (5.4) stand for

$$\begin{aligned} \left\langle Z^m\right\rangle_{J,1}&=\left[Z_H^m\right]^{\mathrm{O}} \quad ; \quad \left\langle Z^m\right\rangle_{M,2}=\frac{\left[Z_E^m\right]^{\mathrm{O}}}{\eta_{\mathrm{O}}^{\,2}} \\ \left\langle Z^m\right\rangle_{J,2}&=\left[Z_H^m\right]^{\mathrm{I}} \quad ; \quad \left\langle Z^m\right\rangle_{M,2}=\frac{\left[Z_E^m\right]^{\mathrm{I}}}{\eta_{\mathrm{I}}^{\,2}} \end{aligned} \tag{5.12}$$

and consequently Z^0_{MFIE} becomes - $m=0$ -

$$Z^0_{MFIE}=\begin{bmatrix} \underline{\underline{0}} & \left\langle \underline{\underline{Z}}_{t,\phi'}^{\,m}\right\rangle_{J,1} & \left\langle \underline{\underline{Z}}_{t,t'}^{\,m}\right\rangle_{M,1} & \underline{\underline{0}} \\ \left\langle \underline{\underline{Z}}_{\phi,t'}^{\,m}\right\rangle_{J,1} & \underline{\underline{0}} & \underline{\underline{0}} & \left\langle \underline{\underline{Z}}_{\phi,\phi'}^{\,m}\right\rangle_{M,1} \\ \underline{\underline{0}} & \left\langle \underline{\underline{Z}}_{t,\phi'}^{\,m}\right\rangle_{J,2} & \left\langle \underline{\underline{Z}}_{t,t'}^{\,m}\right\rangle_{M,2} & \underline{\underline{0}} \\ \left\langle \underline{\underline{Z}}_{\phi,t'}^{\,m}\right\rangle_{J,2} & \underline{\underline{0}} & \underline{\underline{0}} & \left\langle \underline{\underline{Z}}_{\phi,\phi'}^{\,m}\right\rangle_{M,2} \end{bmatrix} \qquad m=-M..+M \tag{5.13}$$

which, following the arrangement carried out before, becomes

$$\begin{bmatrix} \left\langle \underline{\underline{Z}}_{\phi,t'}^{\,m}\right\rangle_{J,1} & \left\langle \underline{\underline{Z}}_{\phi,\phi'}^{\,m}\right\rangle_{M,1} & \underline{\underline{0}} & \underline{\underline{0}} \\ \left\langle \underline{\underline{Z}}_{\phi,t'}^{\,m}\right\rangle_{J,2} & \left\langle \underline{\underline{Z}}_{\phi,\phi'}^{\,m}\right\rangle_{M,2} & \underline{\underline{0}} & \underline{\underline{0}} \\ \underline{\underline{0}} & \underline{\underline{0}} & \left\langle \underline{\underline{Z}}_{t,t'}^{\,m}\right\rangle_{M,2} & \left\langle \underline{\underline{Z}}_{t,\phi'}^{\,m}\right\rangle_{J,2} \\ \underline{\underline{0}} & \underline{\underline{0}} & \left\langle \underline{\underline{Z}}_{t,t'}^{\,m}\right\rangle_{M,1} & \left\langle \underline{\underline{Z}}_{t,\phi'}^{\,m}\right\rangle_{J,1} \end{bmatrix} \qquad m=-M..+M \tag{5.14}$$

The dimensions of the two submatrices groups are $2N_\phi\times(N_t+N_\phi)$ and $2N_t\times(N_t+N_\phi)$, which again form non-square matrices, whereby $\det(Z^0_{MFIE})=0$.

Therefore, in dielectric problems, the *unbalanced* set only allows the use of the PMCHW operator.

5.2 NUMERICAL LIMITATIONS ON THE DEVELOPMENT OF THE DIELECTRIC OPERATORS

The study in the previous section allows the use of any dielectric operator with a *balanced* set. However, to my knowledge, no dielectric BoR-formulation regarding the EFIE or the MFIE has ever been successfully developed. Indeed, the BoR-dielectric formulations present in literature correspond to the PMCHW -either with a *balanced* set [19][20][31] or with an *unbalanced* set [13]-. In the opinion of the author of this dissertation Thesis, this better performance of the PMCHW, as reasoned in the next paragraph, must be attributed to the fact that it manages better the inaccuracy associated to the PeC-MFIE.

In the EFIE -see (5.9)-, the PeC-EFIE and the PeC-MFIE contributions affect only one sort of current -respectively the electric current and the magnetic current-. Analogously, the MFIE -see (5.12)- allows for the dual case so that the electric and the magnetic currents are influenced respectively only by the PeC-MFIE and by the PeC-EFIE terms. The PMCHW, on the other hand, provides both the PeC-EFIE and the PeC-MFIE influences for both the electric and the magnetic currents -see (5.5)-. One can agree that this approach must be more robust to the inaccuracy in the PeC-MFIE contribution since it can be compensated -at least partially- by the well-behaving PeC-EFIE for both source magnitudes. Note that for the EFIE and for the MFIE, the contribution due to one source magnitude -respectively the magnetic and the electric current- is completely misled by the erroneous PeC-MFIE term. This advantageous property of the PMCHW operator appears again in Chapter 8 for the case of 3D penetrable bodies.

Some examples are presented in the following sections for homogeneous penetrable bodies and for PeC-bodies coated with a single dielectric layer, whereby the E-PMCHW operator has to be applied.

5.3 HOMOGENEOUS DIELECTRIC BODIES

The bistatic RCS for a dielectric sphere with $\varepsilon_r = 4$ and radius $0.4775\lambda_0$ with axial incidence are presented for the two polarizations of the incident field. -see Fig. 5.1-. It is also presented the bistatic RCS for a dielectric ellipsoid with $a = 0.7849\lambda_0$, $a/b = 3$ and $\varepsilon_r = 5$ for the field polarization normal to the scan plane. The discretization adopted in both cases is $N_\phi = 35$ and $N_{FFT} = 128$ The results of the sphere are compared with the Mie solution. The results for the spheroid are compared with the Null-field solution of Barber Yeh and the MoM solution of L. N. Medgyesi [19].

The system of equations in these cases presents a condition number higher than in the conducting case -it is commented this aspect in detail in Chapter 8 for 3D dielectric operators-. For the cases tested is never lower than 1e4 -and increases when heading the high-frequency modes-. So, the extraction of the singularity through the recurrence formula must be carried out carefully. The bound adopted to allow the extraction of the singularity is set to $0.1\lambda_0$.

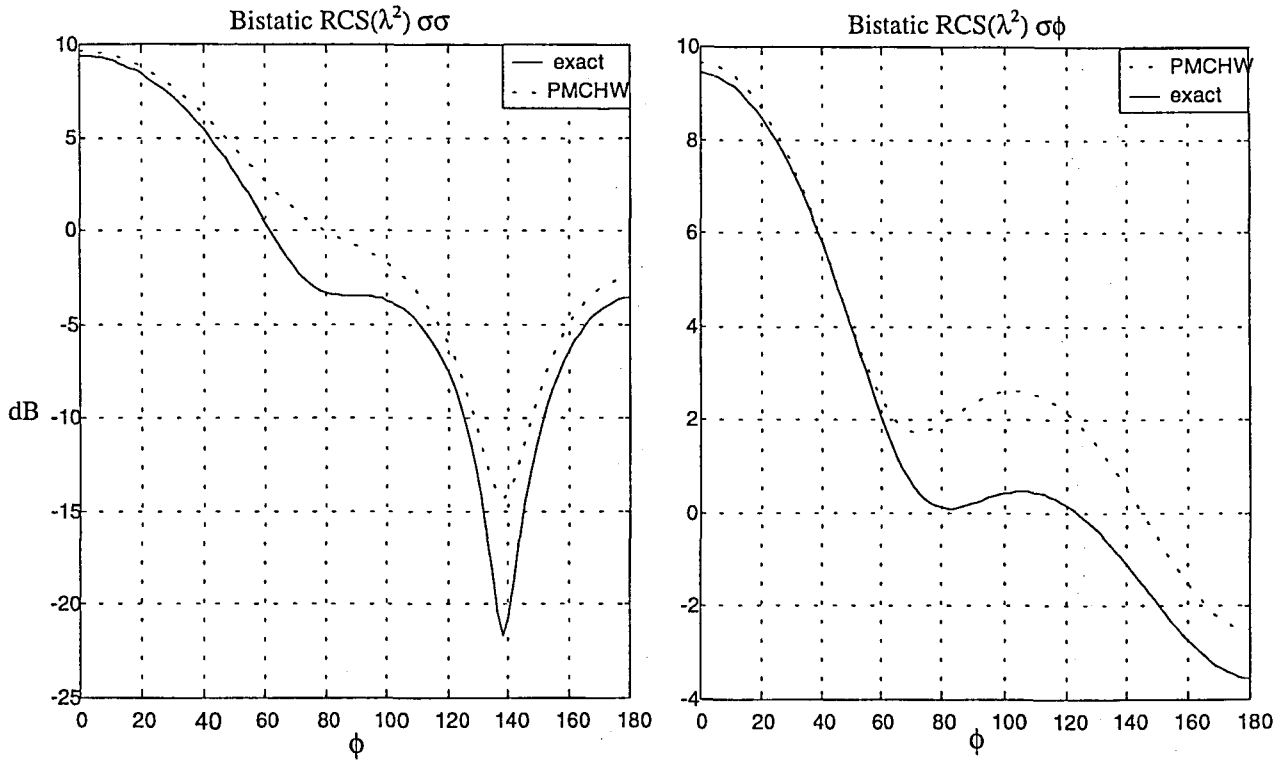

Fig. 5.1 RCS for the sphere - $\varepsilon_r = 4$ - *with* $N_\phi = 35$

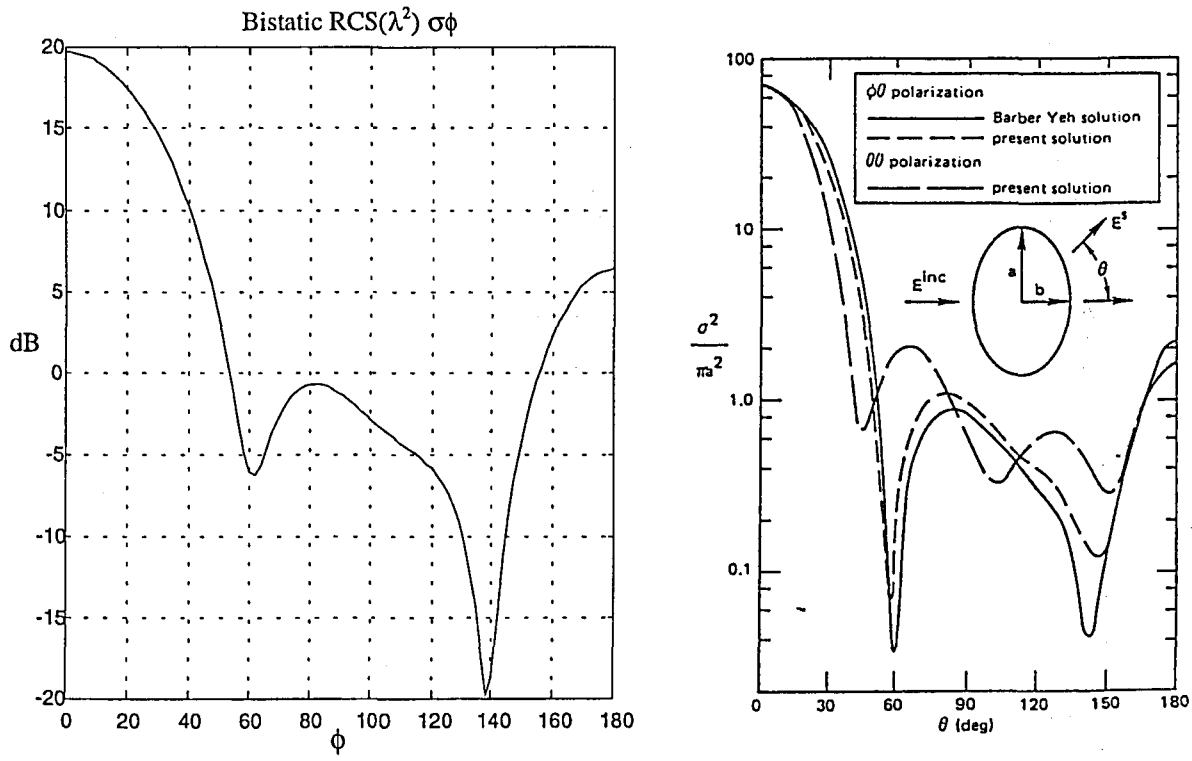

Fig. 5.2 RCS for the ellipsoid - $\varepsilon_r = 5$ - *with* $N_\phi = 35$

5.4 PEC-BODIES WITH FULL DIELECTRIC COATING

The bistatic RCS for a PeC-sphere completely coated with a penetrable layer -$\varepsilon_r = 4$- are presented in Fig. 5.3 for the two polarizations of the incident field. The outer radius -$a_1 = 0.477\lambda_0$- and the interior radius -a_2- satisfy $a_2/a_1 = 0.25$. The discretization adopted in the outer and the inner layers is respectively $N_{\phi,1} = 35$ and $N_{\phi,2} = 12$. The results for the spheroid are compared with the extended Mie solution and the MoM-BoR solution of L.N. Medgyesi [19].

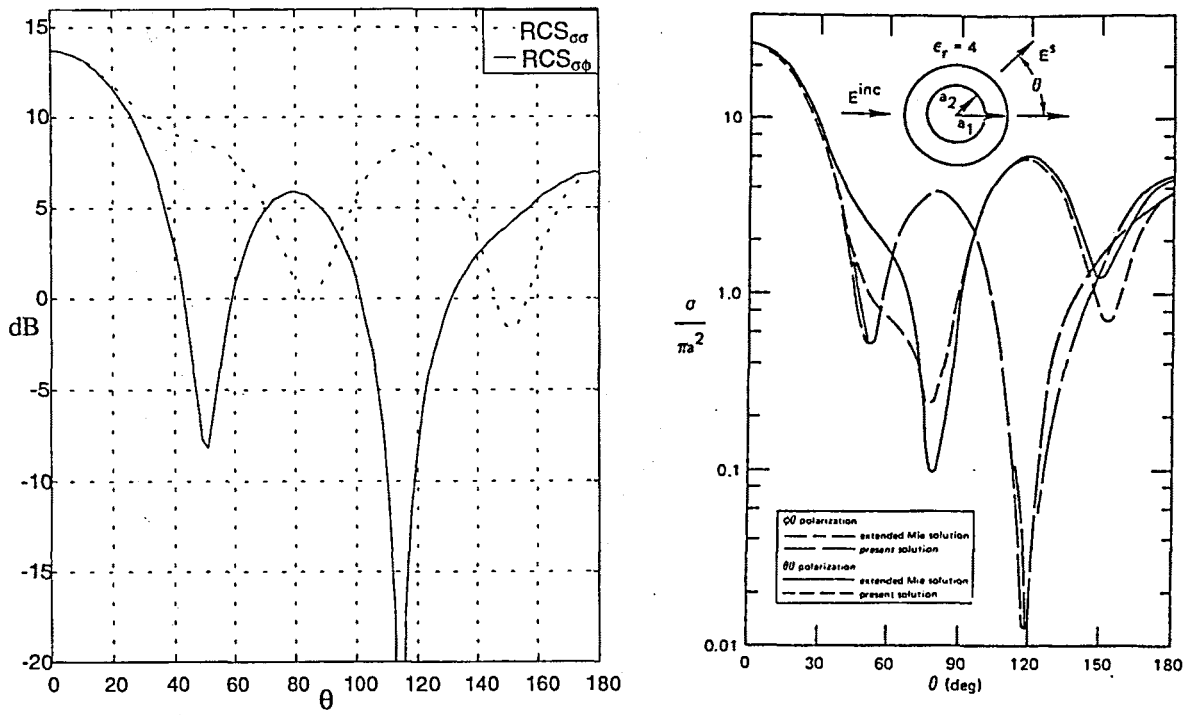

Fig. 5.3 RCS for the completely coated PeC-sphere with a layer with $\varepsilon_r = 4$ -

The error in the results Fig. 5.1, Fig. 5.2 and Fig. 5.3 are evident for these objects, that in any case present electrical dimensions considerably larger than those objects analysed with the BoR PeC-MFIE -see Chapter 4-.

Chapter 6 RWG BASED METHOD OF MOMENTS FOR PEC 3D BODIES

6.1 DEFINITION OF THE BASIS FUNCTIONS

In accordance with the purpose of this dissertation Thesis, the basis functions must be patches, whereby the current domain of each expanding function is confined in a determined area of the body surface.

As explained in Chapter 2, one cannot assume in the patch-based methods the expansion of the current over edges or vertices, which represent the borders of the basic expanding domain. As there is a discontinuity on the value of the function at both sides of the edge, one cannot foresee in advance which the value over the edges is. One expects, though, if the development of the electromagnetic operator is adequate, that the final current solution will converge at both sides of the edges to the correct value as the discretization becomes finer. In other integral methods, such as the Boundary Element Methods (BEM) [6][22], where one uses node-based finite elements, the current interpolation is effectuated up from the unknown values over the vertices. This lets the unknown globally defined over any point of the body surface, no matter if a vertex, an edge or a facet.

Two very closely related patch-based functions sets, *RWG* and *unxRWG*, are used to develop the MoM electromagnetic operators regarding either the expanding functions or the weighting functions. These sets associate the unknown to every interior edge of the body surface so that the edges placed along the end borders for the very particular case of open surfaces are dismissed.

The current value for any point inside the triangular facets is obtained from the contribution of the interior edges that shape the triangle where the point is placed -when dealing with a closed surface, the three bordering edges do contribute-.

Let us i, j, k be the three edges that form the triangle, the value for the current $\vec{J}(\vec{r})$ inside the triangle yields -see Fig. 6.1-

$$\vec{J}(\vec{r}) = \sum_{s=i,j,k} \vec{B}_s(\vec{r}) I_s \tag{6.1}$$

where I_s represent the current unknowns and $\vec{B}_s(\vec{r})$ stands for any of both sets, *RWG* or *unxRWG*, to be presented next.

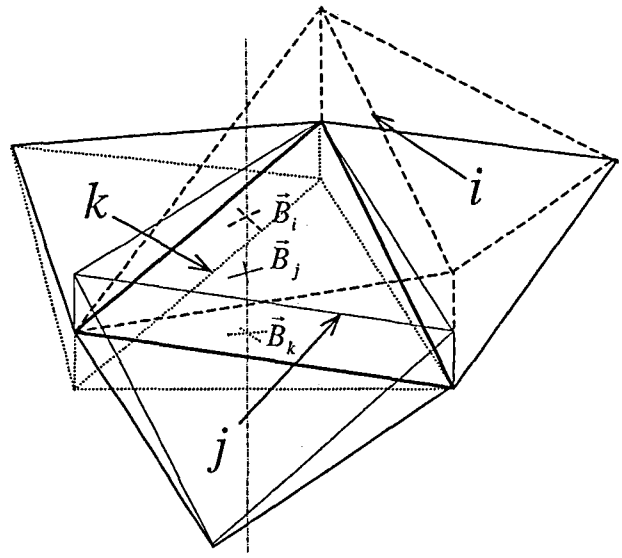

Fig. 6.1 The surrounding edges i, j, k contribute on the current value over the triangle

They turn out antagonistic and independent since they rely on the two orthogonal polar fundamental canonical directions: respectively ρ and ϕ. *RWG* and *unxRWG* are respectively included into the general groups of divergence-conforming and curl-conforming functions[14], where they stand for low-order functions defined over planar triangular facets. The curl-conforming functions were first presented by Nedelec [32] and used in the numerical methods by Bossavit and Vérité [42], Hano [43], and Barton and Cendes [35]. The earliest use of divergence-conforming functions for numerical solutions can be attributed to Raviart and Thomas [27], Rao *et al.* [28], and Shcaubert *et al.* [29].

6.1.1 RWG basis functions

Sadasiva M. Rao, Donald R. Wilton and Allen W. Glisson, [28], presented a revolutionary set of patch-based basis functions to apply on the PeC-EFIE approach for any closed PeC surface of arbitrary shape. Similarly, R. E. Hodges and Y. Rahmat-Samii [11] presented later on an accurate formulation, with the same set of functions, for PeC bodies by means of the alternative PeC-MFIE operator.

This set of basis functions $\{\vec{w}_i\}$, the so-called *RWG* basis functions, is defined as

[14] The curl-conforming and the divergence-conforming bases have, respectively, continuous tangential and normal components across adjacent elements [33].

$$\vec{w}_i(\vec{r}) = \begin{cases} \dfrac{1}{2A_i^+}\vec{f}_i^{\,+}(\vec{r}), & \vec{r} \in T_i^+ \\ \dfrac{1}{2A_i^-}\vec{f}_i^{\,-}(\vec{r}), & \vec{r} \in T_i^- \end{cases} \tag{6.2}$$

where $A_i^{\pm}$ and $\vec{f}_i^{\,\pm}(\vec{r})$ respectively stand for the area and the expanding part over each triangle $T_i^{\pm}$, associated to the edge i. Particularly,

$$\vec{f}_i^{\,\pm}(\vec{r}) = (\pm)_i\left(\vec{r} - \vec{r}_{oi}^{\,\pm}\right) = (\pm)_i\,\vec{\rho}_i^{\,\pm} \tag{6.3}$$

with $\vec{r}_{oi}^{\,\pm}$ being the local coordinates origin placed at the vertex opposite to the edge i, -see Fig. 6.2-. The convention adopted forces the current to flow from T_i^+ to T_i^- through the common i edge, as shown in the figure below.

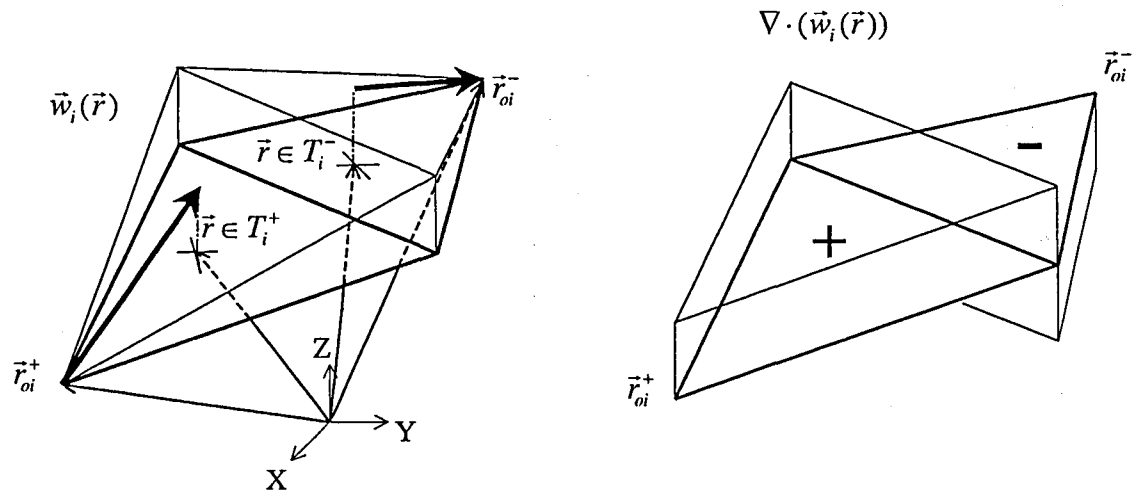

Fig. 6.2 RWG basis function

- $\vec{\rho}_i^{\,\pm}$ in (6.3) denotes that the *RWG* set effectuates a radially directed expansion of the current over each triangular facet $T_i^{\pm}$.

- The component perpendicular to the common edge i of the *RWG* function at both sides $T_i^{\pm}$ is equal[15], as shown right away

$$\left.\frac{1}{2A_i^+}\vec{f}_i^{\,+}(\vec{r})\cdot\hat{n}_{out,i}^{+}\right|_{\vec{r}\in\partial\left(T_i^+\cap T_i^-\right)} = \frac{1}{2A_i^+}h_i^+ = l_i$$

[15] The original definition of the *RWG* basis functions allowed for a product of (6.2) by the length of the edge, which normalise the current coefficient to the normal component of the current; later on, though, this formulation was simplified and the multiplication by this constant factor was left out. Both developments are equivalent and the results are the same.

$$-\frac{1}{2A_i^-}\vec{f}_i^-(\vec{r})\cdot\hat{n}_{out,i}^-\Big|_{\vec{r}\in\partial(T_i^+\cap T_i^-)}=\frac{1}{2A_i^-}h_i^-=l_i \tag{6.4}$$

where it is taken for granted the well-known equality for the area of the triangle $A_i^\pm=h_i^\pm l_i/2$. $\partial(T_i^+\cap T_i^-)$ denotes the border common to both triangles, l_i stands for the length of the i edge, $h_i^\pm$ denotes the heights of $T_i^\pm$ from $\vec{r}_{oi}^{\,\pm}$ and $\hat{n}_{out,i}^+$, $-\hat{n}_{out,i}^-$ are the unit vectors that are at the same time perpendicular to $\partial(T_i^+\cap T_i^-)$, coplanar with T_i^+, T_i^- and following the + to - flux. As the normal component across the four exterior edges is null, any *RWG* expansion ensures the normal components across the edges to be continuous.

- Resorting to the polar divergence expression,

$$\nabla\cdot\vec{f}_i^{\,\pm}(\vec{r})=(\pm)_i\nabla\cdot\vec{\rho}_i^{\,\pm}=(\pm)_i\frac{1}{\rho_i^\pm}\frac{\partial}{\partial\rho_i^\pm}\left(\rho_i^{\pm 2}\right)=(\pm)_i 2 \tag{6.5}$$

the surface divergence of the *RWG* basis functions yields

$$\nabla\cdot\vec{w}_i(\vec{r})=\begin{cases}\dfrac{1}{2A_i^+}\nabla\cdot\vec{f}_i^{\,+}(\vec{r})=\dfrac{1}{A_i^+}, & \vec{r}\in T_i^+\\[2ex] \dfrac{1}{2A_i^-}\nabla\cdot\vec{f}_i^{\,-}(\vec{r})=-\dfrac{1}{A_i^-}, & \vec{r}\in T_i^-\end{cases} \tag{6.6}$$

which lets the PeC-EFIE operator well-defined at least with regard to the Scalar potential term, that depends on the surface charge density σ -related with the divergence of the current through the continuity equation-. The charge throughout the i expanding function Q_i, in view of (6.5), is ensured to be zero; that is,

$$Q_i=\iint_{T_i^+\cup T_i^-}\sigma_i(\vec{r})dS=\frac{-1}{j\varpi}\iint_{T_i^+\cup T_i^-}\nabla\cdot\vec{w}_i(\vec{r})dS=\frac{-1}{j\varpi}\left[\frac{1}{A_i^+}\iint_{T_i^+}dS-\frac{1}{A_i^-}\iint_{T_i^-}dS\right]=0 \tag{6.7}$$

because the charge-density pulses -see Fig. 6.2- in $T_i^\pm$ compensate each other. This of course sets to zero the total amount of charge Q_i over the body surface

$$Q_T=\sum_{i=1}^{N}Q_i=0 \tag{6.8}$$

that is a condition that all the correct MoM expanding functions, as referred in Chapter 2, must accomplish.

- The basic structure of the *RWG* functions may be understood as an elementary electric dipole since the application of the curl operator yields zero.

6.1.2 unxRWG basis functions

An antagonistic set to *RWG* appears by means of the following definition

$$(\vec{w}\times\hat{n})_i(\vec{r})=\begin{cases}\dfrac{1}{2A_i^+}\vec{f}_i^{\,+}(\vec{r})\times\hat{n}_i^+, & \vec{r}\in T_i^+\\ \dfrac{1}{2A_i^-}\vec{f}_i^{\,-}(\vec{r})\times\hat{n}_i^-, & \vec{r}\in T_i^-\end{cases} \tag{6.9}$$

which I name *unxRWG* because it is derived from the cross-product between *RWG* and $\hat{n}_i^{\pm}$, the normal vectors to the planar facets $T_i^{\pm}$. That is,

$$\vec{f}_i^{\,\pm}(\vec{r})\times\hat{n}_i^{\pm}=(\pm)_i\left(\vec{r}-\vec{r}_{oi}^{\,\pm}\right)\times\hat{n}_i^{\pm}=(\pm)_i\,\vec{\rho}_i^{\,\pm}\times\hat{n}_i^{\pm} \tag{6.10}$$

which, in view of Fig. 6.3, replaces the original *RWG* polar unit vectors $(\pm)_i\,\hat{\rho}_i^{\pm}$ by the other, azimuthal, local direction $\hat{\phi}_i^{\pm}$ over both triangles $T_i^{\pm}$.

$$\vec{f}_i^{\,\pm}(\vec{r})\times\hat{n}_i^{\pm}=\left|\vec{\rho}_i^{\,\pm}\right|\left\{(\pm)_i\,\hat{\rho}_i^{\pm}\times\hat{n}_i^{\pm}\right\}=\left|\vec{\rho}_i^{\,\pm}\right|\hat{\phi}_i^{\pm}=\rho_i^{\pm}\hat{\phi}_i^{\pm} \tag{6.11}$$

The convention adopted compels the current to flow from one side of both triangles $T_i^{\pm}$ to the other side; indeed,

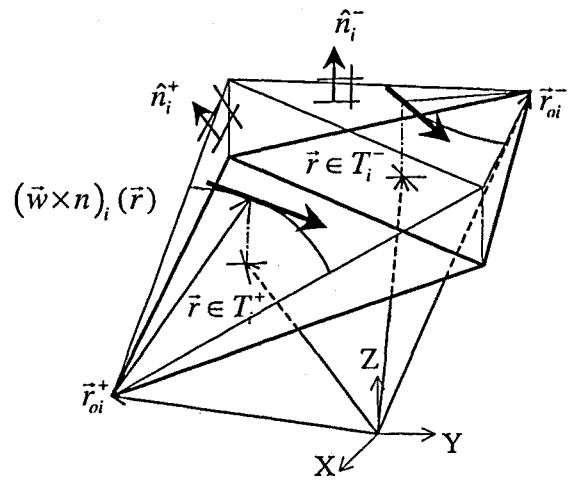

Fig. 6.3 unxRWG basis function

- $\hat{\phi}_i^{\pm}$ in (6.11) denotes that the *unxRWG* set effectuates an angularly oriented expansion of the current over each triangular facet $T_i^{\pm}$.

- In contrast with (6.4), the component parallel to the common edge i of the *unxRWG* function at both sides $T_i^{\pm}$ is that which now becomes equal,

$$\frac{1}{2A_i^+}\left\{\vec{f}_i^{\,+}(\vec{r})\times\hat{n}_i^+\right\}\cdot\hat{l}_i\Big|_{\vec{r}\in\partial\left(T_i^+\cap T_i^-\right)}=\frac{1}{2A_i^+}\vec{f}_i^{\,+}(\vec{r})\cdot\left\{\hat{n}_i^+\times\hat{l}_i\right\}\Big|_{\vec{r}\in\partial\left(T_i^+\cap T_i^-\right)}$$

$$=\frac{1}{2A_i^+}\vec{f}_i^{\,+}(\vec{r})\cdot\hat{n}_{out,i}^+\Big|_{\vec{r}\in\partial\left(T_i^+\cap T_i^-\right)}=l_i$$

$$\frac{1}{2A_i^-}\left\{\vec{f}_i^{\,-}(\vec{r})\times\hat{n}_i^-\right\}\cdot\hat{l}_i\Big|_{\vec{r}\in\partial\left(T_i^+\cap T_i^-\right)}=\frac{1}{2A_i^-}\vec{f}_i^{\,-}(\vec{r})\cdot\left\{\hat{n}_i^-\times\hat{l}_i\right\}\Big|_{\vec{r}\in\partial\left(T_i^+\cap T_i^-\right)}$$

$$=-\frac{1}{2A_i^-}\vec{f}_i^{\,-}(\vec{r})\cdot\hat{n}_{out,i}^-\Big|_{\vec{r}\in\partial\left(T_i^+\cap T_i^-\right)}=l_i \qquad (6.12)$$

As the component parallel to the four exterior edges is null, any *unxRWG* expansion ensures the tangential components along the edges to be continuous.

- The divergence of the *unxRWG* functions yields zero because there is only ρ dependence along the ϕ component,

$$\nabla\cdot\left(\vec{f}_i^{\,\pm}(\vec{r})\times\hat{n}_i^{\pm}\right)=\frac{1}{\rho}\frac{\partial\left(\rho_i^{\pm}\right)}{\partial\phi}=0 \qquad (6.13)$$

which lets the surface charge density σ be identically null at any point over the body surface. Therefore, in any closed domain inside $T_i^+\cup T_i^-$, the entering and the leaving current flux coincide. Hence, the charge inside any arbitrary domain all over the body surface is identically zero, which accomplishes the required preliminary MoM condition of $Q_T=0$ but, as shown later on, lets the scalar potential gradient in PeC-EFIE badly defined.

- In contrast with *RWG*, the basic structure of the *unxRWG* functions represents an elementary magnetic dipole; indeed, according to (6.13), its electric dipolar moment is null.

- Although it is required for $\hat{n}_i^+$ and $\hat{n}_i^-$ to point to the same medium so that the rotation of the function has the same sense across T_i^+ and T_i^-, there is no constraint on the choice of the sign for $\hat{n}_i^{\pm}$. On PeC-Bodies, it has been adopted the convention to direct $\hat{n}_i^{\pm}$ towards the outer free-space medium.

6.2 VALID PEC-OPERATORS

It has been presented in Chapter 2 the construction of the system of equations that leads to the general matrix expression for PeC-bodies. The impedance matrix elements z_{sq} present the general form

$$z_{sq} = \left\langle \vec{W}_s, \vec{S}\left(\vec{B}_q\right)\right\rangle \qquad s=1..N,\ q=1..N \tag{6.14}$$

where N, $\vec{W}$ and $\vec{B}$ are respectively the number of unknowns and the sets of weighting and expanding functions and $\vec{S}$ is the chosen electromagnetic operator, which in essence is the PeC-EFIE or the PeC-MFIE. The PeC-CFIE -Combined Field Integral Equation- results from their addition. As detailed in Chapter 2, in the development of the PeC-operators $\vec{r} \in S^-$ is assumed.

The weighting functions must be so that they constitute a complete basis of the rank space of the operator. This obviously links the weighting -$\vec{W}_s$- with the expanding -$\vec{B}_q$- functions, which in turn must be appropriate with the characteristics of the operator.

In the next section it is given a descriptive insight into the characteristics of the valid PeC-operators in order to assess its good behaviour. A thorough analysis of the required characteristics of the field -rank- and current -domain- spaces for each operator is given in section 6.5. It is then justified the right choice of *RWG* and *unxRWG* as weighting or expanding functions in the following valid operators.

6.2.1 PeC-EFIE(RWG,RWG): $\left\langle \vec{w}_s, \vec{E}^S_{PeC}\left(\vec{w}_q\right)\Big|_{\vec{r}\in S^-}\right\rangle$

6.2.1.1 Mathematical development

S. Rao, D. Wilton and A. Glisson [28] developed this Galerkin MoM approach making use of their *RWG* functions. The impedance terms stand for

$$Z_{efie}(s,q) = \left\langle \vec{w}_s, \vec{E}^S_{PeC}\left(\vec{w}_q\right)\Big|_{\vec{r}\in S^-}\right\rangle = -j\omega\left\langle \vec{w}_s, \vec{A}\left(\vec{w}_q\right)\right\rangle - \left\langle \vec{w}_s, \nabla\Phi\left(\vec{w}_q\right)\right\rangle \qquad s=1..N,\ q=1..N \tag{6.15}$$

which, examined separately for each plus-minus field-source triangle contribution, in view of the definition for the *RWG* functions in (6.6) and in Fig. 6.2, stands for

$$\begin{aligned}
&\left\langle \frac{1}{2A_s^{\pm}}\vec{f}_s^{\pm}(\vec{r}), \vec{A}\left(\frac{1}{2A_q^{\pm}}\vec{f}_q^{\pm}(\vec{r}\,')\right)\right\rangle \\
&\quad = \mu\iint_{T_s^{\pm}} \frac{1}{2A_s^{\pm}}\vec{f}_s^{\pm}(\vec{r})\cdot\left[\iint_{T_q^{\pm}} \frac{1}{2A_q^{\pm}}\vec{f}_q^{\pm}(\vec{r}\,')G(\vec{r}-\vec{r}\,')dS'\right]dS \\
&\quad = \mu\iint_{T_s^{\pm}} \frac{(\pm)_s}{2A_s^{\pm}}\vec{\rho}_s^{\pm}\cdot\left[\iint_{T_q^{\pm}} \frac{(\pm)_q}{2A_q^{\pm}}\vec{\rho}\,'^{\pm}_q G(\vec{r}-\vec{r}\,')dS'\right]dS \qquad s=1..N,\ q=1..N
\end{aligned} \tag{6.16}$$

and

$$\left\langle \frac{1}{2A_s^{\pm}}\vec{f}_s^{\pm}(\vec{r}),\nabla\Phi\left(\frac{1}{2A_q^{\pm}}\vec{f}_q^{\pm}(\vec{r}')\right)\right\rangle$$
$$=\frac{-1}{j\omega\varepsilon}\iint_{T_s^{\pm}}\frac{1}{2A_s^{\pm}}\vec{f}_s^{\pm}(\vec{r})\cdot\left[\iint_{T_q^{\pm}}\frac{1}{2A_q^{\pm}}\nabla'\cdot\vec{f}_q^{\pm}(\vec{r}')\nabla G(\vec{r}-\vec{r}')dS'\right]dS$$
$$=\frac{-1}{j\omega\varepsilon}\iint_{T_q^{\pm}}\frac{1}{2A_q^{\pm}}\nabla'\cdot\vec{f}_q^{\pm}(\vec{r}')\iint_{T_s^{\pm}}\frac{1}{2A_s^{\pm}}\vec{f}_s^{\pm}(\vec{r})\cdot\nabla G(\vec{r}-\vec{r}')dSdS' \qquad (6.17)$$
$$s=1..N,\ q=1..N$$

The field integrand in (6.17) can be equivalently expressed as

$$\vec{f}_s^{\pm}(\vec{r})\cdot\nabla G(\vec{r}-\vec{r}')=\nabla\left(\vec{f}_s^{\pm}(\vec{r})G(\vec{r}-\vec{r}')\right)-\nabla\cdot\left(\vec{f}_s^{\pm}(\vec{r})\right)G(\vec{r}-\vec{r}') \qquad (6.18)$$

The first addend when field-integrated throughout the pair of edge triangles -resorting to the surface gradient theorem- becomes

$$\iint_{T_s^+\cup T_s^-}\nabla\cdot\left(\vec{w}_s(\vec{r})G(\vec{r}-\vec{r}')\right)dS=\iint_{T_s^+\cup T_s^-}\nabla_S\cdot\left(\vec{w}_s(\vec{r})G(\vec{r}-\vec{r}')\right)dS$$
$$=\oint_{\partial(T_s^+\cup T_s^-)}G(\vec{r}-\vec{r}')\vec{w}_s(\vec{r})\cdot\hat{n}_{out}(\vec{r})dl$$
$$=\oint_{\partial T_s^+}G(\vec{r}-\vec{r}')\frac{\vec{f}_s^{+}(\vec{r})}{2A_s^{+}}\cdot\hat{n}_{out}^{+}(\vec{r})dl+\oint_{\partial T_s^-}G(\vec{r}-\vec{r}')\frac{\vec{f}_s^{-}(\vec{r})}{2A_s^{-}}\cdot\hat{n}_{out}^{-}(\vec{r})dl \qquad (6.19)$$

where $\hat{n}_{out}^{\pm}$ denotes the unit vector pointing out across the borders. Since there is no leak of current outwards -the current is parallel to the outer borders-, the previous expression, in accordance with (6.4), yields zero

$$=\int_{\partial(T_i^+\cap T_i^-)}G(\vec{r}-\vec{r}')\frac{\vec{f}_s^{+}(\vec{r})}{2A_s^{+}}\cdot\hat{n}_{out}^{+}(\vec{r})dl+\int_{\partial(T_i^+\cap T_i^-)}G(\vec{r}-\vec{r}')\frac{\vec{f}_s^{-}(\vec{r})}{2A_s^{-}}\cdot\hat{n}_{out}^{-}(\vec{r})dl$$
$$=\int_{\partial(T_i^+\cap T_i^-)}G(\vec{r}-\vec{r}')\left[\frac{\vec{f}_s^{+}(\vec{r})}{2A_s^{+}}\cdot\vec{n}_{out,i}^{+}(\vec{r})+\frac{\vec{f}_s^{-}(\vec{r})}{2A_s^{-}}\cdot\vec{n}_{out,i}^{-}(\vec{r})\right]dl=0 \qquad (6.20)$$

Therefore, back to (6.17), with the modifications due to (6.18), (6.19) and (6.20), the scalar potential term stands for:

$$\left\langle \frac{1}{2A_s^{\pm}}\vec{f}_s^{\pm}(\vec{r}),\nabla\Phi\left(\frac{1}{2A_q^{\pm}}\vec{f}_q^{\pm}(\vec{r}')\right)\right\rangle$$
$$=\frac{1}{j\omega\varepsilon}\iint_{T_s^{\pm}}\frac{1}{2A_s^{\pm}}\nabla\cdot\vec{f}_s^{\pm}(\vec{r})\cdot\left[\iint_{T_q^{\pm}}\frac{1}{2A_q^{\pm}}\nabla'\cdot\vec{f}_q^{\pm}(\vec{r}')G(\vec{r}-\vec{r}')dS'\right]dS$$

$$= \frac{1}{j\varpi\varepsilon} \iint_{T_s^{\pm}} \frac{(\pm)_s}{A_s^{\pm}} \cdot \left[\iint_{T_q^{\pm}} \frac{(\pm)_q}{A_q^{\pm}} G(\vec{r} - \vec{r}\,') dS' \right] dS \qquad s = 1..N,\ q = 1..N \qquad (6.21)$$

which is a very advantageous expression because the dependence on the Green's function gradient disappears [16].

6.2.1.2 Theoretical considerations

To assess the prospective good behaviour of a Galerking operator, it is advantageous to use a self-adjoint operator. In this case, the validity relies merely on the skill of the expanding functions set in spanning the operator domain, since both, rank and domain spaces, are the same.

By viewing each of the terms corresponding to the Vector and Scalar potentials in (6.16) and (6.21), one remarks that the field terms and the source terms in each of these integrals can be switched so that

$$Z_{efie}(s,q) = \left\langle \vec{w}_s, \vec{E}^S_{PeC}(\vec{w}_q) \right\rangle = \left\langle \vec{w}_q, \vec{E}^S_{PeC}(\vec{w}_s) \right\rangle = Z_{efie}(q,s) \qquad (6.22)$$

which implies that Z_{efie} is a symmetric matrix.

According to the inner-product definition presented in Chapter 2, one can remark through the observation of (6.22) that the adjoint operator of $\vec{E}^S$ is the complex conjugate of $\vec{E}^S$: $\vec{E}^{S^*}$. Of course, the domain space of both conjugate operators must be the same and the implication must be the same as if the operator was self-adjoint. Therefore, in view of the good behaviour of the operator, one has to consider *RWG* as good expanding set for the domain of $\vec{E}^S$.

(6.22) can also be inferred from the application of the reciprocity theorem on two electric current distributions $\vec{w}_s$ and $\vec{w}_q$. This involves that $\vec{w}_s$ and $\vec{w}_q$ present a physical behaviour. Indeed, as shown before, thanks to the fact that there is no leak of current in $\vec{w}$, one can simplify the testing of the scalar potential gradient and yield a symmetric impedance term.

6.2.2 PeC-MFIE(unxRWG,RWG): $\left\langle (\vec{w}\times\hat{n})_s, \vec{H}^S_{PeC}(\vec{w}_q)\big|_{r\in S^-} \right\rangle$

6.2.2.1 Mathematical development

The detailed development of the impedance terms for the PeC-MFIE operator with the *RWG* expanding functions and the *unxRWG* weighting functions, according to R.E. Hodges and Y. Rahmat-Samii [11], yields

[16] The absence of the Green's function gradient dependence in the PeC-EFIE operator was also expounded when developing the BoR PeC-EFIE operator (Chapter 3) and it happens whenever there is no leak of current all over the weighting function domain.

$$Z_{mfie}(s,q)=\left\langle (\vec{w}\times\hat{n})_s, \vec{H}^{s}_{PeC}(\vec{w}_q)\big|_{\vec{r}\in S^-}\right\rangle=\frac{1}{\mu}\left\langle (\vec{w}\times\hat{n})_s, \nabla\times\vec{A}(\vec{w}_q)\right\rangle \qquad s=1..N,\ q=1..N \tag{6.23}$$

which, examined separately for each plus-minus field-source triangle contribution and resorting to the vector equality $\nabla\times(\psi\vec{A})=\nabla\psi\times\vec{A}+\psi\nabla\cdot\vec{A}$, stands for

$$\begin{aligned}
&\frac{1}{\mu}\left\langle \frac{1}{2A_s^{\pm}}\vec{f}_s^{\pm}(\vec{r})\times\hat{n}_s^{\pm}, \nabla\times\vec{A}\left(\frac{1}{2A_q^{\pm}}\vec{f}_q^{\pm}(\vec{r}')\right)\right\rangle \\
&\quad=\iint_{T_s^{\pm}}\left(\frac{1}{2A_s^{\pm}}\vec{f}_s^{\pm}(\vec{r})\times\hat{n}_s^{\pm}\right)\cdot\nabla\times\left[\iint_{T_q^{\pm}}\frac{1}{2A_q^{\pm}}\vec{f}_q^{\pm}(\vec{r}')G(\vec{r}-\vec{r}')dS'\right]dS \\
&\quad=\iint_{T_s^{\pm}}\left(\frac{1}{2A_s^{\pm}}\vec{f}_s^{\pm}(\vec{r})\times\hat{n}_s^{\pm}\right)\cdot\iint_{T_q^{\pm}}\frac{1}{2A_q^{\pm}}\nabla G(\vec{r}-\vec{r}')\times\vec{f}_q^{\pm}(\vec{r}')dS'dS \\
&\quad=\iint_{T_s^{\pm}}\frac{(\pm)_s}{2A_s^{\pm}}(\vec{\rho}_s^{\pm}\times\hat{n}_s^{\pm})\cdot\left[\iint_{T_q^{\pm}}\frac{(\pm)_q}{2A_q^{\pm}}\nabla G(\vec{r}-\vec{r}')\times\vec{\rho}\,'^{\pm}_q dS'\right]dS \qquad s=1..N,\ q=1..N
\end{aligned} \tag{6.24}$$

Moreover, (6.24) can be simplified, as described in [11], through the expression

$$\hat{R}\times\vec{\rho}\,'^{\pm}_q=\frac{1}{R}(\vec{r}-\vec{r}^{\pm}_{oq}+\vec{r}^{\pm}_{oq}-\vec{r}')\times(\vec{r}'-\vec{r}^{\pm}_{oq})=\frac{1}{R}(\vec{r}-\vec{r}^{\pm}_{oq})\times(\vec{r}'-\vec{r}^{\pm}_{oq}) \tag{6.25}$$

so that the cross-product is left out of the source-integral; that is,

$$\begin{aligned}
&\iint_{T_s^{\pm}}\frac{(\pm)_s}{2A_s^{\pm}}(\vec{\rho}_s^{\pm}\times\hat{n}_s^{\pm})\cdot\left[\iint_{T_q^{\pm}}\frac{\partial G}{\partial R}\hat{R}\times\vec{\rho}\,'^{\pm}_q\frac{(\pm)_q}{2A_q^{\pm}}dS'\right]dS \\
&\quad=\iint_{T_s^{\pm}}\frac{(\pm)_s}{2A_s^{\pm}}(\vec{\rho}_s^{\pm}\times\hat{n}_s^{\pm})\cdot(\vec{r}-\vec{r}^{\pm}_{oq})\times\left[\iint_{T_q^{\pm}}\frac{(\pm)_q}{2A_q^{\pm}}\frac{\partial G}{\partial R}\frac{\vec{\rho}\,'^{\pm}_q}{R}dS'\right]dS \qquad s=1..N,\ q=1..N
\end{aligned} \tag{6.26}$$

which is more advantageous in computational terms for the cross-product is moved out of the source integral.

6.2.2.2 Theoretical considerations

The PeC-MFIE operator demands special attention when the source-integration is carried out since two different integrals determine the result when $\vec{r}'\to\vec{r}$. The Principal Cauchy value contribution, which is the term coming from the routine source-integration, turns out null when the field and source triangles coincide because it is perpendicular to the plane where the *unxRWG* weighting function lies. Indeed, when $\vec{r}'\to\vec{r}$, $\nabla G(\vec{r}-\vec{r}')\propto(\vec{r}-\vec{r}')$ is coplanar with $\vec{\rho}\,'^{\pm}_q$, whereby $\left[\nabla G(\vec{r}-\vec{r}')\times\vec{\rho}\,'^{\pm}_q\right]\perp(\vec{\rho}_s^{\pm}\times\hat{n}_s^{\pm})$.

As usual when developing PeC-MFIE and $\vec{r}' \to \vec{r}$, the key term from the source integration comes from the integration of the singularity, whose analytical expression is presented in Chapter 2. According to the convention sign expounded in 6.1.2 for $\hat{n}$, with opposite sense to $\hat{n}^-$, the singular contribution to the impedance element becomes

$$Z_{\text{sing},mfie}(s,q) = \frac{\Omega_0^-}{4\pi}\left\langle (\vec{w}\times\hat{n})_s, (\hat{n}^-\times\vec{w}_q)\right\rangle = \frac{\Omega_0^-}{4\pi}\iint_{T_\cap}(\vec{w}_s(\vec{r})\times\hat{n})\cdot(\hat{n}^-\times\vec{w}_q(\vec{r}))dS$$
$$= \frac{\Omega_0^-}{4\pi}\iint_{T_\cap}\vec{w}_q(\vec{r})\cdot((\vec{w}_s(\vec{r})\times\hat{n})\times\hat{n}^-)dS = \frac{\Omega_0^-}{4\pi}\iint_{T_\cap}\vec{w}_q(\vec{r})\cdot\vec{w}_s(\vec{r})dS \qquad (6.27)$$

which is only applicable for those s, q-edges pairs that have common $T_s^\pm, T_q^\pm$ associated triangles. Particularly, if $s=q$ $T_\cap = T_s^+ \cup T_s^-$, and if $s \neq q$, $T_\cap$ corresponds to that triangle that is common to the domain of both functions $\vec{w}_s$ and $\vec{w}_q$. (6.27) can be seen as the inner-product between all the elements of the *RWG* set, which must be in general non null.

The application of the operator $\vec{H}^S_{PeC}\big|_{\vec{r}\in S^-}$ on a given function $\vec{w}_i(\vec{r})$ can be analytically computed, as shown in Chapter 2, for the specific case of the terms due to the singularity. To build the complete rank space, though, one should assess in addition the influence from the Cauchy Principal Value. Even though, as above-mentioned, it tends to zero for the functions that are nearly coplanar with the edge i -usually the closest ones for smooth-varying bodies-, its influence in general all over the rank subdomain $\vec{r}\in T_i^+ \cup T_i^-$ cannot be considered negligible.

In any case, as we have the closed expression of a very important part of the rank, it makes sense to use *unxRWG* as weighting functions because they expand perfectly this important part of the rank

$$\vec{H}^S_{PeC}(\vec{w}_i(\vec{r}'))\big|_{\text{sing},\vec{r}\in S^-} = \frac{\Omega_0^-}{4\pi}\hat{n}^-\times\vec{w}_i(\vec{r}) \propto (\vec{w}\times\hat{n})_i \qquad \vec{r}\in T_i^+\cup T_i^- \qquad (6.28)$$

This property has suggested the author of this dissertation Thesis that the reasoning would be likewise fit if the expanding and weighting functions, respectively *RWG* and *unxRWG*, were exchanged, which leads to the next section.

6.2.3 PeC-MFIE(RWG,unxRWG): $\left\langle \vec{w}_s, \vec{H}^S_{PeC}((\vec{w}\times\hat{n})_q)\big|_{\vec{r}\in S^-}\right\rangle$

6.2.3.1 Mathematical development

Analogously to (6.23), the impedance elements for this case become

$$Z_{mfiexun}(s,q) = \left\langle \vec{w}_s, \vec{H}^S_{PeC}((\vec{w}\times\hat{n})_q)\right\rangle = \frac{1}{\mu}\left\langle \vec{w}_s, \nabla\times\vec{A}((\vec{w}\times\hat{n})_q)\right\rangle \qquad s=1..N,\ q=1..N \qquad (6.29)$$

and an arrangement more in detail yields

$$\frac{1}{\mu}\left\langle \frac{1}{2A_s^{\pm}}\vec{f}_s^{\pm}(\vec{r}),\nabla\times\vec{A}\left(\frac{1}{2A_q^{\pm}}\left(\vec{f}_q^{\pm}\times\hat{n}_q^{\pm}\right)(\vec{r}\,')\right)\right\rangle$$
$$=\iint_{T_s^{\pm}}\frac{(\pm)_s}{2A_s^{\pm}}\vec{\rho}_s^{\pm}\cdot\left[\iint_{T_q^{\pm}}\nabla G(\vec{r}-\vec{r}\,')\times\left(\vec{\rho}\,'^{\pm}_q\times\hat{n}_q^{\pm}\right)\frac{(\pm)_q}{2A_q^{\pm}}dS'\right]dS \qquad (6.30)$$
$$s=1..N,\ q=1..N$$

6.2.3.2 Theoretical considerations

Since one can indistinctly turn either *RWG* into *unxRWG* or *unxRWG* into *RWG* through the normal vector cross-product, the previous expressions (6.27) and (6.28) can now be easily adapted

$$Z_{\text{sing},mfiexun}(s,q)=\frac{\Omega_0^-}{4\pi}\left\langle\vec{w}_s,\left(\hat{n}^-\times\left(\vec{w}_q\times\hat{n}\right)\right)\right\rangle=\frac{\Omega_0^-}{4\pi}\iint_{T_n}\vec{w}_s\cdot\left(\hat{n}^-\times\left(\vec{w}_q\times\hat{n}\right)\right)dS$$
$$=-\frac{\Omega_0^-}{4\pi}\iint_{T_n}\vec{w}_s(\vec{r})\cdot\left(\left(\vec{w}_q(\vec{r})\times\hat{n}\right)\times\hat{n}^-\right)dS=-\frac{\Omega_0^-}{4\pi}\iint_{T_n}\vec{w}_q(\vec{r})\cdot\vec{w}_s(\vec{r})dS \qquad (6.31)$$

$$\vec{H}^S_{PeC}\left(\left(\vec{w}\times\hat{n}\right)_i\right)\Big|_{\text{sing},\vec{r}\in S_i^-}=\frac{\Omega_0^-}{4\pi}\hat{n}^-\times\left(\left(\vec{w}\times\hat{n}\right)_i(\vec{r})\right)=-\frac{\Omega_0^-}{4\pi}\vec{w}_i(\vec{r})\qquad\vec{r}\in T_i^+\cup T_i^- \qquad (6.32)$$

whereby it is clear that *RWG* expands the rank of the singular integration contribution to the operator, when the domain is expanded through *unxRWG*.

Through the application of the rule $\vec{a}\cdot\left(\vec{b}\times\vec{c}\right)=\vec{b}\cdot\left(\vec{c}\times\vec{a}\right)=\vec{c}\cdot\left(\vec{a}\times\vec{b}\right)$ and the fact that $\nabla G=-\nabla' G$, one can express (6.30) as

$$Z_{mfiexun}(s,q)=\frac{(\pm)_s}{2A_s^{\pm}}\frac{(\pm)_q}{2A_q^{\pm}}\iint_{T_s^{\pm}}\iint_{T_q^{\pm}}\vec{\rho}_s^{\pm}\cdot\left[\nabla G(\vec{r}-\vec{r}\,')\times\left(\vec{\rho}\,'^{\pm}_q\times\hat{n}_q^{\pm}\right)\right]dS'dS$$
$$=\frac{(\pm)_s}{2A_s^{\pm}}\frac{(\pm)_q}{2A_q^{\pm}}\iint_{T_s^{\pm}}\iint_{T_q^{\pm}}\left(\vec{\rho}\,'^{\pm}_q\times\hat{n}_q^{\pm}\right)\left[\vec{\rho}_s^{\pm}\cdot\times\nabla G(\vec{r}-\vec{r}\,')\right]dS'dS$$
$$=\frac{(\pm)_s}{2A_s^{\pm}}\frac{(\pm)_q}{2A_q^{\pm}}\iint_{T_s^{\pm}}\left(\vec{\rho}\,'^{\pm}_s\times\hat{n}_s^{\pm}\right)\cdot\iint_{T_q^{\pm}}\nabla' G(\vec{r}-\vec{r}\,')\times\vec{\rho}_q^{\pm}dSdS' \qquad (6.33)$$

which is the same expression as in (6.24) by switching the field and source domains. Whenever the triangles associated to the edges s and q accomplish $T_s^{\pm}\neq T_q^{\pm}$, in view of (6.33), one can state

$$Z_{mfie}(s,q)=Z_{mfiexun}(q,s) \qquad (6.34)$$

In case both edges have in common at least one triangle, one cannot say so since what rules now is the term due to the integration of the singularity. By comparing the contribution of this term for operators, (6.27) and (6.31), one can infer particularly for the self-impedance elements

$$Z_{mfie}(s,s) \cong -Z_{mfiexun}(s,s) \tag{6.35}$$

as long as T_s^+ and T_s^- are nearly co-planar to dismiss the Cauchy principal value contribution, which is normally the case.

Furthermore, let one apply the reciprocity theorem to a pair of sources $(\vec{w}\times\hat{n})_q$, electric, and $\vec{w}_s$, magnetic,

$$\iint_{T_q^+\cup T_q^-} (\vec{w}\times\hat{n})_q \vec{E}^S(\vec{w}_s)\Big|_{\vec{r}\in T_q^+\cup T_q^-} dS = -\iint_{T_s^+\cup T_s^-} \vec{w}_s \vec{H}^S\left((\vec{w}\times\hat{n})_q\right)\Big|_{\vec{r}\in T_s^+\cup T_s^-} dS \tag{6.36}$$

According to the field integral expressions presented in Chapter 2, $\vec{H}^S$ can be expressed in terms of $\vec{H}^S_{PeC}$ as

$$\begin{aligned} \vec{H}^S\left((\vec{w}\times\hat{n})_q\right)\Big|_{\vec{r}\in T_s^+\cup T_s^-} &= \vec{H}^S_{PeC}\left((\vec{w}\times\hat{n})_q\right)\Big|_{\vec{r}\in T_s^+\cup T_s^-} \\ \vec{E}^S(\vec{w}_s)\Big|_{\vec{r}\in T_s^+\cup T_s^-} &= -\vec{H}^S_{PeC}(\vec{w}_s)\Big|_{\vec{r}\in T_s^+\cup T_s^-} \end{aligned} \tag{6.37}$$

which leads (6.36) to

$$\iint_{T_q^+\cup T_q^-} (\vec{w}\times\hat{n})_q \vec{H}^S_{PeC}(\vec{w}_s)\Big|_{\vec{r}\in T_q^+\cup T_q^-} dS = \iint_{T_s^+\cup T_s^-} \vec{w}_s \vec{H}^S_{PeC}\left((\vec{w}\times\hat{n})_q\right)\Big|_{\vec{r}\in T_s^+\cup T_s^+} dS \tag{6.38}$$

which is in agreement with the expression (6.34). Although at first glance one may find it contradictory with (6.35), this is not the case. Indeed, $\vec{H}^S_{PeC}$ assumes $\vec{r}\in S^-$; that is, the same side of the surface for both operators. On the other hand, one can imagine this particular case for the reciprocity theorem as two collapsed surfaces, where the normal vector coming from the singularity integration have opposite sign at both sides.

6.3 DISMISSED PEC-OPERATORS

The study of the validity of a given operator must focus firstly on the domain space. Only if the functions expand correctly the domain space -current and charge-, should one care for the right weighting functions for the rank space. The dismissed combinations between the *RWG* and the *unxRWG* sets as weighting and expanding functions for the PeC-MFIE and PeC-EFIE operators are shown right away.

6.3.1 Operators with an inappropriate expansion of the domain space

The *unxRWG* set is inappropriate to expand the PeC-EFIE domain space because, according to its null divergence, (6.13), it is unable to expand the surface charge density σ. Indeed, as σ is null, one cannot develop the Scalar potential term -second addend in (6.15)- which results in a bad definition for the PeC-EFIE operator. One can equivalently understand this through the vector space theory. Indeed, the addition of the dimension of the rank and of the null spaces of a linear transformation yields the dimension of the domain space. In this case, the whole *unxRWG* set expands the Null space of the scalar potential operator, which definitely forces the PeC-EFIE rank to be formed only by the zero. Hence, the two operators that must be dismissed are the PeC-EFIE(*unxRWG,unxRWG)* and the PeC-EFIE(*RWG,unxRWG).*

One must note that although PeC-EFIE(*unxRWG,unxRWG)* -like PeC-EFIE(*RWG,RWG)*- results in a symmetric matrix impedance, the operator is not correct in this case. This confirms that the fact of the operator being self-adjoint -it can be considered so in practice in both cases- is only a sufficient condition of good behaviour provided that the expanding functions form a proper set throughout the domain space, which is not the case now.

Some strategies to deal with the inherent charge accumulation of the *unxRWG* set are shown right away. The results, in general, have turned out unsatisfactory. In section 6.5, it will be given a thorough insight into the properties of the PeC-EFIE operator and it will be reasoned why these strategies have failed.

6.3.1.1 Computation of the accumulated charge along the edges

Some efforts have been poured by the author of this dissertation Thesis to get some PeC-EFIE operator alike to PeC-EFIE(*unxRWG,unxRWG*) but with the introduction of a σ-dependent term that allows for the charge accumulation on the borders inherent to *unxRWG.*

In the literature there are certain examples of basis functions with charge accumulation along the borders. For instance, the use of cubical cells for developing the dielectric electromagnetic operators in accordance with the volume equivalence Tteorem [26], where it is allowed for the remaining charge over the opposite faces along the different current directions.

According to the general idea of providing the radiation due to the residual charge along wires (2D) and faces (3D), the computation of the radiation due to the scalar potential regarding the edges of the triangles as wires has been attempted. One has resorted then to a definition of σ in terms of the Dirac's delta -infinite on the edges-. This is the required mathematical resort to supply a linear charge distribution over the edges. The surface integrals accordingly become line integrals in this case.

However, a major problem appears in the computation of the self-contribution of a wire, which is singular and thus non-integrable. Some results have been programmed without this term, which have turned out, in general terms, unsatisfactory and no real improvement has been noticed.

6.3.1.2 Charge definition on the four neighbouting triangles. Modified *unXRWG* functions

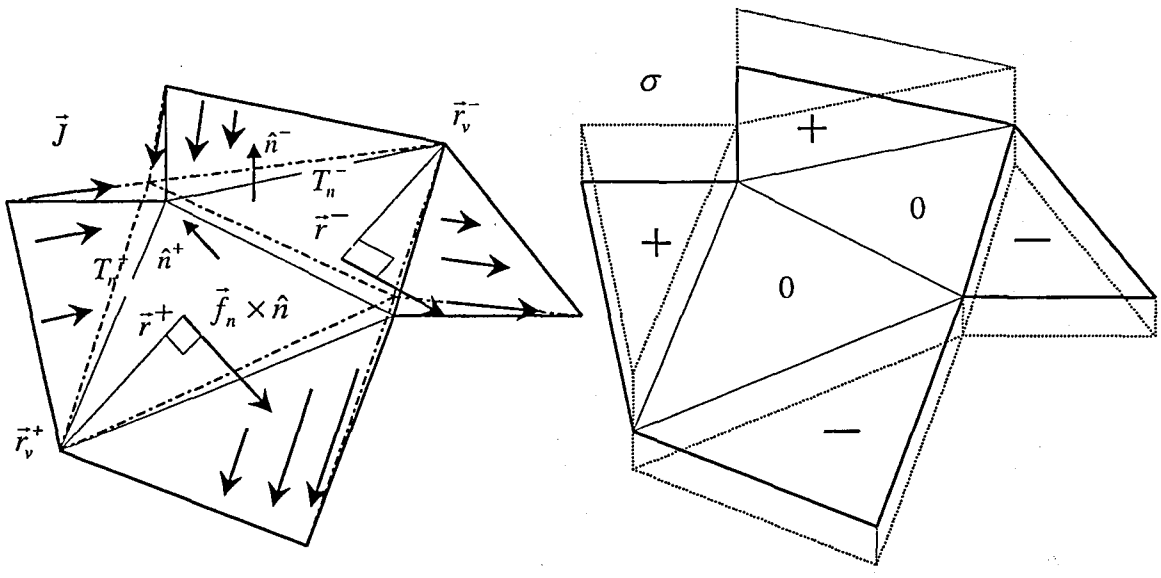

Fig. 6.4 Modified unxRWG functions

Another attempted strategy has been to modify the *unxRWG* basis function definition by extending the basic subdomain of the *unxRWG* expanding functions to the four neighbouring triangles -see Fig. 6.4 -.

The charge associated to the *unxRWG* functions is null inside each patch because the surface charge density is indeed null at each point inside the patch. So, the leaving flux equals the entering flux for each patch. For an arbitrary triangle, one can not assume that the leaking flux at one side compensates the entering flux from the other side, since there is entering and leaving flux across the common edge. Anyway, one has preferred to leave the original pair of triangles untouched and apply a slope for the current over the four adjacent triangles, so that the introduced charge at one side equals the charge at the other side -see Fig. 6.4-. I have called these functions as *modified unxRWG*. Note that under this definition the value of the expanded current inside a triangle is defined not only by the expanding functions linked to the edges shaping the triangle but by the expanding functions linked to the edges shaping the adjacent triangles.

Note that this definition does not ensure the normal current component across the edges to be continuous. This disagrees with the definition of the *RWG* functions [28] or of the Kolundzija's quadrangular functions [14]. However, it is actually consistent with the *unxRWG* definition, which does not allow for the continuity of the normal component across the common edge. With this charge introduction on the four neighbouring patches -see Fig. 6.4-, the function on the two triangles of the middle keeps being orthogonal to *RWG*, which seems intuitively reasonable with regard to the necessary uncoupling properties for developing the dielectric operators. Moreover, σ is not null anymore at any point of the surface. Indeed, now the scalar potential term can be defined with a finite value for σ.

The definition of the *modified unxRWG* has been heuristic. These functions have turned out the only ones -compared to the other attempted *unxRWG* modifications- able to expand the

current over a sphere, which is known beforehand through the Mie series. Note that this is a necessary condition but not sufficient to define properly the PeC-EFIE operator. The results have turned out unsatisfactory in general; it was remarked only some improvement in comparison with the PeC-EFIE(*unxRWG*) for smooth-varying low-frequency surfaces with a coarse mesh.

6.3.2 Operators with an inappropriate expansion of the rank space

In accordance with the sections 6.2 and 6.3.1, PeC-MFIE accepts *RWG* and *unxRWG* as expanding functions meanwhile PeC-EFIE allows only for the *RWG* set. In this section, it is assessed the performance of these operators when the weighting functions -the expansion of the rank space- are chosen to be alternative to the choice for the valid PeC-operators shown in 6.2. The computation of the alternative operators PeC-EFIE(*unxRWG,RWG)*, PeC-MFIE(*RWG,RWG)* and PeC- MFIE(*unxRWG,unxRWG*) yields self-contributions in general close to zero -these contributions are the biggest ones in the valid operators of 6.2-.

In consequence, the condition numbers become very high. For example, for a PeC-sphere with 128 triangles and radius 0.2λ the condition number for the PeC-EFIE(*unxRWG,RWG*) operator yields 1.175e17 -near singular matrix-, while the condition number for the same problem under PeC-EFIE(*RWG,RWG*), PEC-MFIE(*unxRWG,RWG*), PeC-MFIE(*RWG,unxRWG*) are respectively of 46.58, 3.5905, 3.22.

It is thus reasonable that none of the proposed sets of weighting functions can expand the rank space for the presented operators. Particularly, according to the proximity to zero of the self-contributions, it seems that the corresponding chosen weighting spaces represent the worst choice. Indeed, it has to be so because they are orthogonal to those presented in 6.3.1, with a much better performance for the same examples.

The bad behaviour of the alternative combinations - PeC-EFIE(*unxRWG,RWG*), PEC-MFIE(*RWG,RWG*), PeC-MFIE(*unxRWG,unxRWG*)- agrees with the intuitive physical interpretation. Indeed, the electric field radiated by *RWG* is uncoupled with *unxRWG,* and the magnetic field radiated by any of both sets, *RWG, unxRWG,* is uncoupled with itself. One can easily resort to electric dipole antenna examples, where the coupling with the incident field is maximum when the electric incident field is parallel to the electric source current and null when they both are perpendicular.

Finally, it must be noted that with the same set of expanding functions *RWG*, PeC-MFIE and PeC-EFIE require different and orthogonal sets, respectively *RWG* and *unxRWG.* This agrees with the intuitive reasonable idea that the electric and magnetic fields due to the same electric source are uncoupled. For example, an elementary magnetic dipole, which contributes in the dual operator through the basic PeC-MFIE, provides best electromagnetic coupling with an incident electric field in the normal plane [17]. On the other hand, an elementary electric dipole likewise oriented yields a null coupling with the same incident field.

[17] An elementary magnetic dipole corresponds physically to an electric circular spire around the magnetic dipole axis; the normal plane stands for the plane where the spire lies

6.3.2.1 PeC-EFIE(*unxRWG,RWG*)

The PeC-EFIE only accepts *RWG* as expanding functions. The detailed development of the terms of self-impedance due to the PeC-EFIE(*unxRWG,RWG*) operator for any edge yields.

$$z_{qq} = \left\langle (\vec{w}\times\hat{n})_q, \vec{E}^S_{PeC}(\vec{w}_q)\right\rangle = -j\omega\left\langle (\vec{w}\times\hat{n})_q, \vec{A}(\vec{w}_q)\right\rangle - \left\langle (\vec{w}\times\hat{n})_q, \nabla\Phi(\vec{w}_q)\right\rangle \qquad q=1..N \tag{6.39}$$

Assuming that the pair of triangles is symmetric with regard to the common edge, the analysis in detail for each addend yields

$$\left\langle (\vec{w}\times\hat{n})_q, \vec{A}(\vec{w}_q)\right\rangle = \mu \iint\limits_{T_q^+\cup T_q^+} (\vec{w}\times\hat{n})_q \iint\limits_{T_q^+\cup T_q^+} G(\vec{r},\vec{r}')\vec{w}_q dS' dS \tag{6.40}$$

$$\left\langle (\vec{w}\times\hat{n})_q, \nabla\Phi(\vec{w}_q)\right\rangle = -\frac{1}{j\omega\varepsilon} \iint\limits_{T_q^+\cup T_q^+} (\vec{w}\times\hat{n})_q \iint\limits_{T_q^+\cup T_q^+} \nabla G(\vec{r},\vec{r}')\nabla'\cdot\vec{w}'_q dS' dS \tag{6.41}$$

which can be tackled through the addition of the cross- and the self-influences between triangles.

With regard to the cross-influence -$T_q^{\pm}$ over $T_q^{\mp}$-,

$$\begin{aligned} fc^{\pm}_{crs,1} &= \iint\limits_{T_q^{\pm}} \frac{(\pm)_q}{2A_q^{\pm}}(\vec{\rho}_q^{\pm}\times\hat{n}^{\pm}) \iint\limits_{T_q^{\mp}} G(\vec{r},\vec{r}')\frac{(\mp)_q}{2A_q^{\mp}}\vec{\rho}'^{\mp}_q dS' dS \\ &= \frac{-1}{4A_q^{\pm}A_q^{\mp}} \iint\limits_{T_q^{\pm}} (\vec{\rho}_q^{\pm}\times\hat{n}^{\pm}) \iint\limits_{T_q^{\mp}} G(\vec{r},\vec{r}')\vec{\rho}'^{\mp}_q dS' dS \end{aligned} \tag{6.42}$$

$$\begin{aligned} fc^{\pm}_{crs,2} &= \iint\limits_{T_q^{\pm}} \frac{(\pm)_q}{2A_q^{+}}(\vec{\rho}_q^{\pm}\times\hat{n}^{\pm}) \iint\limits_{T_q^{\mp}} \nabla G(\vec{r},\vec{r}')\frac{(\mp)_q}{A_q^{\mp}} dS' dS \\ &= \frac{-1}{2A_q^{\pm}A_q^{\mp}} \iint\limits_{T_q^{\pm}} (\vec{\rho}_q^{\pm}\times\hat{n}^{\pm}) \iint\limits_{T_q^{\mp}} \nabla G(\vec{r},\vec{r}') dS' dS \end{aligned} \tag{6.43}$$

With regard to the self-influence -$T_q^{\pm}$ over $T_q^{\pm}$-,

$$\begin{aligned} fc^{\pm}_{slf,1} &= \iint\limits_{T_q^{\pm}} \frac{(\pm)_q}{2A_q^{\pm}}(\vec{\rho}_q^{\pm}\times\hat{n}^{\pm}) \iint\limits_{T_q^{\pm}} G(\vec{r},\vec{r}')\frac{(\pm)_q}{2A_q^{\mp}}\vec{\rho}'^{\pm}_q dS' dS \\ &= \frac{1}{4A_q^{\pm}A_q^{\pm}} \iint\limits_{T_q^{\pm}} (\vec{\rho}_q^{\pm}\times\hat{n}^{\pm}) \iint\limits_{T_q^{\pm}} G(\vec{r},\vec{r}')\vec{\rho}'^{\pm}_q dS' dS \end{aligned} \tag{6.44}$$

$$\begin{aligned} fc^{\pm}_{slf,1} &= \iint\limits_{T_q^{\pm}} \frac{(\pm)_q}{2A_q^{\pm}}(\vec{\rho}_q^{\pm}\times\hat{n}^{\pm}) \iint\limits_{T_q^{\mp}} \nabla G(\vec{r},\vec{r}')\frac{(\pm)_q}{A_q^{\pm}} dS' dS \\ &= \frac{1}{2A_q^{\pm}A_q^{\pm}} \iint\limits_{T_q^{\pm}} (\vec{\rho}_q^{\pm}\times\hat{n}^{\pm}) \iint\limits_{T_q^{\mp}} \nabla G(\vec{r},\vec{r}') dS' dS \end{aligned} \tag{6.45}$$

There is symmetry with regard to the common edge in the previous expressions with regard to the source functions and the Green's function terms. However, the field term $\left(\vec{\rho}_q^{\pm}\times\hat{n}^{\pm}\right)$ is antisymmetric, which lets the relative inner-products defined with opposite sign; indeed, the previous expressions become related as $fc^{+}_{slf,1}=-fc^{-}_{slf,1}$, $fc^{+}_{slf,2}=-fc^{-}_{slf,2}$, $fc^{+}_{crs,1}=-fc^{-}_{crs,1}$, $fc^{+}_{crs,2}=-fc^{-}_{crs,2}$, which makes the self-impedance term in (6.39) zero.

Despite this being concluded for symmetric pairs of triangles, which is actually quite a common case in regular discretizations, in a general case, according to the same reasoning, the inner-product with $\left(\vec{w}\times\hat{n}\right)_q$ tends to cancel both source-triangle contributions too.

6.3.2.2 PeC-MFIE(unxRWG,unxRWG), PeC-MFIE(RWG,RWG)

As previously pointed out, the PeC-MFIE accepts both sets to span the domain space. If on the testing of $\vec{H}^s$, one makes the chosen weighting functions set to coincide with the expanding functions set, be it *RWG* or *unxRWG,* the key term coming from the integration of the singularity, in view of (6.27) and (6.31), becomes

$$\left\langle \vec{w}_s, \vec{H}^s_{PeC}\left(\vec{w}_q\right)\Big|_{\text{sing}}\right\rangle = \frac{\Omega_0^-}{4\pi}\left\langle \vec{w}_s, \left(\hat{n}^-\times\vec{w}_q\right)\right\rangle = \frac{\Omega_0^-}{4\pi}\iint_{T_0^-}\left(\hat{n}^-\times\vec{w}_q\right)\cdot\vec{w}_s\left(\vec{r}\right)dS$$

$$\left\langle \left(\vec{w}\times\hat{n}\right)_s, \vec{H}^s_{PeC}\left(\left(\vec{w}\times\hat{n}\right)_q\right)\Big|_{\text{sing}}\right\rangle = \frac{\Omega_0^-}{4\pi}\iint_{T_0^-}\left(\hat{n}^-\times\left(\vec{w}\times\hat{n}\right)_q\right)\cdot\left(\vec{w}\times\hat{n}\right)_s\left(\vec{r}\right)dS$$

$$= -\frac{\Omega_0^-}{4\pi}\iint_{T_0^-}\vec{w}_q\cdot\left(\vec{w}\times\hat{n}\right)_s\left(\vec{r}\right)dS \qquad (6.46)$$

which for $s=q$ yields zero. The diagonal row of the resulting matrix for both operators PeC-MFIE(*unxRWG,unxRWG),* PeC-MFIE(*RWG,unxRWG)* is then quasi-null -it is only left the Cauchy Principal Value that, anyway, as explained before, is usually very close to zero too in this case-.

6.4 NUMERICAL DEVELOPMENT OF THE PEC-OPERATORS

The development of the valid operators PeC-EFIE(*RWG,RWG),* PeC-MFIE(*unxRWG, RWG*) and PeC-MFIE(*RWG,unxRWG*) has been thoroughly undertaken so as to enable a further precise formulation for the derived dielectric operators.

The computation of the impedance terms Z_{sq} focuses on the influence between the pairs of triangles $T_q^+ - T_q^-$ over $T_s^+ - T_s^-$. It is efficient to compute first the influences between the triangles and after update the corresponding impedance terms in accordance with the characteristics, + or −, of each source and field triangle. Hence, through the computation of the interaction between two triangles one updates nine impedance terms at most -nine impedance terms actually when all the edges are interior-.

6.4.1 Analytical integration

The source integration has been carried out analytically for the highest order terms, which contribute most at very near distances of the field point $\vec{r}$. One has followed the analytical developments presented in [9] that have been used by S. M. Rao, D. R. Wilton and A. W. Glisson to develop the PeC-EFIE(*RWG,RWG*) [28] and by R. E. Hodges and Y. Rahmat-Samii to develop the PeC-MFIE(*unxRWG,RWG*) [11]. The PeC-EFIE formulation of Rao *et al.*, which allowed for the precise integration only for the self-contribution, has been in this work extended to the influence due to the neighbouring source triangles. Furthermore, the PeC-MFIE(*RWG,unxRWG*) operator, that has been developed from scratch, has made use of these fundamental integrals too.

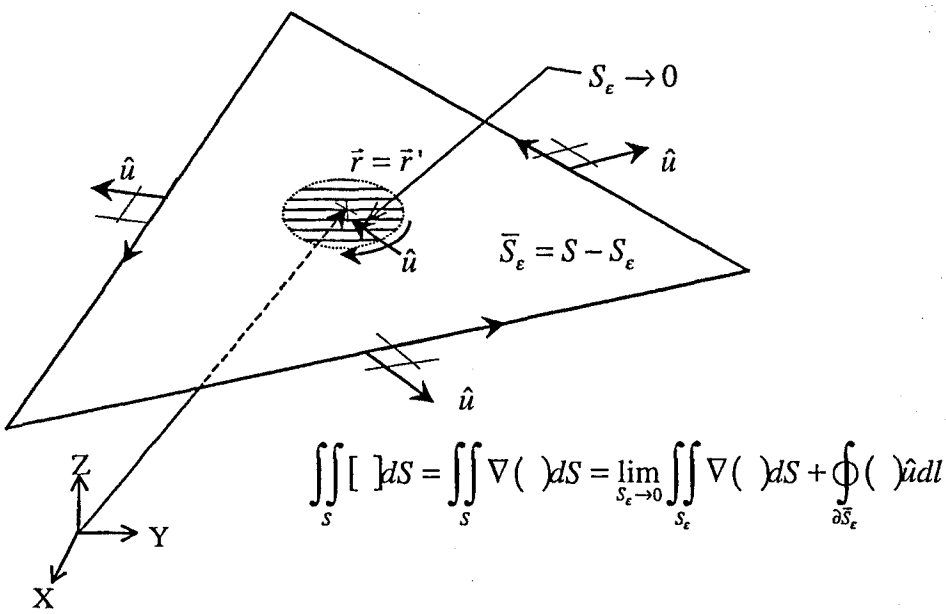

Fig. 6.5 Decomposition in the analytical development of the source-surface integral

The developments in [9] are based on analytical formulas for the potentials due to uniform and linearly varying source distributions defined over triangular facets. They derive from the addition of the contributions from the non-singular and singular parts of the integrand. While one can obtain an analytical expression for the non-singular part through the application of the surface divergence and gradient theorems[18], the singular part is provided as the limit of a surface integral embracing a domain around the singularity with radius approaching zero -see Fig. 6.5-

The analytical expressions for the fundamental high-order terms yield [9][11],

$$I_{1/R}(\vec{r}) = \int_T \frac{dS'}{R} = \sum_{i=1,2,3} \left(\hat{P}_i^0 \cdot \hat{u}_i\right) P_i^0 \ln \frac{R_i^+ + l_i^+}{R_i^- + l_i^-} - |d| \sum_{i=1,2,3} \left(\hat{P}_i^0 \cdot \hat{u}_i\right) \left(\tan^{-1} \frac{P_i^0 l_i^+}{\left(R_i^0\right)^2 + |d| R_i^+} - \tan^{-1} \frac{P_i^0 l_i^-}{\left(R_i^0\right)^2 + |d| R_i^-} \right) \tag{6.47}$$

$$I_{\vec{\rho}/R}(\vec{r}) = \int_T \frac{\vec{\rho}' - \vec{\rho}}{R} dS' = \frac{1}{2} \sum_{i=1,2,3} \hat{u}_i \left[\left(R_i^0\right)^2 \ln \frac{R_i^+ + l_i^+}{R_i^- + l_i^-} + l_i^+ R_i^+ - l_i^- R_i^- \right] \tag{6.48}$$

[18] The surface integral theorems are only valid over non-singular domains

$$I_{1/R^3}(\vec{r}) = \int_T \frac{dS'}{R^3} = -\frac{1}{|d|}\sum_{i=1,2,3}\left(\hat{P}_i^0 \cdot \hat{u}_i\right)\left(\tan^{-1}\frac{|d|l_i^+}{P_i^0 R_i^+} - \tan^{-1}\frac{|d|l_i^-}{P_i^0 R_i^+}\right) + \frac{1}{|d|}\sum_{i=1,2,3}\left(\hat{P}_i^0 \cdot \hat{u}_i\right)\left(\tan^{-1}\frac{l_i^+}{P_i^0} - \tan^{-1}\frac{l_i^-}{P_i^0}\right) \tag{6.49}$$

$$I_{\vec{\rho}/R^3}(\vec{r}) = \int_T \frac{\vec{\rho}\,' - \vec{\rho}}{R^3} dS' = -\sum_{i=1,2,3} \hat{u}_i \ln\frac{R_i^+ + l_i^+}{R_i^- + l_i^-} \tag{6.50}$$

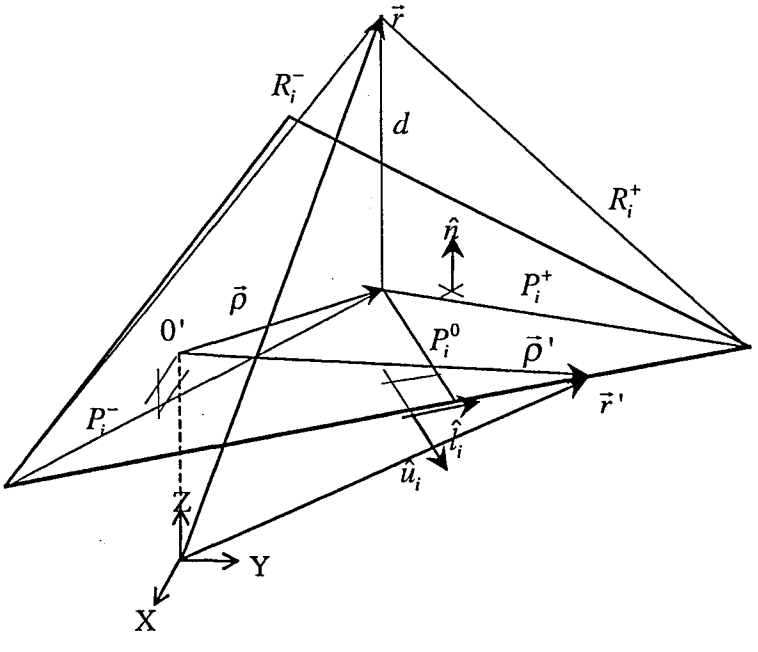

Fig. 6.6 Parameters of the analytical source-integration over a triangle

The parameters, associated to an arbitrary side of the source triangle T_s, are defined as -see Fig. 6.6-

$$\hat{l}_i = \frac{\vec{\rho}_i^+ - \vec{\rho}_i^-}{\left|\vec{\rho}_i^+ - \vec{\rho}_i^+\right|} \qquad \hat{u}_i = \hat{l}_i \times \hat{n}$$

$$l_i^\pm = \left(\vec{\rho}_i^\pm - \vec{\rho}\right)\cdot \hat{l}_i \qquad P_i^0 = \left|\left(\vec{\rho}_i^\pm - \vec{\rho}\right)\cdot \hat{u}_i\right|$$

$$\hat{P}_i^0 = \frac{\left(\vec{\rho}_i^\pm - \vec{\rho}\right) - l_i^\pm \hat{l}_i}{P_i^0} \qquad P_i^\pm = \sqrt{\left(P_i^0\right)^2 + \left(l_i^\pm\right)^2}$$

$$R_i^0 = \sqrt{\left(P_i^0\right)^2 + d_i^2} \qquad R_i^\pm = \sqrt{\left(P_i^\pm\right)^2 + d_i^2} \tag{6.51}$$

The development of these integrals with the field point outside T_s for certain cases where some of the parameters - P_i^0, $l_i^\pm$, $|d|$- is zero, brings about singularities for the corresponding sides and addends. This is meaningless since the real contribution of that addend for that side in this case must be taken as zero, as one can check when obtaining the theoretical expressions.

6.4.2 Integration according to a Gaussian quadrature rule

With regard to the computation of the field integrals or of the low-order source contributions, which become comparatively increasingly important as the source triangle is less near from the field triangle, it is undertaken through Gaussian quadrature rules for triangles.

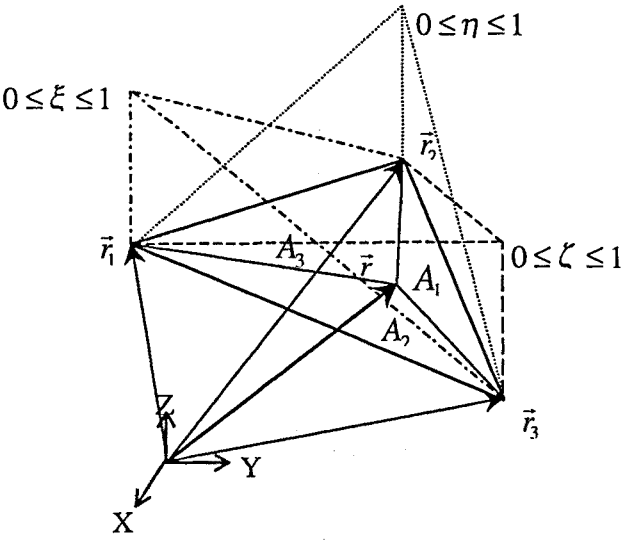

Fig. 6.7 Local linear interpolation over the triangle

One makes use of a local coordinate system especially aimed to generate linear facets. For the case of a triangle, it becomes -see Fig. 6.7-

$$\vec{r} = \xi \vec{r}_1 + \eta \vec{r}_2 + \zeta \vec{r}_3 \tag{6.52}$$

where $\vec{r}_1$, $\vec{r}_2$, $\vec{r}_3$ correspond to the position vector at the vertices of the triangle and ξ, η, ζ are the local coordinates assigned to each vertex, defined as the relative area of the portion embraced by $\vec{r}$ and the opposite side to the corresponding vertex.

$$\xi = \frac{A_1}{A} \qquad \eta = \frac{A_2}{A} \qquad \zeta = \frac{A_3}{A} \tag{6.53}$$

so that $\xi + \eta + \zeta = 1$, which means that two variables are only really needed.

The integration is performed by a Gaussian quadrature rule such that

$$\int_T f(\xi, \eta, \zeta) dS = A \sum_{i=1}^{ng} w_i f(\xi_i, \eta_i, \zeta_i) \tag{6.54}$$

where for the ith Gaussian point of location (ξ_i, η_i, ζ_i), there corresponds a Gaussian weight w_i. The points and the weights are tabulated in advance according to the value of ng; for example, for $ng = 1$ one point is placed at the centroid of the triangle with weight $1/3$. The points are disposed symmetrically over the triangle.

The computation of the integral can be precisely accomplished whenever the integrands are not singular. The choice of *ng* depends on the varying order of the integrand; for example, with regard to the computation of the impedance elements, the far interactions require lower values of *ng* than the near ones.

6.4.3 PeC-EFIE(RWG,RWG)

The integrand inside the vector and scalar potential contributions relies on the Green's function. The extraction of the highest order terms in (6.16) and (6.21), can be effectuated through the Taylor's expansion of the Green's function

$$G(R)=\frac{e^{-jkR}}{4\pi R}=\frac{1}{4\pi}\left[\frac{1}{R}-jk-\frac{k^2}{2}R+...\right] \tag{6.55}$$

where only the first term is fast-varying when $R\to 0$. Therefore, meanwhile the $1/R$ dependence is analytically source-integrated at small distances, the rest are numerically integrated by means of a Gauss quadrature rule.

The source contribution in the scalar potential expression (6.21), in view of (6.47), yields

$$\iint_{T_q^\pm} G(\vec{r}-\vec{r}\,')dS'=\frac{1}{4\pi}\left[I_{1/R}(\vec{r})+\iint_{T_q^\pm}\frac{e^{-jkR}-1}{R}dS'\right] \tag{6.56}$$
$$s=1..N,\ q=1..N$$

Analogously, the source contribution in the vector potential expression (6.16), in accordance with (6.47) and (6.48), becomes

$$\begin{aligned}\iint_{T_q^\pm}\vec{\rho}\,'^{\pm}_{q}G(\vec{r}-\vec{r}\,')dS' &= \iint_{T_q^\pm}\left(\vec{\rho}\,'-\vec{\rho}+\vec{\rho}-\vec{\rho}_{oq}\right)G(\vec{r}-\vec{r}\,')dS' \\ &= \iint_{T_q^\pm}(\vec{\rho}\,'-\vec{\rho})G(\vec{r}-\vec{r}\,')dS'dS+\left(\vec{\rho}-\vec{\rho}^{\pm}_{oq}\right)\iint_{T_q^\pm}G(\vec{r}-\vec{r}\,')dS' \\ &= I_{\vec{\rho}/R}(\vec{r})+\left(\vec{\rho}-\vec{\rho}^{\pm}_{oq}\right)I_{1/R}(\vec{r})+\iint_{T_q^\pm}\vec{\rho}\,'^{\pm}_{q}\frac{e^{-jkR}-1}{R}dS'\end{aligned} \tag{6.57}$$
$$s=1..N,\ q=1..N$$

6.4.4 PeC-MFIE(unxRWG,RWG)

The contribution due to the singular part is analytically expressed in (6.27) in terms of the solid angle. Because of the quadratic dependence of the integrand, the field-integration is performed exactly. Furthermore, since the triangular facets are flat, the solid angle value must be taken as 2π, whereby (6.27) results in

$$Z_{\text{sing},mfie}(s,q)=\frac{1}{2}\iint_{T_o}\vec{w}_q(\vec{r})\cdot\vec{w}_s(\vec{r})dS \tag{6.58}$$

The integrand for the Cauchy value terms relies on $\frac{1}{R}\frac{\partial G}{\partial R}$. Its Taylor's decomposition leads to

$$\begin{aligned}\frac{1}{R}\frac{\partial G}{\partial R}(R) &= -\frac{e^{-jkR}}{4\pi R^2}\left[\frac{1}{R}+jk\right] = -\frac{1}{4\pi R}\left[\frac{1}{R}-jk-\frac{k^2}{2}R+\ldots\right]\left[\frac{1}{R}+jk\right] \\ &= -\frac{1}{4\pi}\left[\frac{1}{R^3}+\frac{k^2}{2R}-\frac{jk^3}{2}+\ldots\right]\end{aligned} \tag{6.59}$$

where the two first terms are fast-varying when R approaching zero. Therefore, these terms are analytically source-integrated at small distances, while the rest are numerically integrated by means of a Gauss quadrature rule.

The numerical computation of the Cauchy principal value in (6.24) is carried out according to (6.59) with the help of the analytical expressions (6.47) (6.48) (6.49) (6.50),

$$\begin{aligned}\iint_{T_q^\pm}\frac{\partial G}{\partial R}\frac{1}{R}\vec{\rho}\,'^{\pm}_q dS' &= \iint_{T_q^\pm}(\vec{\rho}\,'-\vec{\rho})\frac{\partial G}{\partial R}\frac{1}{R}dS' + (\vec{\rho}-\vec{\rho}^{\pm}_{oq})\iint_{T_q^\pm}\frac{\partial G}{\partial R}\frac{1}{R}dS' \\ &= \frac{1}{4\pi}\left[-I_{\vec{\rho}/R^3}(\vec{r})-\frac{k^2}{2}I_{\vec{\rho}/R}(\vec{r})+\iint_{T_q^\pm}(\vec{\rho}\,'-\vec{\rho})\left(\frac{\partial G}{\partial R}\frac{1}{R}+\frac{1}{R^3}+\frac{k^2}{2R}\right)dS'\right] \\ &\quad +\frac{(\vec{\rho}-\vec{\rho}^{\pm}_{oq})}{4\pi}\left[-I_{1/R^3}(\vec{r})-\frac{k^2}{2}I_{1/R^3}(\vec{r})+\iint_{T_q^\pm}\left(\frac{\partial G}{\partial R}\frac{1}{R}+\frac{1}{R^3}+\frac{k^2}{2R}\right)dS'\right] \\ &\qquad\qquad s=1..N,\ q=1..N\end{aligned} \tag{6.60}$$

6.4.5 PeC-MFIE(RWG,unxRWG)

For the same reason as in 6.4.4, the impedance element part due to the integration of the singularity (6.31) becomes

$$Z_{\text{sing},mfiexun}(s,q) = -\frac{1}{2}\iint_{T_Q}\vec{w}_q(\vec{r})\cdot\vec{w}_s(\vec{r})dS \tag{6.61}$$

Unlike 6.4.3 and 6.4.4, one can not now express the principal value of the source contribution in (6.30)

$$\iint_{T_q^\pm}\nabla G(\vec{r}-\vec{r}\,')\times(\vec{\rho}\,'^{\pm}_q\times\hat{n}^{\pm}_q)dS' \tag{6.62}$$

in terms of an analytical expression for the high-order terms.

In any case, making use of the thorough reasoning developed in 6.2.3.2, which is a consequence of the particular characteristics of the $\vec{H}^S_{PeC}$ operator, one can compute the impedance terms $Z_{mfiexun}(s,q)$ from $Z_{mfie}(q,s)$, which can provide a high-order analytical

development -see (6.60)-. This is equivalent to developing $Z_{mflexun}(s,q)$ by first field-integrating and after source-integrating, which, though contrary to the usual MoM implementations, is perfectly possible -see (6.33)-.

6.5 PHYSICAL PROPERTIES ON AN ARBITRARY POLYHEDRON

The purpose of this section, a singular contribution of this dissertation Thesis, is to study the physical properties of the fields and the current over the enclosing surface of an arbitrary polyhedron, which represents the meshed surface -see Fig. 6.8-. From an electromagnetic problem where, in accordance with the theorem of equivalence, the solution is unique for both possible approaches -EFIE and MFIE-, one passes to a discretization of the original problem. The correct PeC-operators must be those that keep the solution correct in electromagnetic terms.

The edges do not exist physically; what is commonly called *edge* is a very steep transition on the curvature angle of a surface but the continuity of the magnitudes is never lost. The edges of the polyhedron represent the break on the continuity properties of the fields and current magnitudes. One can thus consider that the correct patch-based PeC-operators are those that succeed in enforcing correctly the field and current boundary conditions over the edges[19].

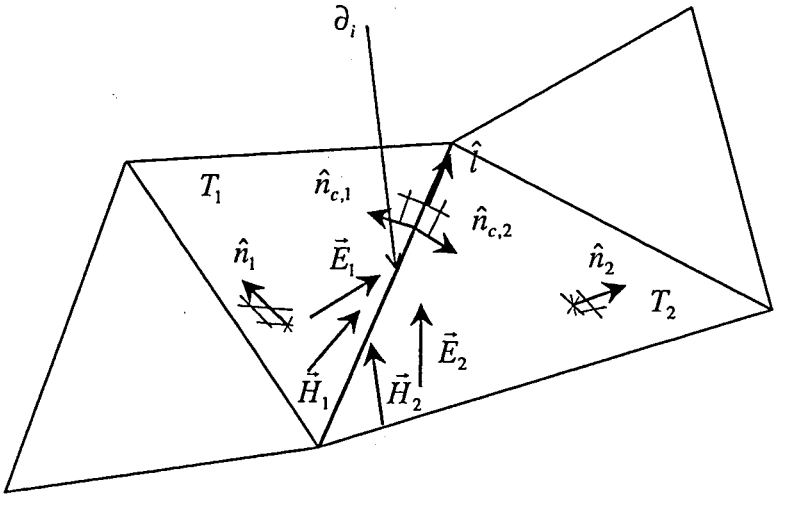

Fig. 6.8 Boundary conditions across the edge ∂_i

6.5.1 Charge boundary conditions

The description of the current behaviour is present in the continuity equation, where the current $\vec{J}$ and the charge density σ are related. Obtaining σ is straightforward whenever $\vec{J}$ is continuous because the divergence operator is well defined

[19] The boundary conditions inside the facets must be accomplished too. Since the functions are continuous there, they are automatically accomplished

$$\sigma(\vec{r}) = -\frac{1}{j\omega}\nabla\cdot\vec{J}(\vec{r}) \tag{6.63}$$

However, as the divergence is a differential operator, some special condition must be provided on the edges, where the expanded current -in accordance with the restrictions of the patch-based functions- is not continuous.

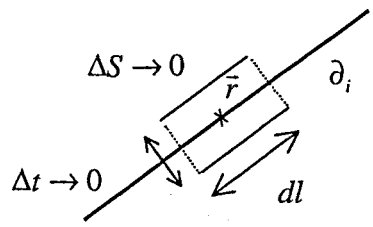

Fig. 6.9 Elementary surface with area $\Delta S \to 0$ around a point over the edge ∂_i

The integration of $\nabla_s\cdot\vec{J}$ over a portion of surface - $\Delta S \to 0$ - around a point on the edge - $\vec{r}\in\partial_i$ - with the length of the transversal side tending to zero - $\Delta t \to 0$ -see Fig. 6.9- yields -see Fig. 6.8-

$$\lim_{\Delta S\to 0}\int_{\Delta S}\nabla_s\cdot\vec{J}dS = \left(\vec{n}_{c,1}\cdot\vec{J}_1 + \vec{n}_{c,2}\cdot\vec{J}_2\right)dl \tag{6.64}$$

where the surface divergence theorem is applied.

Moreover, the integration of $\sigma(\vec{r})$ in the same portion of surface with area tending to zero yields

$$\lim_{\Delta S\to 0}\int_{\Delta S}\sigma dS = \tau dl \tag{6.65}$$

where τ stands for the linear charge density over the edge and it is well-known over the literature as *charge accumulation.* This magnitude is beyond the reach of the patch-based functions because, as explained in Chapter 2, they cannot assume the expansion over the edges.

The comparison of (6.64) and (6.65) -following (6.63)- yields

$$-\frac{1}{j\omega}\left(\vec{n}_{c,1}\cdot\vec{J}_1\Big|_{\vec{r}\in\partial_i} + \vec{n}_{c,2}\cdot\vec{J}_2\Big|_{\vec{r}\in\partial_i}\right) = \tau\Big|_{\vec{r}\in\partial_i} \tag{6.66}$$

which is a condition to define properly the scalar potential since it affects the surface charge. Therefore, any PeC-EFIE approach must supply it.

6.5.2 Field boundary conditions

The field magnitudes have to accomplish the boundary conditions over the surface of the polyhedron. Through the enforcement of the field boundary conditions across the edge, a

description of the current behaviour -and therefore of the expanding functions- inside the patches can be obtained. Likewise, one can also reach a description of the rank of the operators, which justifies the choice of the corresponding weighting functions.

The boundary conditions presented in Chapter 2 -(2.37), (2.38), (2.39), (2.40)- rule the conditions for the fields across an interface surface. The study of the boundary conditions on the polyhedron requires the adaptation of the boundary conditions of Chapter 2 to the 2D case.

6.5.2.1 Magnetic field conditions: MFIE

- $\vec{n}\cdot\left(\vec{B}_1-\vec{B}_2\right)\Big|_{\vec{r}\in S_i}=0$

This condition comes from the adaptation of the boundary condition in (2.40) to 2D with the imposition -characteristic to the PeC case- of no magnetic linear charge density.

According to the equivalence theorem, the medium in the equivalent problem is homogeneous, whereby one can accordingly state for the case of an arbitrary edge ∂_i in the polyhedron -see Fig. 6.8-

$$\vec{n}_{c,1}\cdot\vec{H}_1\Big|_{\vec{r}\in\partial i}+\vec{n}_{c,2}\cdot\vec{H}_2\Big|_{\vec{r}\in\partial_i}=0 \tag{6.67}$$

Since the sources in the equivalent problem are radiating sources, the magnetic field at each side -1,2- of the edge is related with the current through the well-known expression

$$\vec{J}_{\{1|2\}}=\hat{n}_{\{1|2\}}\times\vec{H}_{\{1|2\}} \tag{6.68}$$

which readily yields

$$\vec{H}_{\{1|2\}}=\vec{J}_{\{1|2\}}\times\hat{n}_{\{1|2\}} \tag{6.69}$$

When introduced in (6.67), an expression of the boundary condition in terms of the current is obtained

$$\vec{n}_{c,1}\cdot\left(\vec{J}_1\times\hat{n}_1\right)\Big|_{\vec{r}\in\partial_i}+\vec{n}_{c,2}\cdot\left(\vec{J}_2\times\hat{n}_2\right)\Big|_{\vec{r}\in\partial_i}=0 \tag{6.70}$$

which can be rewritten, in view of Fig. 6.8, as

$$\begin{aligned}&\vec{n}_{c,1}\cdot\left(\vec{J}_1\times\hat{n}_1\right)\Big|_{\vec{r}\in\partial_i}+\vec{n}_{c,2}\cdot\left(\vec{J}_2\times\hat{n}_2\right)\Big|_{\vec{r}\in\partial_i}=0\\&\vec{J}_1\Big|_{\vec{r}\in\partial_i}\cdot\left(\hat{n}_1\times\vec{n}_{c,1}\right)+\vec{J}_2\Big|_{\vec{r}\in\partial_i}\cdot\left(\hat{n}_2\times\vec{n}_{c,2}\right)=0\\&\vec{J}_1\Big|_{\vec{r}\in\partial_i}\cdot\hat{l}=\vec{J}_2\Big|_{\vec{r}\in\partial_i}\cdot\hat{l}\end{aligned} \tag{6.71}$$

It is thus a sufficient condition to accomplish the boundary condition in (6.67) to have the tangential component of the current along each edge continuous. As mentioned in 6.1.2, any magnitude expanded by *unxRWG* -in general, by a curl-conforming set- satisfies this property. Furthermore, with the choice of *RWG* -in general, any divergence-conforming set- as weighting set, the normal component of the magnetic field is ensured to be continuous, which agrees with the field requirement in (6.67). Hence, the operator PeC-MFIE(*RWG,unxRWG*) appears as suitable to satisfy this unambiguous field requirement.

- $\vec{n}\times\left(\vec{H}_1-\vec{H}_2\right)\Big|_{\vec{r}\in S_i}=0$

This condition results from the adaptation of the boundary condition (2.37) to the 2D case. Indeed, when integrating $\nabla_s\times\vec{H}$ over a portion of surface - $\Delta S\to 0$ - around a point on the edge - $\vec{r}\in\partial_i$ - with the length of the transversal side tending to zero - $\Delta t\to 0$ -see Fig. 6.9 -, we have -see Fig. 6.8-

$$\lim_{\Delta S\to 0}\int_{\Delta S}\nabla_s\times\vec{H}dS=\left(\vec{n}_{c,1}\times\vec{H}_1+\vec{n}_{c,2}\times\vec{H}_2\right)dl \tag{6.72}$$

where the surface curl theorem is applied.

The Ampere's law allows the equivalent expression of the left-hand side term as

$$\lim_{\Delta S\to 0}\int_{\Delta S}\nabla_s\times\vec{H}dS=\lim_{\Delta S\to 0}\int_{\Delta S}\left(\vec{J}+j\omega\vec{D}\right)dS=\left(I\hat{l}+j\omega D_l\hat{l}\right)dl \tag{6.73}$$

where I and D_l stand respectively for the electric wire-current and the electric flux density at $\vec{r}\in\partial_i$.

The electric flux density on the edge, according to the Gauss law, coincides with the charge Q on the edge; indeed,

$$dD_l=\tau dl \quad\Rightarrow\quad D_l=Q \tag{6.74}$$

The introduction of (6.74) in (6.73) yields the continuity equation over a wire, which makes (6.73) become zero

$$\left(I+j\omega Q\right)\hat{l}dl=0dl \tag{6.75}$$

and thus the expression for (6.72) yields

$$\vec{n}_{c,1}\times\vec{H}_1\Big|_{\vec{r}\in\partial i}+\vec{n}_{c,2}\times\vec{H}_2\Big|_{\vec{r}\in\partial_i}=0 \tag{6.76}$$

which represents a boundary condition for the magnetic field on an arbitrary edge ∂_i of the polyhedron -see Fig. 6.8-.

The introduction of (6.69) in the field boundary condition -(6.76)- yields

$$\vec{n}_{c,1}\times\left(\vec{J}_1\times\hat{n}_1\right)\Big|_{\vec{r}\in\partial_i}+\vec{n}_{c,2}\times\left(\vec{J}_2\times\hat{n}_2\right)\Big|_{\vec{r}\in\partial_i}=0 \tag{6.77}$$

Moreover, one can easily express

$$\begin{aligned}\vec{n}_{c,\{12\}}\times\left(\vec{J}_{\{12\}}\times\hat{n}_{\{12\}}\right)\Big|_{\vec{r}\in\partial_i} &= \left(\vec{n}_{c,\{12\}}\cdot\hat{n}_{\{12\}}\right)\vec{J}_{\{12\}}\Big|_{\vec{r}\in\partial_i}-\left(\vec{n}_{c,\{12\}}\cdot\vec{J}_{\{12\}}\Big|_{\vec{r}\in\partial_i}\right)\hat{n}_{\{12\}}\\ &=-\left(\vec{n}_{c,\{12\}}\cdot\vec{J}_{\{12\}}\Big|_{\vec{r}\in\partial_i}\right)\hat{n}_{\{12\}}\end{aligned} \tag{6.78}$$

which, back to (6.77), yields

$$\left(\vec{n}_{c,1}\cdot\vec{J}_1\Big|_{\vec{r}\in\partial_i}\right)\hat{n}_1+\left(\vec{n}_{c,2}\cdot\vec{J}_2\Big|_{\vec{r}\in\partial_i}\right)\hat{n}_2=0 \tag{6.79}$$

which is a sufficient condition for the current to satisfy (6.76). Due to the planar discretization, though, one cannot assume $\hat{n}_1=\hat{n}_2$ in general, which makes more difficult than before the enforcement of the boundary condition.

For the specific case of $\hat{n}_1=\hat{n}_2$, the field condition in (6.76) is equivalent to -see Fig. 6.8-

$$\hat{l}\cdot\vec{H}_1\Big|_{\vec{r}\in\partial i}-\hat{l}\cdot\vec{H}_2\Big|_{\vec{r}\in\partial_i}=0 \tag{6.80}$$

which, in view of (6.69), becomes

$$\begin{aligned}\hat{l}\cdot\left(\vec{J}_1\times\hat{n}_1\right)\Big|_{\vec{r}\in\partial i}-\hat{l}\cdot\left(\vec{J}_2\times\hat{n}_2\right)\Big|_{\vec{r}\in\partial_i}&=0\\ \left(\hat{n}_1\times\hat{l}\right)\cdot\vec{J}_1\Big|_{\vec{r}\in\partial i}-\left(\hat{n}_2\times\hat{l}\right)\vec{J}_2\Big|_{\vec{r}\in\partial_i}&=0\\ \hat{n}_{c,1}\cdot\vec{J}_1\Big|_{\vec{r}\in\partial i}+\hat{n}_{c,2}\cdot\vec{J}_2\Big|_{\vec{r}\in\partial_i}&=0\end{aligned} \tag{6.81}$$

which is obviously equivalent to (6.79) when $\hat{n}_1=\hat{n}_2$.

RWG -and any divergence-conforming set- excels as the expanding set that fulfils (6.81). Similarly, the use of *unxRWG* -in general, any curl-conforming set- as weighting functions satisfies the field requirement in (6.80).

Nonetheless, these unambiguous current and field spaces are wrong in physical terms since its behaviour is not in general in agreement with the behaviour of the magnetic field, derived from the boundary condition (6.76). In consequence, in the solution due to PeC-MFIE(*unxRWG,RWG)* there must always be some inherent error that declines when $\hat{n}_1$ and $\hat{n}_2$ approach. A deeper insight into this fact is given in Chapter 7 and a heuristic method of correction is provided.

6.5.2.2 Electric field conditions: PeC-EFIE

- $\vec{n}\cdot\left(\vec{D}_1-\vec{D}_2\right)\Big|_{\vec{r}\in\partial_i}=\tau\Big|_{\vec{r}\in\partial_i}$

This condition comes from the adaptation of the boundary condition in (2.39) to 2D. In this case one must allow for the electric linear charge density. Note that this is a new fact because in the magnetic field boundary conditions either there is no linear charge density -(6.67)- or the influences of the wire-magnitudes sum zero -(6.76)-.

The integration of $\nabla_s\cdot\vec{E}$ over a portion of surface -$\Delta S\to 0$- around a point on the edge -$\vec{r}\in\partial_i$- with the length of the transversal side tending to zero -$\Delta t\to 0$-see Fig. 6.9-yields -see Fig. 6.8-

$$\lim_{\Delta S\to 0}\int_{\Delta S}\nabla_s\cdot\vec{E}dS=\left(\vec{n}_{c,1}\cdot\vec{E}_1+\vec{n}_{c,2}\cdot\vec{E}_2\right)dl \tag{6.82}$$

where the surface divergence theorem is applied.

The Gauss' law enables the equivalent expression of the left-hand side term as

$$\lim_{\Delta S\to 0}\int_{\Delta S}\nabla_s\cdot\vec{E}dS=\frac{1}{\varepsilon}\left[\lim_{\Delta S\to 0}\int_{\Delta S}\sigma dS\right]=\frac{1}{\varepsilon}\tau dl \tag{6.83}$$

where τ stands for the electric linear charge density at $\vec{r}\in\partial_i$.

Therefore, the expression in (6.82) becomes

$$\vec{n}_{c,1}\cdot\vec{E}_1\Big|_{\vec{r}\in\partial_i}+\vec{n}_{c,2}\cdot\vec{E}_2\Big|_{\vec{r}\in\partial_i}=\frac{\tau}{\varepsilon}\Big|_{\vec{r}\in\partial_i} \tag{6.84}$$

which represents a boundary condition for the electric field on an arbitrary edge ∂_i in the polyhedron -see Fig. 6.8-.

Furthermore, according to the continuity equation, (6.83) can be expressed in terms of the electric current through the application of the surface divergence theorem

$$\begin{aligned}\lim_{\Delta S\to 0}\int_{\Delta S}\nabla_s\cdot\vec{E}dS&=\frac{1}{\varepsilon}\left[\lim_{\Delta S\to 0}\int_{\Delta S}\sigma dS\right]=\frac{1}{-j\omega\varepsilon}\lim_{\Delta S\to 0}\int_{\Delta S}\nabla_s\cdot\vec{J}dS\\&=\frac{1}{-j\omega\varepsilon}\left(\vec{n}_{c,1}\cdot\vec{J}_1+\vec{n}_{c,2}\cdot\vec{J}_2\right)dl\end{aligned} \tag{6.85}$$

which, in accordance with (6.82), yields the following boundary condition for the electric field

$$\vec{n}_{c,1}\cdot\vec{E}_1\Big|_{\vec{r}\in\partial_i}+\vec{n}_{c,2}\cdot\vec{E}_2\Big|_{\vec{r}\in\partial_i}=\frac{1}{-j\omega\varepsilon}\left(\vec{n}_{c,1}\cdot\vec{J}_1+\vec{n}_{c,2}\cdot\vec{J}_2\right)\Big|_{\vec{r}\in\partial_i} \tag{6.86}$$

The comparison of (6.84) and (6.86) provides the condition for the current to let the rank well defined in electromagnetic terms

$$\frac{1}{-j\omega\varepsilon}\left(\vec{n}_{c,1}\cdot\vec{J}_1+\vec{n}_{c,2}\cdot\vec{J}_2\right)\Big|_{\vec{r}\in\partial_i}=\frac{\tau}{\varepsilon}\Big|_{\vec{r}\in\partial_i} \tag{6.87}$$

which coincides with the charge condition in (6.66). This is very important because with (6.87) it is enforced on the polyhedron at the same time the physical requirements regarding the charge and the electric flux density, which is a definition of the rank -field- and domain -current and charge- spaces.

Since only one condition is imposed over each edge and it relates two independent source magnitudes - $\vec{J}$ and τ -, this problem is ambiguously defined. That is, one cannot set at the same time the field and current spaces without imposing a value for τ. It is thus an undetermined problem -it has infinite solutions- and the degrees of freedom are the number of edges of the polyhedron. Logically, the problem must be more undetermined -the degrees of freedom increase- as more edges are set in the discretization.

The only way to undertake this problem is to impose a constriction in the domain space so that the solution suits best the physical behaviour. If we take into consideration the fact that on a physical *edge* the *charge accumulation* is null, it seems reasonable to impose $\tau=0$ over the edges of the polyhedron. According to the charge condition, this involves

$$\vec{n}_{c,1}\cdot\vec{J}_1\Big|_{\vec{r}\in\partial_i}+\vec{n}_{c,2}\cdot\vec{J}_2\Big|_{\vec{r}\in\partial_i}=0 \tag{6.88}$$

which ensures the electric field to accomplish

$$\vec{n}_{c,1}\cdot\vec{E}_1\Big|_{\vec{r}\in\partial_i}+\vec{n}_{c,2}\cdot\vec{E}_2\Big|_{\vec{r}\in\partial_i}=0 \tag{6.89}$$

The current and field conditions in (6.88) and in (6.89) impose the continuity of the normal component of these magnitudes across an arbitrary edge of the polyhedron ∂_i -see Fig. 6.9-.

It makes thus sense the use of the *RWG* set as expanding and weighting functions because, as explained in 6.1.1, any expansion undertaken through *RWG* enforces the continuity of the normal component of the magnitude across the edges.

Similarly, it is justified the dismissal of the antagonistic *unxRWG* as expanding functions of the domain of the PeC-EFIE operator. One can also understand why all the strategies to deal with the *unxRWG* charge accumulation -see 6.3.1.1- have turned out unsuccessful. They all cannot ensure this condition.

It must be noted that the good behaviour of the operator PeC-EFIE(*RWG*,*RWG*) relies on the capacity of the operator to assume the implicit imposition $\tau=0$. Since the apparition of τ is a consequence of the discretization, it is reasonable that, as long as the amount edges is not very high, the assumption for τ can be well-accomplished and the system well-defined. However, as long as the discretization becomes finer, the

solution for the current becomes increasingly undetermined. Indeed, it is well-known that the PeC-EFIE(*RWG,RWG*) condition number for increasingly fine meshings increases accordingly.

It is important to point out that the PeC-EFIE is undetermined in any case. As the number of edges increases -the number of degrees of freedom of the problem-, the system becomes increasingly undetermined and the condition number augments accordingly. The fact of having good condition numbers for PeC-EFIE(*RWG,RWG*) with a restricted amount of edges shows that the group of possible solutions are very near the physical assumption $\tau = 0$ over each edge. As the degree of meshing increases, the polyhedron is less physical and the range of possible solutions becomes gradually less near the assumption of no charge accumulation. That is why, from a certain bound the solution cannot be determined anymore since the degree of the ambiguity of the system is too high.

In the original physical problem, the solution obtained through the theorem of equivalence and EFIE is unique. However, the discretization unavoidably compels the apparition of the magnitude τ, which brings about an ambiguity in the values of the normal components of the electric field and the current on the edges of the polyhedron. Note that the magnetic field boundary conditions, on the other hand, show no dependence on any wire-magnitude -see 6.5.2.1-. Therefore, the uniqueness of the solution for the PeC-MFIE is maintained after discretizing the body, whereby the condition number must be low and stable for increasing degrees of meshing.

The condition in (6.88) ensures the charge over the surface to be null. Indeed, the integration of the left-hand side term over the line-path defined by the whole set of N edges over the polyhedron consequently yields

$$\sum_{i=1}^{N} \int_{\partial_i} \left(\vec{n}_{c,1} \cdot \vec{J}_1 + \vec{n}_{c,2} \cdot \vec{J}_2 \right) dl = 0 \tag{6.90}$$

By grouping together the paths $j(I)$, $k(I)$, $l(I)$ that surround an arbitrary triangular facet I and by selecting the addend placed on that triangle, the left-hand side term of (6.90) can be equivalently expressed as

$$\sum_{I=1}^{2N/3} \left[\int_{\partial_{i(I)}} \vec{n}_{c,i(I)} \cdot \vec{J}_{i(I)} dl + \int_{\partial_{j(I)}} \vec{n}_{c,j(I)} \cdot \vec{J}_{j(I)} dl + \int_{\partial_{k(I)}} \vec{n}_{c,k(I)} \cdot \vec{J}_{k(I)} dl \right] = 0 \tag{6.91}$$

which can be better written in terms of the number of triangular facets[20] $N_t = 2N/3$ and the path around the I triangle ∂T_I as

$$\sum_{I=1}^{N_t} \int_{\partial T_I} \vec{n}_{c,I} \cdot \vec{J}_I dl = 0 \tag{6.92}$$

Thanks to the surface divergence theorem, this expression becomes

[20] For the sake of simplicity, triangular facets are chosen, in agreement with the type of facets used in this work. One can likewise build the reasoning for any type of facet, such as rectangles for example.

$$-\sum_{I=1}^{N_t}\int_{T_i}\nabla_s\cdot\vec{J}_I dS = j\omega\sum_{I=1}^{N_t}\int_{T_i}\sigma dS = j\omega\sum_{I=1}^{N_t}Q_I = 0 \Rightarrow Q_T = 0 \tag{6.93}$$

which stands for the charge conservation principle.

- $\vec{n}\times\left(\vec{E}_1-\vec{E}_2\right)\Big|_{\vec{r}\in S_i} = 0$

This condition comes from the adaptation of the boundary condition in (2.38) to 2D. The integration of $\nabla_s\times\vec{E}$ over a portion of surface - $\Delta S\to 0$ - around a point on the edge - $\vec{r}\in\partial_i$ - with the length of the transversal side tending to zero - $\Delta t\to 0$ -see Fig. 6.9- yields -see Fig. 6.8-

$$\lim_{\Delta S\to 0}\int_{\Delta S}\nabla_s\times\vec{E}dS = \left(\vec{n}_{c,1}\times\vec{E}_1+\vec{n}_{c,2}\times\vec{E}_2\right)dl \tag{6.94}$$

where the surface curl theorem is applied.

The Faraday's law allows the equivalent expression of the left-hand side term as

$$\lim_{\Delta S\to 0}\int_{\Delta S}\nabla_s\times\vec{E}dS = \lim_{\Delta S\to 0}-\int_{\Delta S}j\omega\vec{B}dS = 0 \tag{6.95}$$

because the integration of a finite magnitude -the magnetic flux density $\vec{B}$ -over a portion of surface with area tending to zero yields zero.

Therefore, the expression in (6.94) becomes

$$\vec{n}_{c,1}\times\vec{E}_1\Big|_{\vec{r}\in\partial i}+\vec{n}_{c,2}\times\vec{E}_2\Big|_{\vec{r}\in\partial_i} = 0 \tag{6.96}$$

which represents a boundary condition for the electric field on an arbitrary edge ∂_i of the polyhedron -see Fig. 6.8-.

Unlike the previous cases -see (6.70),(6.77),(6.86)-, it is not possible now to introduce a term due to the electric current in the field boundary condition. Indeed, from the value of $\vec{B}$ on a wire -the edge- it is not possible to set the value the value of the electric current. That is, the field requirements are incompatible with the electric current.

This can be better understood through the analysis of the electromagnetic solution for a wire with electric current flowing. It is well known that in this case the magnetic field in the proximity of the wire rotates around the wire -the magnetic field cannot impinge the electric source-. In the limit case of a point on the wire - $\vec{r}\in\partial_i$ - the magnetic field cannot be defined. Indeed, the magnetic field there must accordingly maintain the rotation, which is absurd because it allows infinite directions for the value of the magnetic field at one single point, $\vec{r}\in\partial_i$. In mathematical terms this means that the limit of $\vec{B}$ in (6.95) does not exist and thus the limit of the surface integral in (6.95) with area tending to zero yields zero.

As reasoned in detail for the dual magnetic condition in (6.76), *unxRWG* expands a space that approaches to a certain extent the electric field requirements in (6.96). According to the reasoning of the previous paragraph, it is not possible to implement any PeC-EFIE approach with *unxRWG* -or any curl-conforming set- as weighting functions. That is why all the attempts for the PeC-EFIE with *unxRWG* as weighting set shown in the sections 6.3.1.1 and 6.3.1.2 failed.

6.5.3 Conclusions

From the previous study it can be concluded

1. The correct operators to obtain the solution for an arbitrary polyhedron, a constraint of a planar facet approach, come from compatible current and field boundary conditions over the edges. That is why the number of edges sets the number of unknowns of the system.

2. PeC-MFIE(*RWG,unxRWG*) and PeC-MFIE(*unxRWG,RWG*) show a perfect correspondence between the rank generated by the expanding functions and the space expanded by the weighting functions. They both correspond to compatible problems with unique solution. Therefore, for the PeC-MFIE, the discretization does not add any ambiguity and the solution keeps being unique. In consequence, the condition number for the PeC-MFIE must be low and stable when yielding the meshing finer -as long as the impedance elements are accurately computed-.

3. In general, the electric flux density boundary condition over each edge allows infinite solutions; the solution is thus undetermined. This is a consequence of the discretization because the equivalence theorem ensures the uniqueness of the solution in the physical problem without discretization. Through the a priori imposition of no charge accumulation $-\tau = 0-$, one can set a system that best approaches the physical behaviour. The ambiguity of the system increases as the degree of discretization augments and more edge conditions appear. The condition number must increase accordingly. This accounts for the fact that the condition number of PeC-EFIE(*RWG,RWG*) is always higher than those of PeC-MFIE(*unxRWG,RWG*) and PeC-MFIE(*RWG,unxRWG*).

4. PeC-MFIE(*RWG,unxRWG*) ensures the required physical boundary conditions for any kind of discretization. PeC-MFIE(*unxRWG,RWG*), on the contrary, enforces tangent continuity for the magnetic field over the edges, which only approaches the corresponding magnetic field boundary condition if the normal vectors of adjacent facets tend to become parallel. Therefore, with the same degree of discretization and accuracy, the PeC-MFIE(*RWG,unxRWG*) results must be better than those from the PeC-MFIE(*unxRWG,RWG*).

5. Since both PeC-MFIE approaches -corresponding to the two canonical directions across the edge- are defined with no restrictions, one can infer that a global interpolatory technique, such as the node-based Finite elements, applied to the PeC-MFIE can be possible too. Indeed, node-based finite element PeC-MFIE formulations with current interpolation have been carried out [22]. The PeC-EFIE, though, has to impose a charge constraint over the edges, which is not inherently assumed by the

electric field over the edges of a polyhedron. That is why no node-based finite-element formulations for the PeC-EFIE operator have ever been published.

6. No patch-based formulations can be developed for PeC-EFIE with *unxRWG* - or any curl-conforming set- as weighting set because the problem cannot be posed.

7. This study has focused on the necessary conditions for the field and the current. The *RWG* and *unxRWG* sets represent low-order expanding bases over the triangle subdomain. The higher-order bases enclosed in the wide families of the divergence-conforming and curl-conforming bases -where *RWG* and *unxRWG* respectively belong- accomplish the required edge conditions too. One has to assume thus in the results of this work the error due to the low-order expansion of the current, which is different for the *RWG* and *unxRWG* sets. This fact is commented more in detail in Chapter 7.

8. PeC-EFIE(*RWG*,*RWG*) ensures the charge conservation principle through the accomplishment of the charge condition over the edges. PeC-MFIE does not impose this condition over the edges but *unxRWG* and *RWG* fulfil it by definition because it is a requirement of the patch-based functions. On an PeC-MFIE approach with boundary elements, though, the charge condition is not needed to be explicitly set since it is not required for the definition of the PeC-MFIE operator for both canonical directions over the edge, tangential and normal. This implies that the PeC-MFIE must incorporate implicitly the charge conservation principle on the solution with node-based finite elements.